Chemical Constituents from the Root Woods of *Ochna integerrima* (Lour.) Merr. and Their Biological Activities

Sirilug Wongpakham

A Thesis Submitted in Partial Fulfillment of Requirements for
degree of Master of Science in Chemistry
April 2025

สารองค์ประกอบทางเคมีจากเนื้อไม้ส่วนรากของช้างน้าว (*Ochna integerrima* (Lour.) Merr.) และฤทธิ์ทางชีวภาพ

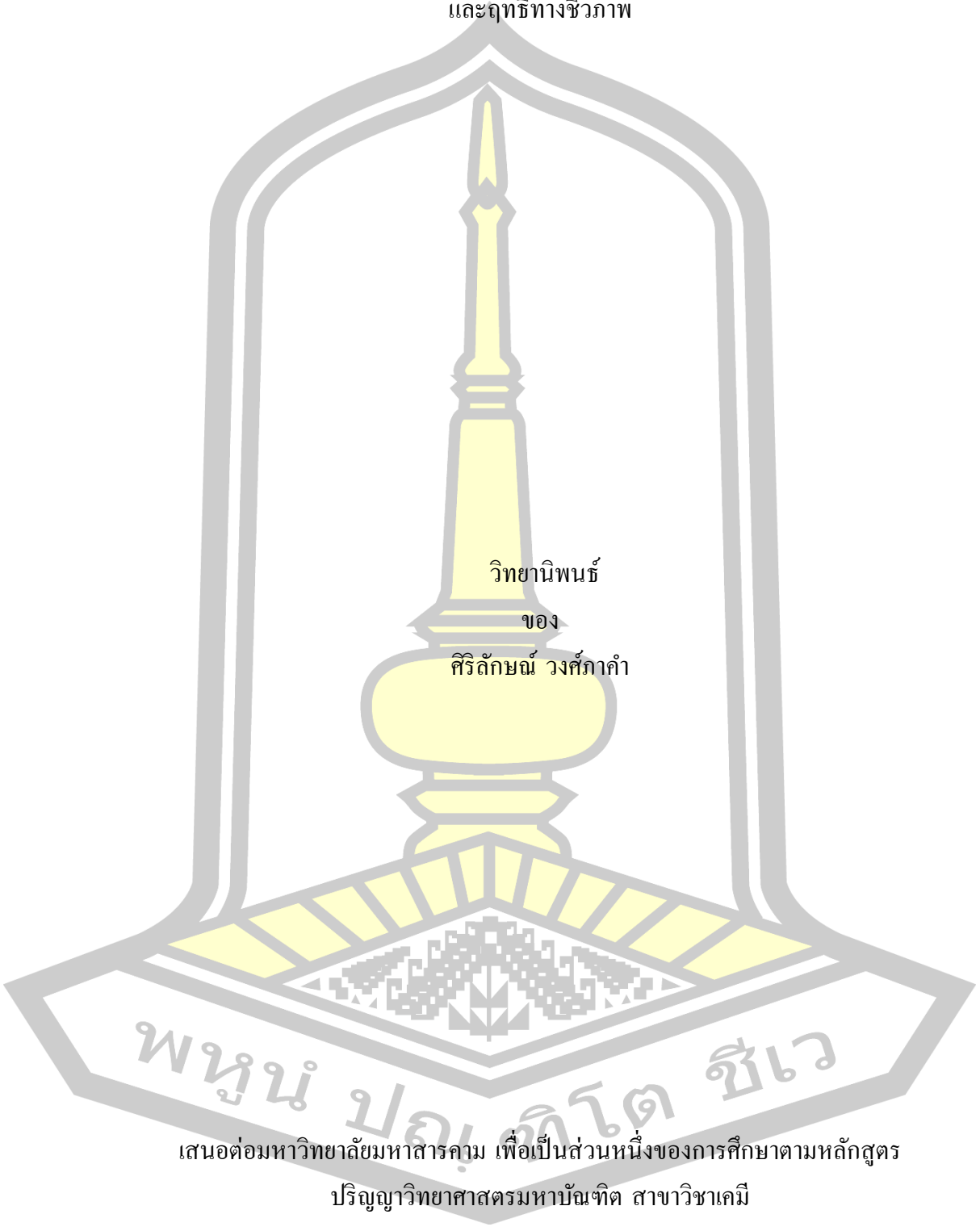

วิทยานิพนธ์

ของ

ศิริลักษณ์ วงศ์ภาคำ

เสนอต่อมหาวิทยาลัยมหาสารคาม เพื่อเป็นส่วนหนึ่งของการศึกษาตามหลักสูตร

ปริญญาวิทยาศาสตรมหาบัณฑิต สาขาวิชาเคมี

เมษายน 2568

Chemical Constituents from the Root Woods of *Ochna integerrima* (Lour.) Merr. and Their Biological Activities

Sirilug Wongpakham

A Thesis Submitted in Partial Fulfillment of Requirements

for Master of Science (Chemistry)

April 2025

The examining committee has unanimously approved this Thesis, submitted by Miss Sirilug Wongpakham , as a partial fulfillment of the requirements for the Master of Science Chemistry at Mahasarakham University

Examining Committee

.....Chairman
(Assoc. Prof. Panawan Moosophon , Ph.D.)

.....Advisor
(Assoc. Prof. Prapairat Seephonkai , Ph.D.)

.....Co-advisor
(Assoc. Prof. Aphidech Sangdee , Ph.D.)

.....Committee
(Assoc. Prof. Chatthai Kaewtong , Ph.D.)

.....Committee
(Asst. Prof. Pakin Noppawan , Ph.D.)

Mahasarakham University has granted approval to accept this Thesis as a partial fulfillment of the requirements for the Master of Science Chemistry

.....	.....
(Prof. Pairot Pramual , Ph.D.)	(Prof. Anongrit Kangrang , Ph.D.)
Dean of The Faculty of Science	Acting Dean of Graduate School

TITLE Chemical Constituents from the Root Woods of *Ochna integerrima* (Lour.) Merr. and Their Biological Activities

AUTHOR Sirilug Wongpakham

ADVISORS Associate Professor Prapairat Seephonkai , Ph.D.

Associate Professor Aphidech Sangdee , Ph.D.

DEGREE Master of Science **MAJOR** Chemistry

UNIVERSITY Mahasarakham University **YEAR** 2025

ABSTRACT

Ochna integerrima (Louri) Merr. is one of the two species of the genus *Ochna* (family Ochnaceae) found in Thailand. Its barks and roots are used in traditional Thai medicine to treat digestive disorders, the leaves have historically been utilized to treat a range of conditions such as asthma, dysentery, epilepsy, gastric disorders, menstrual disorders, lumbago, ulcers, and snakebites. Phytochemical investigation of the crude methanol extract of the root woods of *O. integerrima* furnished an unreported isoflavone glycoside, gerontoisoflavone A-4'-*O*-*β*-D-xylopyranoside (35), together with the previously described iriskumaonin methyl ether (11), irisolone methyl ether (12), a flavone glycoside, vitexin (13), a chromone derivative, lophilone A (20), isoprunetin (26), gerontoisoflavone A (27), and iriskumaonin (36). The structure of 35 was elucidated by 1D and 2D NMR spectral analysis as well as HRMS data. All the compounds except compound 20 were evaluated for antimalarial activity against a chloroquine- and pyrimethamine-resistant strain of *Plasmodium falciparum* (multidrug-resistant strain K1), antibacterial activity against methicillin-susceptible *Staphylococcus aureus* (MSSA), methicillin-resistant *S. aureus* (MRSA), and *Bacillus cereus*, and their 2,2-diphenyl-1-picrylhydrazil radical ($DPPH^{\bullet}$) scavenging activity. Compounds 27 exhibited strongest scavenging activity, with SC_{50} of 137.7 μM, while 36 and 26 displayed weak scavenging activity, with SC_{50} values of 4 and 5 times higher than that of 27. None of the tested compounds showed antimalarial activity against *P. falciparum* (K1) at a concentration of 5 μg/mL and compound 36 showed antibacterial activity against the *S. aureus* MSSA with a MIC and MBC values of 0.25 and >0.25 mg/mL, respectively.

Keyword : Ochna integerrima, Ochnaceae, Gerontoisoflavone A-4'-O-β-D-xylopyranoside, Isoflavones glycosides, Antimalarial activity, Antibacterial activity, DPPH radical scavenging activity

ACKNOWLEDGEMENTS

This thesis would not have been possible without the guidance and the help of several individuals who in one way or another contributed and extended their valuable assistance in the preparation and completion of this study, it is a pleasure to thank those who made it a possibility. I would like to express my sincere gratitude and deep appreciation to my beloved adviser, Assoc. Prof. Prapairat Seephonkai, for her supported to me in all stages of this thesis, kind supervision, valuable guidance, teaching encouragement, advice, taking, care and helpful discussion. Sincere gratefulness is also extended to my co-advisor, Assoc. Prof. Aphidech Sangdee, for the helpful antibacterial activity assay, suggestions and comments for completion of this thesis. I would like to thank Dr. Rapatbhorn Patrapuvich, head of the Drug Research Unit for Malaria (DRUM), Mahidol University, and her research team for the antimalarial activity assay. I also would like to thank Asst. Prof. Worrawat Promden, Buriram Rajabhat University, for antioxidant activity assay, Prof. Anake Kijjoa, for conceptualization, suggestions, and revision of the manuscript of the paper, Ms. Thanatcha Samsee, for UV, IR, and optical rotation measurement, and Mr. Komgrit Wongpakam, for the plant material identification.

I am grateful to thank Assoc. Prof. Panawan Moosophon, Department of Chemistry, Faculty of Science, Khon Kaen University, Assoc. Prof. Chatthai Kaewtong, and Asst. Prof. Pakin Noppawan, Department of Chemistry, Faculty of Science, Mahasarakham University, for they kind comments and supports as members of my examining committee.

I would like to thank the financial support from Mahasarakham University (Postgraduate Research Scholarship), Faculty of Sciences, Mahasarakham University (MSU), and Center of Excellence for Innovation in Chemistry (PERCH-CIC).

Last and most of all, I wish to express my heartfelt gratitude here to my family for their tender love, definitely care, encouragement, and constant support throughout my studies. Without them, I could not imagine how I could complete my master's degree

study.

Sirilug Wongpakham

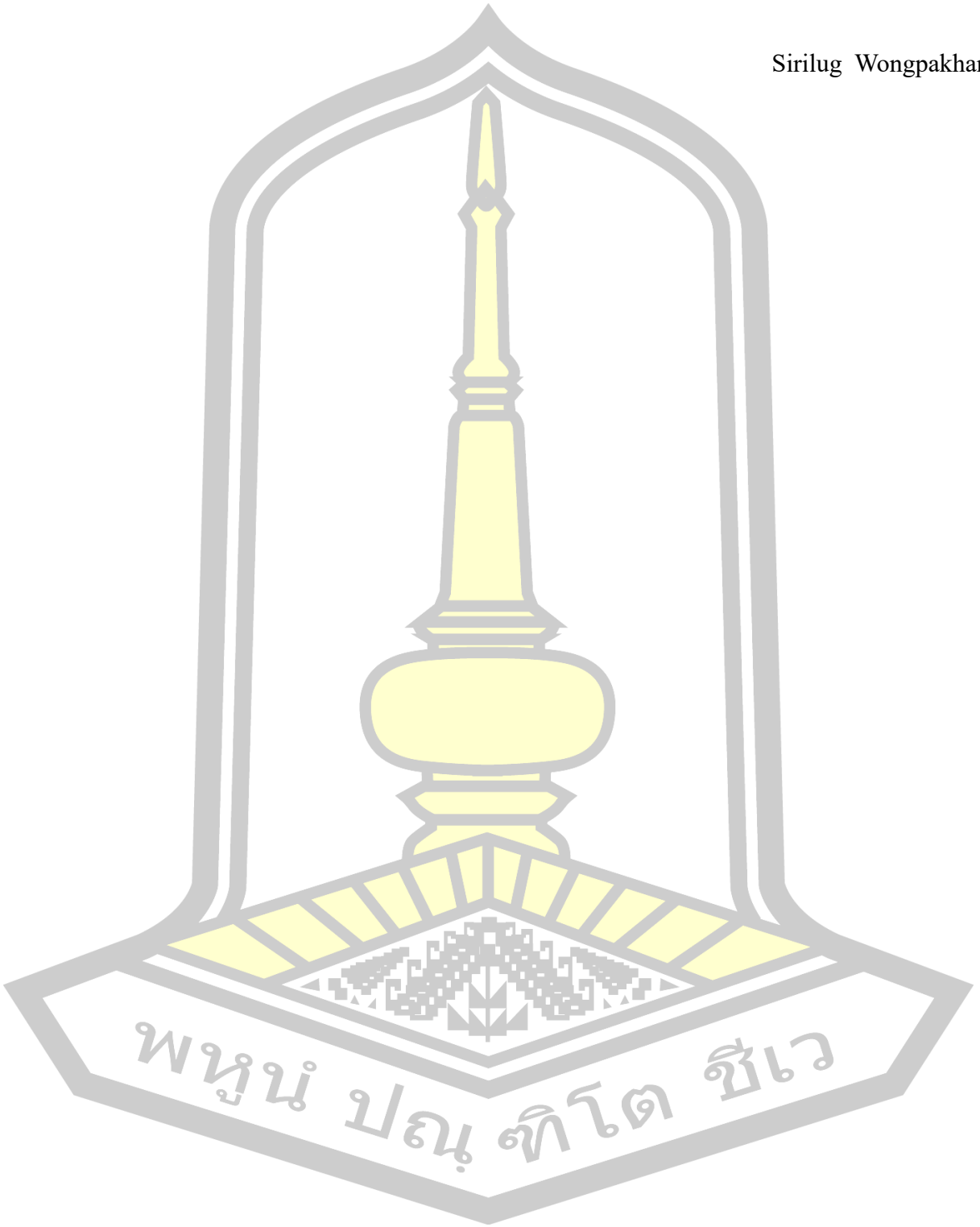

TABLE OF CONTENTS

Page

LIST OF TABLES

Page

LIST OF FIGURE

Page

LIST OF FLOW CHART

Page

LIST OF ABBREVIATIONS

Abbreviation	Full word
%RSA	%Radical scavenging activity
1D	1-Dimensional
ABTS	2,2'-Azino-bis (3-ethylbenzthiazoline-6-sulphonic acid)
DPPH$^{\bullet}$	2,2-Diphenyl-1- picrylhydrazyl radical
2D	2-Dimensional
MTT assay	3-(4,5-Dimethylthiazol-2-yl)-2,5-diphenyltetrazolium bromide assay
m/z	A value of mass divided by charge
A	Absorbance
B. cereus	*Bacillus cereus*
BuOH	Butanol
CO_2	Carbon dioxide
CCl_4	Carbon tetrachloride
^{13}C-NMR	Carbon-13 nuclear magnetic resonance
PERCH-CIC	Center of Excellence for Innovation in Chemistry
cm	Centimeter
KKU-100	Cholangiocarcinoma
ca.	Circa
CC	Column chromatography
COSY	Correlation spectroscopy

Abbreviation	Full word
J	Coupling constant
°C	Degree Celsius
DNA	Deoxyribonucleic acid
DMST	Department of Medical Sciences Thailand
Acetone-d_6	Deuterated acetone
$CDCl_3$	Deuterated chloroform
DMSO-d_6	Deuterated dimethyl sulfoxide
CD_3OD	Deuterated methanol
DMSO	Dimethyl sulfoxide
DEPT	Distortion less enhancement by polarization transfer
d	Doublet (spectral multiplicity)
dd	Doublet of doublet (spectral multiplicity)
DRUM	Drug Research Unit for Malaria
FCR3	Drug-sensitive strains
EtOH	Ethanol
EtOAc	Ethyl acetate
e.g.	Exempli gratia
FRAP	Ferric reducing ability power
U.N. FAO	Food and agriculture organization of the United Nations
FTIR	Fourier transform infrared
Fr.	Fraction
g	Gram

Abbreviation	Full word
Huh-7	Hepatocellular carcinoma
Hz	Hertz
HMBC	Heteronuclear multiple bond correlation
HSQC	Heteronuclear single quantum coherence
HRESIMS	High resolution electrospray ionization mass spectroscopy
HRMS	High resolution mass spectroscopy
h	Hour
HaCaT	Human epidermal keratinocytes
HepG2	Human hepatocellular carcinoma cell line
HIV-1	Human immunodeficiency virus type 1
H_2O_2	Hydrogen peroxide
i.e.	Id est (in other words)
IR	Infrared radiation
IC_{50}	Inhibitory concentration at 50%
kcal/mol	Kilocalorie per mole
L	Liter
RAW 264.7 cell	Macrophage cell line
MSU	Mahasarakham University
MS	Mass spectrometry
MHz	Megahertz
m	Meter
MeOH	Methanol

Abbreviation	Full word
MRSA	Methicillin-resistant *Staphylococcus aureus*
MSSA	Methicillin-susceptible *Staphylococcus aureus*
OMe	Methoxy group
µg/mL	Microgram by milliliter
µL	Microliter
µM	Micromolar
mg	Milligram
mg/mL	Milligram per milliliter
mL	Milliliter
mm	Millimeter
MBC	Minimum bactericidal concentration
MIC	Minimum inhibitory concentration
min	Minute
MHA	Mueller Hinton Agar
K1	Multidrug-resistant strain
m	Multiplet (spectral multiplicity)
mult.	Multiplicity
nm	Nanometer
nM	Nanomolar
NO	Nitric oxide
N_2	Nitrogen gas
n-BuOH	Normal butanol

Abbreviation	Full word
n-Hexane	Normal hexane
NHDF	Normal human dermal fibroblasts
ND	Not determine
NT	Not tested
NMR	Nuclear magnetic resonance
NOESY	Nuclear overhauser effect spectroscopy
O. integerrima	*Ochna integerrima*
O_2	Oxygen gas
P. falciparum	*Plasmodium falciparum*
^{1}H NMR	Proton-1 nuclear magnetic resonance
ROS	Reactive oxygen species
SC_{50}	Scavenging concentration at 50%
s	Singlet (spectral multiplicity)
km^2	Square kilometer
SD	Standard deviation
S. aureus	*Staphylococcus aureus*
TLC	Thinlayer chromatography
MDA-MB231	Triple-negative breast cancer
UV	Ultraviolet radiation
UV-vis	Ultraviolet-visible spectroscopy
viz.	Videlicet
v/v	Volume by volume

Abbreviation	Full word
WRBRI	Walai Rukkhavej Botanical Research Institute
cm^{-1}	Wave number unit

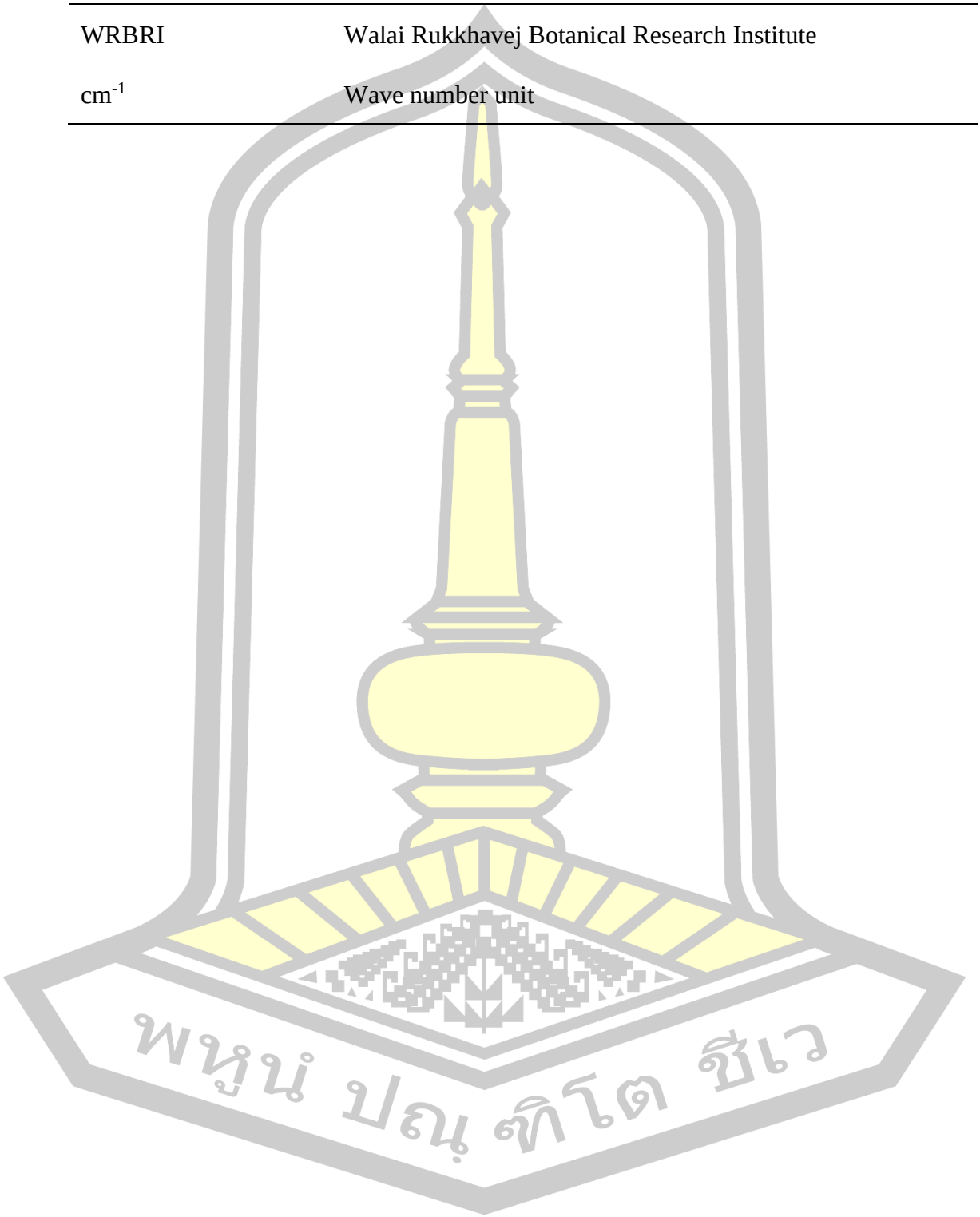

CHAPTER 1

INTRODUCTION

1.1. Background

Thailand is one of the most biodiversity-rich countries in Southeast Asia. The small country but rich in biodiversity of plants, animals, fungi, and microorganisms, comprising approximately 6–10% of the total species known thus far (Baimai, 2010). Based on the U.N. FAO, 37.1% or about 18,972,000 ha of Thailand is forested (Mongabay, 2011). Thailand has a total area of about 513,000 km^2, 70 percent of the total land area was covered with various kinds of tropical forest including broad-leaved evergreen, dry dipterocarp and pine forest, mixed deciduous forest, peat swamp forest and mangrove forest along coastlines. About 1/3 of the coastal areas are bordered by mangrove forests. Thailand's tropical forests support some 12,000 species of vascular plants, roughly 15,000 known species of animals and about 10,000 known species of microorganisms. It is believed that more than 100,000 species of living organisms in these forests await discovery. Thus, Thailand is situated in one of the richest areas of the world with regard to biological resources (Baimai, 2010).

Plants are important sources of bioactive compounds with a huge variety of different molecules and have long been used as natural medicine for centuries. The plant-derive compounds are commonly called "phytochemicals" or referred to "secondary metabolites". Although these compounds are not required for the growth

and performance of basic life of functions, they show many of biological properties (Newman and Cragg, 2016; Kennedy and Wightman, 2011). The people of Thailand have used medicinal plants as sources of drugs for traditional remedies of ailments throughout this country's long history. Such indigenous knowledge has been perpetuated by being passed down from generation to generation within ethnic tribes. For instance, *Curcuma longa* Linn., has been used for treatment of peptic ulcer and dyspepsia, *Diospyros mollis* Griff., has been used to eliminate hookworm (Baimai, 2010), the barks of *Ochna integerrima* (Lour.) Merr. has been used as a digestive tonic, and the roots as an anthelmintic. Infusion of its roots and leaves is reputed for its antidysenteric and antipyretic properties (Bandi et al., 2012), and *Croton sublyratus* Kurz (Family Euphorbiaceae) which has been used by local people for a long time as an effective treatment for peptic ulcer (Baimai, 2010).

The genus *Ochna* (Family Ochnaceae) comprises of *ca*. 85 species. Several members of the genus *Ochna* are used in folk medicine for treatment of malaria, diarrhea, hemorrhoids, ulcers, epilepsy, dysentery, asthma, snake bite, and menstrual pain or as abortifacient agents (Bandi et al., 2012; Makhafola et al., 2012; Ndoile and Heerden, 2018). Flavonoids are a major group of compounds isolated from the plants of this genus, e.g. *O. afzelii* (Kakabi et al., 2024; Pegnyemb et al., 2003), *O. calodendron* (Messanga et al., 2002), *O. holstii* (Kalenga et al., 2021), *O. integerrima* (Chokchaisiri et al., 2024; Ichino et al., 2006), *O. kibbiensis* (Ismail et al., 2017), *O. kirkii* (Kalenga et al., 2021), *O. lanceolata* (Reddy et al., 2008), and *O. schweinfurthiana* (Ndongo et al., 2015).

Therefore, in this study, the root woods of *Ochna integerrima* collected in northeastern Thailand were selected for phytochemical investigation and biological activity evaluation.

1.2. Research objective

This research aims to phytochemical investigate the root woods of *Ochna integerrima* and to evaluate the biological activities of the isolated compounds from this species.

1.3. Expected result

The expected results of this research are information of phytochemicals produced in the root woods of *Ochna integerrima* and their biological activities.

1.4. Scope of research

Scope of research are; (1) phytochemical investigation of the root woods of *O. integerrima*, and (2) evaluation of biological activities of the isolated compounds from the root woods of *Ochna integerrima* wich include antimalarial, antibacterial, and DPPH radical scavenging activities.

CHAPTER 2

LITERATURE REVIEWS

2.1. *Ochna integerrima*

In Thailand, only two species of the genus *Ochna* have been recorded, *viz*. *Ochna integerrima* (Louri) Merr. and *Ochna kirkii* Oliv (Smitinand and Larsen, 1970). *O. integerrima* (Lour.) Merr. (**Figure 1**), a deciduous shrub in the family of Ochnaceae, is a great source of active compounds and is used as a medicinal plant in tropical Asia, Africa, and America (Moh and Kato-Noguchi, 2022). *O. integerrima* can grow up to 12 m tall. The short bole can be straight or twisted and is 6–16 cm in diameter. It is a very popular ornamental garden plant in east Asia, the bark is dark brown and broken into scaly deep grooves. Leaves simple, alternate and distichous, obovate, glabrous, apex obtuse, base rounded to acute, margin dentate (Phargarden, 2010). Flowers yellow, arranged in a few-flowered inflorescence, axillary on leafless twigs, bisexual, pedicels longer than 0.5 cm. The fruit is green, 8–9 mm wide and 1–1.2 cm long. When the fruit matures, it turns glossy black fruit, which protrude from the swollen base of the bright red calyx (Med Thai, 2020).

The barks of *O. integerrima* ("kamlang chang san" in Thai), which is widely distributed in Thailand, is used in traditional Thai medicine as a digestive aid. On the other hand, its roots and leaves are used in traditional Indonesian medicine to treat dysentery and reduce fever (Bandi et al., 2012). Previous studies reported the isolation of various flavonoids (monomeric and dimeric flavonoids and flavonoid glycosides)

and stilbenoids, including oligostilbenoids, from the leaves, stems, stem barks, and roots of *O. integerrima* (Chokchaisiri et al., 2024; Ichino et al., 2006; Reutrakul et al., 2007; Kaewamatawong et al., 2002; Likhitwitayawuid et al., 2001; Likhitwitayawuid et al., 2005), some of which exhibited antimalarial (Ndoile and Heerden, 2018; Chokchaisiri et al., 2024), anti-human immunodeficiency virus type 1 (anti HIV-1) (Reutrakul et al., 2007), antibacterial (Seephonkai et al., 2021), and antioxidant activities (Buranasudja et al., 2022). To the best of our knowledge, there is only one report on phytochemical constituents of the root woods of *O. integerrima* (Likhitwitayawuid et al., 2005).

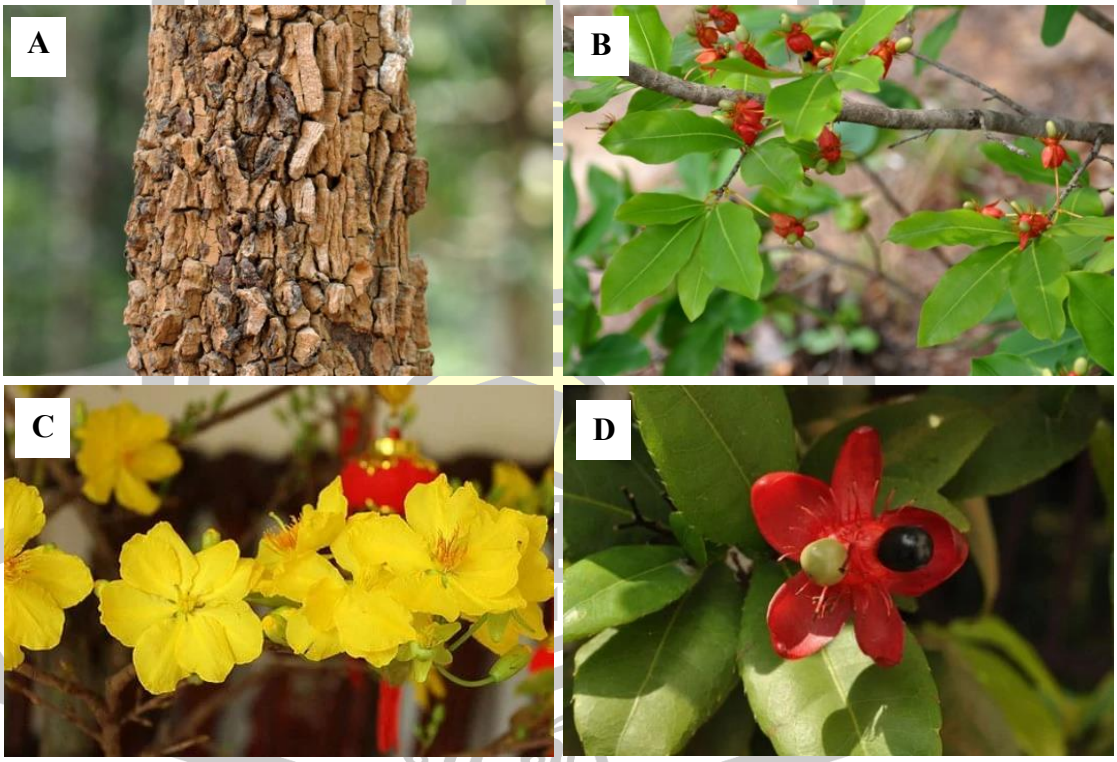

Figure 1. Stems (**A**), leaves (**B**), flowers (**C**), and fruits (**D**) of *O. integerrima*. (Med Thai, 2020; Phargarden, 2010)

There are numbers of reports on chemical constituents of *Ochna integerrima*. These are a summary of phytochemical investigations of *O. integerrima* which reported in ScienceDirect and PubMed databases since the year 2000.

2.2. Isolated compounds from the leaves and twigs of *O. integerrima*

In 2001, the isolation of two new bioflavonoids, 2",3"-dihydroochnaflavone (**1**) and 2",3"-dihydroochnaflavone 7"-*O*-methyl ether (**2**), and a flavonoid glycosides, 6-*γ,γ*-dimethylallyltaxifolin 7-*O*-*β*-D-glucoside (**3**), from the ethyl acetate (EtOAc) extract from the leaves of *O. integerrima* has been reported (Likhitwitayawuid et al., 2001). This plant was collected from Nakhon Ratchasima Province, Thailand.

In 2007, five new flavonoid glycosides, 6-*γ,γ*-dimethylallyldihydrokaempferol 7-*O*-*β*-D-glucoside (**4**), 6-*γ,γ*-dimethylallylkaempferol 7-*O*-*β*-D-glucoside (**5**), 6-*γ,γ*-dimethylallylquercetin 7-*O*-*β*-D-glucoside (**6**), 6-(3-hydroxy-3-methylbutyl)taxifolin 7-*O*-*β*-D-glucoside (**7**) and 6-(3-hydroxy-3-methylbutyl)quercetin 7-*O*-*β*-D-glucoside (**8**), five known flavonoids, ochnaflavone (**9**), ochnaflavone 7"-*O*-methyl ether (**10**), 2",3"-dihydroochanaflavone 7"-*O*-methyl ether (**2**), 5,3',4'-trimethoxy-6,7-methyl enedioxy isoflavone (**11**) and 5,4'-dimethoxy-6,7-methylenedioxy isoflavone (**12**), and two known flavonoid glycosides, 6-*γ,γ*-dimethylallyltaxifolin 7-*O*-*β*-D-glucoside (**3**) and vitexin (**13**), were isolated from the EtOAc extract from the leaves and twigs of *O. integerrima* (Reutrakul et al., 2007). This plant was collected from Uthai Thani Province, Thailand. All isolated compounds were tested for anti HIV–1 activity. Compounds **10** and **2** were found to be the most effective with inhibitory concentration at 50% (IC_{50}) values of 2.0 and 2.4 μg/mL, respectively.

2.3. Isolated compounds from the flowers and seeds of *O. integerrima*

In 2022, three flavonoid glycosides **4**–**6** and luteolin (**14**), were isolated for the first time from the EtOAc extract from the flowers of *O. integerrima* (Buranasudja et al., 2022). EtOAc extract exhibited the strongest antioxidant activity with IC_{50} 11.44 µg/mL, followed by butanol (BuOH) with IC_{50} 24.84 µg/mL and methanol (MeOH) with IC_{50} 48.51 µg/mL. From EtOAc extract, compound **14** showed the strongest DPPH radical scavenging activity with IC_{50} 8.77 µM. The study demonstrated that EtOAc and BuOH extracts protected human epidermal keratinocytes (HaCaT) keratinocytes from H_2O_2–induced oxidative stress, highlighting their potential as anti–aging agents. Molecular docking analysis suggested that compounds **5**, **6**, and **14** strongly inhibited tyrosinase, with free binding energies ranging from -70 to -78.9 kcal/mol, an enzyme involved in melanin synthesis.

In 2024, three flavonoid glycosides **4**–**6** and luteolin (**14**), were isolated from the EtOAc extract from the flowers of *O. integerrima* (Nguyen et al., 2024). The research has been extended by analyzing both the flowers and seeds of *O. integerrima* to evaluate their antioxidant, anti-tyrosinase, hepatoprotective, and anti–inflammatory properties. The study employed multiple antioxidant assays, including 2,2'-azino-bis (3-ethylbenzthiazoline-6-sulphonic acid) (ABTS), ferric reducing ability power (FRAP), hydroxyl radical scavenging, and ferrous ion chelation, revealing that *n*-butanol (*n*-BuOH) extracts from both flowers and seeds had the highest antioxidant activity. Tyrosinase inhibition assays confirmed that **14** and its derivatives effectively reduced enzyme activity, reinforcing their potential for skin-whitening applications. Additionally, aqueous extracts exhibited significant hepatoprotective effects,

protecting human hepatocellular carcinoma cell line (HepG2) from CCl_4-induced oxidative damage, with efficacy comparable to quercetin. The study also highlighted the anti-inflammatory potential of *O. integerrima*, demonstrating that *n*-hexane and EtOAc extracts from flowers significantly reduced nitric oxide (NO) production in macrophage cell line (RAW 264.7 cell). The findings suggest that *O. integerrima* is a versatile medicinal plant with applications in skincare, liver protection, and anti-inflammatory treatments, further supporting its traditional medicinal uses and potential for pharmaceutical and cosmeceutical industry.

2.4. Isolated compounds from the stem barks and roots of *O. integerrima*

In 2002, two new bioflavonoids, 6'''-hydroxylophirone B (**15**) and 6'''-hydroxy lophirone B 4'''-*O*-*β*-D-glucoside (**16**), and five known biflavonoids, 3-(2,4-dihydroxy benzoyl)-4,6-dihydroxy-2-(4-hydroxyphenyl)-1-benzofuran-7-yl 2-(4-hydroxyphenyl) ethenyl ketone (**17**), 3-(2,4-dihydroxybenzoyl)-2,3-dihydro-4,6-dihydroxy-2-(4-hydroxyphenyl)-1-benzofuran-7-yl 2-(4-hydroxyphenyl) ethenyl ketone (**18**), lophirone C (**19**), lophirone A (**20**), calodenone (**21**), were isolated from the MeOH extract from the stem barks of *O. integerrima* (Kaewamatawong et al., 2002). This plant was collected from Nakhon Ratchasima Province, Thailand.

In 2006, a new biflavanone A_1 (**22**), and its stereoisomer A_2 (**23**), were isolated from the ethanol (EtOH) extract of the outer barks of *O. integerrima* (Ichino et al., 2006). This plant was collected from Ubon Ratchathani Province, Thailand. Compounds A_1 (**22**) and A_2 (**23**) showed antimalarial activities against multidrug-resistant strain *P. falciparum* (K1) and drug-sensitive strains *P. falciparum* (FCR3)

with IC_{50} values of 0.08, 5.2, and 0.26, 4.5 μg/mL, respectively. The antimalarial activity of **22** against *P. falciparum* was three times more active against K1 than FCR3.

In 2005, six known isoflavones, 5,3',4'-trimethoxy-6,7-methylenedioxy isoflavone (**11**), 5,4'-dimethoxy-6,7-methylenedioxy isoflavone (**12**), 5-hydroxy-4'-methoxy-6,7-methylenedioxy isoflavone (**24**), 3',4'-dimethoxy-6,7-methylenedioxy isoflavone (**25**), 7,4'-dihydroxy-5-methoxy isoflavone (**26**), 7,4'-dihydroxy-5,3'-dimethoxy isoflavone (**27**), were isolated from the MeOH extract from the stem woods of *O. integerrima*. Two known isoflavones, 5,3',4'-trimethoxy-6,7-methylenedioxy isoflavone (**11**), 5,4'-dimethoxy-6,7-methylenedioxy isoflavone (**12**), and five known chalcones, 6'''-hydroxylophirone B (**15**), 3-(2,4-dihydroxybenzoyl)-4,6-dihydroxy-2-(4-hydroxyphenyl)-1-benzofuran-7-yl 2-(4-hydroxyphenyl) ethenyl ketone (**17**), lophirone C (**19**), lophirone A (**20**), calodenone (**21**), were isolated from the MeOH extract from the root barks of *O. integerrima*. Three known isoflavones, 5,3',4'-trimethoxy-6,7-methylenedioxy isoflavone (**11**), 5,4'-dimethoxy-6,7-methylenedioxy isoflavone (**12**), 7,4'-dihydroxy-5-methoxy isoflavone (**26**), and six known chalcones, 6'''-hydroxylophirone B (**15**), 3-(2,4-dihydroxybenzoyl)-4,6-dihydroxy-2-(4-hydroxyphenyl)-1-benzofuran-7-yl 2-(4-hydroxyphenyl) ethenyl ketone (**17**), 3-(2,4-dihydroxybenzoyl)-2,3-dihydro-4,6-dihydroxy-2-(4-hydroxy phenyl)-1-benzofuran-7-yl 2-(4-hydroxyphenyl) ethenyl ketone (**18**), lophirone C (**19**), lophirone A (**20**), calodenone (**21**), were isolated from the MeOH extract from the root woods of *O. integerrima* (Likhitwitayawuid et al., 2005).

In 2024, a new oligostilbenoid, integerrimol A (**28**), and six known oligostilbenoids, hexacosyl ferulate (**29**), balanocarpol (**30**), hopeafuran (**31**), vaticanol B (**32**), diptoindonesin G (**33**), and roxburghiol A (**34**), were isolated from the EtOAc extract of the stems of *O. integerrima* (Chokchaisiri et al., 2024). The cytotoxicity assessment of compounds **28**–**34** against triple-negative breast (MDA-MB231), hepatocellular carcinoma (Huh-7), cholangiocarcinoma (KKU-100), and normal human dermal fibroblasts (NHDF), was conducted using the 3-(4,5-dimethylthiazol-2-yl)-2,5-diphenyltetrazolium bromide assay (MTT), with doxorubicin as the positive control. It was found that compounds **28** and **34** exhibited mild cytotoxic activity against the examined cancer cell lines. Conversely, compounds **29** through **33** manifest negligible activity in terms of suppressing cancer cell proliferation.

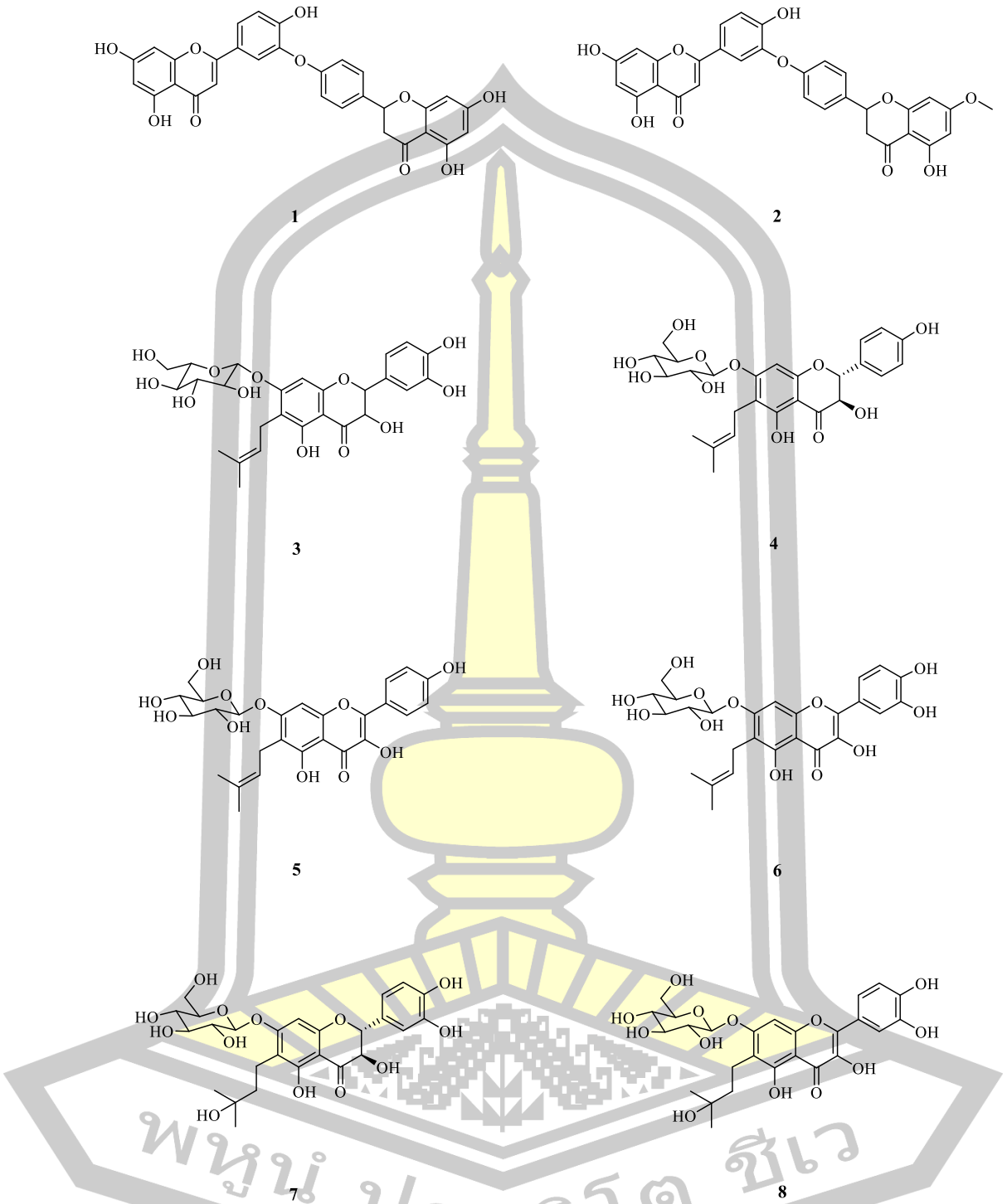

Figure 2. Structures of compounds **1**–**34**.

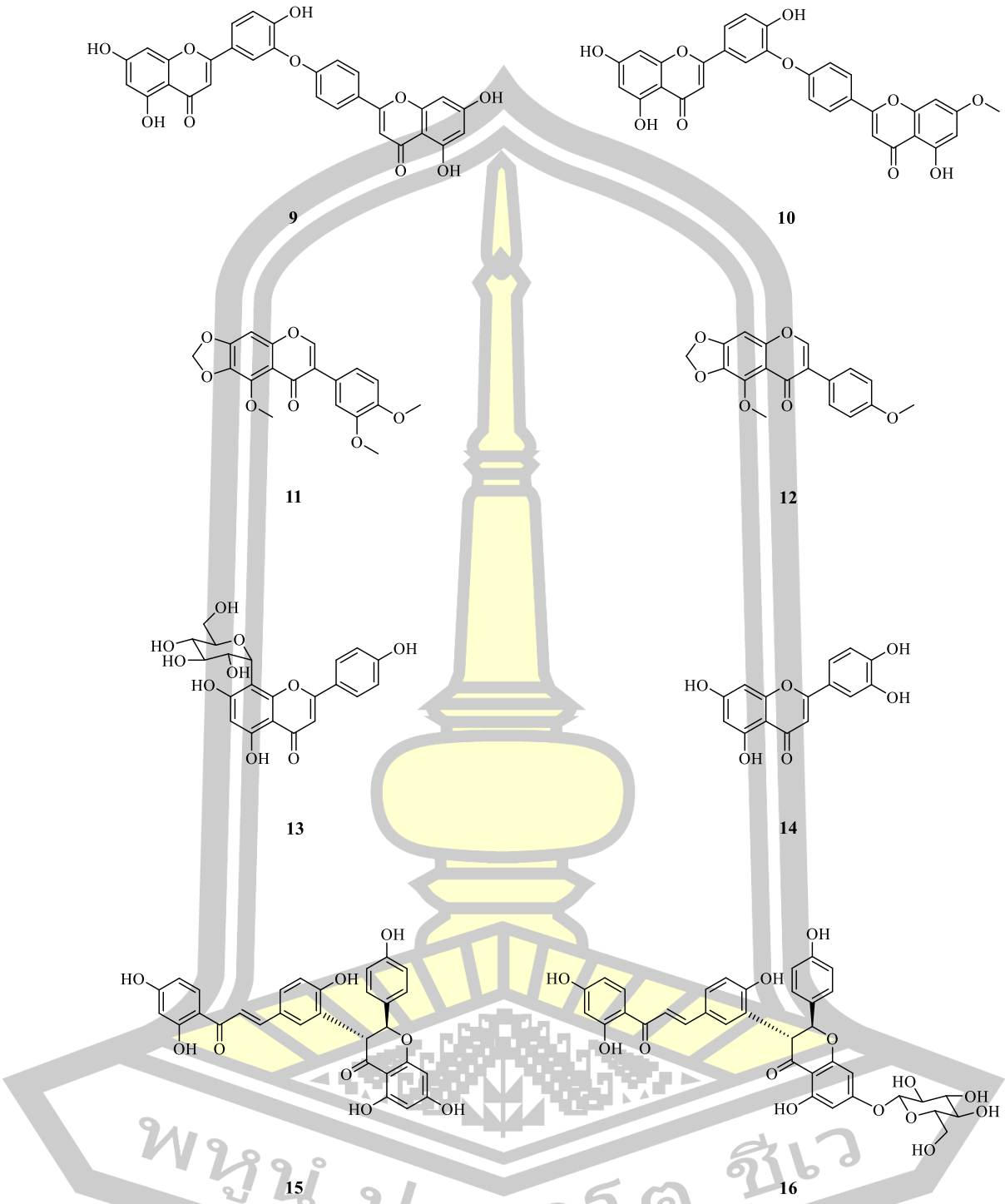

Figure 2 (continued)**.** Structures of compounds **1**–**34**.

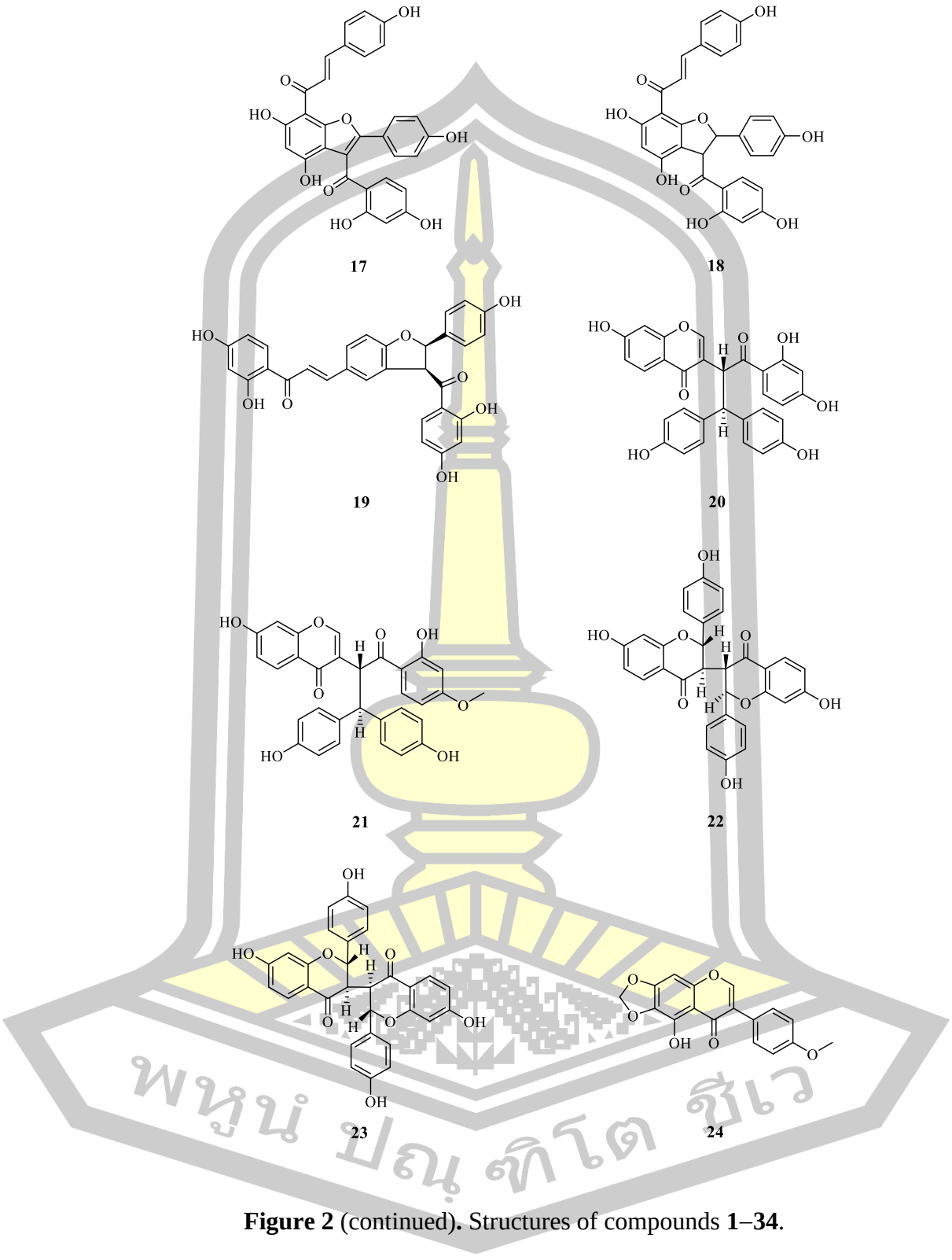

Figure 2 (continued)**.** Structures of compounds **1**–**34**.

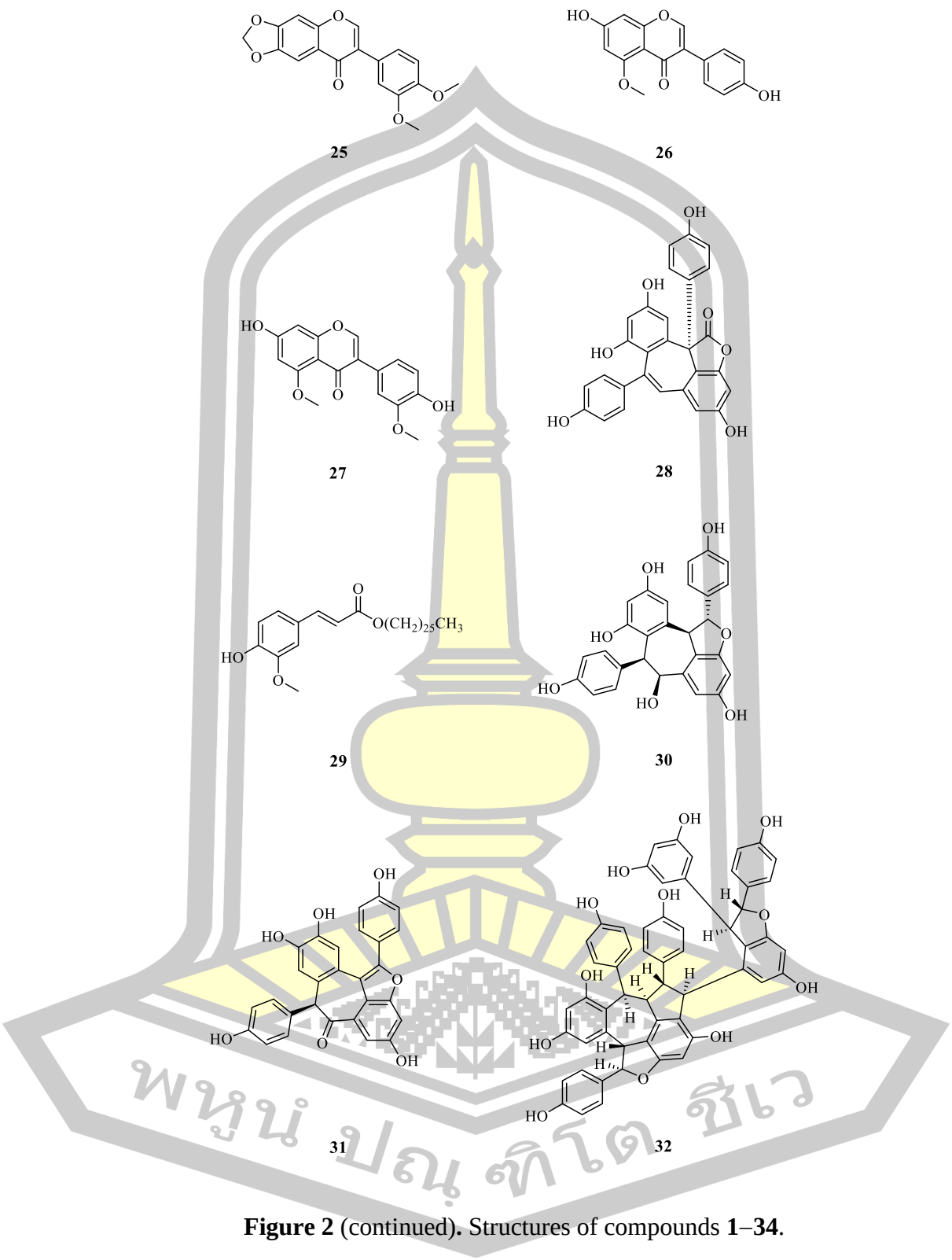

Figure 2 (continued)**.** Structures of compounds **1**–**34**.

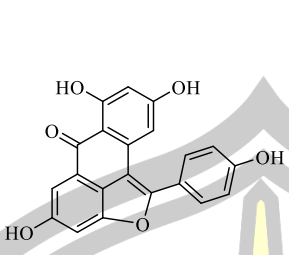

33

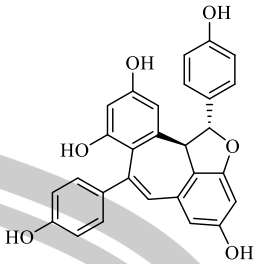

34

Figure 2 (continued)**.** Structures of compounds **1**–**34**.

CHAPTER 3

MATERIALS AND METHODS

3.1. General experimental procedure

Optical rotations were measured using an ADP430 Series polarimeter. Ultraviolet (UV) spectra were recorded on a JASCO V-730 spectrophotometer. Fourier transform infrared (FTIR) spectra were acquired using a Bruker INVENNIO-S spectrometer. Nuclear magnetic resonance (NMR) spectra (^{1}H NMR 400 MHz, ^{13}C NMR 100 MHz) were recorded on a Bruker Ascend-400 (Prodigy unit) with deuterated solvents; deuterated chloroform ($CDCl_3$) (δ_H 7.26/δ_C 77.0 ppm), deuterated methanol (CD_3OD) (δ_H 3.31/δ_C 49.0 ppm), deuterated acetone (acetone-d_6) (δ_H 2.05/δ_C 29.8 ppm), and deuterated dimethylsulphoxide (DMSO-d_6) (δ_H 2.50/δ_C 39.5 ppm). High-resolution electrospray ionization mass (HRESIMS) spectra were measured using a Bruker micrOTOF mass spectrometer. Column chromatography (CC) was performed using silica gel 60 (Merck), silica gel 60H (Merck) and Sephadex LH-20 (Sigma). Pre-coated silica gel 60 F_{254} on Aluminium sheets (Merck) were used for analytical thinlayer chromatography (TLC).

3.2. Plant material

The roots of *O. integerrima* (**Figure 3**), were collected on May 24, 2022, from Walai Rukkhavej Botanical Research Institute (WRBRI), Na Dun District, Maha Sarakham Province, Thailand. The plant samples were authenticated by K. Wongpakam, WRBRI, Mahasarakham University. The voucher specimens of

Wongpakam 19–02 were deposited at WRBRI, Mahasarakham University. The root woods was separated from the root barks, The samples were chopped into small pieces, dried, and then kept in a plastic bag for further extraction.

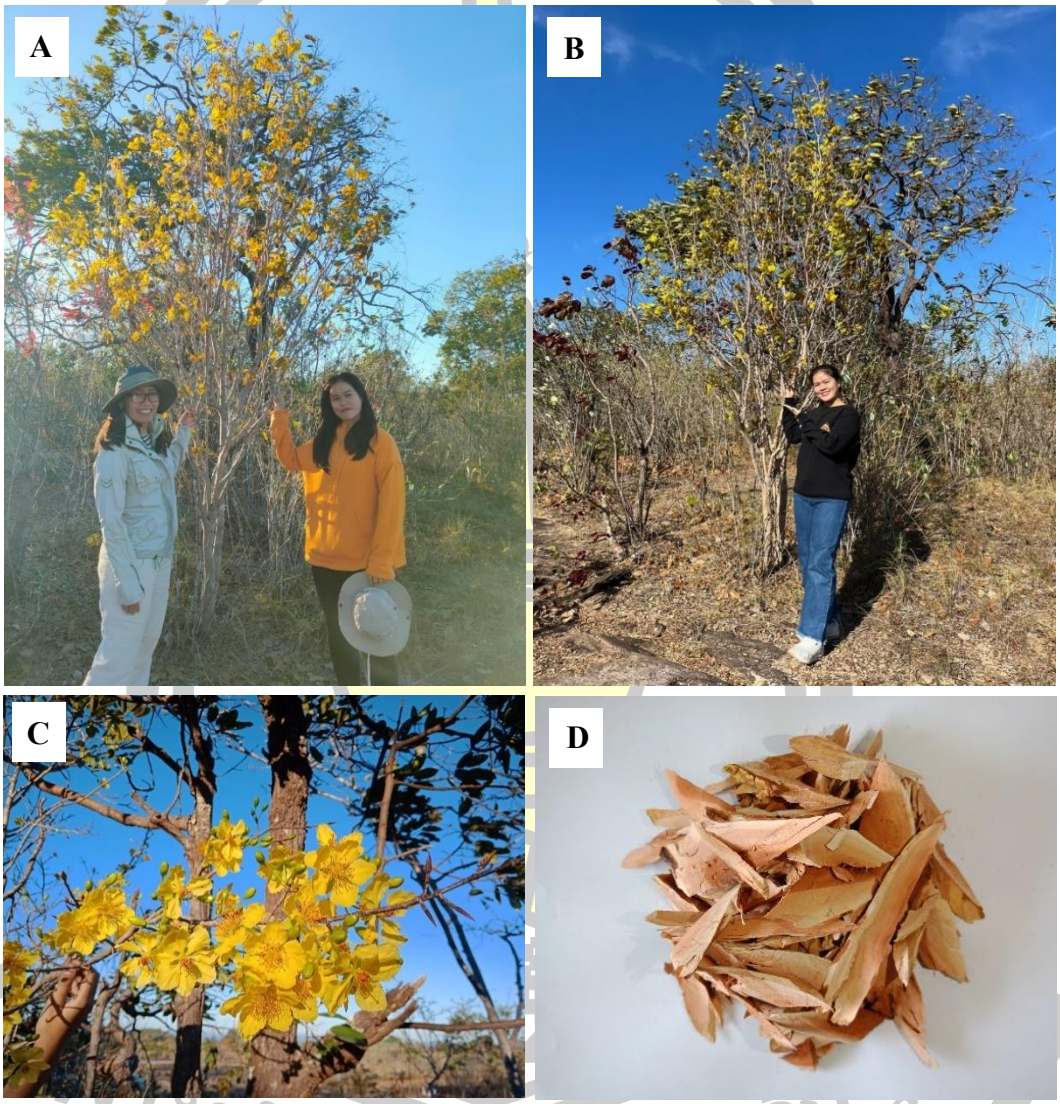

Figure 3. Tree (**A** and **B**), flowers (**C**), root woods (**D**) of *O. integerrima*.

3.3. Extraction

The air-dried root woods of *O. integerrima* (400 g) was cut into small pieces and extracted by refluxing in MeOH (3.5 L, 4 h) (**Figure 4**). After cooling to room temperature, the mixture was filtered by a filter paper and the MeOH solution was evaporated under reduced pressure at 45 ℃ to obtain dark brown gum MeOH extract (13.07 g).

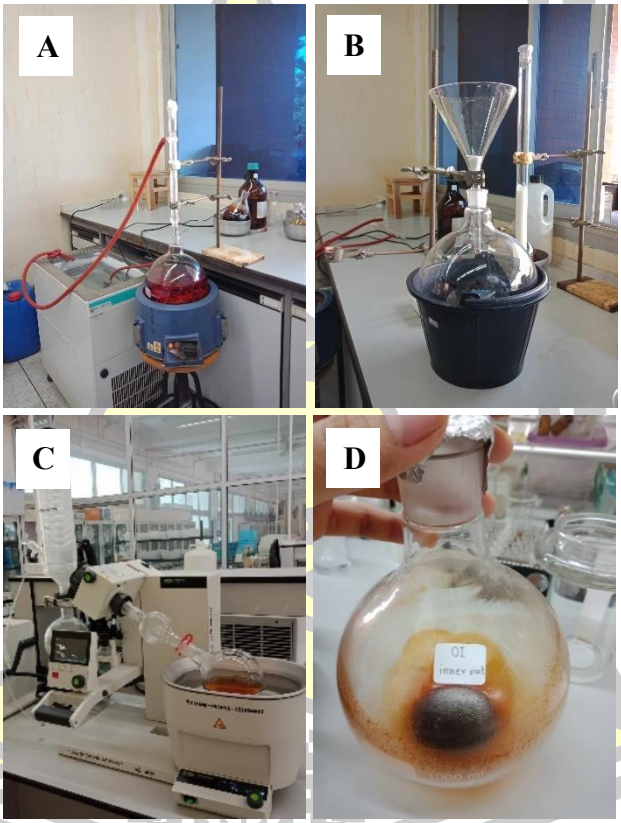

Figure 4. Reflux apparatus (**A**), filtration (**B**), evaporation (**C**), crude MeOH extract (**D**) of the root woods of *O. integerrima*.

3.4. Isolation

Dark brown gum MeOH extract (1 3.07 g) of the root woods which was applied on a silica gel column, eluted with gradient mixtures of hexane–EtOAc from 70:30 to 0:100, and then EtOAc–MeOH, 90:10 to 80:20 to provide four main fractions (Fr.A–D).

Fr.A (141.7 mg) was applied over a silica gel column, eluted with the same mobile phase described above to provide a major subfraction Fr.A1 (69.7 mg) which was further applied on a Sephadex LH-20 column, eluted with MeOH to afford **12** (48.6 mg).

Fr.B (229.2 mg) was applied on a silica gel column, eluted with gradient mixtures of hexane–EtOAc from 70:30 to 0:100, and then EtOAc–MeOH from 90:10 to 80:20 to provide two main subfractions (Fr.B1 and Fr.B2). Fr. B1 (16.7 mg) was purified over Sephadex LH-20 column, eluted with MeOH to yield **12** (2.6 mg). Fr.B2 (52.1 mg) was applied on a silica gel column and eluted with the same eluent described above to provide two main subfractions (Fr.B2a and Fr.B2b). Compound **12** (4.3 mg) was isolated from Fr.B2a (10.2 mg) when **11** (14.2 mg) was obtained from Fr.B2b (32.5 mg) by silica gel column CC.

Fr.C (317.1 mg) was washed with MeOH (5 mL × 2), stirred in a small vial for 15 min, and then filtered. The MeOH soluble portion (Fr.C1) and the residue (Fr.C2) were separated. Fr.C1 (227.5 mg) was applied on a silica gel column, eluted with gradient mixtures of hexane–EtOAc from 70:30 to 0:100, and then EtOAc–MeOH

from 90:10 to 80:20 to provide two main subfractions (Fr.C1a and Fr.C1b). Fr.C1a (97.5 mg) was applied over a silica gel column, eluted with same mobile phase described above to effort **12** (3.2 mg) and **11** (9.9 mg). Fr.C1b (72.7 mg) was applied on a silica gel column, eluted with the same mobile phase described above to yield **36** (2.6 mg), and a main subfraction Fr.C1b1 (37.6 mg) which was subjected to apply on a Sephadex LH-20 column, eluted with MeOH to yield **20** (3.0 mg). Fr.C2 (63.7 mg) was applied over a silica gel, eluted with the same eluent described above to provide a collected fraction which was further purified over Sephadex LH-20 column, eluted with MeOH to yield **27** (21.4 mg).

Fr.D (3.7 g) was applied on a silica gel column, eluted with gradient mixtures of hexane–EtOAc from 70:30 to 0:100, and then EtOAc–MeOH from 90:10 to 80:20 to provide three subfractions (Fr.D1–3). Fr.D1 (35.5 mg) was applied on a silica gel column, eluted with the same eluent described above to provide two main subfractions (Fr.D1a and Fr.D1b). Compound **12** (5.7 mg) was isolated from Fr.D1a (9.5 mg) when **11** (12.7 mg) was obtained from Fr.D1b (18.2 mg) by silica gel CC. Fr.D2 (125.1 mg) was applied over a silica gel column, eluted with the same eluent described above to provide two main subfractions (Fr.D2a and Fr.D2b). Compound **27** (3.9 mg) was obtained from Fr.D2a (40.2 mg) when **26** (3.8 mg) was isolated from Fr.D2b (37.1 mg) by CC of silica gel. Fr.D3 (2.86 g) was applied on a silica gel column, eluted with the same manner of mobile phase described above to provide a main subfraction Fr.D3a (132.7 mg) which was further applied on silica gel column using the same eluent described above. A collected fraction obtained from silica gel

column was subjected to purify over Sephadex LH-20 to yield **35** (10.3 mg) and **13** (7.2 mg).

The isolation of the crude MeOH extract from the root woods of *O. integerrima* is shown in **Flow chart 1**.

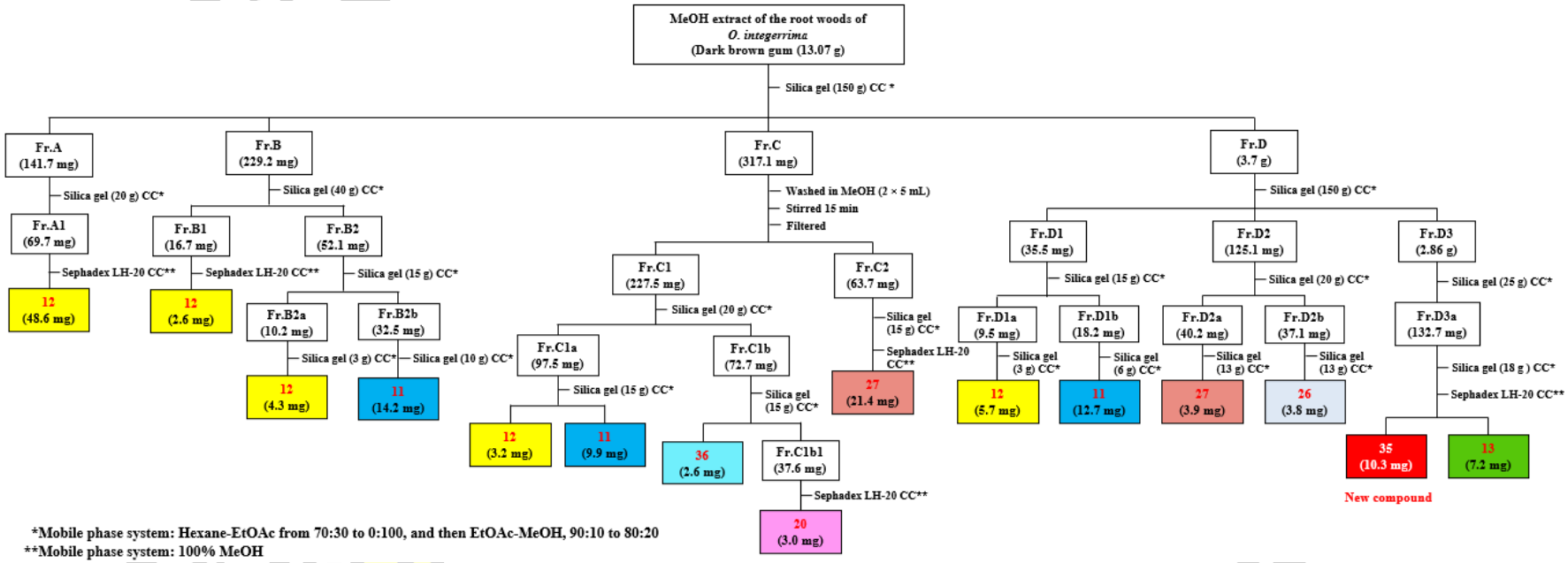

Flow chart 1. Isolation of the crude MeOH extract.

3.5. Structure elucidation

The structures of pure compounds were analyzed by spectroscopic methods (1D and 2D nuclear magnetic resonance (NMR) spectroscopy, mass (MS) spectrometry, infrared (IR) spectroscopy, and ultraviolet-visible (UV-Vis) spectroscopy). Structures of the known compounds were identified and confirmed by the comparison of their spectroscopic data of those reported in literatures.

3.6. Biological activity assay

The antimalarial, antibacterial, and DPPH$^{\bullet}$ radical scavenging activities of the extracts and the isolated pure compounds were evaluated.

3.6.1. Antimalarial activity assay

The antimalarial activity of the samples was tested against a multidrug-resistant *P. falciparum* (K1) reference strain using a standardized fluorescent SYBR Green-based 96-microplate assay (Bennett et al., 2004; Smilkstein et al., 2004). Parasites were cultured according to a reference procedure, (Trager and Jensen, 2005) with slight modifications. Sample solutions were prepared in dimethyl sulfoxide (DMSO) and 50 µL were used for the test. For screening, parasites were treated with 5 µg/mL of the samples (MeOH extract, and **11**–**13**, **26**, **27**, **35**, and **36**), 200 nM artesunate (standard antimalarial drug), or with 0.1% DMSO (control) and then incubated at 37 °C for 72 h under a gas mixture of 5% CO_2, 5% O_2, and 90% N_2. To determine parasite growth inhibition, fluorescence associated with SYBR green-intercalate parasitic deoxyribonucleic acid (DNA) of the samples and control was measured at 490 nm excitation and 540 nm emission using the EnVision Multilabel

Reader. Parasite growth values were normalized to those for the DMSO solvent control. The results are reported as %inhibition. The assays were carried out in triplicate.

$$\%\text{Inhibition} = \frac{(\text{A control} - \text{A sample})}{\text{A control}} \times 100$$

Human blood used in this study was performed under the human use protocol TMEC 18–004, approved by the Institute Ethical Review Committee of the Faculty of Tropical Medicine, Mahidol University, Bangkok, Thailand. *P. falciparum* K1 strain, a chloroquine- and pyrimethamine-resistant strain isolated in Thailand was used (Thaithong et al., 1983).

3.6.2. Antibacterial activity assay

3.6.2.1. Bacterial strains and cultivation

The antibacterial activity of samples was assayed against three Gram-positive bacteria, methicillin-susceptible *Staphylococcus aureus* (MSSA) DMST 2933, methicillin-resistant *S. aureus* (MRSA) DMST 20651 and *Bacillus cereus* 11778. The selected strain was cultured on Mueller Hinton Agar (MHA) medium at 37 °C for 16–18 h.

3.6.2.2. Agar well diffusion method

The agar well diffusion method was performed to determine the antibacterial activity of the samples (Sangdee et al., 2018). The sample solutions

(50 mg/mL) were added to each well (0.1 mL per well). The zone of inhibition was measured after 16–18 h incubation of the plates at 37 ℃. The negative controls of 10% (v/v) methanol and 10% DMSO were used. A standard positive control was tetracycline (250 μg/mL).

3.6.2.3. MIC and MBC determination

The minimum inhibitory concentration (MIC) and minimum bactericidal concentration (MBC) values were investigated using the microdilution method (Sangdee et al., 2018). MICs were determined by identifying the solutions that were clear after incubation compared with the control well. MBCs were determined by transferring bacterial suspensions from the MIC assay onto MHA plates. The MBC referred to the lowest concentration that showed no growth after 24 h incubation. A reference standard antibiotic tetracycline (250 μg/mL) was used in the study.

3.6.3. DPPH radical scavenging activity assay

DPPH radical scavenging activity assay was performed as previously described by Promden (Promden et al., 2024). Briefly, 20 μL of each sample solution (1 mg/mL in DMSO) was mixed with 180 μL of DPPH solution (100 μM in MeOH) in a 96-well microplate. The mixture was incubated at 37 ℃ for 30 min in the dark. The absorbance (A) of the samples and control was measured at 515 nm using the FLUOstar® Omega plate reader. The DPPH radical scavenging activity was calculated in term of %radical scavenging activity (%RSA). For the active samples, the scavenging concentration at 50% (SC_{50}) was determined using a calibration curve

within the linear range, plotting concentrations against %RSA. The experiments were performed in triplicate and reported as average ± standard deviation (SD). Ascorbic acid was used as a standard compound.

$$\%RSA = \frac{(A\ control - A\ sample)}{A\ control} \times 100$$

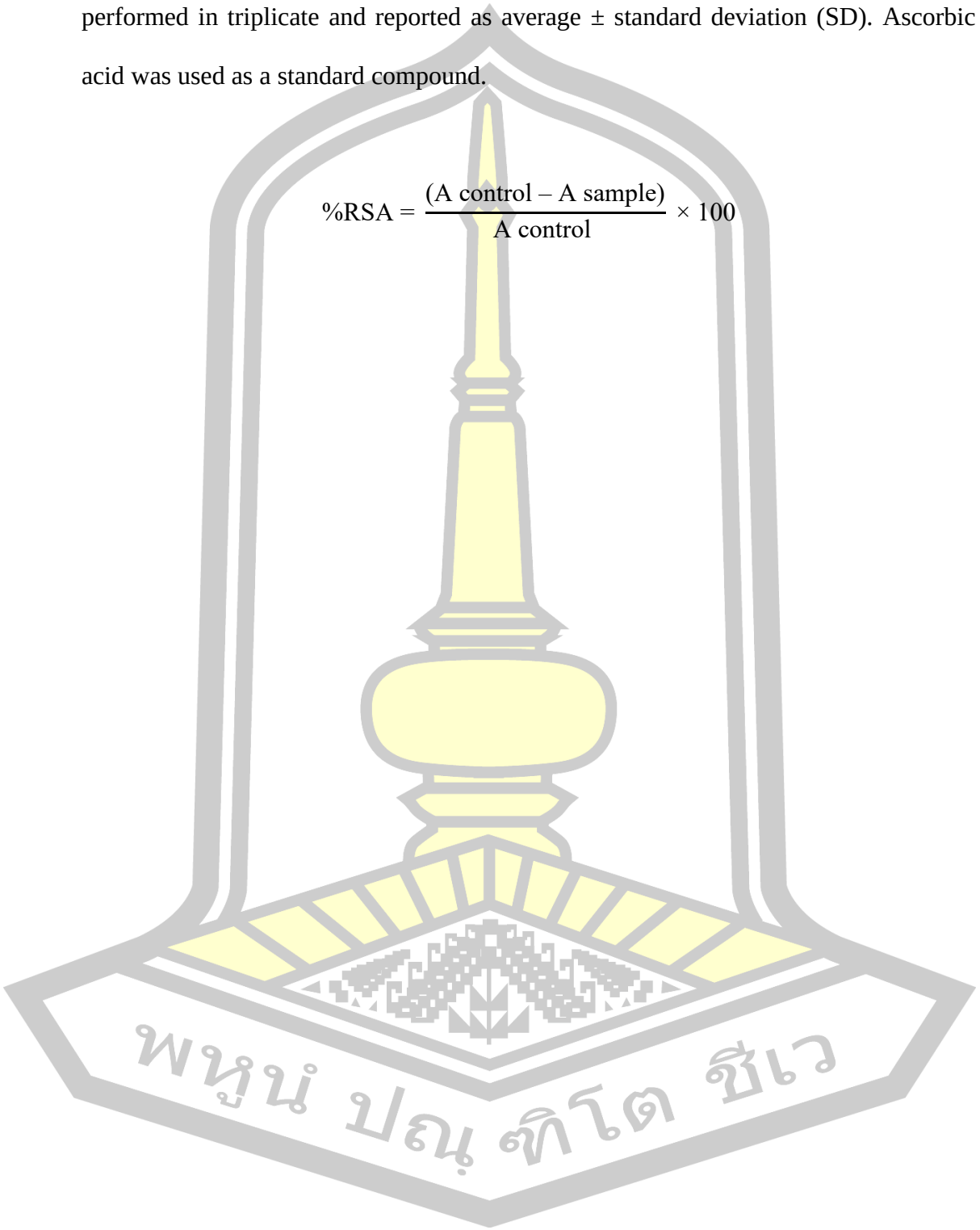

CHAPTER 4

RESULTS AND DISCUSSION

4.1. Biological activities of the crude MeOH extract and the main fractions

The crude MeOH extract of the root woods of *O. integerrima* and the isolated main fractions (Fr.A–D) were tested for their antimalarial activity against the chloroquine- and pyrimethamine-resistant strain of *P. falciparum* (K1), antibacterial activity assay toward three Gram-positive bacteria, methicillin-susceptible *S. aureus* (MSSA), methicillin-resistant *S. aureus* (MRSA), and *B. cereus*, and DPPH$^{\bullet}$ radical scavenging activity. The results are shown in **Table 1**.

Table 1. Biological activities of crude MeOH extract and the main fractions.

Sample	Antimalarial activity (%inhibition)	Antibacterial activity (MIC/MBC; mg/mL)			DPPH$^{\bullet}$ scavenging activity (%RSA)
		S. aureus (MSSA)	*S. aureus* (MRSA)	*B. cereus*	
MeOH extract	26.67	>25.00/>25.00	>25.00/>25.00	>25.00/>25.00	62.70 ± 1.4
Fr.A	38.22	NT	NT	NT	NT
Fr.B	37.21	>5.00/>5.00	>5.00/>5.00	>5.00/>5.00	NT
Fr.C	100	>5.00/>5.00	>5.00/>5.00	>5.00/>5.00	NT
Fr.D	22.57	5.00/>5.00	5.00/>5.00	>5.00/>5.00	NT

NT = Not teste

Among the isolated fractions (Fr.A–D), Fr.C exhibited the most potent antimalarial activity of 100% inhibition at 5 μg/mL on the screening assay. The MeOH extract showed weak antimalarial activity against *P. falciparum* (K1) of 26.7% inhibition at 5 μg/mL. This extract displayed good DPPH$^{\bullet}$ radical scavenging activity of 62.70% at 50 μg/mL.

4.2. Isolation of the crude MeOH extract

Phytochemical investigation of the crude MeOH extract of the root woods of *O. integerrima* furnished an unreported isoflavone glycoside, gerontoisoflavone A-4'-*O*-*β*-D-xylopyranoside (**35**), together with the seven known compounds, the structure of the previously reported **11**–**13**, **20**, **26**, **27**, and **36** were elucidated by comparison of their ^{1}H and ^{13}C NMR as well as other physical data with those reported in the literature. These compounds were identified as iriskumaonin methyl ether (**11**) (Veitch et al., 2003), irisolone methyl ether (**12**) (Veitch et al., 2003), a flavone glycoside, vitexin (**13**) (Choo et al., 2012), a chromone derivative, lophilone A (**20**) (Ghogomu et al., 1987), isoprunetin (**26**) (Kerkatou et al., 2013), gerontoisoflavone A (**27**) (Chang et al., 1995), and iriskumaonin (**36**) (Kalla et al., 1978) (**Figure 5**).

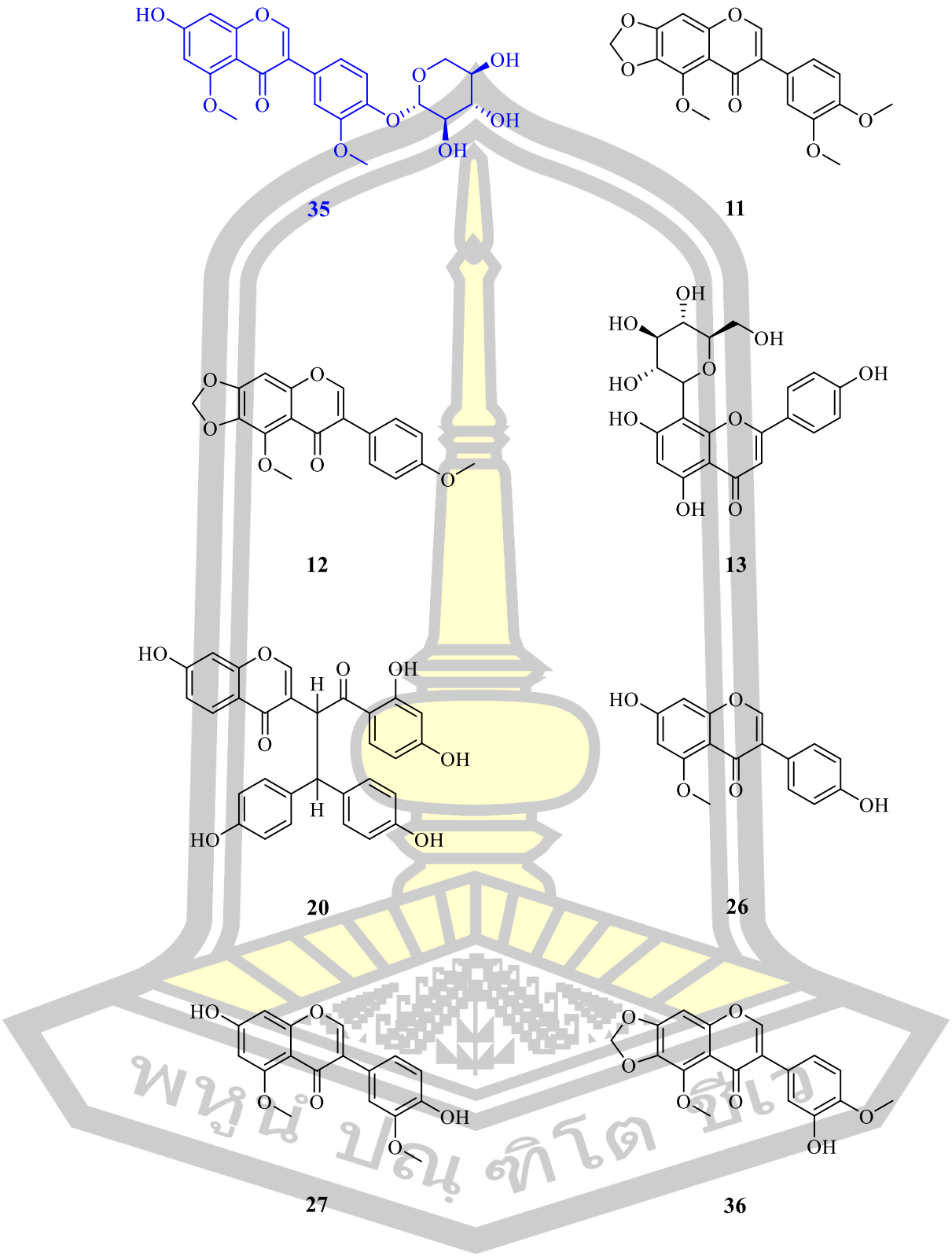

Figure 5. Structures of compounds **11**–**13**, **20**, **26**, **27**, **35**, and **36**.

4.3. Structural elucidation

4.3.1. Gerontoisoflavone A-4'-*O*-*β*-D-xylopyranoside (**35**)

Compound **35** was isolated as a colorless amorphous solid. Its molecular formula $C_{22}H_{22}O_{10}$ was determined based on HRESIMS *m/z* 469.1109 $[M+Na]^+$ (calcd for $C_{22}H_{22}O_{10}Na$, 469.1105 (**Figure A25**). The IR spectrum revealed the presence of hydroxyl (3439 cm^{-1}), conjugated carbonyl (1630 cm^{-1}), aromatic (1574, 1513, 1464 cm^{-1}) and C–O (1305, 1263, 1201 cm^{-1}) (**Figure A26**). The UV spectrum showed characteristic absorptions of the flavonoid scaffold at 254 and 285 nm (**Figure A27**). Analysis of the ^1H and ^{13}C NMR, DEPT spectra, together with HSQC correlations, revealed the presence of a flavonoid aglycone and sugar moiety. The ^1H NMR spectrum of **35** displayed an olefinic singlet at δ_H 8.15 (δ_C 151.1), characteristic of the proton at C-2 of the isoflavone skeleton (**Table 2** and **Figures A3**–**A6**). The ^{13}C NMR spectrum, in combination with DEPT and HSQC spectra, revealed, in addition to the fifteen carbons of the C6–C3–C6 unit of the isoflavone, i. e. a conjugated carbonyl carbon (δ_C 173.7), eight tetrasubstituted non-protonated sp^2 carbons (δ_C 162.5, 161.2, 159.1, 148.8, 145.7, 126.5, 124.3, 107.8), six protonated sp^2 carbons (δ_C 151.1, 121.2, 115.8, 113.8, 96.5, 94.8), five carbons of a pentose sugar unit (δ_C 100.9 CH, 76.5 CH, 73.0 CH, 69.4 CH, 65.7 CH_2) (**Table 2** and **Figures A7**–**A11**, and **A13**–**A16**). Based on HMBC and COSY correlations, the structures of the isoflavone and the sugar moiety were established (**Figures 6** and **7**). The substitution pattern of the A-ring was deduced from the presence of two doublets of two *meta*-coupled aromatic protons at δ_H 6.41 (J = 2.2 Hz, H-8/δ_C 94.8) and δ_H 6.39 (J = 2.2 Hz, H-6/δ_C 96.5), and HMBC correlations from these two protons to C-4a (δ_C 107.8). The presence of a methoxy

group at C-5 was supported by HMBC correlations from the methoxy singlet at δ_H 3.80 (5-OMe/δ_C 55.7) to C-5 (δ_C 161.2), and H-6 to C-5, as well as by the NOESY correlation between 5-OMe and H-6 (**Table 2** and **Figure 8**). That the B-ring is 1,3,4-trisubstituted was evidenced by the presence of two doublets at δ_H 7.14, J = 2.0 Hz, H-2'/δ_C 113.8) and δ_H 7.06 (J = 8.5 Hz, H-5'/δ_C 115.8), and a double of doublet at δ_H 6.98 (J = 8.5, 2.0 Hz, H-6'/δ_C 121.2). This was supported by HMBC correlations from H-2' to C-3 (δ_C 126.5) and H-2 (δ_H 8.15/δ_C 151.1) to C-1' (δ_C 124.3). The HMBC correlation from 3'-OCH_3 at δ_H 3.78, s (δ_C 55.9) to C-3' (δ_C 148.8), aligned with the NOESY correlation between 3'-OCH_3 and H-2', confirmed the position of this methoxy group on the B-ring (**Table 2** and **Figure 8**). The HBMC correlations from H-2 to C-8a, C-1', C-4 (δ_C 173.7) and C-3 (δ_C 126.5) confirmed the structure of an isoflavone in **35** as gerontoisoflavone A, and its ^{1}H and ^{13}C NMR data were in agreement with those reported for gerontoisoflavone A (in DMSO-d_6) (Chang et al., 1995). Moreover, gerontoisoflavone A (**27**) was also co-isolated from this extract. The sugar moiety was identified as a pentopyranose on the basis of the difference between the molecular formula of **35** and its aglycone portion, as well as by HMBC correlations from the anomeric proton, H-1" (δ_H 4.92, d, J = 7.1 Hz/δ_C 100.9) to C-3" (δ_C 76.5) and C-5" (δ_C 65.7) (**Table 2** and **Figure 6**). The structure of the pentopyranose in **35** was identified as β-D-xylopyranose by comparison of its ^{13}C chemical shift values with those reported for the sugar moiety of luteolin 7-*O*-xyloside (in DMSO-d_6) (Gulluce et al., 2012; Lin et al., 2003). That the β-D-xylopyranose is connected to gerontoisoflavone A, through the oxygen bridge, between C-1" of the former and C-4' of the latter was substantiated by HMBC correlation from H-1" to C-4' (**Figure 6**). Therefore, **35** was elucidated as

gerontoisoflavone A-4'-*O*-*β*-D-xylopyranoside. To the best of our knowledge, the structure of **35** has never been previously reported. Although a number of flavonoid glycosides have been previously reported from *O. integerrima* (Buranasudja et al., 2022; Reutrakul et al., 2007; Kaewamatawong et al., 2002; Likhitwitayawuid et al., 2001) only glucopyranose was found to be a sugar moiety of the glycosides. Therefore, **35** is an undescribed isoflavone glycoside whose sugar moiety is a xylopyranose. The NMR spectroscopic data (^{1}H NMR in DMSO-d_6, and CD_3OD, and ^{13}C NMR in DMSO-d_6) of **35** is shown in **Table 3**. The ^{1}H NMR spectra of **35** in CD_3OD is shown in **Figures A22**–**A24**.

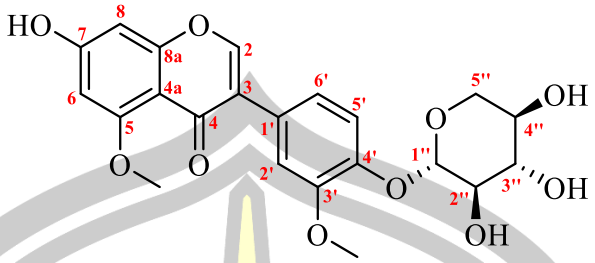

Table 2. ^{1}H, ^{13}C, and 2D NMR spectroscopic data of **35** in DMSO-d_6.

Position	δ_H, mult. (J in Hz)	δ_C	COSY	NOESY	HMBC
2	8.15, s	151.1		2′, 6′	3, 4, 8a, 1′
3		126.5			
4		173.6			
4a		107.8			
5		161.2			
6	6.39, d (2.2)	96.5		5-OCH_3	5, 7, 8, 4a
7		162.5			
8	6.41, d (2.2)	94.8			6, 7, 4a, 8a
8a		159.1			
1′		124.3			
2′	7.14, d (2.0)	113.8	5′, 6′	2, 3′-OCH_3	3, 1′, 3′, 4′, 6′
3′		148.8			
4′		145.7			
5′	7.06, d (8.5)	115.8	2′, 6′	1″	3, 3′, 4′
6′	6.98, dd (8.5, 2.0)	121.2	2′, 5′	2	1′, 2′, 4′
1″	4.92, d (7.1)	100.9	2″	5′, 5″	4′
2″	3.29, m	73.0	1″	5″	
3″	3.29, m	76.5	2″	2″-OH	
4″	3.29, m	69.4	5″, 3″		
5″	3.72, dd (11.2, 5.1)	65.7	4″	1″, 2″	1″, 4″
	3.29, m				1″, 3″, 4″
7-OH	10.73, s				
2″-OH	5.28, d (5.0)			4″-OH	1″, 2″, 3″
3″-OH	5.09, d (4.4)				2″
4″-OH	5.05, d (4.8)			2″-OH	3″, 5″
5-OCH_3	3.80, s	55.7		6	5
3′-OCH_3	3.78, s	55.9		2′	3′

Calibration of DMSO-d_6 δ_H 2.50/δ_C 39.5.

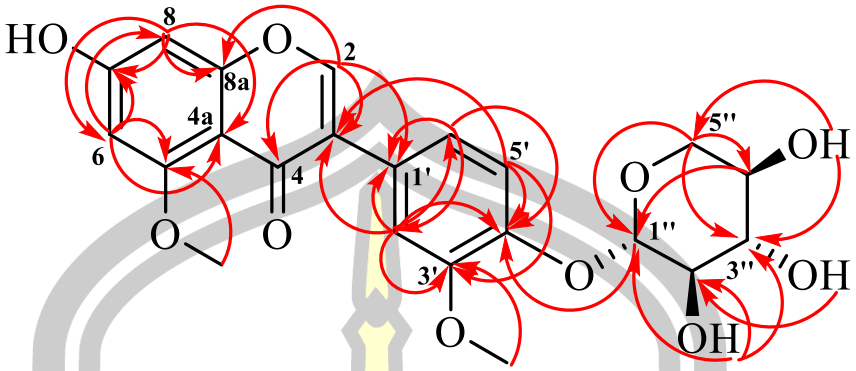

Figure 6. HMBC correlations of **35**.

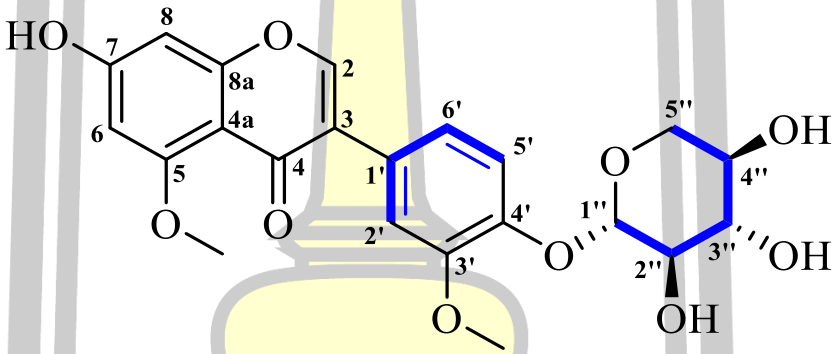

Figure 7. COSY correlations of **35**.

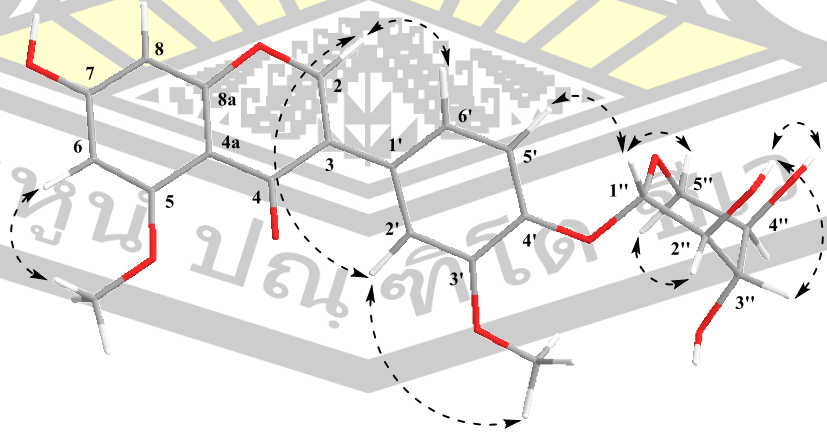

Figure 8. NOESY correlations of **35**.

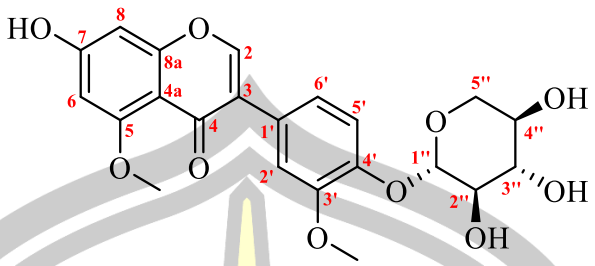

Table 3. ^{1}H and ^{13}C NMR spectroscopic data of **35** in DMSO-d_6 and CD_3OD.

Position	**35**[a] (DMSO-d_6)		**35**[b] (CD_3OD)
	δ_H, mult. (*J* in Hz)	δ_C	δ_H, mult. (*J* in Hz)
2	8.15, s	151.1	8.02, s
3		126.5	
4		173.6	
4a		107.8	
5		161.2	
6	6.39, d (2.2)	96.5	6.42, s
7		162.5	
8	6.41, d (2.2)	94.8	6.42, s
8a		159.1	
1′		124.3	
2′	7.14, d (2.0)	113.8	7.23, d (2.0)
3′		148.8	
4′		145.7	
5′	7.06, d (8.5)	115.8	7.12, d (8.4)
6′	6.98, dd (8.5, 2.0)	121.2	7.02, dd (8.4, 2.0)
1″	4.92, d (7.1)	100.9	4.91, d (7.2)
2″	3.29, m	73.0	3.35–4.59, m
3″	3.29, m	76.5	3.35–4.59, m
4″	3.29, m	69.4	3.35–4.59, m
5″	3.72, dd (11.2, 5.1)	65.7	3.35–4.59, m
	3.29, m		3.35–4.59, m
7-OH	10.73, s		
2″-OH	5.28, d (5.0)		
3″-OH	5.09, d (4.4)		
4″-OH	5.05, d (4.8)		
5-OCH_3	3.80, s	55.7	3.90, s
3′-OCH_3	3.78, s	55.9	3.89, s

[a]Calibration of DMSO-d_6 δ_H 2.50/δ_C 39.5; [b]Calibration of CD_3OD δ_H 3.31.

4.3.2. Iriskumaonin methyl ether (**11**)

Compound **11** ($C_{19}H_{16}O_7$) was isolated as a colorless needle solid. Based on spectroscopic data compared with those reported in the literature, **11** was identified as iriskumaonin methyl ether (Veitch et al., 2003). The NMR spectroscopic data (^{1}H and ^{13}C NMR in $CDCl_3$) of **11** is shown in **Table 4**. The NMR spectra of **11** are shown in **Figures A28**–**A32**.

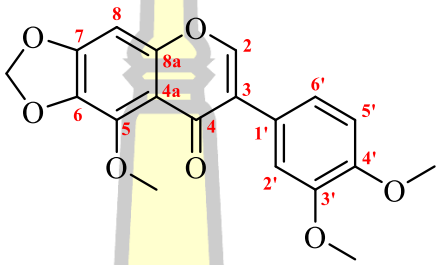

Table 4. ^{1}H and ^{13}C NMR spectroscopic data of **11** compared with literature in $CDCl_3$.

Position	**11**[a]		Iriskumaonin methyl ether[b]	
	δ_H, mult. (*J* in Hz)	δ_C	δ_H, mult. (*J* in Hz)	δ_C
2	7.80, s	150.4	7.78, s	150.4
3		125.4		125.4
4		175.5		175.4
4a		113.8		113.9
5		141.7		141.8
6		135.5		135.5
7		152.8		152.8
8	6.64, s	93.2	6.62, s	93.2
8a		154.7		154.7
1'		124.6		124.7
2'	7.19, d (2.0)	112.8	7.18, d (2.0)	113.0
3'		148.7		148.8
4'		149.0		149.1
5'	6.90, d (8.3)	111.0	6.89, d (8.3)	111.2
6'	7.01, dd (8.3, 2.0)	121.3	7.00, dd (8.3, 2.0)	121.4
OCH_2O	6.07, s	102.2	6.05, s	102.2
5-OCH_3	4.09, s	61.3	4.08, s	61.2
3'-OCH_3	3.92, s	56.0	3.91, s	56.1
4'-OCH_3	3.90, s	55.9	3.89, s	56.0

[a]Calibration of $CDCl_3$ δ_H 7.26/δ_C 77.0; [b]Veitch et al. 2003.

4.3.3. Irisolone methyl ether (**12**)

Compound **12** ($C_{18}H_{14}O_6$) was isolated as a brown amorphous solid. Based on spectroscopic data compared with those reported in the literature (**Table 5**), **12** was identified as irisolone methyl ether (Veitch et al., 2003). The NMR spectroscopic data (1D and 2D NMR in $CDCl_3$) of **12** is shown in **Table 6**. HMBC, COSY, and NOESY correlations of **12** are shown in **Figures 9**–**11**. The NMR spectra of **12** are shown in **Figures A33**–**A44**.

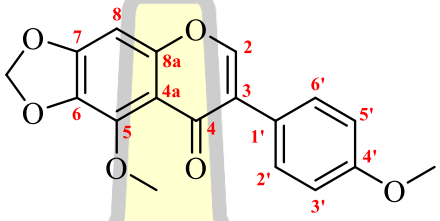

Table 5. ^{1}H and ^{13}C NMR spectroscopic data of **12** compared with literature in $CDCl_3$.

Position	**12**[a]		Irisolone methyl ether[b]	
	δ_H, mult. (*J* in Hz)	δ_C	δ_H, mult. (*J* in Hz)	δ_C
2	7.77, s	150.2	7.77, s	150.2
3		125.3		125.4
4		175.5		175.4
4a		113.8		114.0
5		141.6		141.8
6		135.5		135.6
7		152.8		152.8
8	6.62, s	93.2	6.63, s	93.3
8a		154.7		154.8
1′		124.1		124.2
2′/6′	7.46, d (8.8)	130.3	7.47, d (8.8)	130.4
3′/5′	6.94, d (8.8)	113.8	6.94, d (8.8)	113.9
4′		159.5		159.6
OCH_2O	6.06, s	102.1	6.06, s	102.2
5-OCH_3	4.08, s	61.2	4.08, s	61.3
4'-OCH_3	3.82, s	55.3	3.83, s	55.4

[a]Calibration of $CDCl_3$ δ_H 7.26/δ_C 77.0; [b]Veitch et al. 2003.

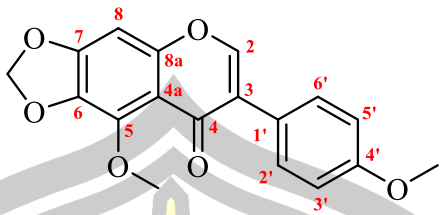

Table 6. ^{1}H, ^{13}C, and 2D NMR spectroscopic data of **12** in $CDCl_3$.

Position	δ_H, mult. (*J* in Hz)	δ_C	COSY	NOESY	HMBC
2	7.77, s	150.2		2′, 6′	3, 4, 8a, 1′
3		125.3			
4		175.5			
4a		113.8			
5		141.6			
6		135.5			
7		152.8			
8	6.62, s	93.2			4, 6, 7, 4a, 8a
8a		154.7			
1′		124.1			
2′/6′	7.46, d (8.8)	130.3	3′, 5′	2, 3′, 5′	3, 2′, 4′, 6′
3′/5′	6.94, d (8.8)	113.8	2′, 6′	2′, 6′, 4′-OCH_3	1′, 3′, 4′, 5′
4′		159.5			
OCH_2O	6.06, s	102.1			6, 7
5-OCH_3	4.08, s	61.2			5
4'-OCH_3	3.82, s	55.3		3′	4′

Calibration of $CDCl_3$ δ_H 7.26/δ_C 77.0.

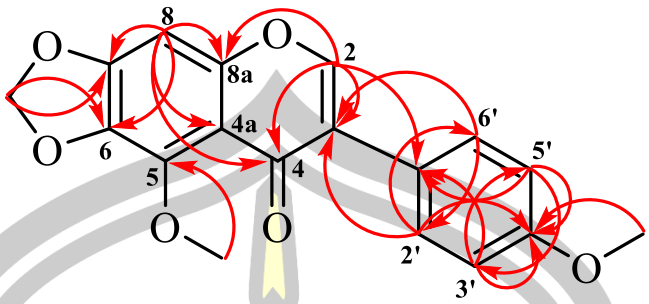

Figure 9. HMBC correlations of **12**.

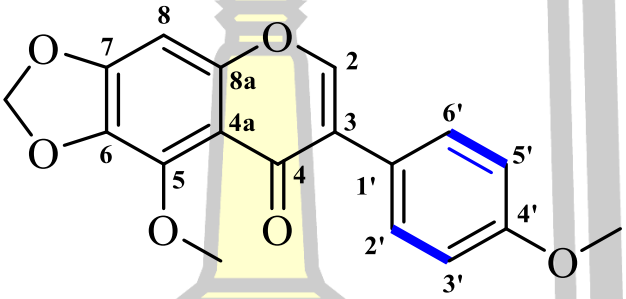

Figure 10. COSY correlations of **12**.

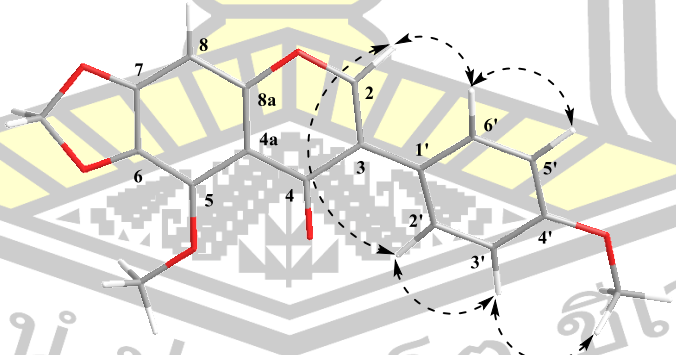

Figure 11. NOESY correlations of **12**.

4.3.4. Vitexin (**13**)

Compound **13** ($C_{21}H_{20}O_{10}$) was isolated as a yellow amorphous solid. Based on spectroscopic data compared with those reported in the literature (**Table 7**), **13** was identified as vitexin (Choo et al., 2012). The NMR spectroscopic data (1D and 2D NMR in DMSO-d_6) of **13** is shown in **Table 8**. HMBC, COSY, and NOESY correlations of **13** are shown in **Figures 12**–**14**. The NMR spectra of **13** are shown in **Figures A45**–**A59**.

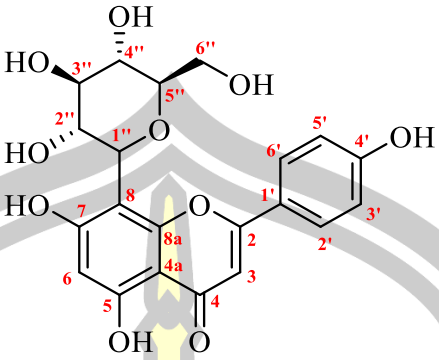

Table 7. ^{1}H and ^{13}C NMR spectroscopic data of **13** compared with literature in DMSO-d_6.

Position	**13**[a]		Vitexin[b]	
	δ_H, mult. (*J* in Hz)	δ_C	δ_H, mult. (*J* in Hz)	δ_C
2		163.9		164.3
3	6.78, s	102.4	6.7, s	102.8
4		182.0		182.4
4a		104.0		104.3
5		160.4		161.5
6	6.26, s	98.2	6.2, s	98.6
7		162.7		161.5
8		104.5		105.0
8a		156.0		156.4
1'		121.6		122.0
2'/6'	8.02, d (8.2)	128.9	8.0, d (7.2)	129.3
3'/5'	6.89, d (8.5)	115.8	6.9, d (8.5)	116.2
4'		161.1		160.8
1"	4.69, d (9.7)	73.4	4.9, d (8.5)	73.8
2"	3.84, m	70.8	3.1–3.9	71.3
3"	3.25, m	78.6	3.1–3.9	79.1
4"	3.37, m	70.5	3.1–3.9	70.9
5"	3.24, m	81.8	3.1–3.9	82.2
6"	3.75, m	61.2	3.1–3.9	61.7
	3.52, m		3.1–3.9	
5-OH	13.16, s			
7-OH	10.36, br s			
2″-OH	4.98, d (4.2)			
3″-OH	5.00, d (5.3)			
4″-OH	4.60, s			
6″-OH	4.60, s			

[a]Calibration of DMSO-d_6 δ_H 2.50/δ_C 39.5; [b]Choo et al. 2012.

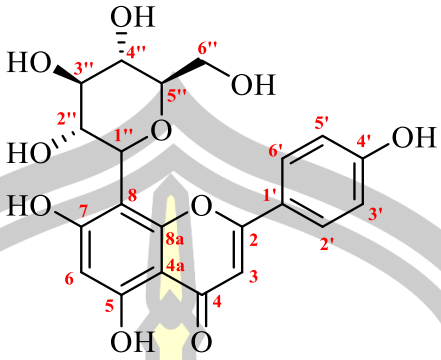

Table 8. ^{1}H, ^{13}C, and 2D NMR spectroscopic data of **13** in DMSO-d_6.

Position	δ_H, mult. (J in Hz)	δ_C	COSY	NOESY	HMBC
2		163.9			
3	6.78, s	102.4		2′, 6′	2, 4, 1'
4		182.0			
4a		104.0			
5		160.4			
6	6.26, s	98.2			5, 7, 8
7		162.7			
8		104.5			
8a		156.0			
1'		121.6			
2'/6'	8.02, d (8.2)	128.9	3′, 5′	3, 3′, 5′	2, 2', 4', 6'
3'/5'	6.89, d (8.5)	115.8	2′, 6′	2′, 6′	1', 3', 4', 5'
4'		161.1			
1"	4.69, d (9.7)	73.4	2"		8, 8a
2"	3.84, m	70.8	1", 3"		1", 3"
3"	3.25, m	78.6	2"		
4"	3.37, m	70.5		3″-OH	
5"	3.24, m	81.8	6"		
6"	3.75, m	61.2	5"		
	3.52, m				
5-OH	13.16, s				6, 4a
7-OH	10.36, br s				
2″-OH	4.98, d (4.2)			4″-OH	
3″-OH	5.00, d (5.3)				2", 5"
4″-OH	4.60, s			2″-OH	
6″-OH	4.60, s				

Calibration of DMSO-d_6 δ_H 2.50/δ_C 39.5.

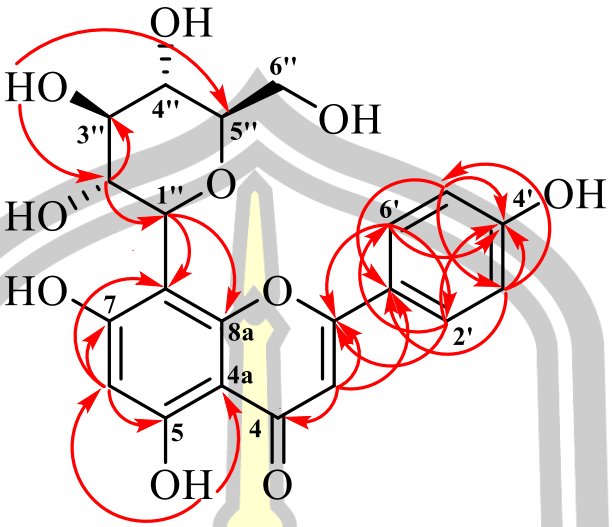

Figure 12. HMBC correlations of **13**.

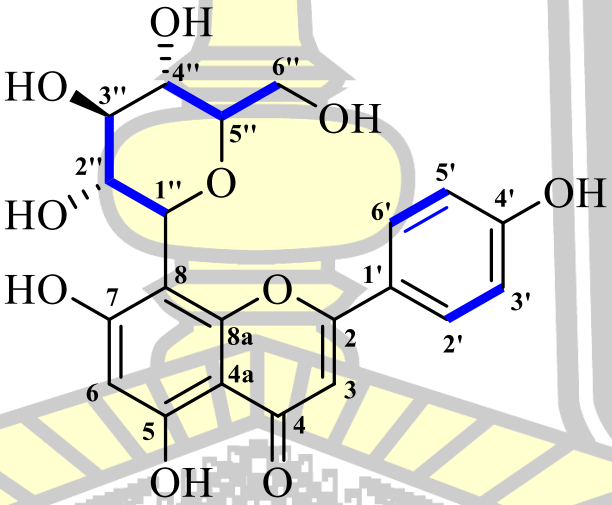

Figure 13. COSY correlations of **13**.

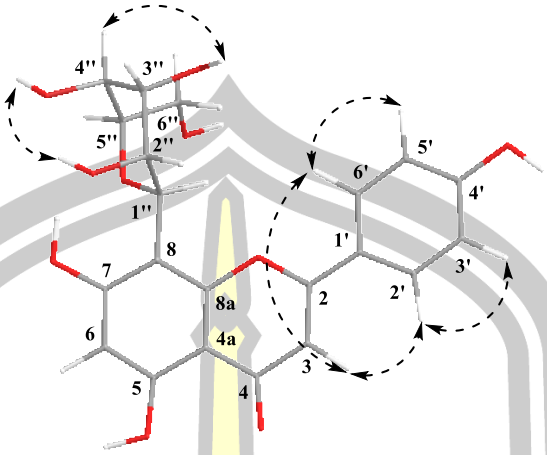

Figure 14. NOESY correlations of **13**.

4.3.5. Lophilone A (**20**)

Compound **20** ($C_{30}H_{22}O_8$) was isolated as a white amorphous solid and the first reported from the stem bark of *Liphira lanceolata* (Ochnaceae) (Ghogomu et al., 1987). The ^{1}H and ^{13}C NMR data (in acetone-d_6) of **20** were similar to those reported for lophilone A in the literature (**Table 9**) (Ghogomu et al., 1987). The *trans*-configuration between H-9 (δ_H 6.13, d, J = 12.3 Hz/δ_C 43.9) and H-17 (δ_H 4.78, d, J = 12.3 Hz/δ_C 53.4) in **20** is consistent with that reported in the literature (Ghogomu et al., 1987). However, **20** displayed opposite signs of optical rotation ($[\alpha]^{26}_D$ = -2.3 (c = 0.52, MeOH)) to that reported for lophilone A ($[\alpha]^{23}_D$ = +56 (c = 0.56, MeOH) (Ghogomu et al., 1987). A small value of the optical rotation of **20** suggested that this compound is most likely an enantiomeric mixture. The NMR spectroscopic data (1D and 2D NMR in CD_3OD) of **20** is shown in **Table 10**. HMBC, COSY, and NOESY correlations of **20** are shown in **Figures 15**–**17**. The NMR spectra of **20** in CD_3OD are shown in **Figures A60**–**A78**. The NMR spectroscopic data (^{1}H and ^{13}C NMR in CD_3OD and acetone-d_6) of **20** is shown in **Table 11**. The NMR spectra of **20** in acetone-d_6 are shown in **Figures A79**–**A87**.

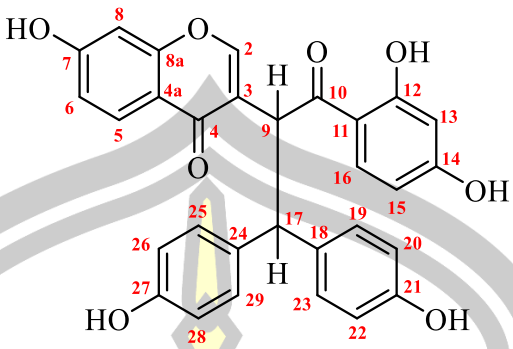

Table 9. ^{1}H and ^{13}C NMR spectroscopic data of **20** compared with literature in acetone-d_6.

Position	**20**[a]		Lophirone A[b]	
	δ_H, mult. (*J* in Hz)	δ_C	δ_H, mult. (*J* in Hz)	δ_C
2	8.25, s	156.1	8.27, s	155.4
3		122.2		122.1
4		175.1		175.4
4a		117.3		117.2
5	7.92, d (8.8)	128.3	7.94, d (8.8)	128.2
6	6.90, dd (8.8, 2.3)	115.9	6.91, dd (8.8, 2.3)	115.9
7		163.3		163.4
8	6.76, d (2.3)	103.1	6.77, d (2.3)	103.2
8a		158.5		158.5
9	6.12, d (12.3)	43.9	6.14, d (12.3)	43.9
10		204.6		204.5
11		114.1		114.1
12		166.8		166.8
13	6.19, d (2.4)	103.3	6.20, d (2.4)	103.3
14		166.0		166.1
15	6.43, d (8.9)	108.9	6.44, dd (9.0, 2.4)	109.0
16	8.32, d (8.9)	134.5	8.34, d (9.0)	134.4
17	4.78, d (12.3)	53.4	4.79, d (12.3)	53.4
18		134.6		134.6
19/23	7.23, d (1.9)	130.1	7.26, m	130.0
20/22	6.59, d (8.6)	115.7	6.61, m	115.8
21		156.4		156.4
24		135.7		135.6
25/29	7.25, d (1.9)	129.4	7.26, m	129.4
26/28	6.64, d (8.6)	115.8	6.65, m	115.9
27		156.5		156.5
12-OH	12.65, d (2.2)			

[a]Calibration of acetone-d_6 δ_H 2.05/δ_C 29.8.; [b]Ghogomu et al. 1987.

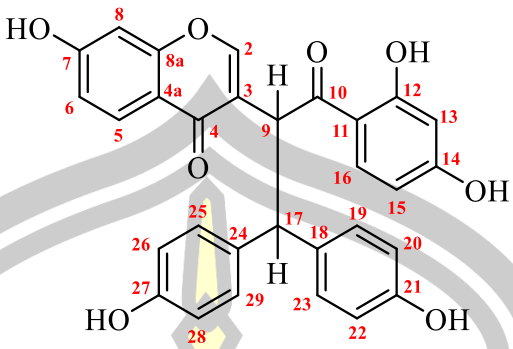

Table 10. ^{1}H, ^{13}C, and 2D NMR spectroscopic data of **20** in CD_3OD.

Position	δ_H, mult. (*J* in Hz)	δ_C	COSY	NOESY	HMBC
2	8.23, s	157.3		16, 17	4, 8a
3		122.5			
4		177.1			
4a		117.0			
5	7.88, d (8.9)	128.2	6	6	4, 7, 8a
6	6.84, dd (8.9, 2.3)	116.7	5, 8	5	8, 4a
7		165.0			
8	6.71, d (2.3)	103.3	6		6, 7, 8a
8a		159.4			
9	5.99, d (12.2)	44.7	17	16, 17, 19, 23, 25, 29	2, 4, 10, 17
10		204.8			
11		114.2			
12		166.9			
13	6.13, d (2.4)	103.5	15	15	15
14		167.0			
15	6.33, dd (8.9, 2.4)	109.3	13, 16	13, 16	11
16	8.14, d (8.9)	134.3	15	2, 9, 15	10, 12, 14
17	4.66, d (12.2)	54.3	9	2, 9, 19, 23, 25, 29	9, 18, 19, 23, 24
18		134.9			
19/23	7.12, d (8.6)	130.4	20, 22	9, 17, 20, 22	17, 19, 21, 23
20/22	6.55, d (8.6)	116.0	19, 23	19, 23	18, 20, 21, 22
21		156.6			
24		135.9			
25/29	7.15, d (8.6)	129.8	26, 28	9, 17, 26, 28	17, 24, 25, 27, 29
26/28	6.59, d (8.6)	116.1	25, 29	25, 29	24, 26, 27, 28,
27		156.7			
12-OH					

Calibration of CD_3OD δ_H 3.31/δ_C 49.0.

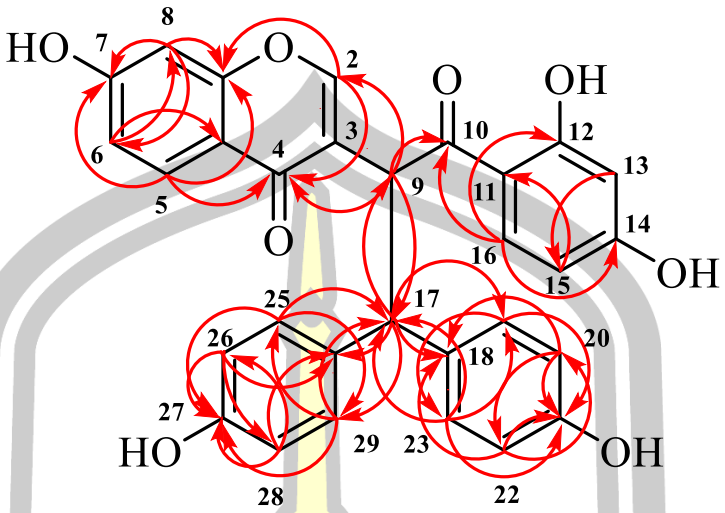

Figure 15. HMBC correlations of **20**.

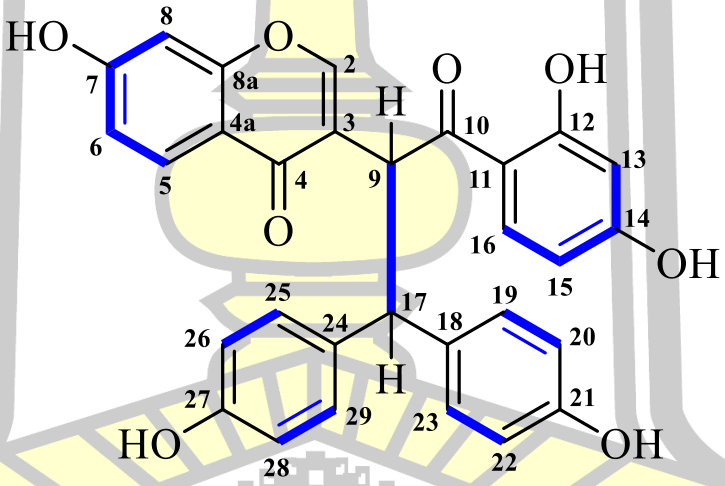

Figure 16. COSY correlations of **20**.

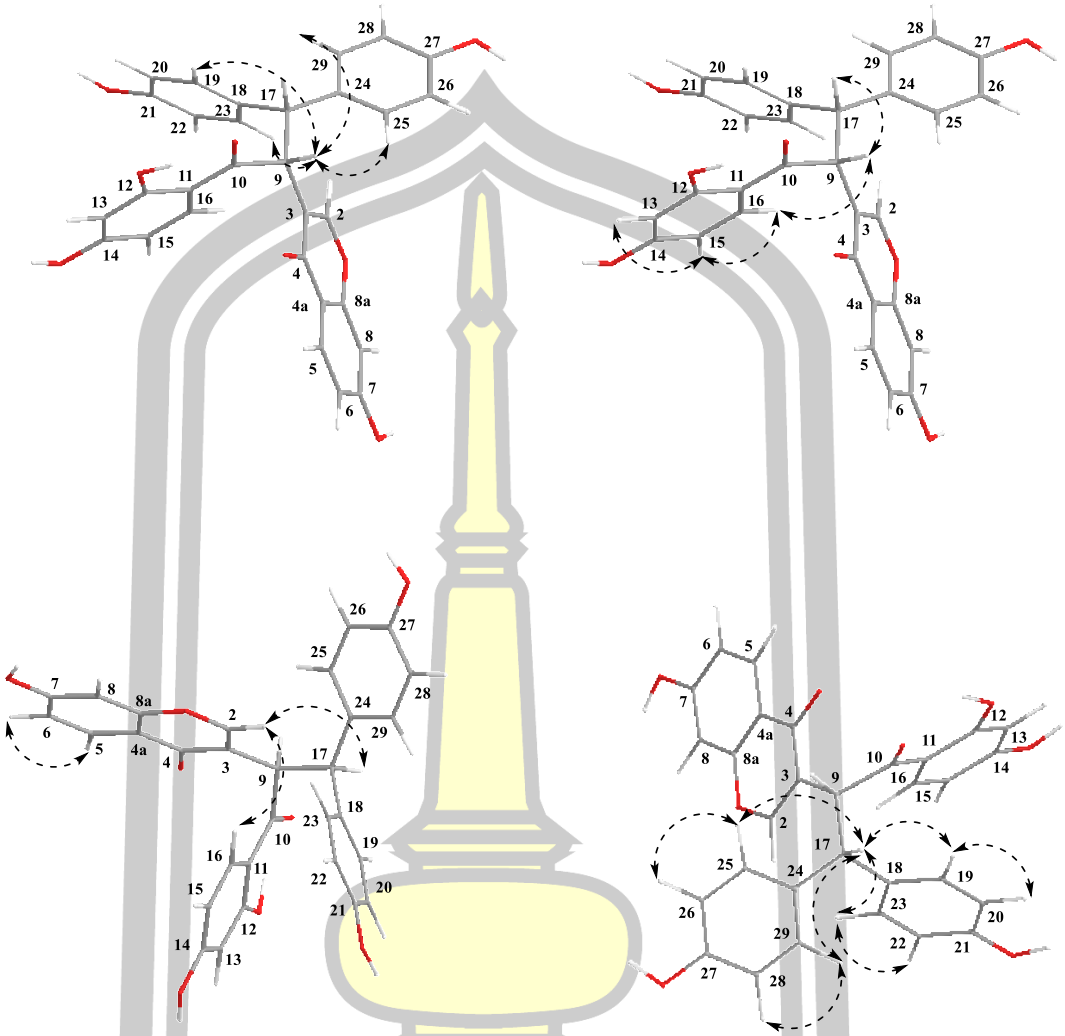

Figure 17. NOESY correlations of **20**.

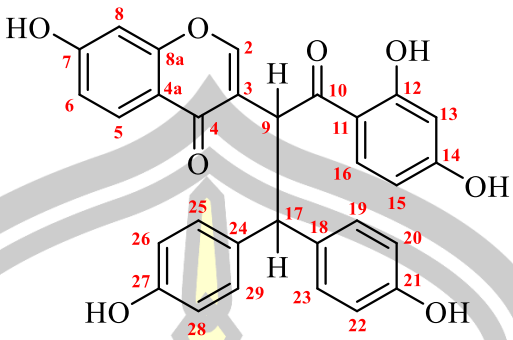

Table 11. ^{1}H and ^{13}C NMR spectroscopic data of **20** in CD_3OD and acetone-d_6.

Position	**20**[a] (CD_3OD)		**20**[b] (acetone-d_6)	
	δ_H, mult. (J in Hz)	δ_C	δ_H, mult. (J in Hz)	δ_C
2	8.23, s	157.3	8.25, s	156.1
3		122.5		122.2
4		177.1		175.1
4a		117.0		117.3
5	7.88, d (8.9)	128.2	7.92, d (8.8)	128.3
6	6.84, dd (8.9, 2.3)	116.7	6.90, dd (8.8, 2.3)	115.9
7		165.0		163.3
8	6.71, d (2.3)	103.3	6.76, d (2.3)	103.1
8a		159.4		158.5
9	5.99, d (12.2)	44.7	6.12, d (12.3)	43.9
10		204.8		204.6
11		114.2		114.1
12		166.9		166.8
13	6.13, d (2.4)	103.5	6.19, d (2.4)	103.3
14		167.0		166.0
15	6.33, dd (8.9, 2.4)	109.3	6.43, d (8.9)	108.9
16	8.14, d (8.9)	134.3	8.32, d (8.9)	134.5
17	4.66, d (12.2)	54.3	4.78, d (12.3)	53.4
18		134.9		134.6
19/23	7.12, d (8.6)	130.4	7.23, d (1.9)	130.1
20/22	6.55, d (8.6)	116.0	6.59, d (8.6)	115.7
21		156.6		156.4
24		135.9		135.7
25/29	7.15, d (8.6)	129.8	7.25, d (1.9)	129.4
26/28	6.59, d (8.6)	116.1	6.64, d (8.6)	115.8
27		156.7		156.5
12-OH			12.65, d (2.2)	

[a]Calibration of CD_3OD δ_H 3.31/δ_C 49.0; [b]Calibration of acetone-d_6 δ_H 2.05/δ_C 29.8.

4.3.6. Isoprunetin (**26**)

Compound **26** ($C_{16}H_{12}O_5$) was isolated as a light brown amorphous solid. Based on spectroscopic data compared with those reported in the literature, **26** was identified as isoprunetin (Kerkatou et al., 2013). The NMR spectroscopic data (^{1}H NMR in CD_3OD, and DMSO-d_6 and ^{13}C NMR in CD_3OD) of **26** is shown in **Table 12**. The NMR spectra of **26** are shown in **Figures A88**–**A94**.

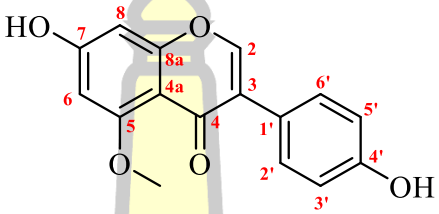

Table 12. ^{1}H and ^{13}C NMR spectroscopic data of **26** compared with literature in CD_3OD.

Position	**26**[a] (CD_3OD)		**26**[b] (DMSO-d_6)	Isoprunetinc[c] (CD_3OD)	
	δ_H, mult. (*J* in Hz)	δ_C	δ_H, mult. (*J* in Hz)	δ_H, mult. (*J* in Hz)	δ_C
2	7.94, s	152.5	8.06, s	7.79, s	152.5
3		126.9			127.0
4		177.8			177.9
4a		109.1			109.4
5		163.0			163.1
6	6.41, s	97.7	6.39, d (2.2)	6.32, s	97.6
7		165.3			164.8
8	6.41, s	96.3	6.37, d (2.2)	6.32, s	97.6
8a		161.5			161.5
1'		124.5			124.6
2'/6'	7.33, d (8.7)	131.6	7.29, d (8.7)	7.23, d (8.8)	131.6
3'/5'	6.82, d (8.7)	116.0	6.77, d (8.7)	6.71, d (8.8)	116.1
4'		158.5			158.5
7-OH			10.69, br s		
4'-OH			9.48, s		
5-OCH_3	3.88, s	56.4	3.79, s	3.78, s	56.5

[a]Calibration of CD_3OD δ_H 3.31/δ_C 49.0; [b]Calibration of DMSO-d_6 δ_H 2.50/δ_C 39.5; [c]Kerkatou et al. 2013.

4.3.7. Gerontoisoflavone A (**27**)

Compound **27** ($C_{17}H_{14}O_6$) was isolated as a light brown amorphous solid. Based on spectroscopic data compared with those reported in the literature, **27** was identified as gerontoisoflavone A (Chang et al., 1995). The NMR spectroscopic data (1D and 2D NMR in CD_3OD) of **27** is shown in **Table 13**. HMBC, COSY, and NOESY correlations of **27** are shown in **Figures 18**–**20**. The NMR spectra of **27** are shown in **Figures A95**–**A107**.

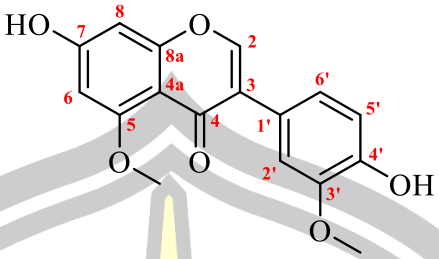

Table 13. ^{1}H, ^{13}C and 2D NMR spectroscopic data of **27** in CD_3OD.

Position	δ_H, mult. (*J* in Hz)	δ_C	COSY	NOESY	HMBC
2	7.98, s	152.7		2′, 6′	3, 4, 8a, 1'
3		126.9			
4		177.8			
4a		109.1			
5		163.0			
6	6.42, s	97.7		5-OCH_3	5, 7, 8, 4a, 8a
7		165.3			
8	6.42, s	96.3			5, 6, 7, 4a, 8a
8a		161.5			
1'		125.1			
2'	7.13, d (2.0)	114.3	6'	2, 6′, 3′-OCH_3	3, 4', 6'
3'		148.6			
4'		147.6			
5'	6.83, d (8.2)	116.0	6'	6′	1', 3'
6'	6.91, dd (8.2, 2.0)	123.0	2', 5'	2, 2′, 5′	3, 2', 4'
7-OH					
4'-OH					
5-OCH_3	3.89, s	56.4		6	5
3'-OCH_3	3.88, s	56.4		2′	3'

Calibration of CD_3OD δ_H 3.31/δ_C 49.0.

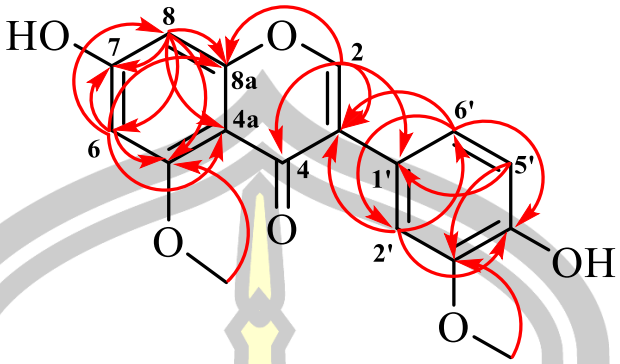

Figure 18. HMBC correlations of **27**.

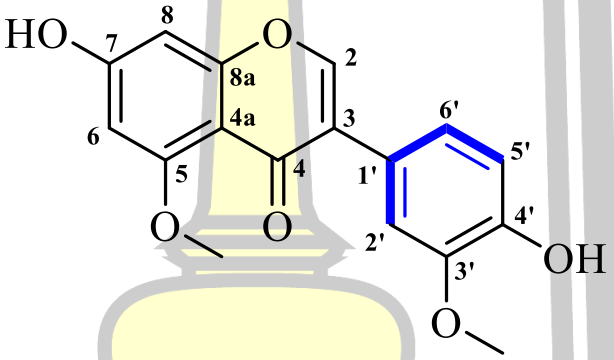

Figure 19. COSY correlations of **27**.

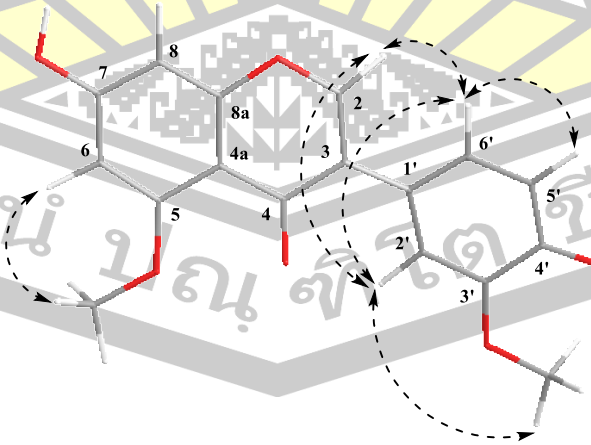

Figure 20. NOESY correlations of **27**.

4.3.8. Iriskumaonin (**36**)

Compound **36** ($C_{18}H_{14}O_7$) was isolated as a white amorphous solid. Based on spectroscopic data compared with those reported in the literature, **36** was identified as iriskumaonin (Kalla et al., 1978). The NMR spectroscopic data (^{1}H and ^{13}C NMR in $CDCl_3$) of **36** is shown in **Table 14**. The NMR spectra of **36** are shown in **Figures A108**–**A112**.

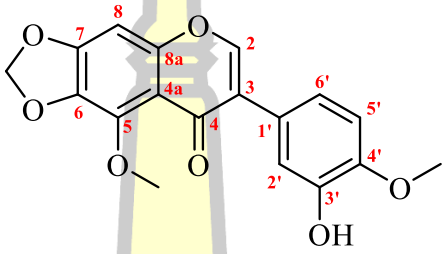

Table 14. ^{1}H and ^{13}C NMR spectroscopic data of **36** compared with literature in $CDCl_3$.

Position	**36**[a]		Iriskumaonin[b]
	δ_H, mult. (*J* in Hz)	δ_C	δ_H, mult. (*J* in Hz)
2	7.79, s	150.4	7.88, s
3		125.4	
4		175.5	
4a		113.8	
5		141.7	
6		135.5	
7		152.8	
8	6.64, s	93.2	6.73, s
8a		154.7	
1'		123.9	
2'	7.24, d (1.8)	112.4	7.36, s
3'		145.7	
4'		146.2	
5'	6.94, d (8.2)	114.2	7.02, s
6'	6.90, dd (8.2, 1.8)	121.8	7.02, s
3'-OH	5.68, br s		5.79, s
OCH_2O	6.07, s	102.2	6.16, s
5-OCH_3	4.09, s	61.3	4.15, s
4'-OCH_3	3.93, s	56.1	3.88, s

[a]Calibration of $CDCl_3$ δ_H 7.26/δ_C 77.0; [b]Kalla et al. 1978.

4.4. Biological activity of the isolated compounds

Compounds **11**–**13**, **26**, **27**, **35**, and **36** were also assayed for antimalarial activity against the chloroquine- and pyrimethamine-resistant strain of *P. falciparum* (K1) and antibacterial activity assay toward three Gram-positive bacteria, methicillin-susceptible *S. aureus* (MSSA) DMST 2933, methicillin-resistant *S. aureus* (MRSA) DMST 20651 and *B. cereus* 11778 and $DPPH^{\bullet}$ scavenging activity. However, since **20** was isolated in a minute quantity, it was not assayed for these activities.

4.4.1. Antimalarial activity

Some isoflavones were found to exhibit *in vitro* antimalarial activity against chloroquine-sensitive strain and chloroquine-resistant clone of *P. falciparum* (Kraft et al., 2000). Additionally, the biflavanones previously isolated from roots and outer barks of *O. integerrima*, exhibited antimalarial activity against chloroquine-resistant strains of *P. falciparum* (FCR-3) and multidrug-resistant *P. falciparum* (K1) (Ndoile and Heerden, 2018; Ichino et al., 2006). This fact led us to screen the crude MeOH extract of root woods of *O. integerrima*, and the isolated compounds (**11**–**13**, **26**, **27**, **35**, and **36**) for antimalarial activity against *P. falciparum* (K1). The result showed a weak inhibitory activity (26.7%) of the crude MeOH extract (at 5 μg/mL), the results are shown in **Table 1**, while **11**–**13**, **26**, **27**, **35**, and **36**, at 5 μg/mL, were void of the activity, the results are shown in **Table 15**.

Table 15. Antimalarial activity of compounds **11**–**13**, **26**, **27**, **35**, and **36**.

Sample	%Inhibition (5 µg/mL)
11	0
12	0
13	2.85
26	0
27	0
35	1.86
36	4.06

4.4.2. Antibacterial activity

From previous report, the antibacterial activities of the MeOH extract and EtOAc extract from the stem bark of *O. integerrima* have been reported (Traisathit et al., 2021). Its activity against Gram-positive bacteria *S. aureus* (MSSA), and *B. cereus*, with MIC and MBC values in the range of 3.12–6.25 mg/mL and 3.12–25.0 mg/mL were determined (Traisathit et al., 2021). Information from previous research indicated that this plant has the potential to be an antibacterial source of compounds. Antibacterial activity of compounds **11**–**13**, **26**, **27**, **35**, and **36** was evaluated. Results indicated that compounds **13**, **26**, **27**, **35**, and **36** showed inhibition zone toward *S. aureus* MSSA (**Table 16**).

Table 16. Antibacterial activity of compounds **11**–**13**, **26**, **27**, **35**, and **36**.

Sample	Antibacterial activity (MIC/MBC; mg/mL)
	S. aureus **(MSSA)**
11	ND
12	ND
13	> 0.25/> 0.25
26	> 0.25/> 0.25
27	> 0.25/> 0.25
35	> 0.25/> 0.25
36	0.25/> 0.25

ND = Not detected.

4.4.3. DPPH radical scavenging activity

Isoflavones were found to protect cells against reactive oxygen species (ROS) by reducing free radicals and downregulating the expression of the stress–response related genes. It is well known that ROS could induce severe DNA damage, which plays an important role in carcinogenesis. Therefore, oxidative stress from ROS accumulation could be one of the mechanisms responsible for the development and progression of cancer. In fact, many isoflavones also inhibit cancer development and progression by regulating multiple cellular signaling pathways that are related to oxidative stress and significantly regulated in cancer (Li et al., 2013). For this reason, the crude MeOH extract of root woods of *O. integerrima* and the isolated isoflavones and isoflavone glycosides, **11**–**13**, **26**, **27**, **35**, and **36**, were assayed for DPPH$^{\bullet}$ scavenging activity.

Therefore, the SC_{50} of **26**, **27**, and **36** were determined. The results showed that **27** exhibited the highest DPPH radical scavenging activity among the three compounds, with SC_{50} 137.7 μM (**Table 17**), which is nearly two times less than that of ascorbic acid (SC_{50} 76.1 μM), a standard compound used in this experiment. Flavonoids display a myriad of biological activities that are related to their antioxidant capacity (Chen et al., 2023). The chemical structures of flavonoids have important effects on their antioxidant activity. Flavonoids with certain numbers and different positions of the hydroxyl groups, especially on the B-ring, a double bond between C2 and C3 on the C-ring, and the presence of methoxy groups, increase the antioxidant activity while the presence of a sugar moiety reduces antioxidant activity (Wang et al., 2018; Heim et al., 2002; Cai et al., 2006). While numerous flavonoids have been isolated from *O. integerrima*, only a few reports have focused on the antioxidant activity of the isolated compounds. To the best of our knowledge, there are no reports on the antioxidant activity of flavonoids isolated from the roots of this plant. Only recently that the antioxidant and other biological properties of flavonoids from the flowers and seeds of *O. integerrima* have been reported (Buranasudja et al., 2022; Nguyen et al., 2024).

Table 17. DPPH radical scavenging activity of compounds **11**–**13**, **26**, **27**, **35**, and **36**.

Sample	%RSA (50 μg/mL)	SC_{50} (μM)
11	4.18 ± 2.4	ND
12	1.33 ± 0.1	ND
13	1.52 ± 0.5	ND
26	24.34 ± 1.7	662.0 ± 58.0
27	65.48 ± 1.4	137.7 ± 7.1
35	2.31 ± 1.0	ND
36	33.21 ± 1.4	510.5 ± 37.8
Ascorbic acid	–	76.1 ± 1.4

ND = Not determined (%RSA < 20 from the screening assay).

CHAPTER 5

CONCLUSION

The phytochemical investigation of the MeOH extract of root woods of *O. integerrima* led to the isolation of an undescribed isoflavone glycoside, gerontoisoflavone A-4'-*O*-*β*-D-xylopyranoside (**35**), along with six previously reported isoflavone derivatives (**11**–**13**, **26**, **27**, and **36**), and a chromone derivative (**20**). These flavonoids have been commonly isolated from the plants of the family Ochnaceae. The isoflavones and isoflavone glycosides **11**–**13**, **26**, **27**, **35**, and **36** were evaluated for antimalarial activity against the multidrug-resistant *P. falciparum* (K1), antibacterial activity against *S. aureus* (MSSA and MRSA) and *B. cereus*, and their DPPH radical scavenging activity. Compounds **11**–**13**, **26**, **27**, **35**, and **36** are inactive with *P. falciparum* (K1), compounds **13**, **26**, **27**, **35**, and **36**, exhibited antibacterial activities against *S. aureus* (MSSA) with MIC and MBC values in the range of 0.25 and >0.25 mg/mL, and compound **27** displayed DPPH radical scavenging activity twofold less than that of ascorbic acid.

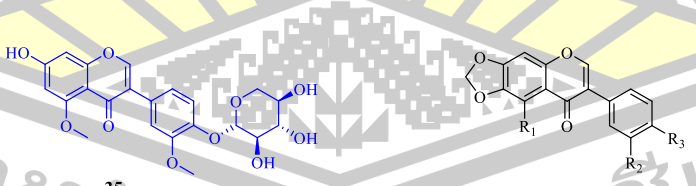

35

11: $R_1 = R_2 = R_3 = OCH_3$
12: $R_1 = OCH_3$, $R_2 = H$, $R_3 = OCH_3$
36: $R_1 = OCH_3$, $R_2 = OH$, $R_3 = OCH_3$

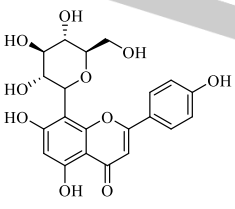

13

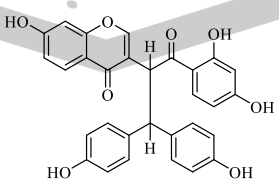

20

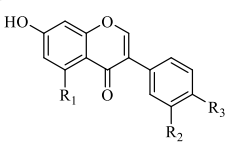

26: $R_1 = OCH_3$, $R_2 = H$, $R_3 = OH$
27: $R_1 = R_2 = OCH_3$, $R_3 = OH$

REFERENCES

REFERENCES

Baimai, V. Biodiversity in Thailand.The Journal of the Royal Institute of Thailand. **2010**; 2: 107–118.

Bandi, A. K. R.; Lee, D. U.; Tih, R. G.; Gunasekar, D.; Bodo, B. Phytochemical and biological studies of Ochna species. Chemistry Biodiversity. **2012**; 9(2): 251–271.

Bennett, T. N.; Paguio, M.; Gligorijevic, B.; Seudieu, C.; Kosar, A. D.; Davidson, E.; Roepe, P. D. Novel, rapid, and inexpensive cell-based quantification of antimalarial drug efficacy. Antimicrobial Agents and Chemotherapy. **2004**; 48(5): 1807–1810.

Buranasudja, V.; Kobtrakul, K.; Vimolmangkang, S.; Binalee, A.; Sanookpan, K.; Vu, T. Y.; Huynh, K. L. V.; Le, B.; Nguyen, H. T.; Do, K. M.; Dang, V. S.; Nguyen, H. M. Some antioxidant properties of components from the flower of Ochna integerrima and their beneficial effects on HaCaT keratinocytes and in Silico analysis on tyrosinase. Chemistry Biodiversity. **2022**; 19(4): e202100882.

Cai, Y. Z.; Sun, M.; Xing, J.; Luo, Q.; Corke, H. Structure–radical scavenging activity relationships of phenolic compounds from traditional Chinese medicinal plants. Life Sciences. **2006**; 78(25): 2872–2888.

Chang, C. H.; Lin, C. C.; Kadota, S.; Hattori, M.; Namba, T. Flavonoids and a prenylated xanthone from *Cudrania cochinchinensis* var. *gerontogea*. Phytochemistry. **1995**; 40(3): 945–947.

Chen, S.; Wang, X.; Cheng, Y.; Gao, H.; Chen, X. A review of classification, biosynthesis, biological activities and potential applications of flavonoids. Molecules. **2023**; 28(13): 4982.

Chokchaisiri, R.; Chaichompoo, W.; Bureekaew, S.; Thepmalee, C.; Ganranoo, L.; Cheenpracha, S.; Suksamrarn, A. A new oligostilbenoid isolated from the stems of *Ochna integerrima*. Phytochemistry Letters. **2024**; 59: 41–44.

Choo, C. Y.; Sulong, N. Y.; Man, F.; Wong, T. W. Vitexin and isovitexin from the leaves of *Ficus deltoidea* with *in-vivo* α-glucosidase inhibition. Journal of Ethnopharmacology. **2012**; 142(3): 776–781.

Ghogomu, R.; Sondengam, B. L.; Martin, M. T.; Bodo, B. Lophirone A, a biflavonoid with unusual skeleton from *Lophira lanceolata*. Tetrahedron Letters. **1987**; 28(26): 2967–2968.

Gulluce, M.; Karadayi, M.; Guvenalp, Z.; Ozbek, H.; Arasoglu, T.; Bari, O. Isolation of some active compounds from *Origanum vulgare* L. ssp. *vulgare* and determination of their genotoxic potentials. Food Chemistry. **2012**; 130(2): 248–253.

Heim, K. E.; Tagliaferro, A. R.; Bobilya, D. J.; Nutr. J. Flavonoid antioxidants: chemistry, metabolism and structure-activity relationships. The Journal of Nutritional Biochemistry. **2002**; 13(10): 572–584.

Ichino, C.; Kiyohara, H.; Soonthornchareonnon, N.; Chuakul, W.; Ishiyama, A.; Sekiguchi, H.; Namatame, M.; Otoguro, K.; Omura, S.; Yamada, H. Antimalarial activity of biflavonoids from *Ochna integerrima*. Planta Medica. **2006**; 72(7): 611–614.

Ismail, A. M.; Musa, A. M.; Nasir, T.; Magaji, M. G.; Jega, Y. A.; Ibrahim, I. Anti-proliferative study and isolation of Ochnaflavone from the ethyl acetate-soluble fraction of *Ochna kibbiensis* Hutch & Dalziel. Natural Product Research. **2017**; 31(18): 2149–2152.

Kaewamatawong, R.; Likhitwitayawuid, K.; Ruangrungsi, N.; Takayama, H.; Kitajima, M.; Aimi, N. Novel biflavonoids from the stem bark of *Ochna integerrima*. Journal of Natural Products. **2002**; 65(7): 1027–1029.

Kakabi, M. H. D.; Mpetga, J. D. S.; Tamokou, J. D. D.; Matsuete, G. T.; Nago, R. D. T.; Bitchagno, G. T. M.; Lenta, B. N.; Sewald, N.; Tene, M.; Ngouela, A. S. Two new flavone glycosides from the leaves of *Ochna afzelii* Oliv. (Ochnaceae). Natural Product Research. **2024**; 38(3): 447–257.

Kalenga, T. M.; Ndoile, M. M.; Atilaw, Y.; Gilissen, P. J.; Munissi, J. J. E.; Rudenko, A.; Bourgard, C.; Sunnerhagen, P.; Nyandoro, S. S.; Erdelyi, M. Biflavanones, chalconoids, and flavonoid analogues from the stem bark of *Ochna holstii*. Journal of Natural Products. **2021**; 84(2): 364–372.

Kalenga, T. M.; Ndoile, M. M.; Atilaw, Y.; Munissi, J. J. E.; Gilissen, P. J.; Rudenko, A.; Bourgard, C.; Sunnerhagen, P.; Nyandoro, S. S.; Erdelyi, M. Antibacterial and cytotoxic biflavonoids from the root bark of *Ochna kirkii*. Fitoterapia. **2021**; 151: 104857.

Kalla, A. K.; Bhan, M. K.; Dhar, K. L. A new isoflavone from *Iris kumaonensis*. Phytochemistry. **1978**; 17(8): 1441–1442.

Kennedy, D. O.; Wightman, E. L. Herbal extracts and phytochemicals: plant secondary metabolites and the enhancement of human brain function. Advances in Nutrition. **2011**; 2(1): 32–50.

Kerkatou, M.; Menad, A.; Sarri, D.; León, F.; Brouard, I.; Bouldjedj, R.; Chalard, P.; Ameddah, S.; Benayache, S.; Benayache, F. Secondary metabolites from *Genista aspalathoides* Lamk ssp. *aspalathoides* M. Der Pharmacia Lettre. **2013**; 5(5): 285–289.

Kraft, C.; Jenett-Siems, K.; Siems, K.; Gupta, M. P.; Bienzle, U.; Eich, E. Antiplasmodial activity of isoflavones from *Andira inermis*. Journal of Ethnopharmacology. **2000**; 73(1–2): 131–135.

Li, Y.; Kong, D.; Ahmad, A.; Bao, B.; Sarkar, F. H. Antioxidant function of isoflavone and 3,3′-diindolylmethane: are they important for cancer prevention and therapy**?**. Antioxidants & Redox Signaling. **2013**; 19(2): 139–150.

Likhitwitayawuid, K.; Kaewamatawong, R.; Ruangrungsi, N. Mono- and biflavonoids of *Ochna integerrima*. Biochemical Systematics and Ecology. **2005**; 33: 527–536.

Likhitwitayawuid, K.; Rungserichai, R.; Ruangrungsi, N.; Phadungcharoen, T. Flavonoids from *Ochna integerrima*. Phytochemistry. **2001**; 56: 353–357.

Lin, Y. L.; Wang, C. N.; Shiao, Y. J.; Liu, T. Y.; Wang, W. Y. Benzolignanoid and polyphenols from *Origanum Vulgare.* Journal of the Chinese Chemical Society. **2003**; 50(5): 1079–1083.

Makhafola, T. J.; Samuel, B. B.; Elgorashi, E. E.; Eloff, J. N. Ochnaflavone and ochnaflavone 7-*O*-methyl ether two antibacterial biflavonoids from *Ochna pretoriensis* (Ochnaceae). Natural Product Communications. **2012**; 7(12): 1601–1604.

Med Thai. (2020). ช้างน้าว สรรพคุณและประโยชน์ของต้นช้างน้าว 24 ข้อ ! (ตาลเหลือง). https://medthai.com/ช้างน้าว/. (February 10, 2023).

Messanga, B. B.; Kimbu, S. F.; Sondengam, B. L.; Bodo, B. Triflavonoids of *Ochna calodendron*. Phytochemistry. **2002**; 59(4): 435–438.

Moh, S. M.; Kato-Noguchi, H. Efficacy of *Ochna integerrima* (Lour.) Merr leaf extracts against seedling growth of six important plants. Australian Journal of Crop Science. **2022**; 16(5): 555–561.

Mongabay. com. (2011). Thailand forest information and data. https://worldrainforests.com/deforestation/2000/Thailand.htm. (January 9, 2025)

Ndoile, M. M.; Heerden, F. R. V. Antimalarial biflavonoids from the roots of *Ochna serrulata* (Hochst.) Walp. International Research Journal of Pure and Applied Chemistry. **2018**; 16(4): 1–9.

Ndongo, J. T.; Issa, M. E.; Messi, A. N.; Mbing, J. N.; Cuendet, M.; Pegnyemb, D. E.; Bochet, C. G. Cytotoxic flavonoids and other constituents from the stem bark of *Ochna schweinfurthiana*. Natural Product Research. **2015**; 29(17): 1684–1687.

Newman, D. J.; Cragg, G. M. Natural products as source of new drugs from 1981 to 2014. Journal of Natural Products. **2016**; 79(3):629–661.

Nguyen, H. M.; Nguyen, K. P.; Le, A. T. P.; Nguyen, N. H. T.; Vu-Huynh, L. K.; Le, C. K. T.; Acharige. A. D.; Hull, K.; Romo, D. Antioxidant, anti-tyrosinase, hepatoprotective, and anti-inflammatory potential in flowers and seeds of *Ochna integerrima* (Lour.) Merr. Natural Product Research. **2024**.

Pegnyemb, D. E.; Tih, R. G.; Sondengam, B. L.; Blond, A.; Bodo, B. Flavonoids from leaves of *Ochna Afzelii*. Biochemical Systematics and Ecology. **2003**; 31(2): 219–221.

Phargarden. (2010). ช้างน้าว. http://www.phargarden.com. (February 10, 2023).

Promden, W.; Chanvorachote, P.; Viriyabancha, W.; Sintupachee, S.; De-Eknamkul, W. *Maclura cochinchinensis* (Lour.) corner heartwood extracts containing resveratrol and oxyresveratrol inhibit melanogenesis in B16F10 melanoma cells. Molecules. **2024**; 29(11): 2473.

Reddy, B. A. K.; Reddy, N. P.; Gunasekar, D.; Blond, A.; Bodo, B. Biflavonoids from *Ochna lanceolata*. Phytochemistry Letters. **2008**; 1(1): 27–30.

Reutrakul, V.; Ningnuek, N.; Pohmakotr, M.; Yoosook, C.; Napaswad, C.; Kasisit, J.; Santisuk, T.; Tuchinda, P. Anti HIV-1 flavonoid glycosides from *Ochna integerrima*. Planta Medica. **2007**; 73(7): 683–688.

Sangdee, A.; Sangdee, K.; Buranrat, B.; Thammawat, S. Effects of mycelial extract and crude protein of the medicinal mushroom, Ophiocordyceps sobolifera, on the pathogenic fungus, Candida albicans. Tropical Journal of Pharmaceutical Research. **2018**; 17(12): 2449–2454.

Seephonkai, P.; Sedlak, S.; Wongpakam, K.; Sangdee, K.; Sangdee, A. Time-kill kinetics and mechanism of action of *Caesalpinia sappan* L. and *Ochna integerrima* (Lour.) Merr. water extractsagainst pathogenic bacteria. Journal of Pharmacy and Pharmacognosy Research. **2021**; 9(6): 813–823.

Smilkstein, M.; Sriwilaijaroen, N.; Kelly, J. X.; Wilairat, P.; Riscoe, M. Simple and inexpensive fluorescence-based technique for high-throughput antimalarial drug screening. Antimicrobial Agents and Chemotherapy. **2004**; 48(5): 1803–1806.

Smitinand, T.; Larsen, K. Flora of Thailand, Vol. 2, Prachachon Publishers, Bangkok **1970**.

Thaithong, S.; Beale, G. H.; Chutmongkonkul, M. Susceptibility of *Plasmodium falciparum* to five drugs: an *in vitro* study of isolates mainly from

Thailand. Transactions of The Royal Society of Tropical Medicine and Hygiene. **1983**; 77(2): 228–231.

Trager, W.; Jensen, J. B. Human malaria parasites in continuous culture. Journal of Parasitology. **2005**; 91(3): 484–486.

Traisathit, R.; Sangdee, A.; Wongpakam, K.; Sedlak, S.; Kanjanasirirat, P.; Borwornpinyo, S.; Thita, T.; Patrapuvich, R.; Seephonkai, P. Antioxidant, antibacterial and antiplasmodial activities of galactogogue plant extracts. Tropical Journal of Natural Product Research. **2021**; 5(4): 698–706.

Veitch, N. C.; Sutton, P. S. E.; Kite, G. C.; Ireland, H. E. Six new isoflavones and a 5-deoxyflavonol glycoside from the leaves of *Ateleia herbert-smithii*. Journal of Natural Products. **2003**; 66(2): 210–216.

Wang, T. Y.; Li, Q.; Bi, K. S. Bioactive flavonoids in medicinal plants: structure, activity and biological fate. Asian Journal of Pharmaceutical Sciences. **2018**; 13(1): 12–23.

APPENDIX

LIST OF APPENDIX

Figure **Page**

Figure **Page**

Figure **Page**

Figure **Page**

Figure **Page**

Figure **Page**

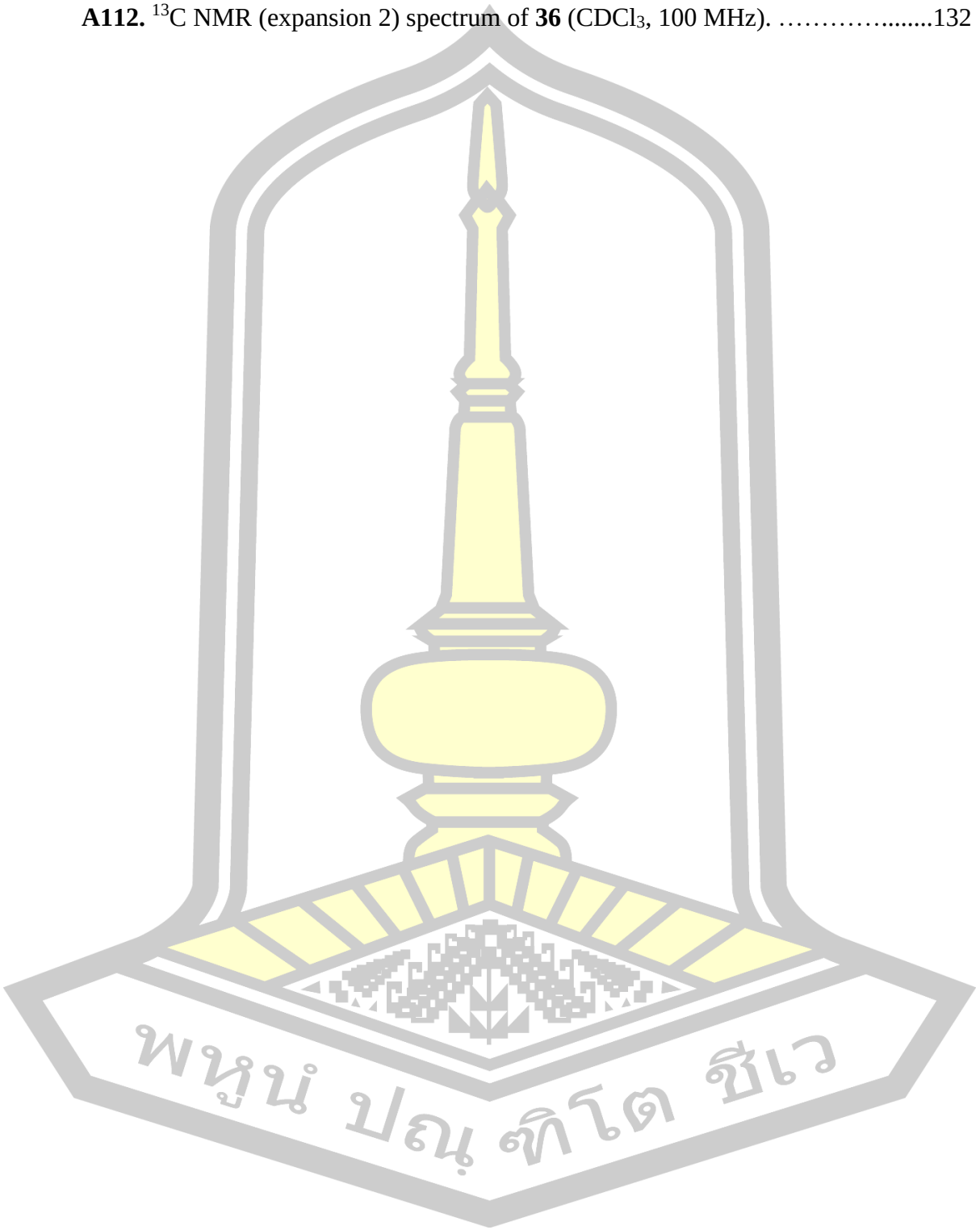

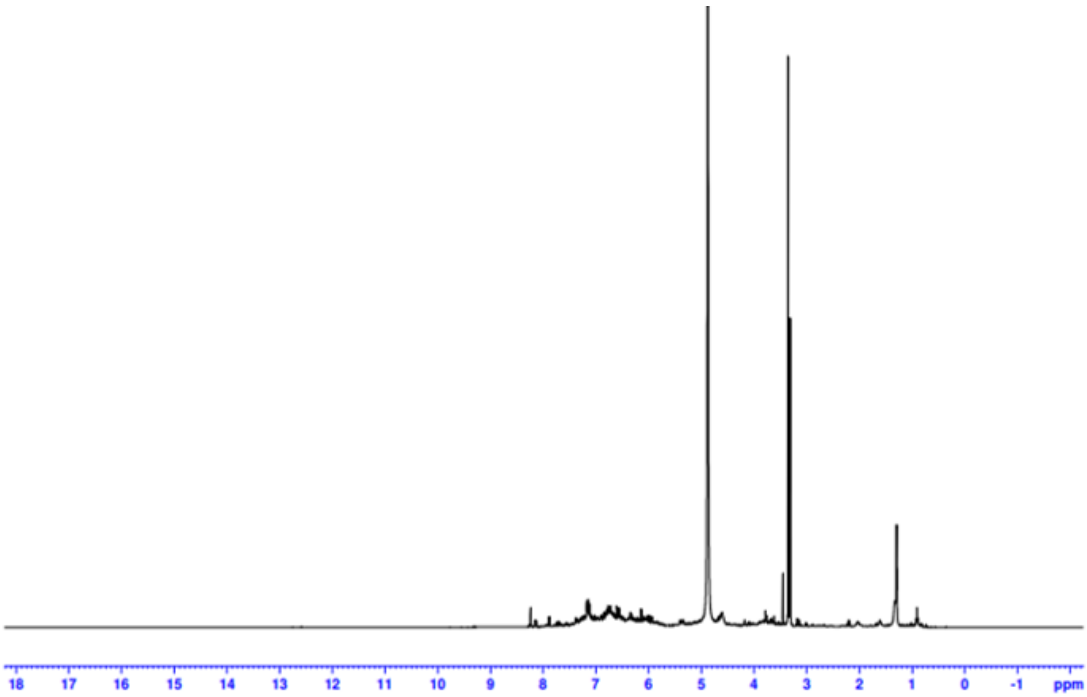

Figure A1. ^{1}H NMR spectrum of the MeOH extract of the root woods of *O. integerrima* (CD_3OD, 400 MHz).

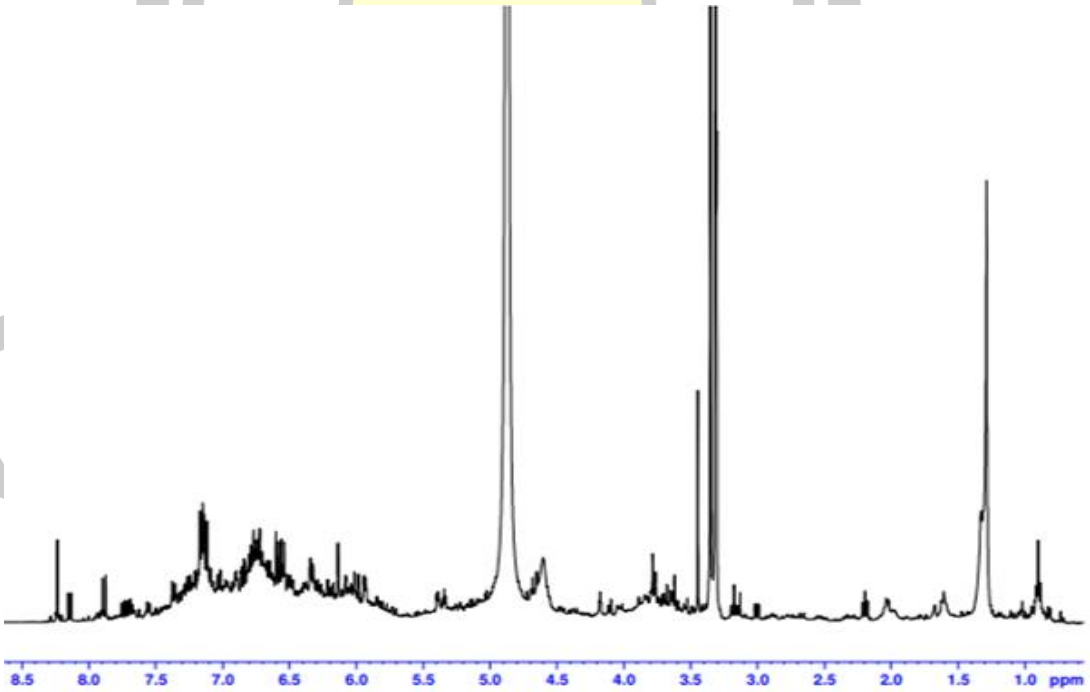

Figure A2. ^{1}H NMR (expansion 1) spectrum of the MeOH extract of the root woods of *O. integerrima* (CD_3OD, 400 MHz).

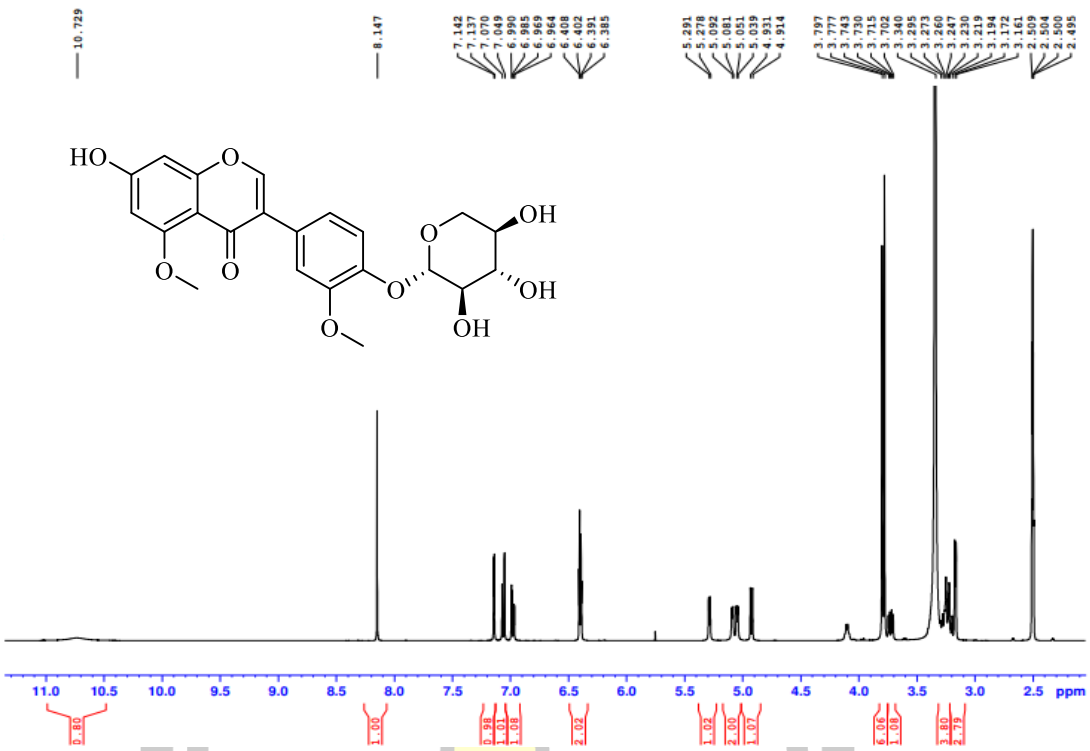

Figure A3. ^{1}H NMR spectrum of **35** (DMSO-d_6, 400 MHz).

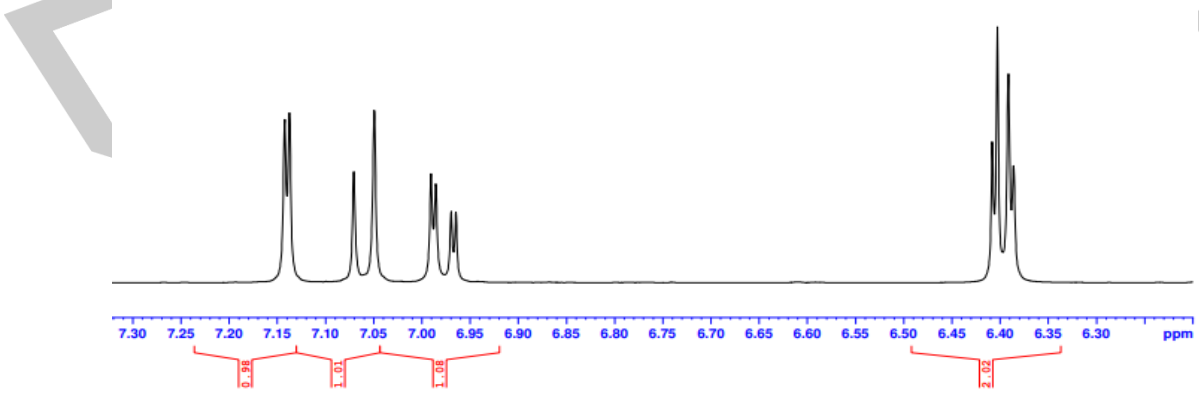

Figure A4. ^{1}H NMR (expansion 1) spectrum of **35** (DMSO-d_6, 400 MHz).

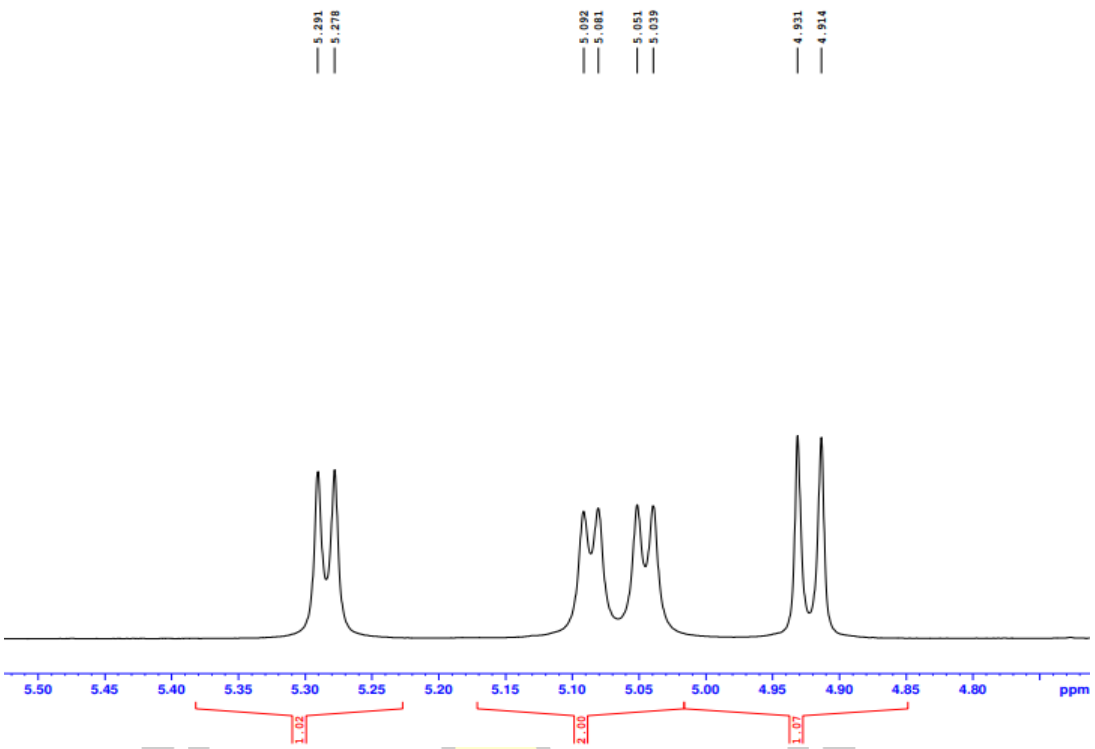

Figure A5. ^{1}H NMR (expansion 2) spectrum of **35** (DMSO-d_6, 400 MHz).

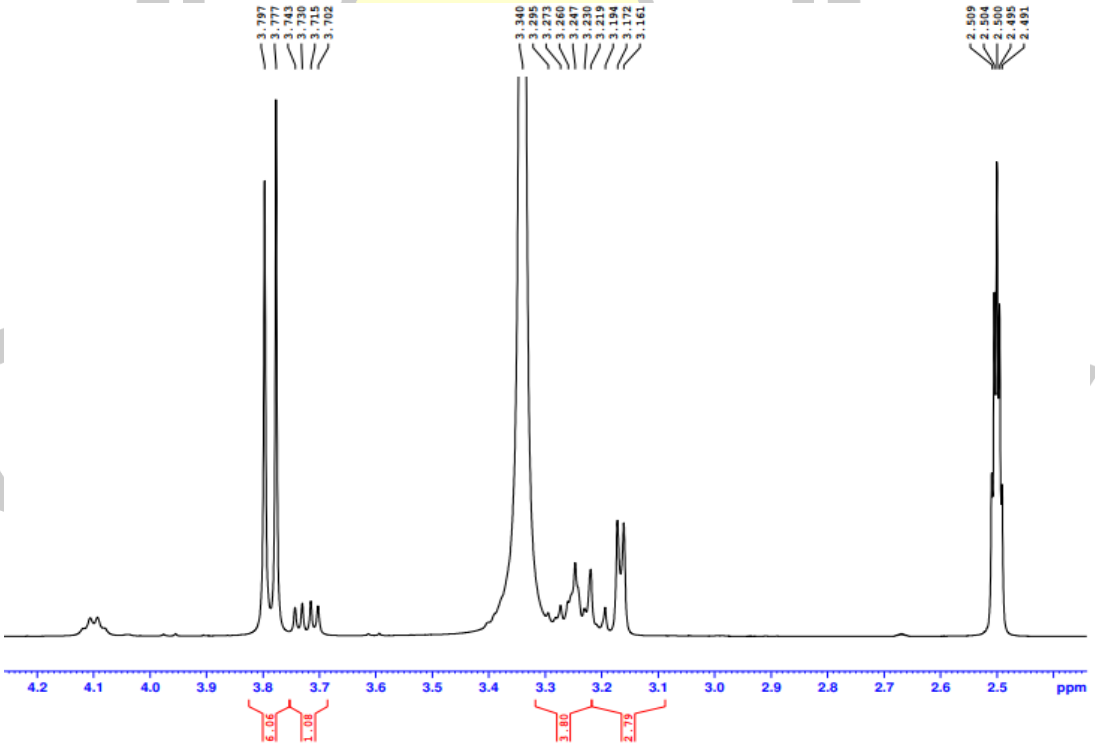

Figure A6. ^{1}H NMR (expansion 3) spectrum of **35** (DMSO-d_6, 400 MHz).

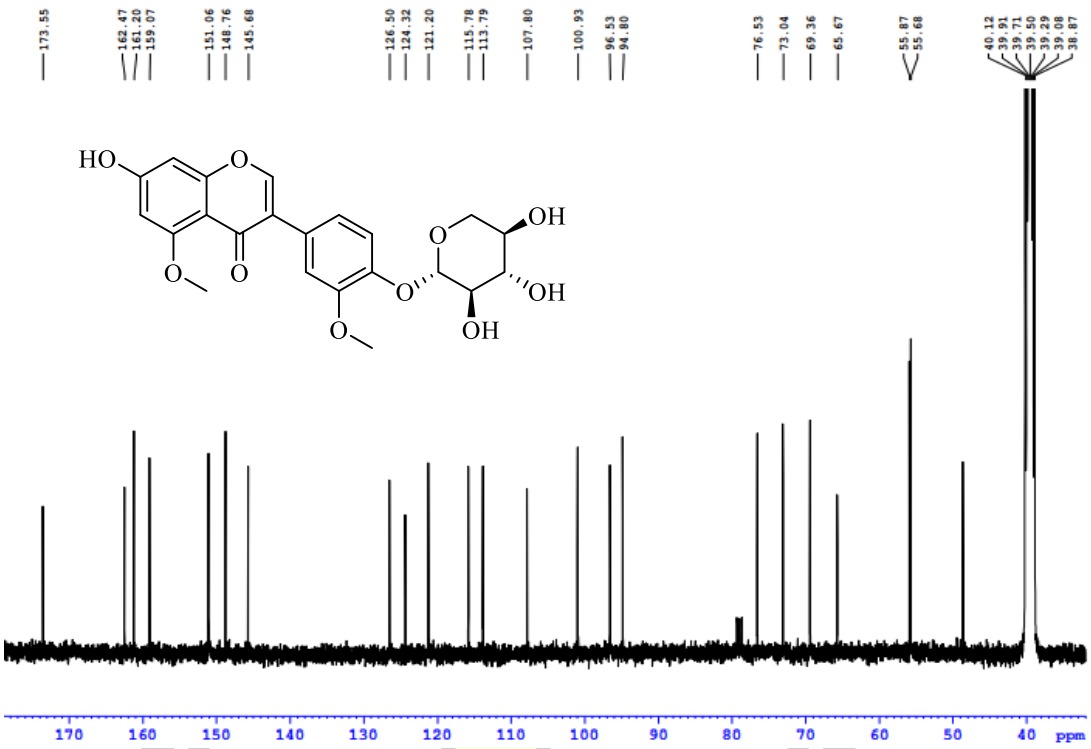

Figure A7. ^{13}C NMR spectrum of **35** (DMSO-d_6, 100 MHz).

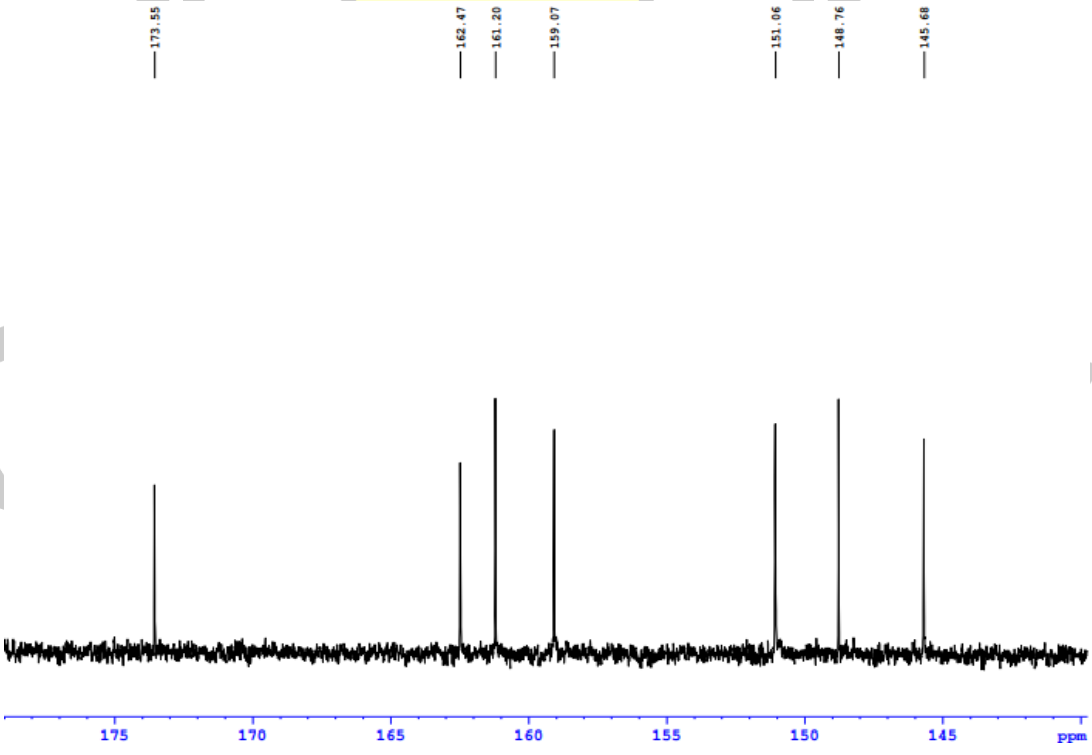

Figure A8. ^{13}C NMR (expansion 1) spectrum of **35** (DMSO-d_6, 100 MHz).

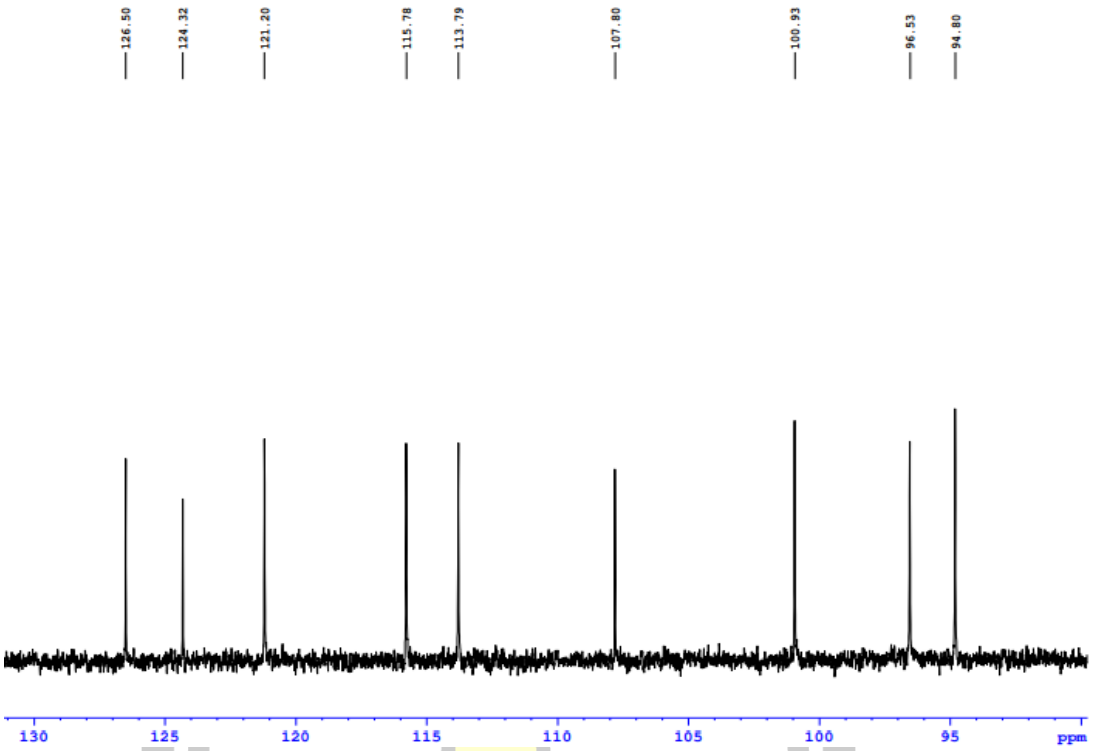

Figure A9. ^{13}C NMR (expansion 2) spectrum of **35** (DMSO-d_6, 100 MHz).

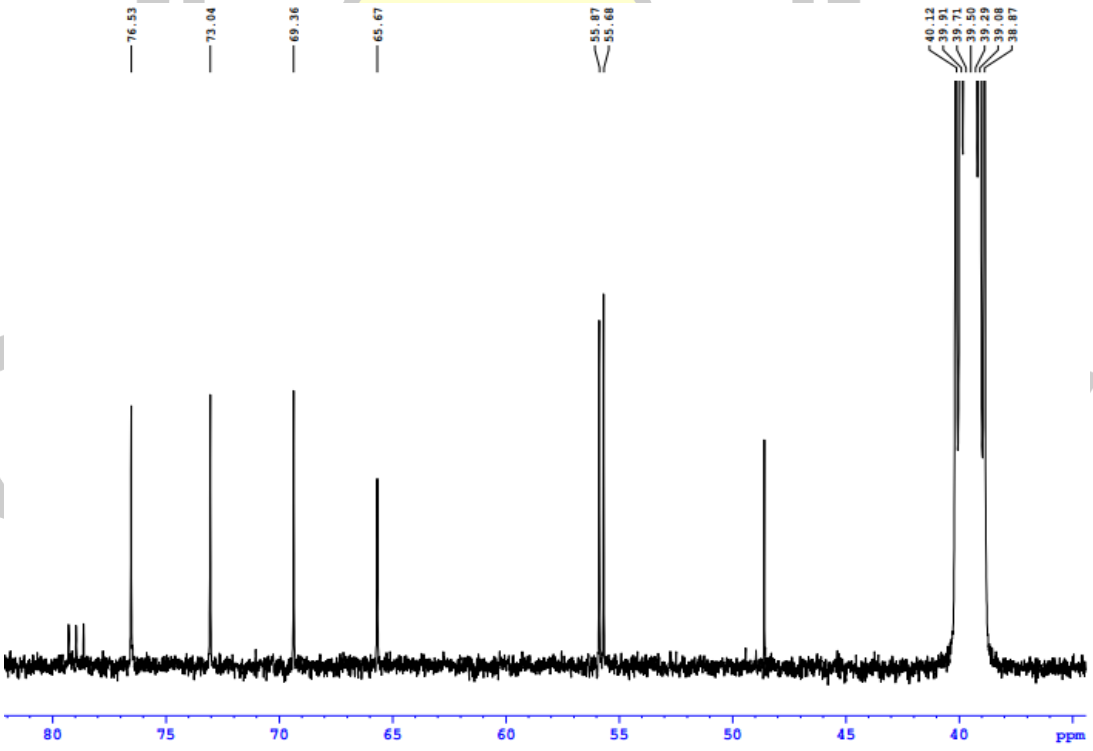

Figure A10. ^{13}C NMR (expansion 3) spectrum of **35** (DMSO-d_6, 100 MHz).

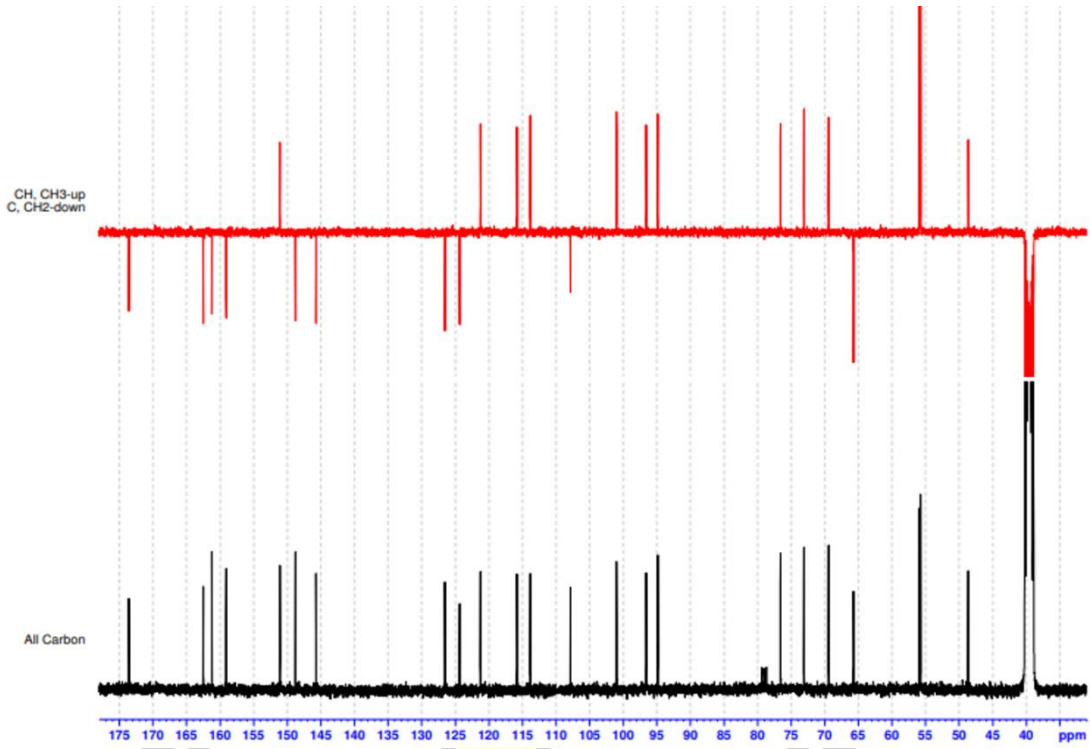

Figure A11. DEPT-135 spectrum of **35** (DMSO-d_6, 100 MHz).

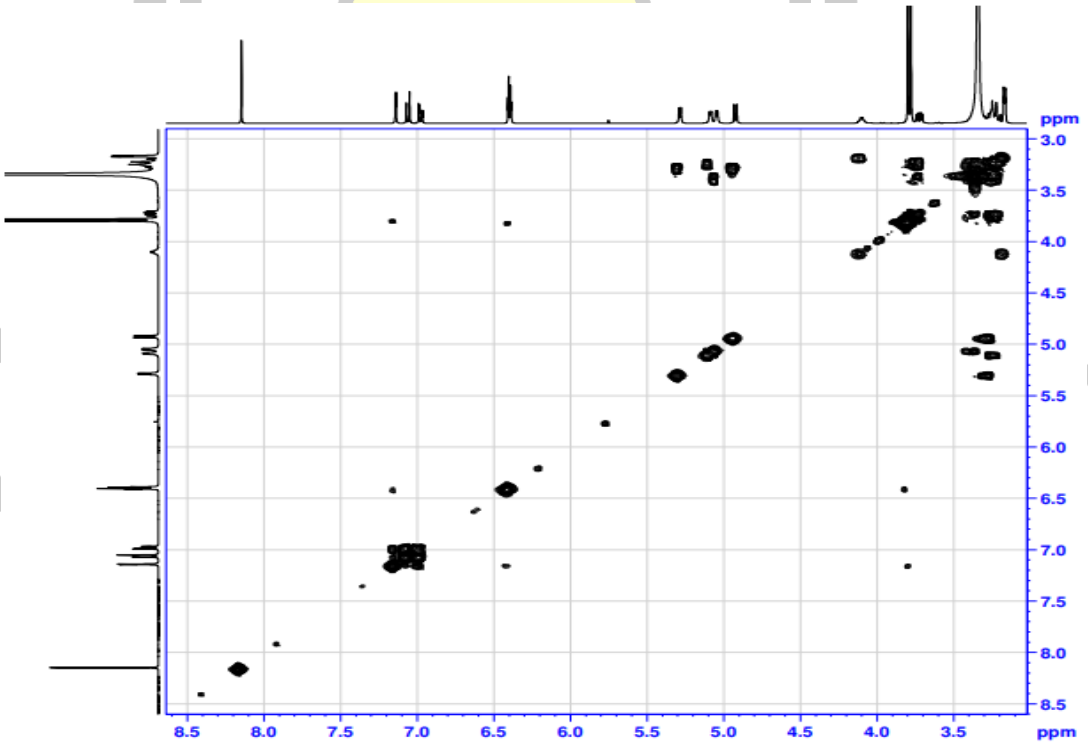

Figure A12. COSY spectrum of **35** (DMSO-d_6, 100 MHz).

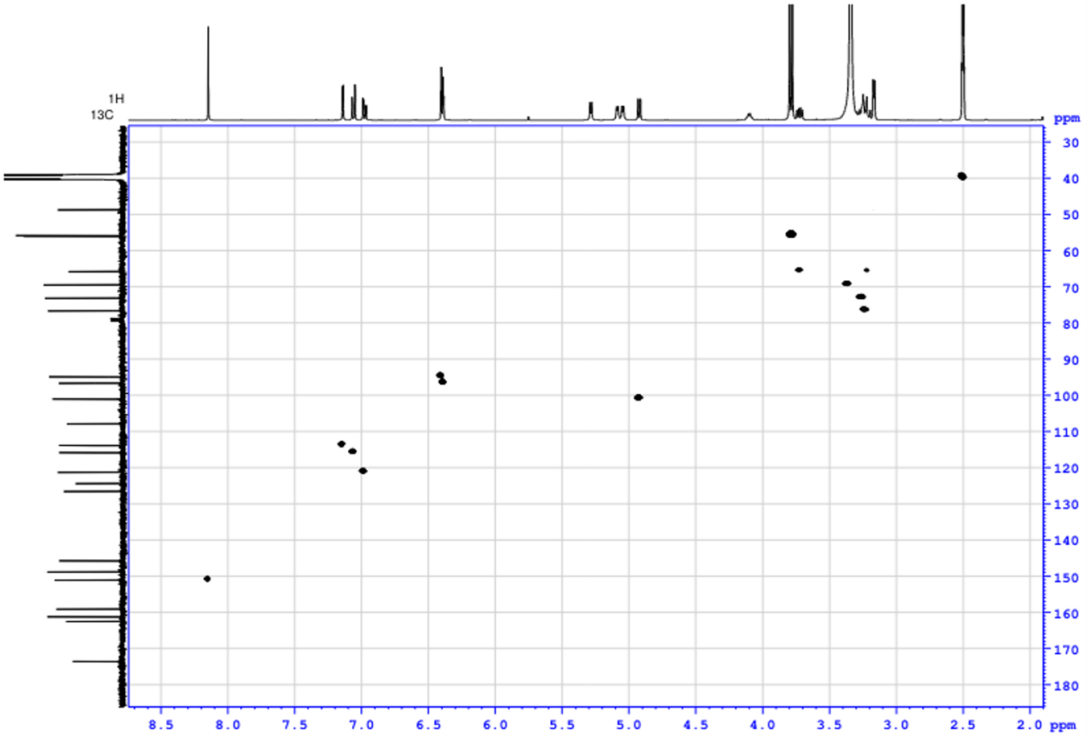

Figure A13. HSQC spectrum of **35** (DMSO-d_6, 100 MHz).

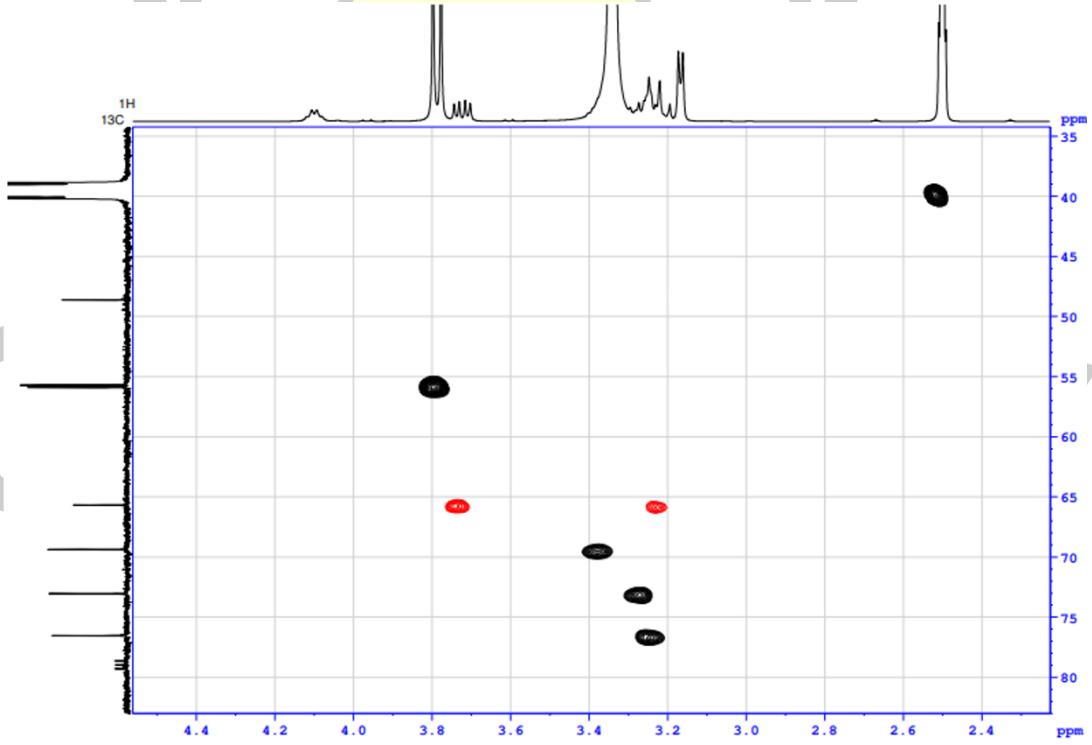

Figure A14. HSQC (expansion 1) spectrum of **35** (DMSO-d_6, 100 MHz).

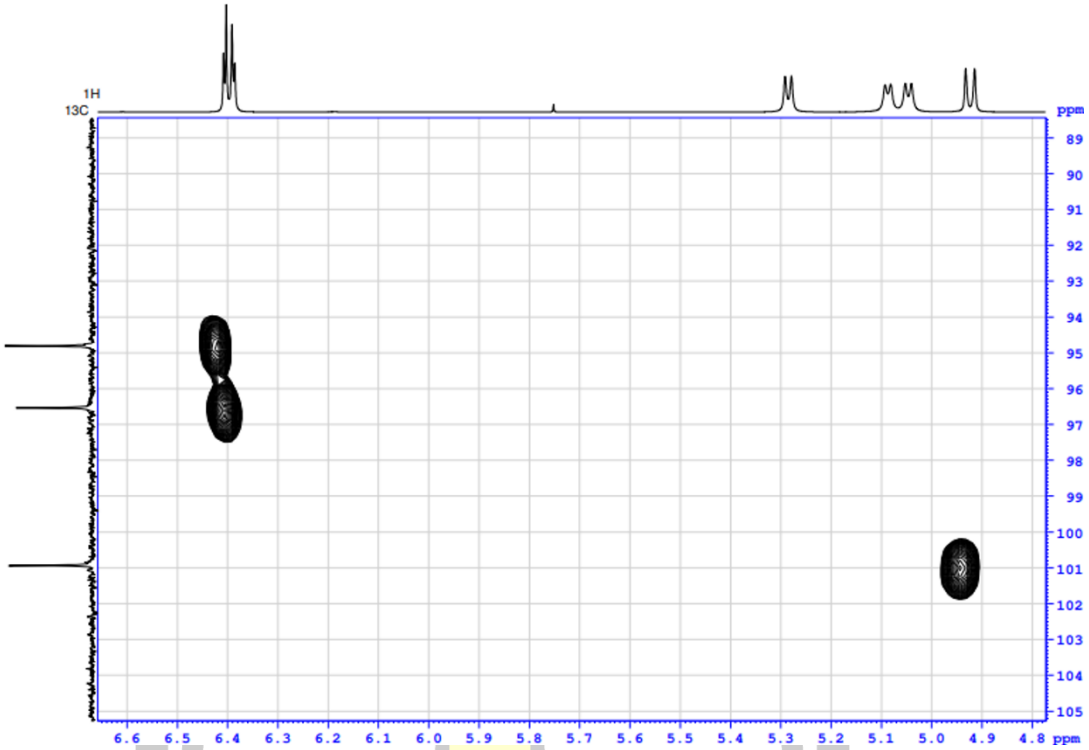

Figure A15. HSQC (expansion 2) spectrum of **35** (DMSO-d_6, 100 MHz).

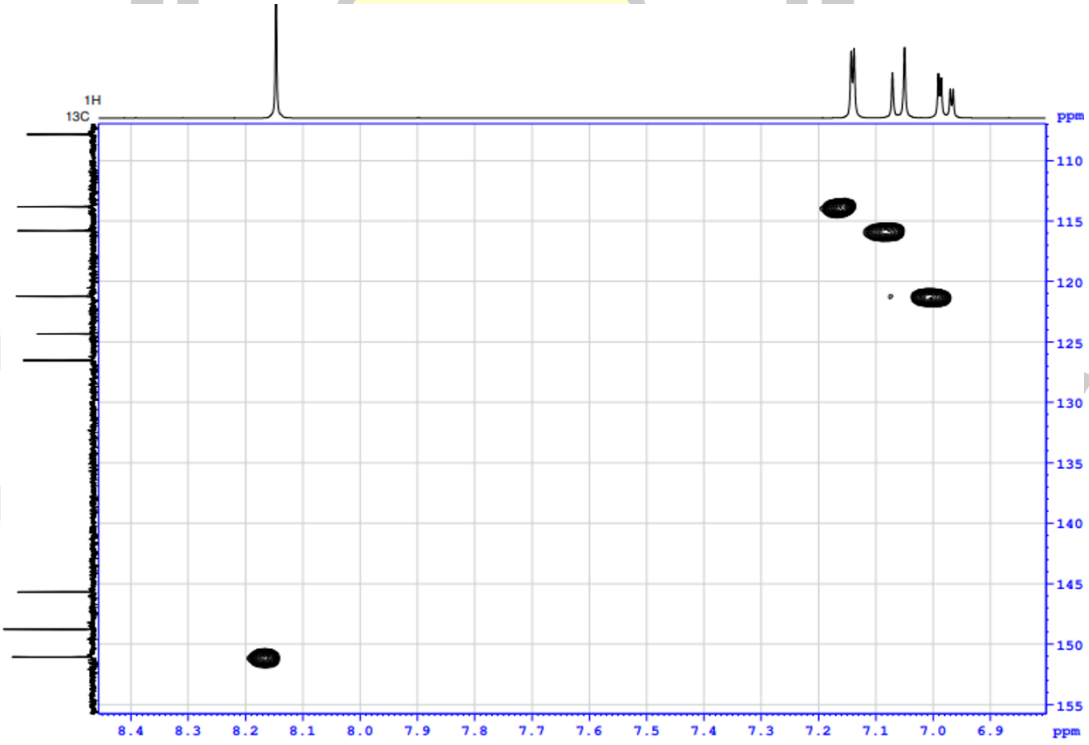

Figure A16. HSQC (expansion 3) spectrum of **35** (DMSO-d_6, 100 MHz).

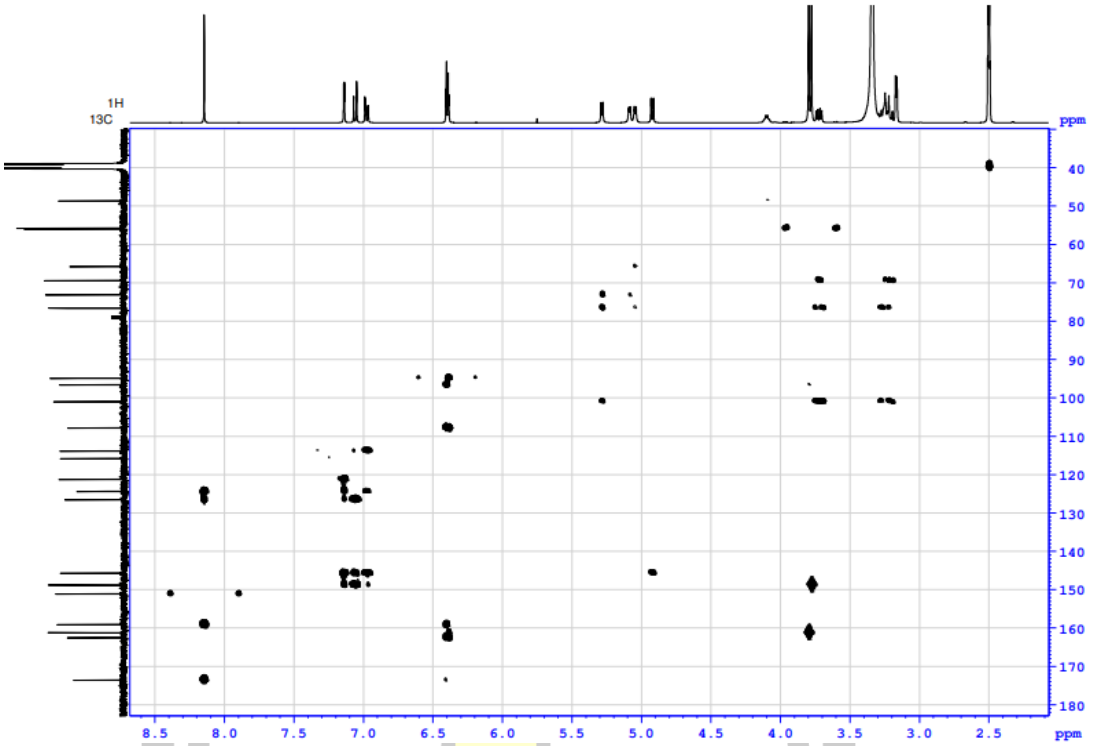

Figure A17. HMBC spectrum of **35** (DMSO-d_6, 100 MHz).

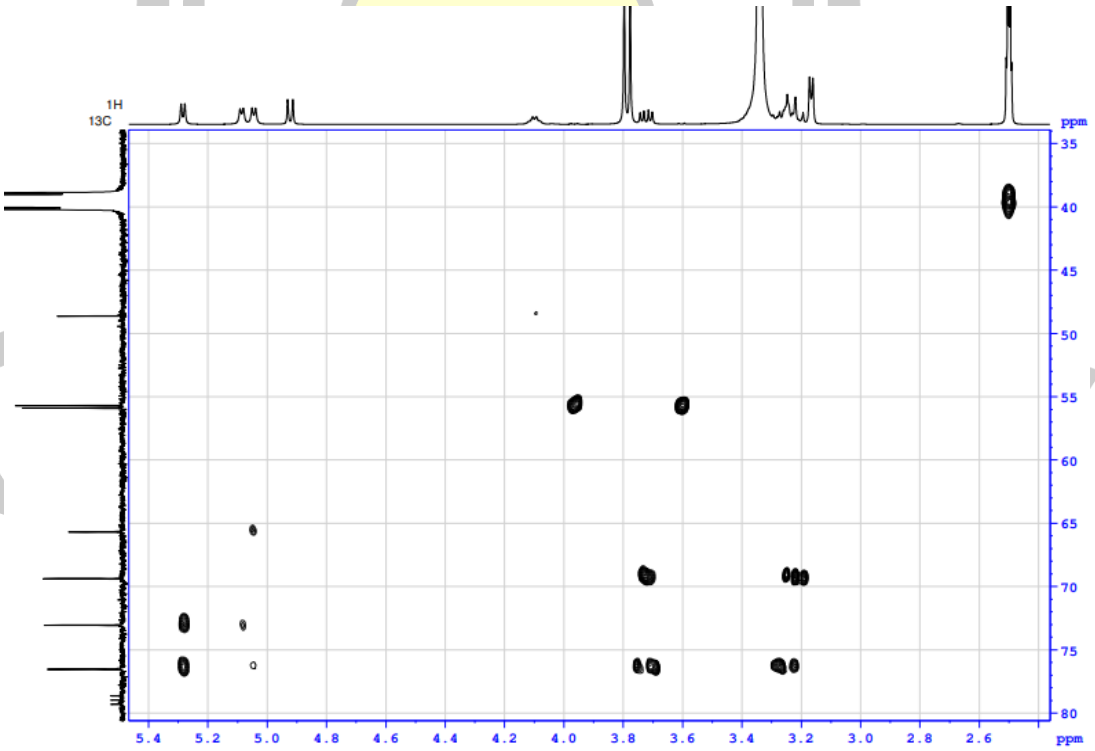

Figure A18. HMBC (expansion 1) spectrum of **35** (DMSO-d_6, 100 MHz).

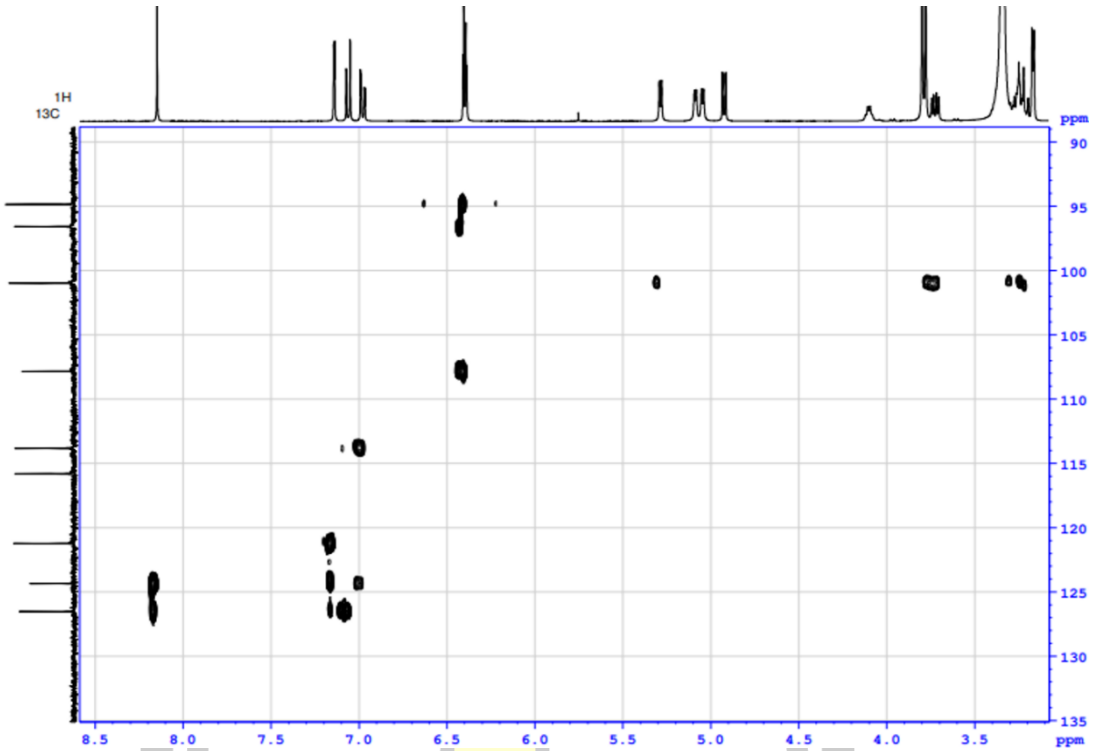

Figure A19. HMBC (expansion 2) spectrum of **35** (DMSO-d_6, 100 MHz).

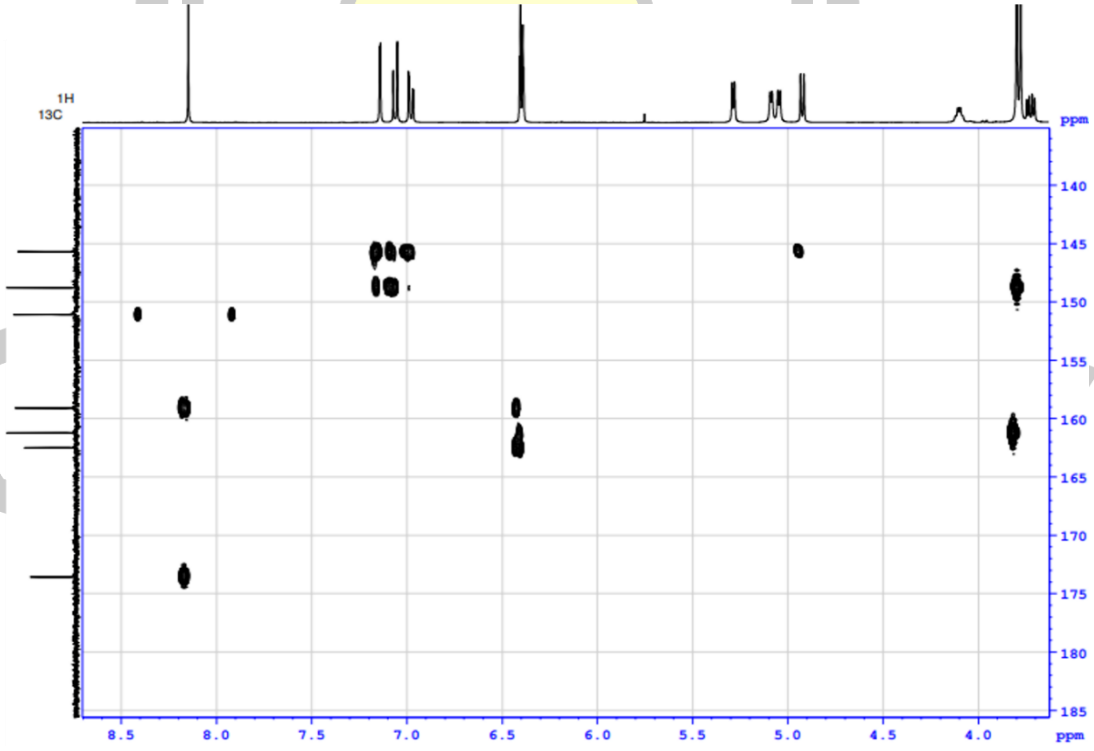

Figure A20. HMBC (expansion 3) spectrum of **35** (DMSO-d_6, 100 MHz).

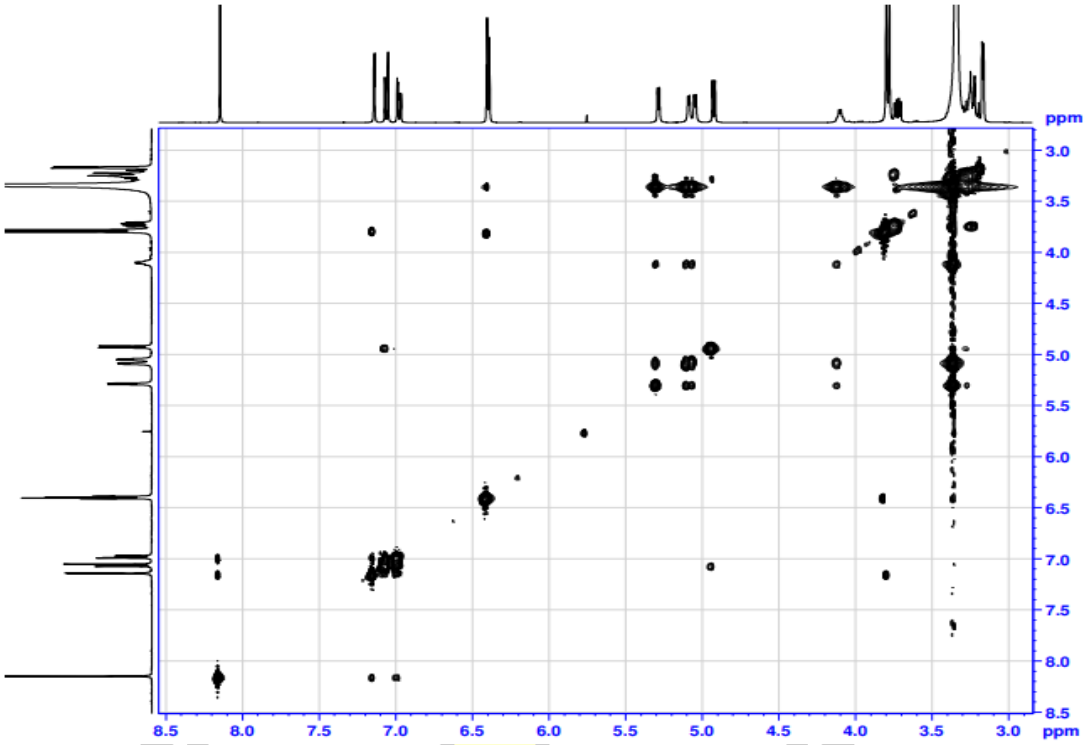

Figure A21. NOESY spectrum of **35** (DMSO-d_6, 100 MHz).

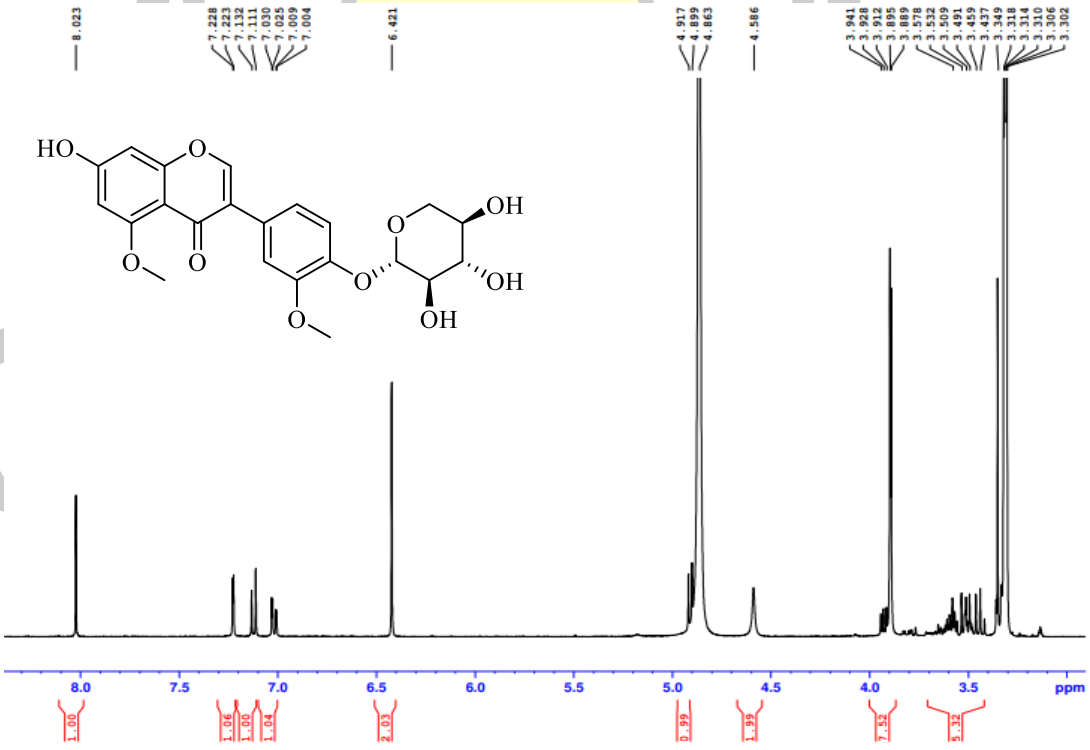

Figure A22. ^{1}H NMR spectrum of **35** (CD_3OD, 400 MHz).

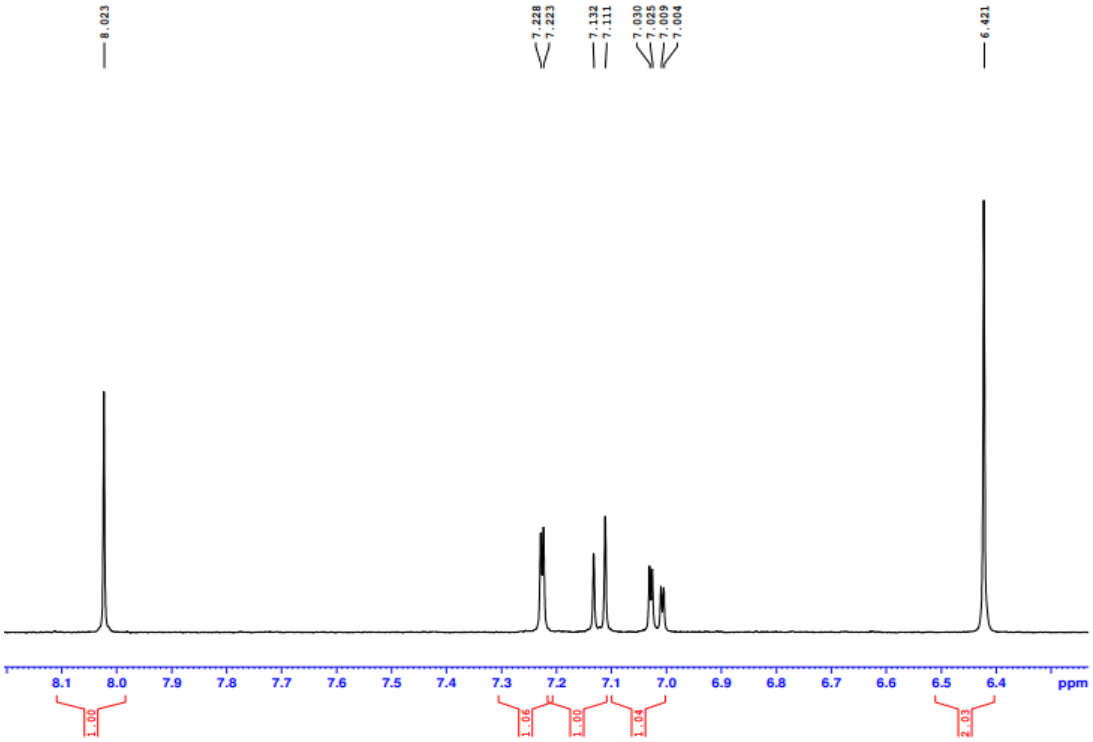

Figure A23. ^{1}H NMR (expansion 1) spectrum of **35** (CD_3OD, 400 MHz).

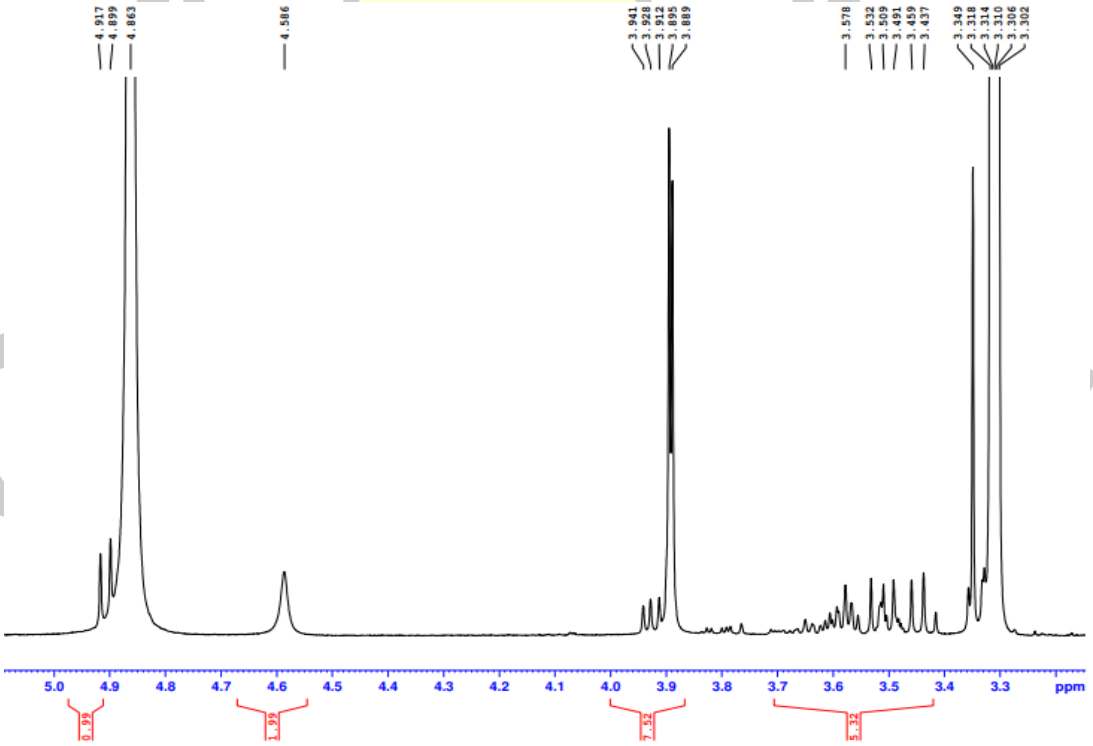

Figure A24. ^{1}H NMR (expansion 2) spectrum of **35** (CD_3OD, 400 MHz).

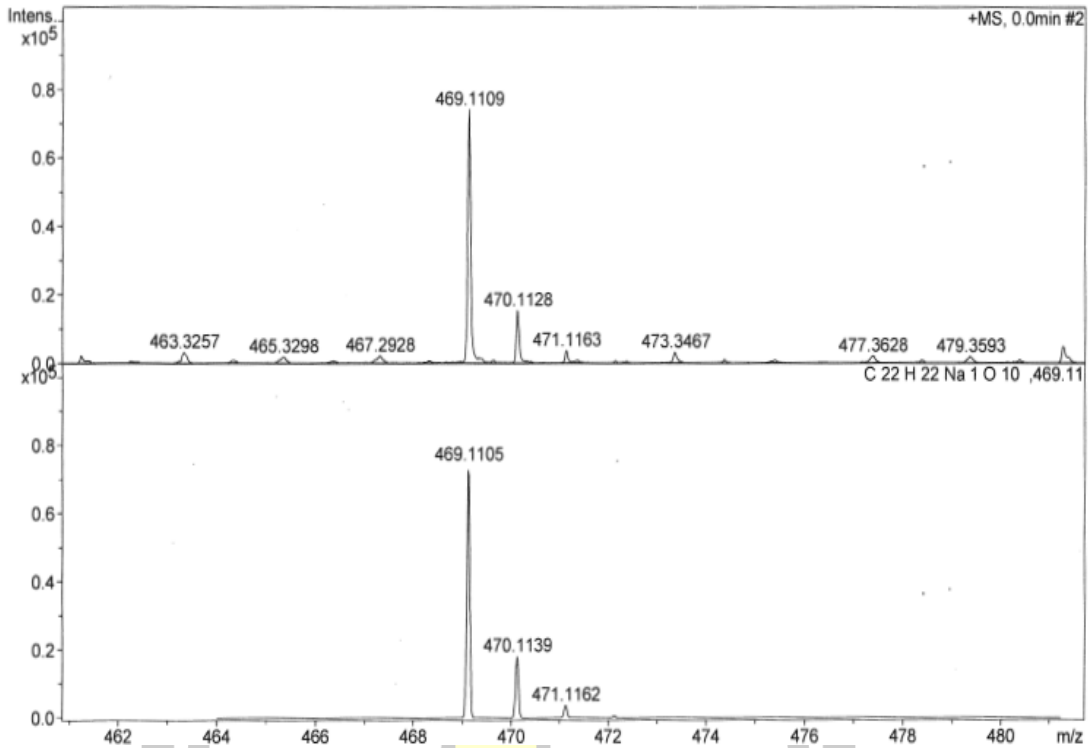

Figure A25. HRESIMS of **35** (positive ion mode).

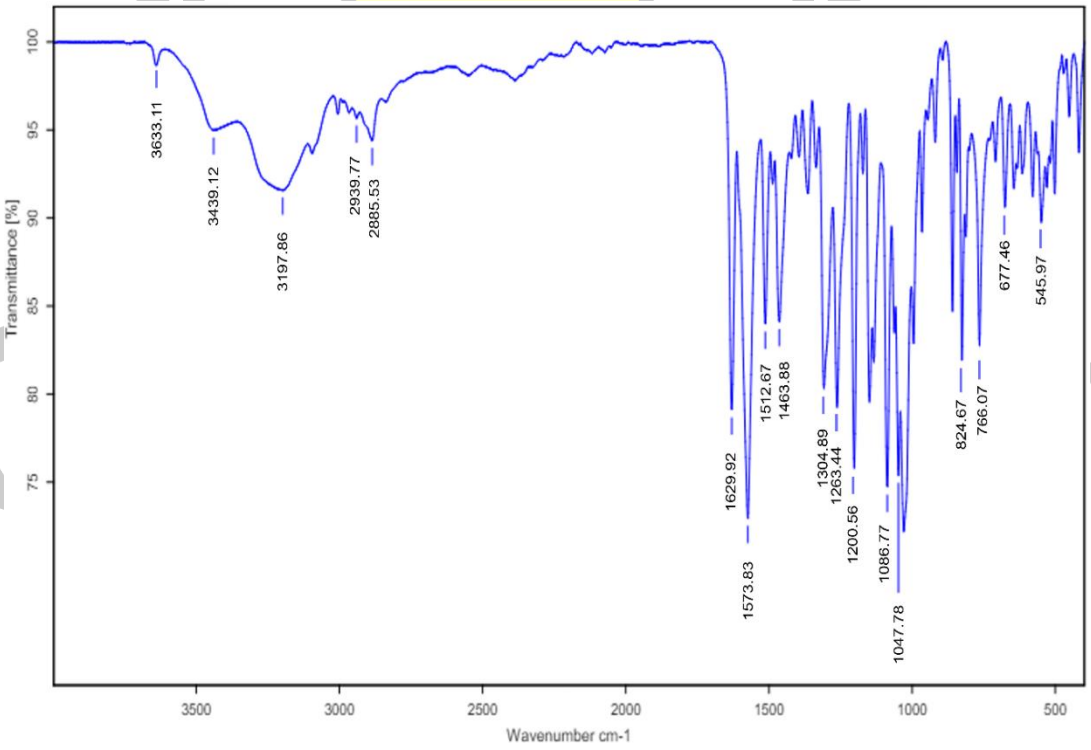

Figure A26. FTIR spectrum of **35**.

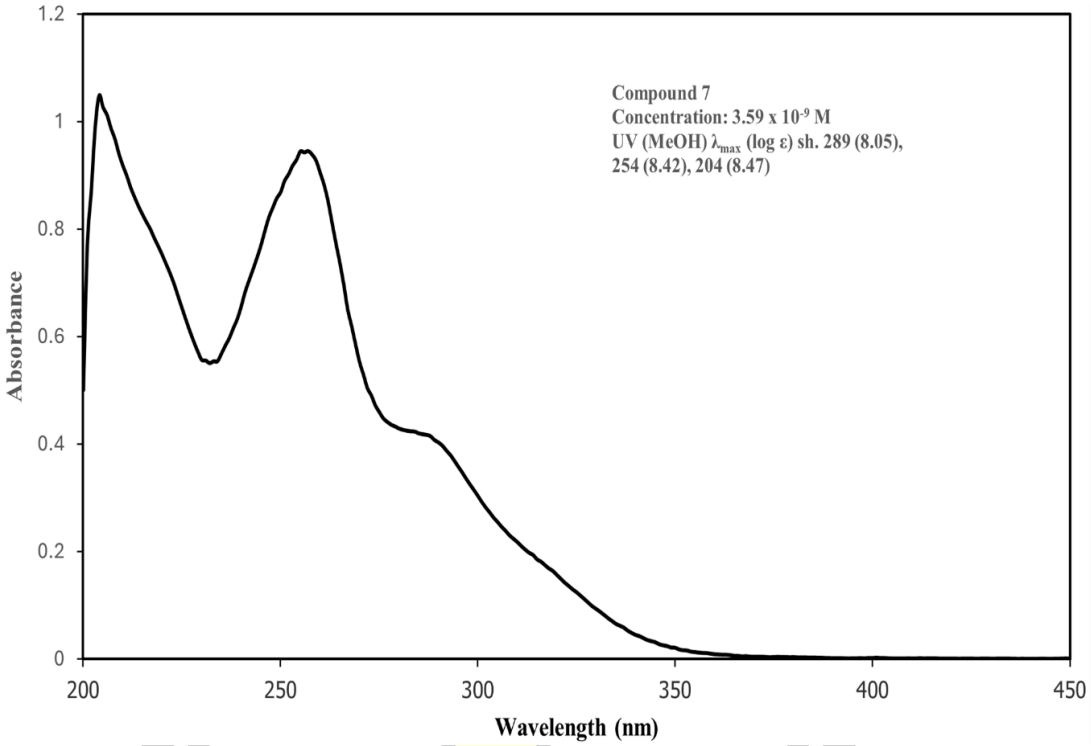

Figure A27. UV spectrum of **35** (MeOH).

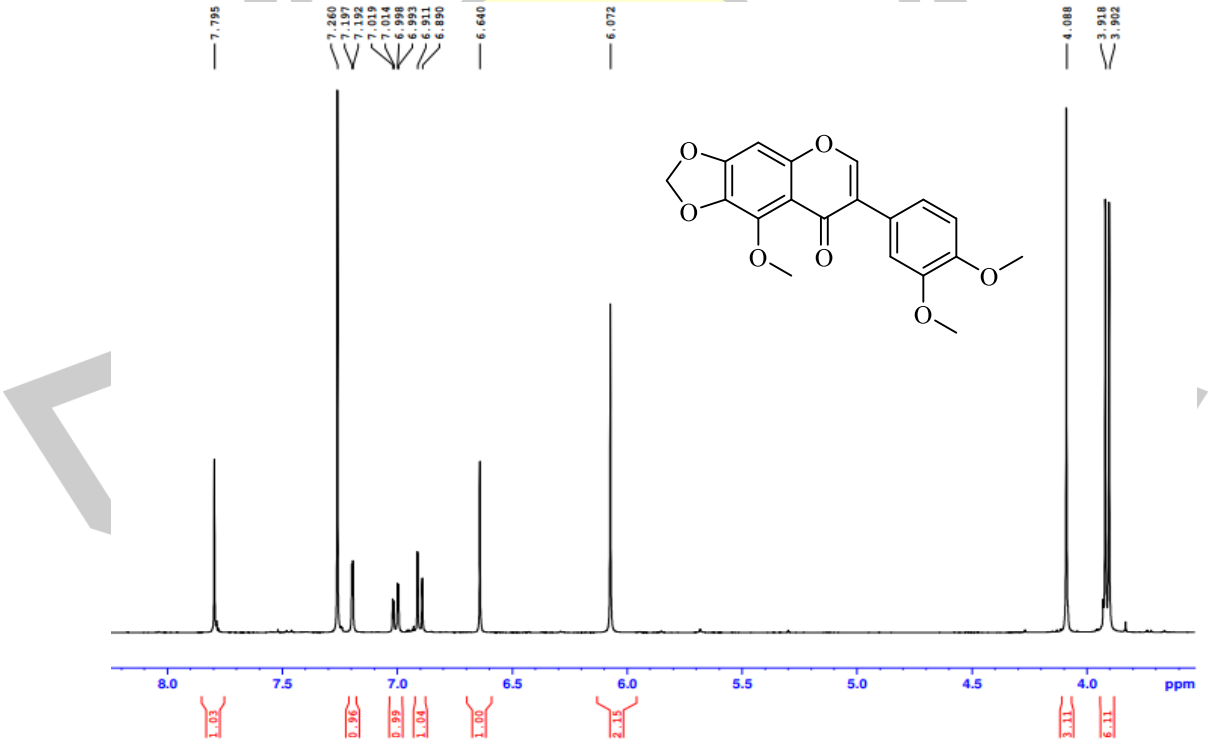

Figure A28. ^{1}H NMR spectrum of **11** ($CDCl_3$, 400 MHz).

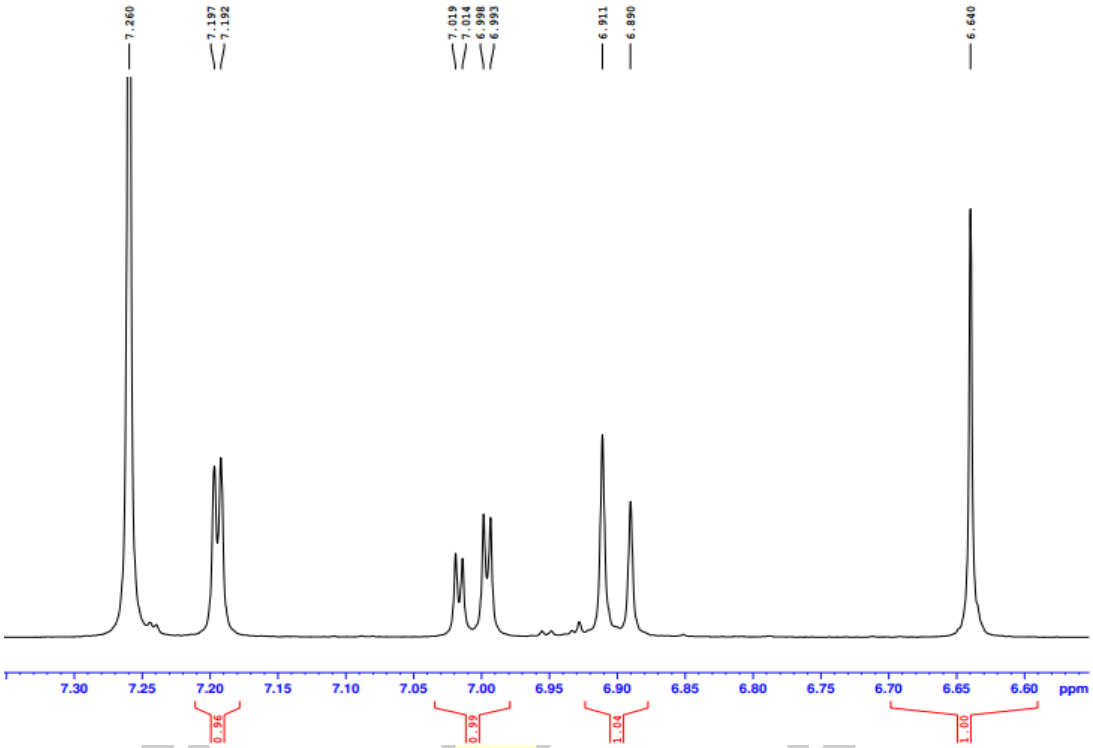

Figure A29. ^{1}H NMR (expansion 1) spectrum of **11** ($CDCl_3$, 400 MHz).

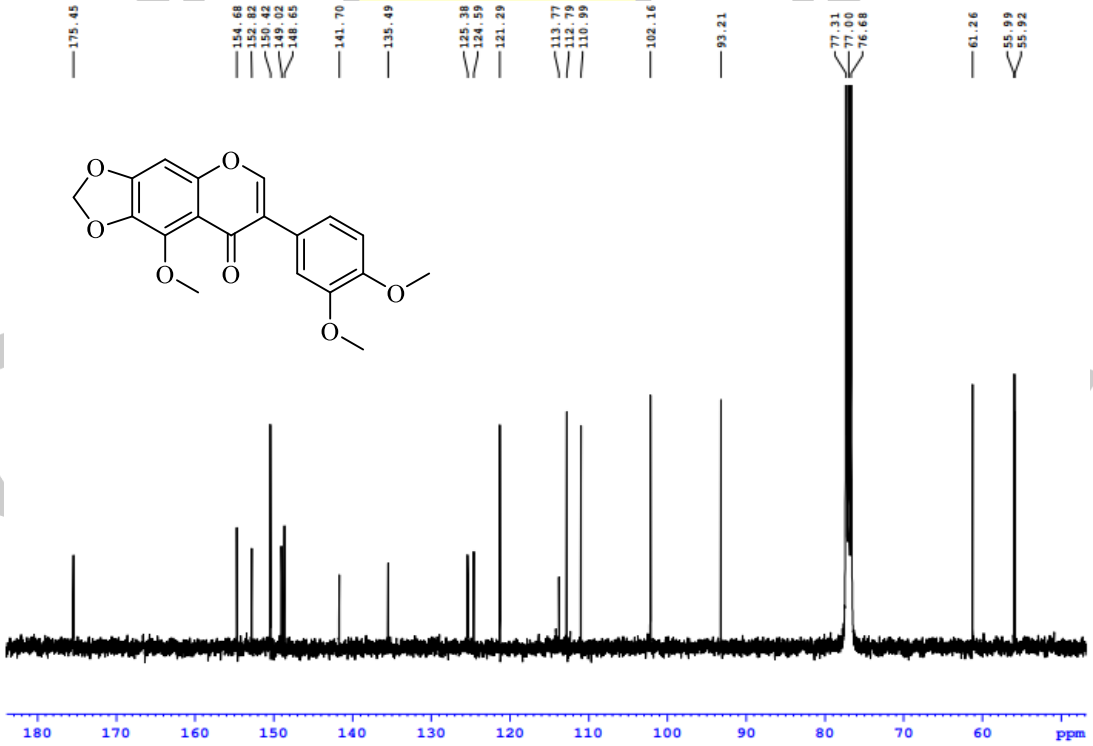

Figure A30. ^{13}C NMR spectrum of **11** ($CDCl_3$, 100 MHz).

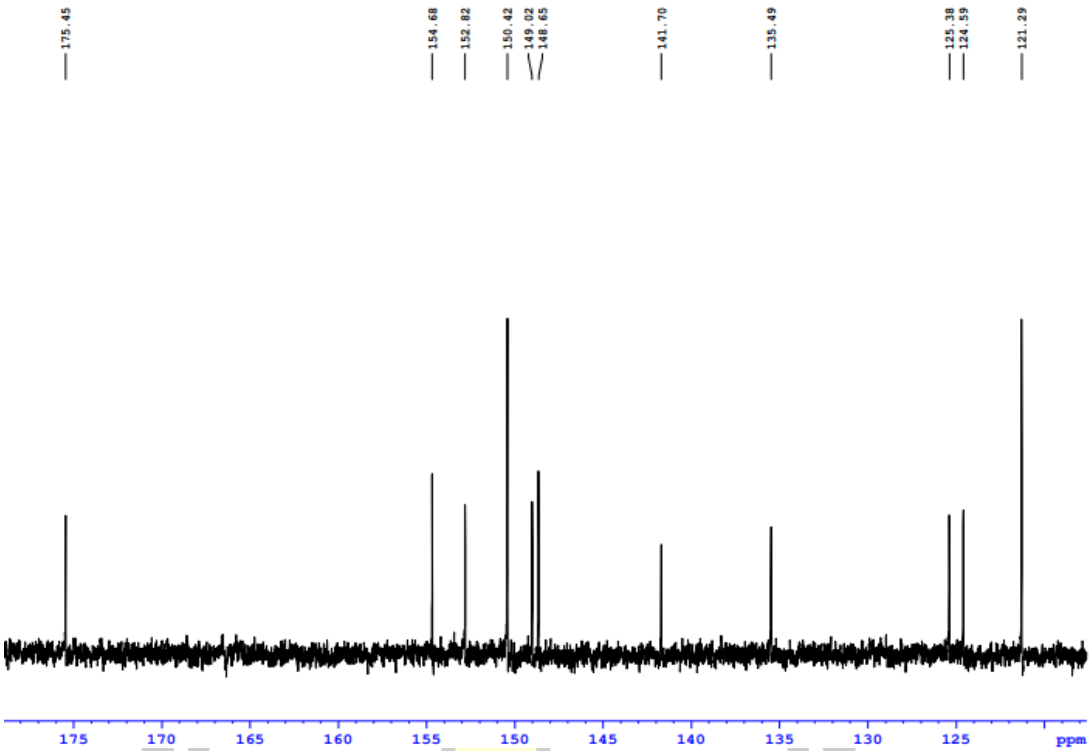

Figure A31. ^{13}C NMR (expansion 1) spectrum of **11** ($CDCl_3$, 100 MHz).

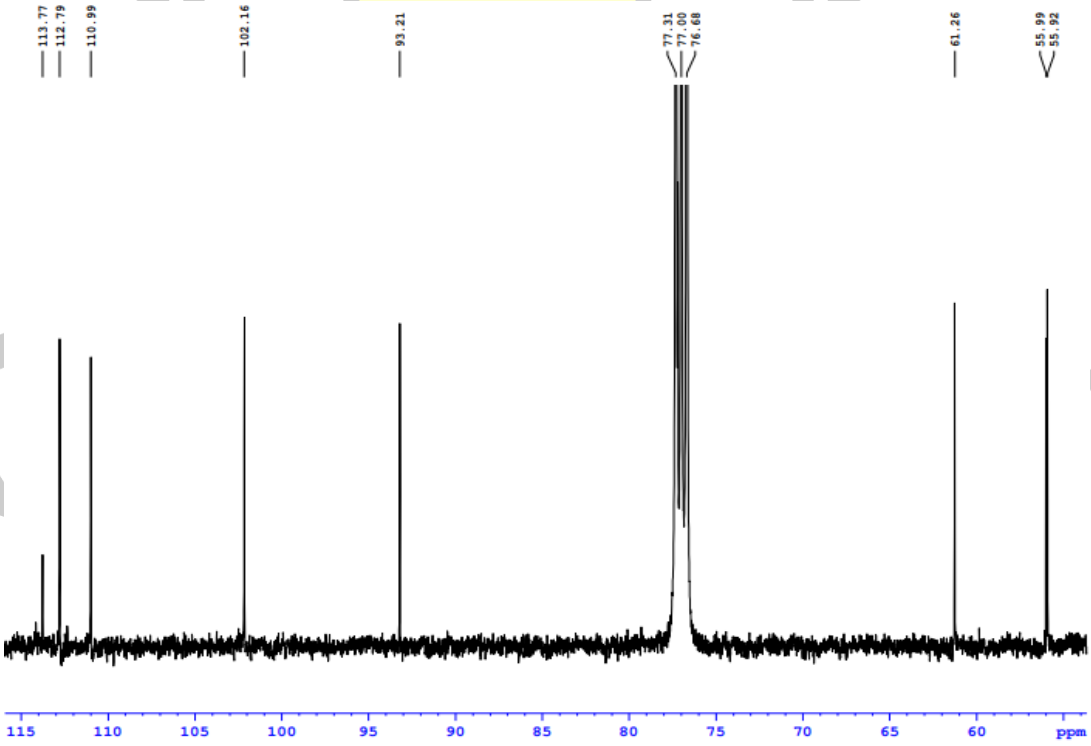

Figure A32. ^{13}C NMR (expansion 2) spectrum of **11** ($CDCl_3$, 100 MHz).

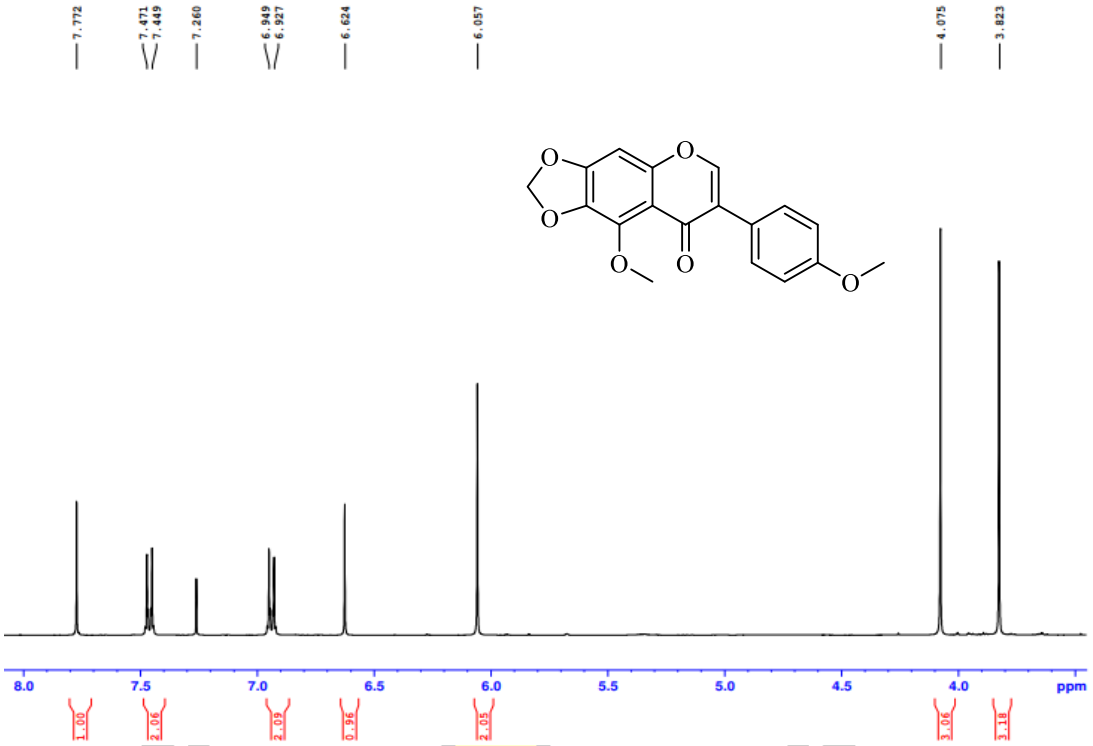

Figure A33. ^{1}H NMR spectrum of **12** ($CDCl_3$, 400 MHz).

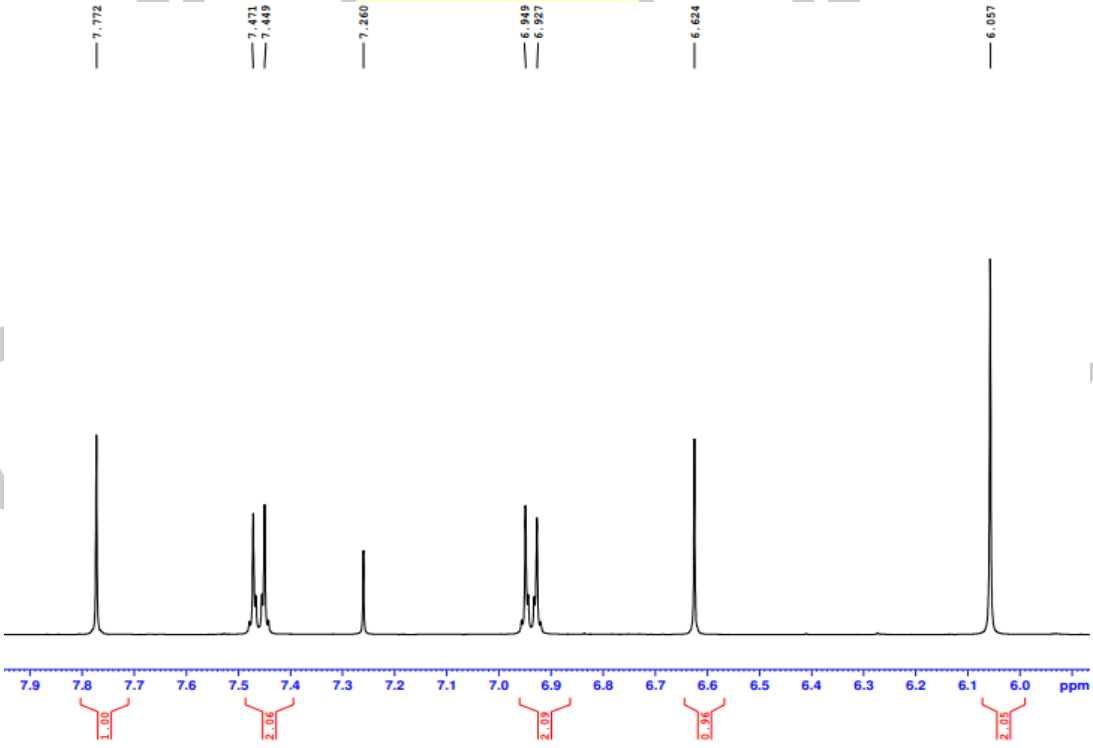

Figure A34. ^{1}H NMR (expansion 1) spectrum of **12** ($CDCl_3$, 400 MHz).

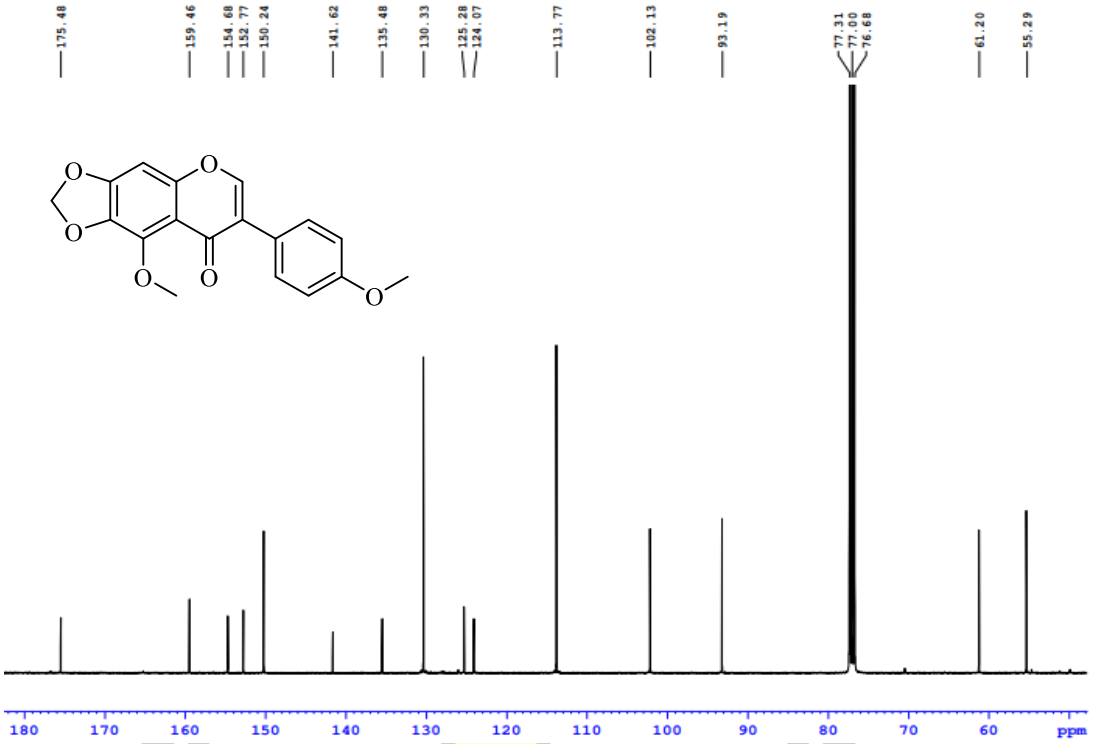

Figure A35. ^{13}C NMR spectrum of **12** ($CDCl_3$, 100 MHz).

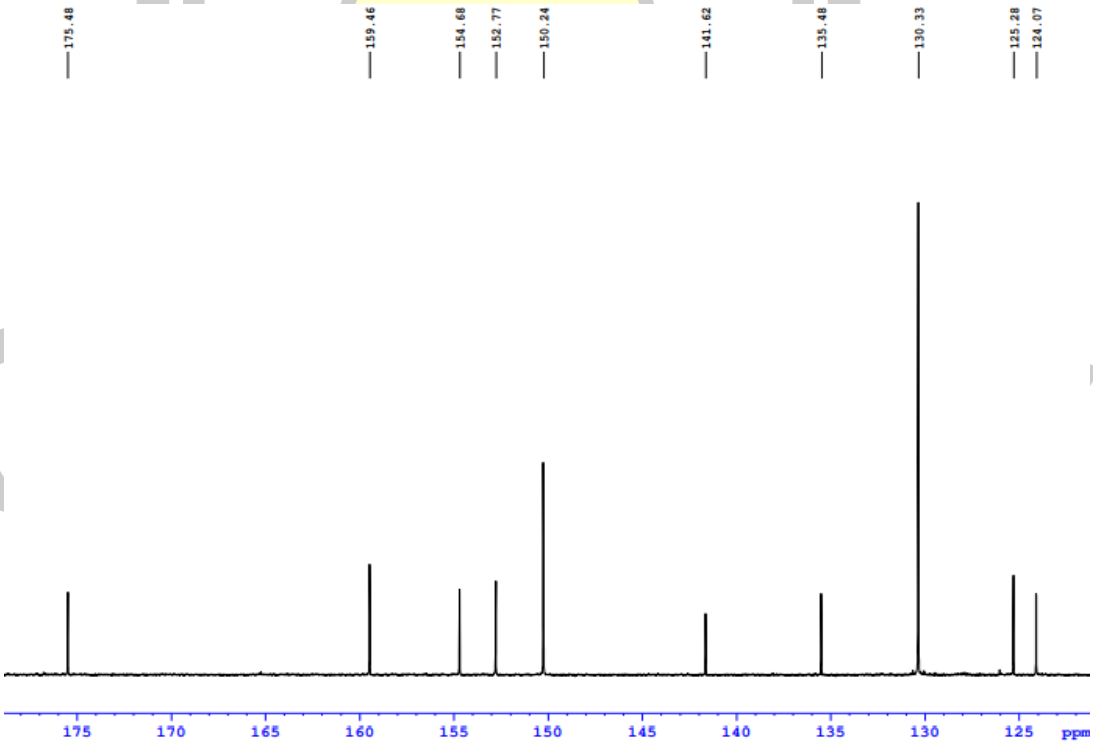

Figure A36. ^{13}C NMR (expansion 1) spectrum of **12** ($CDCl_3$, 100 MHz).

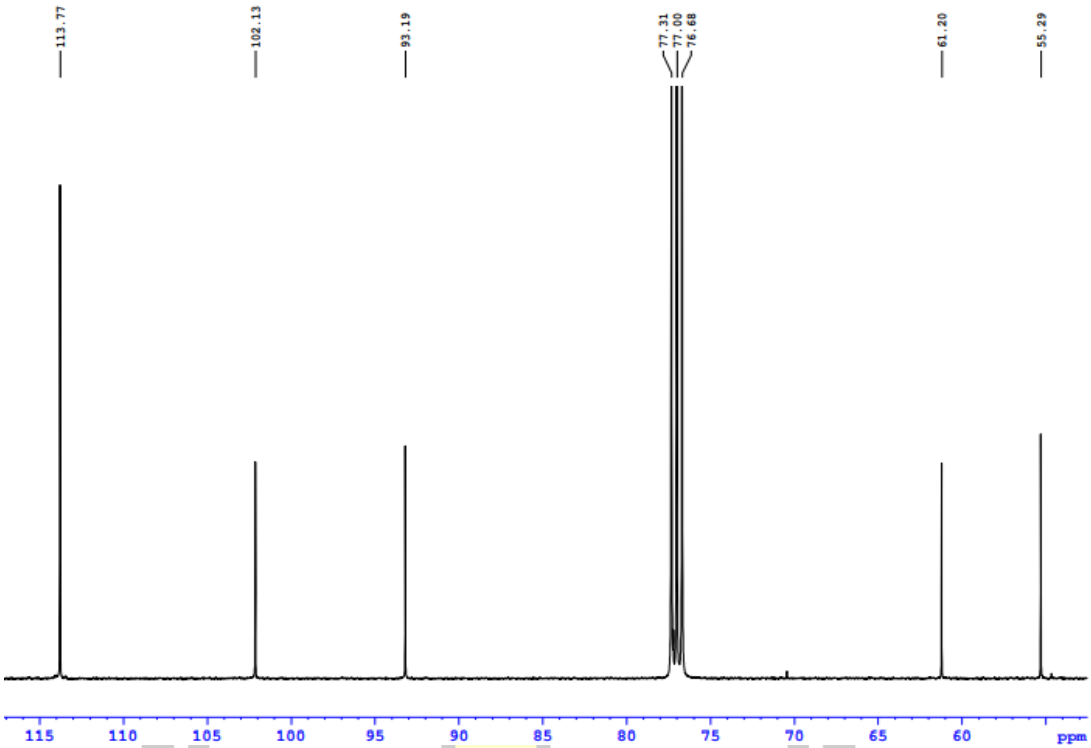

Figure A37. ^{13}C NMR (expansion 2) spectrum of **12** ($CDCl_3$, 100 MHz).

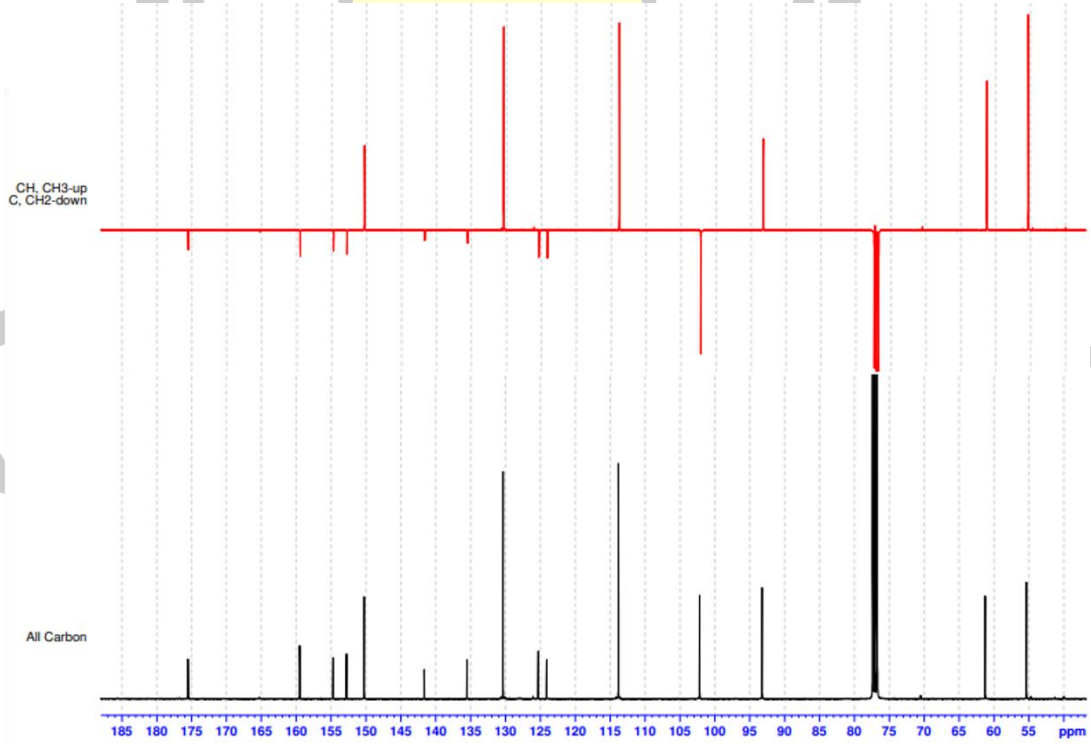

Figure A38. DEPT-135 spectrum of **12** ($CDCl_3$, 100 MHz).

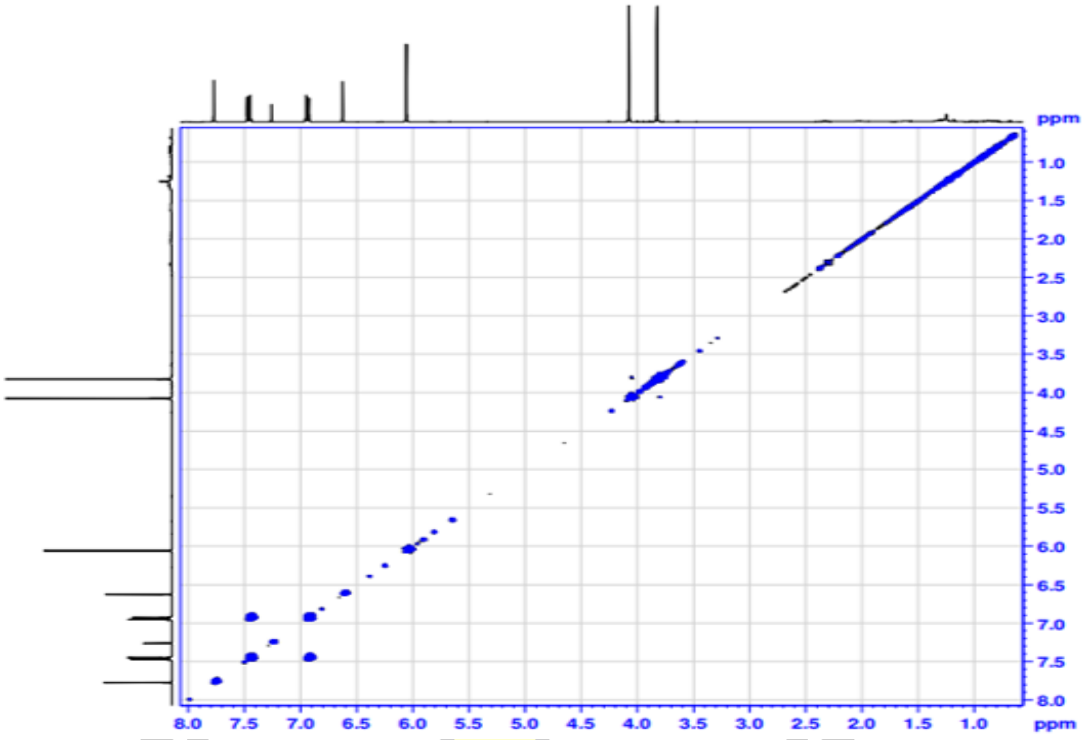

Figure A39. COSY spectrum of **12** ($CDCl_3$, 100 MHz).

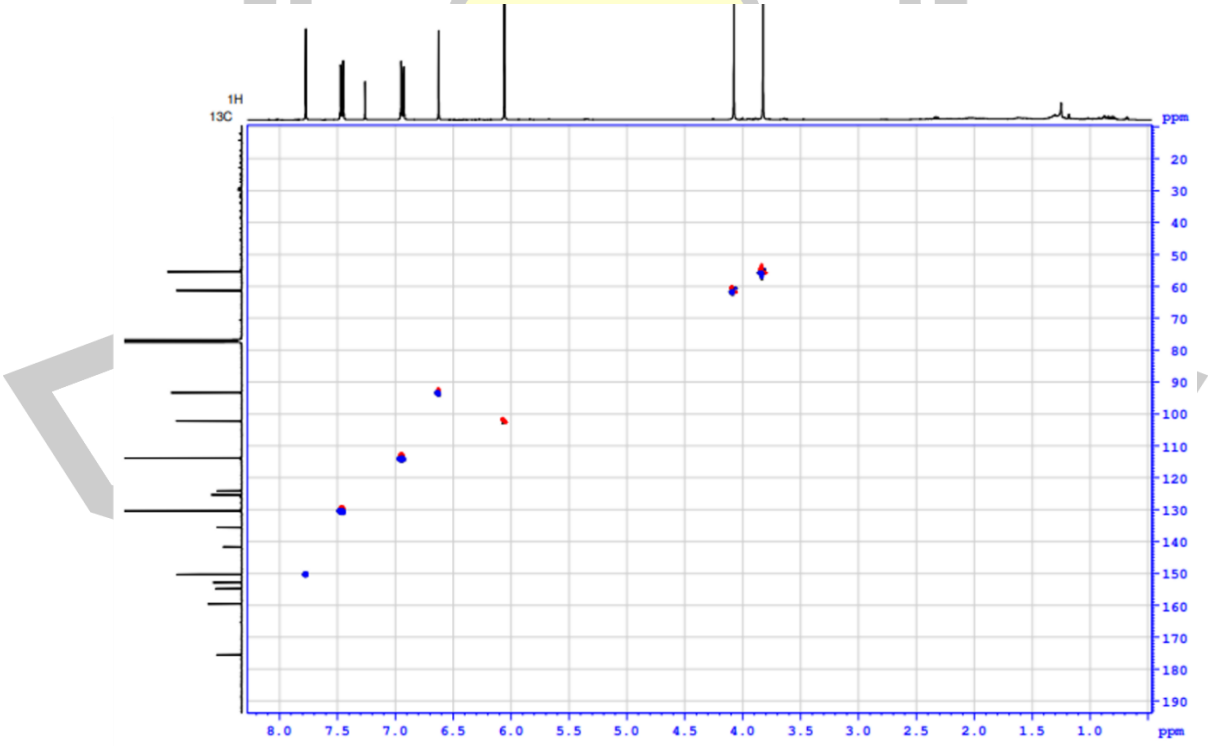

Figure A40. HSQC spectrum of **12** ($CDCl_3$, 100 MHz).

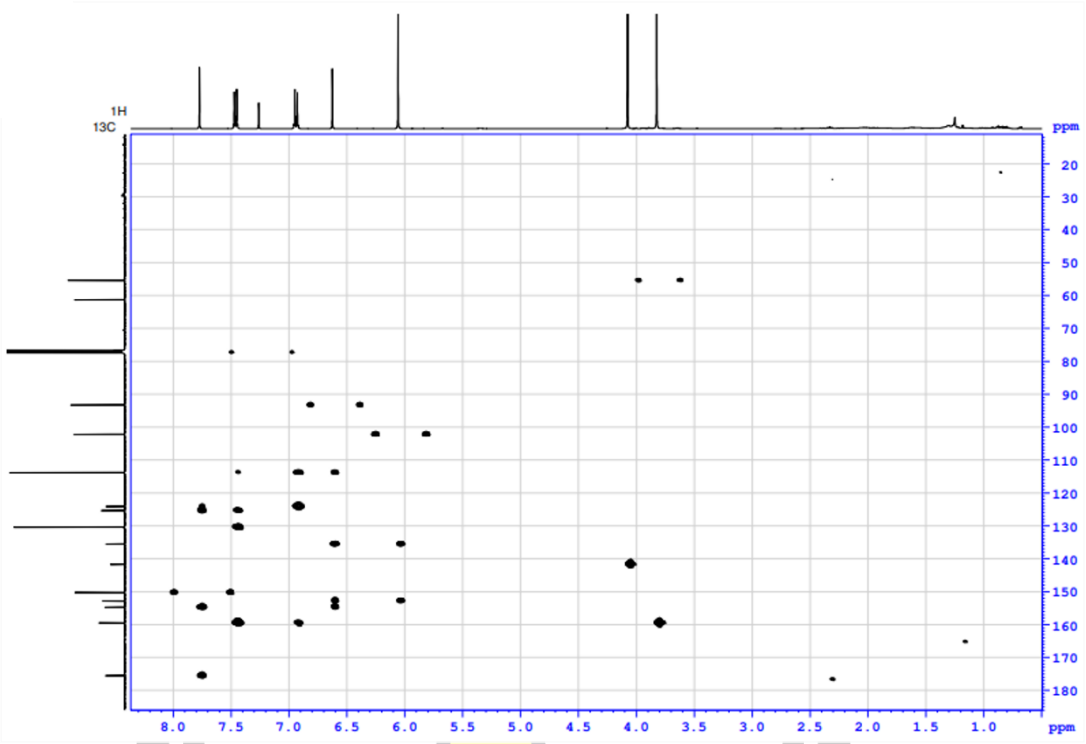

Figure A41. HMBC spectrum of **12** ($CDCl_3$, 100 MHz).

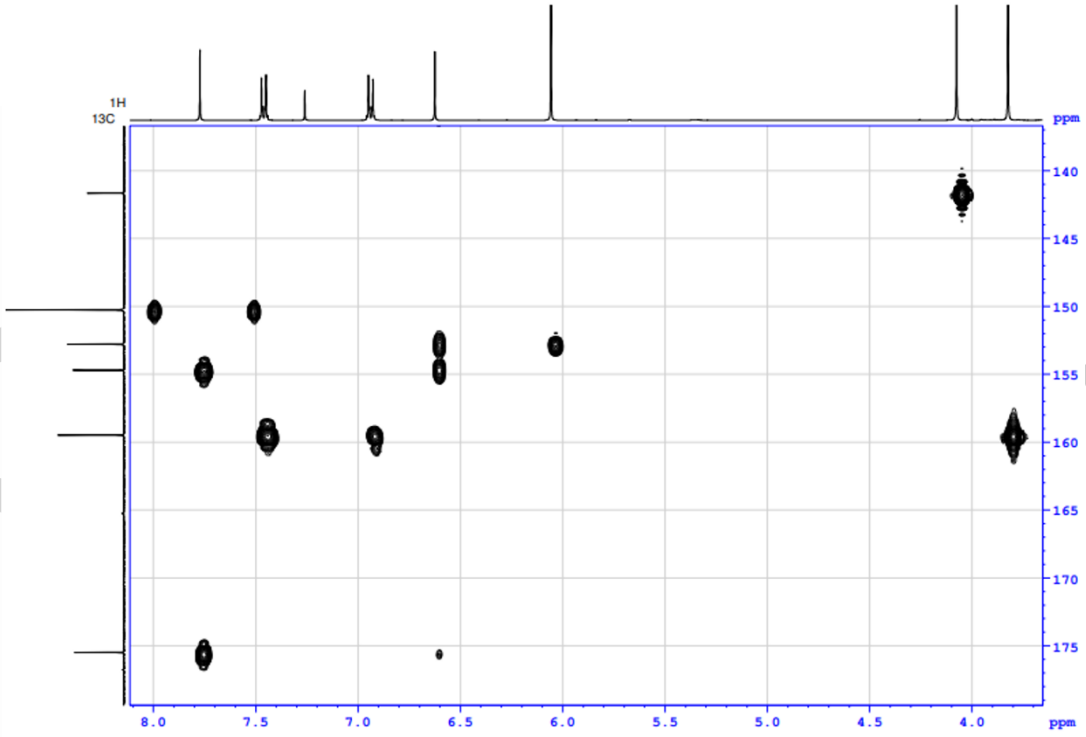

Figure A42. HMBC (expansion 1) spectrum of **12** ($CDCl_3$, 100 MHz).

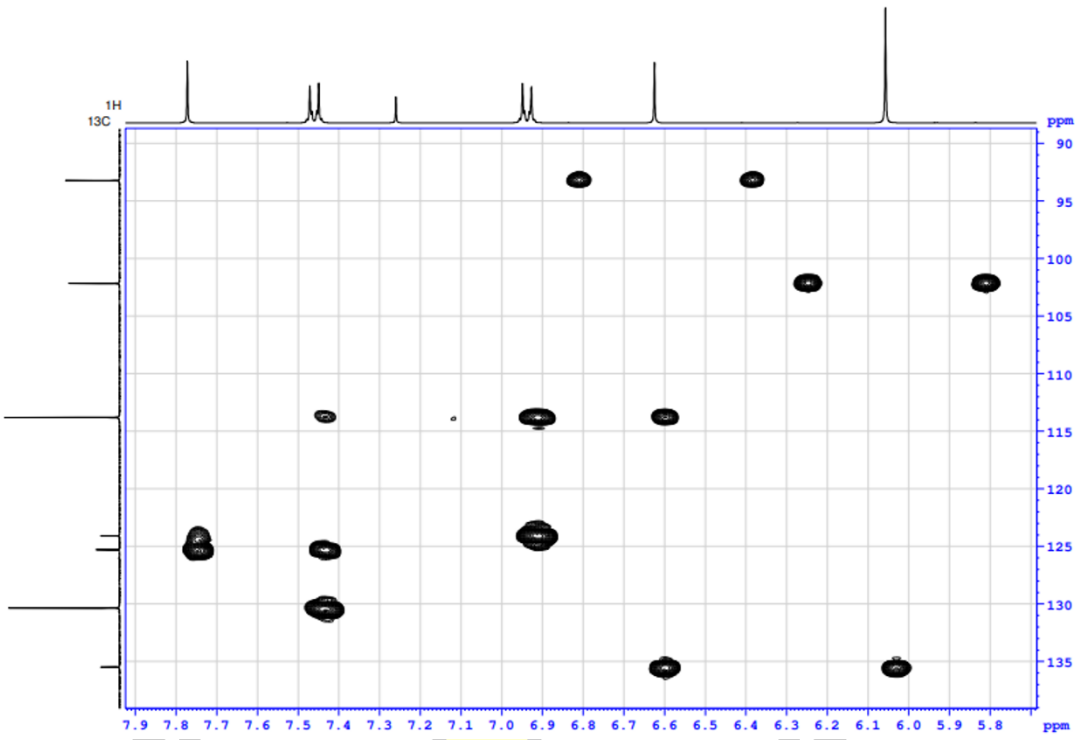

Figure A43. HMBC (expansion 2) spectrum of **12** ($CDCl_3$, 100 MHz).

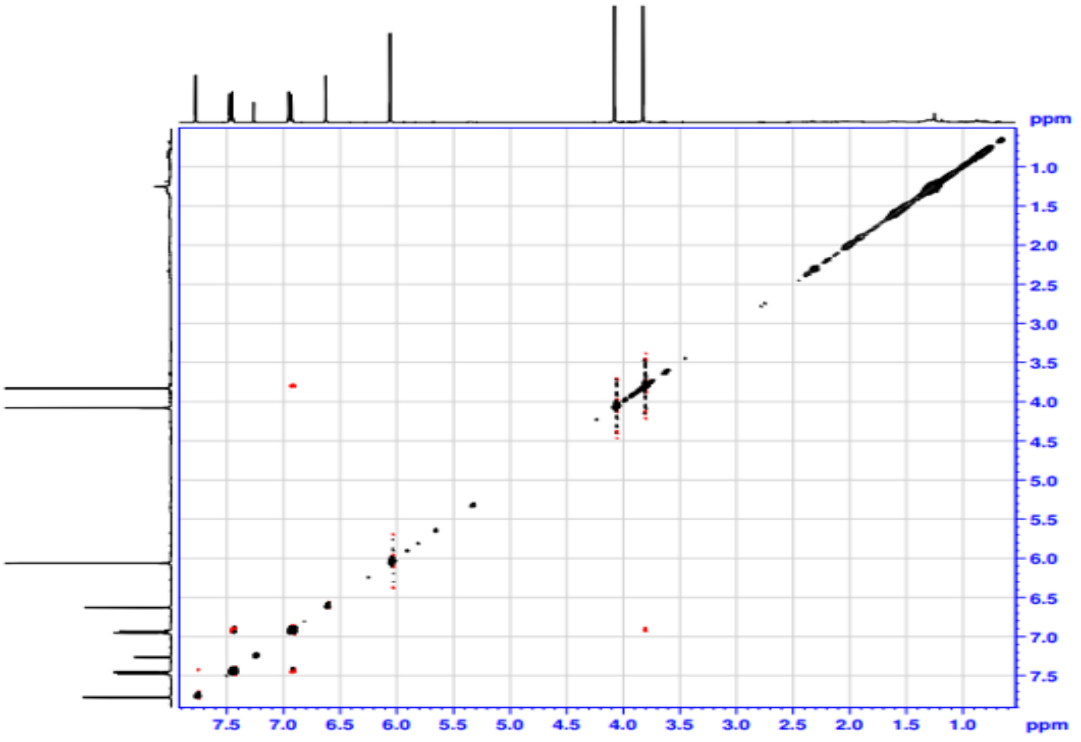

Figure A44. NOESY spectrum of **12** ($CDCl_3$, 100 MHz).

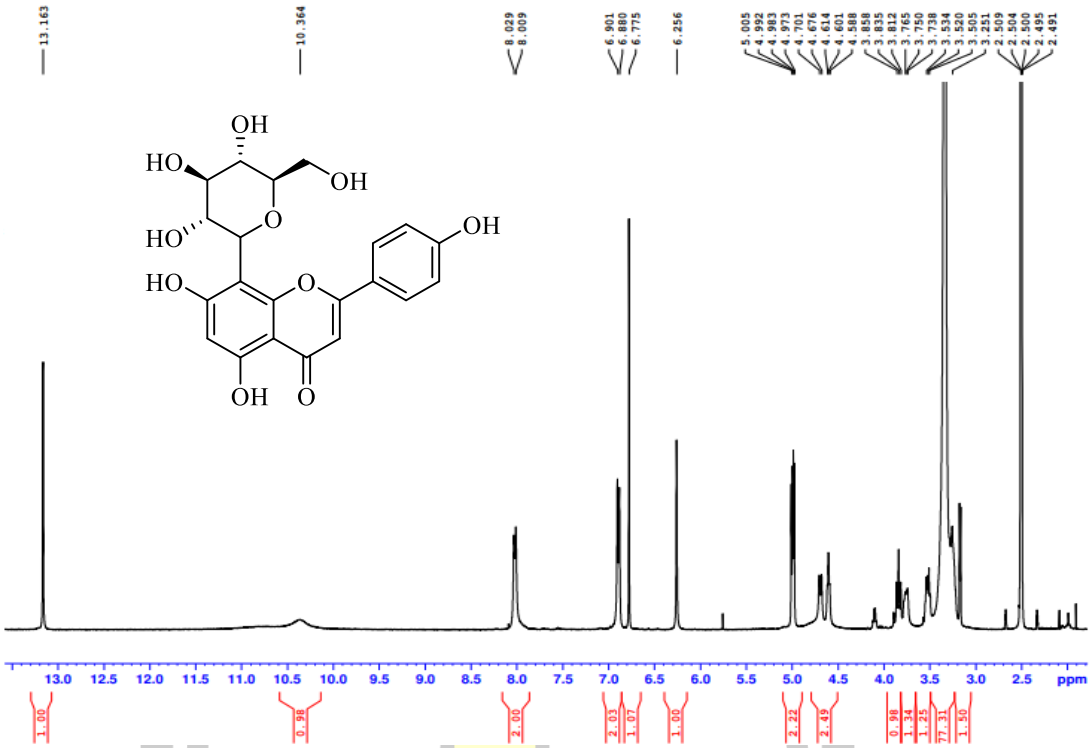

Figure A45. ^{1}H NMR spectrum of **13** (DMSO-d_6, 400 MHz).

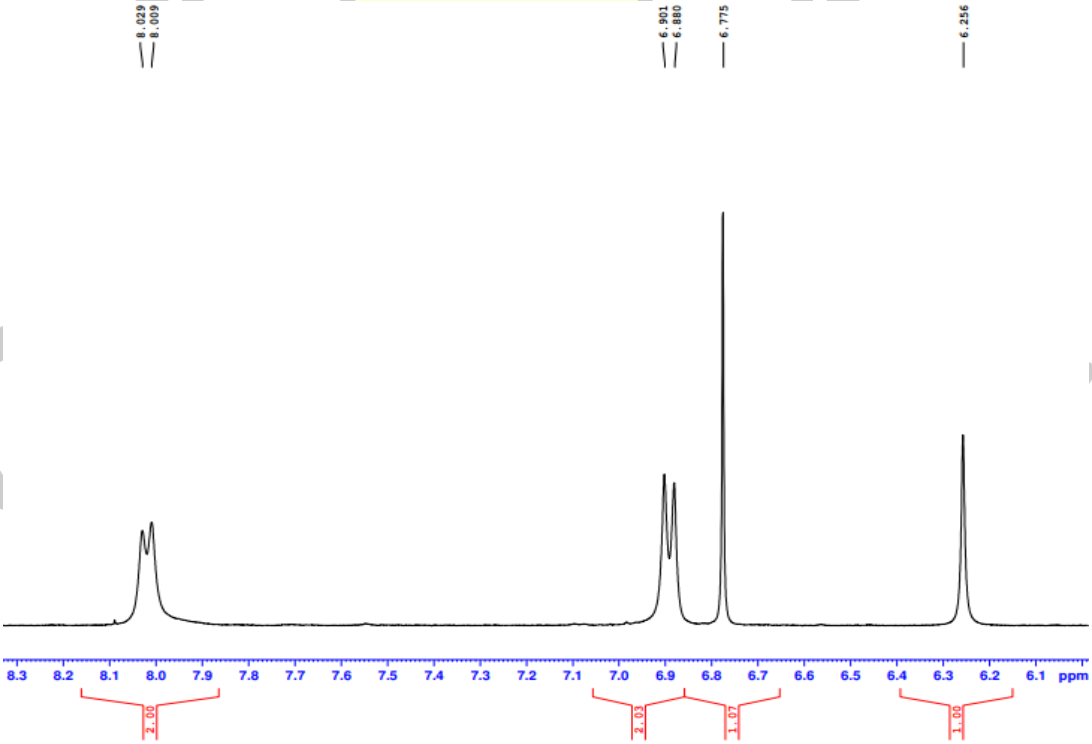

Figure A46. ^{1}H NMR (expansion 1) spectrum of **13** (DMSO-d_6, 400 MHz).

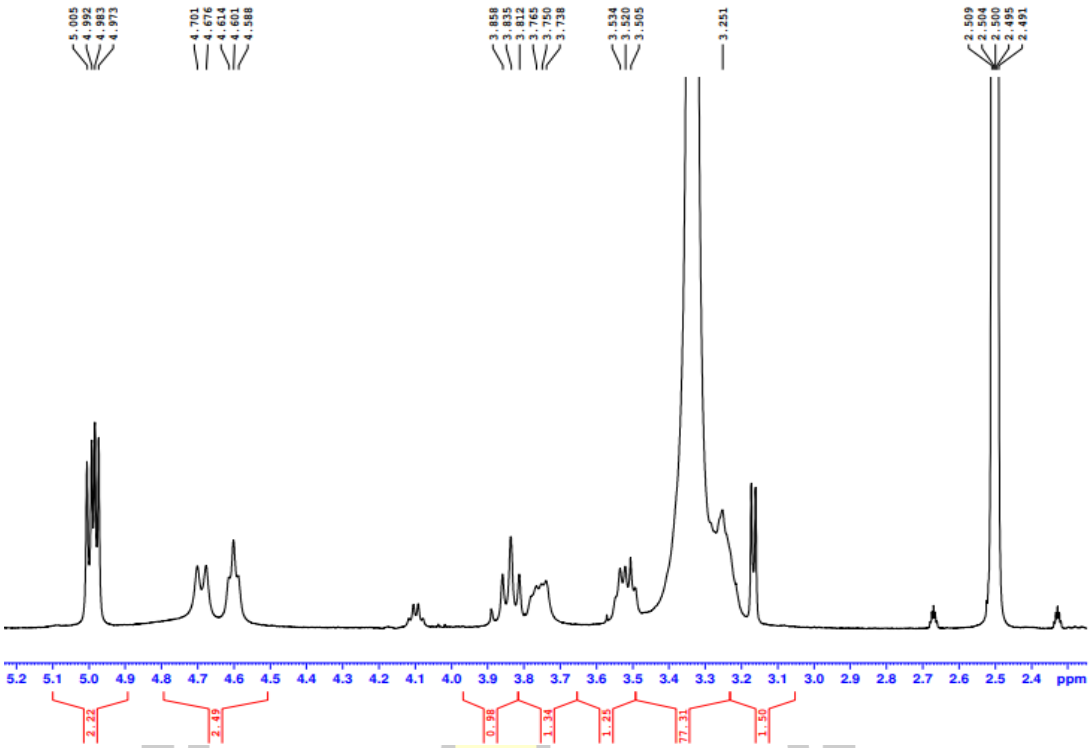

Figure A47. ^{1}H NMR (expansion 2) spectrum of **13** (DMSO-d_6, 400 MHz).

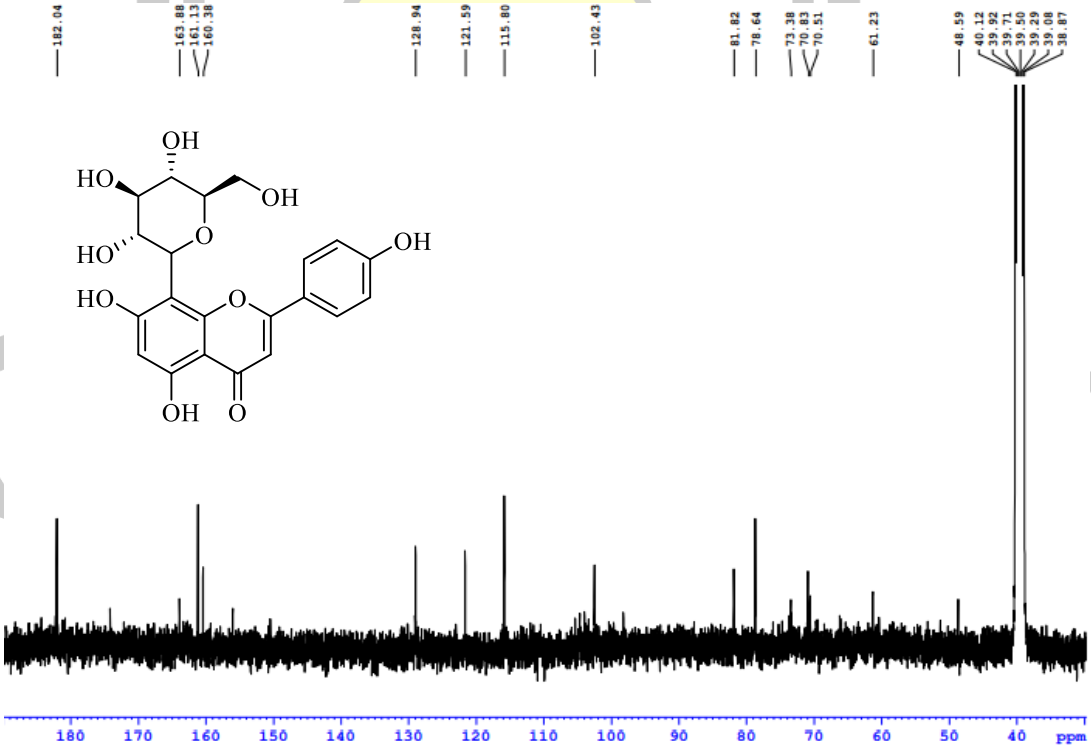

Figure A48. ^{13}C NMR spectrum of **13** (DMSO-d_6, 100 MHz).

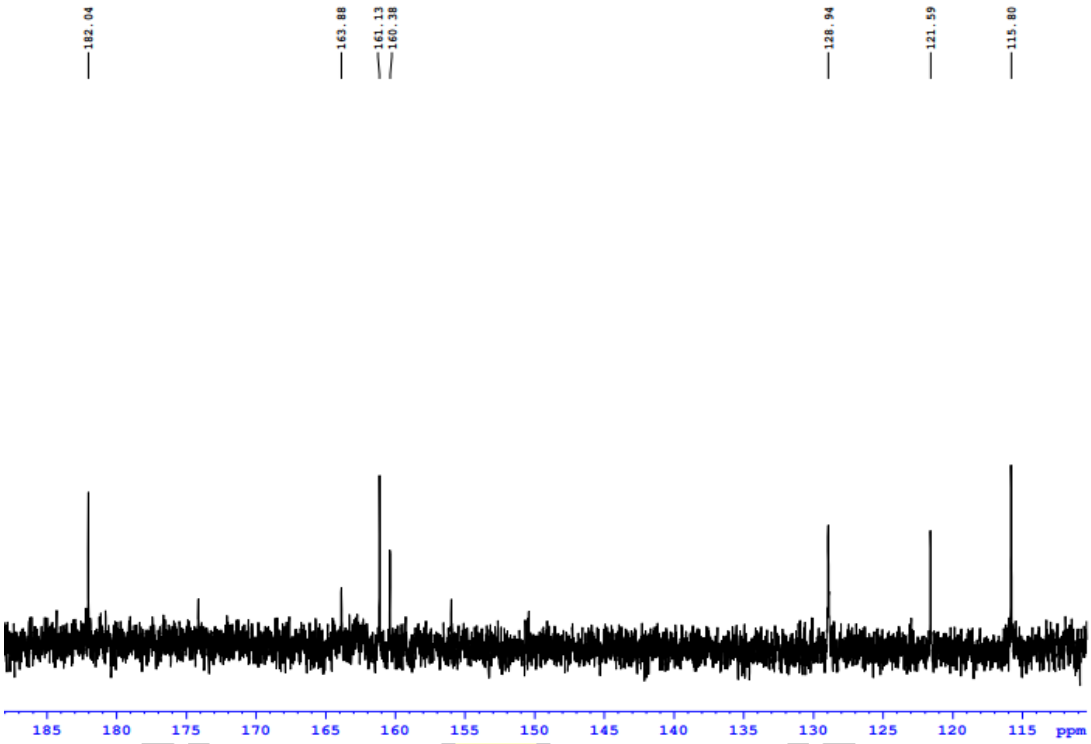

Figure A49. ^{13}C NMR (expansion 1) spectrum of **13** (DMSO-d_6, 100 MHz).

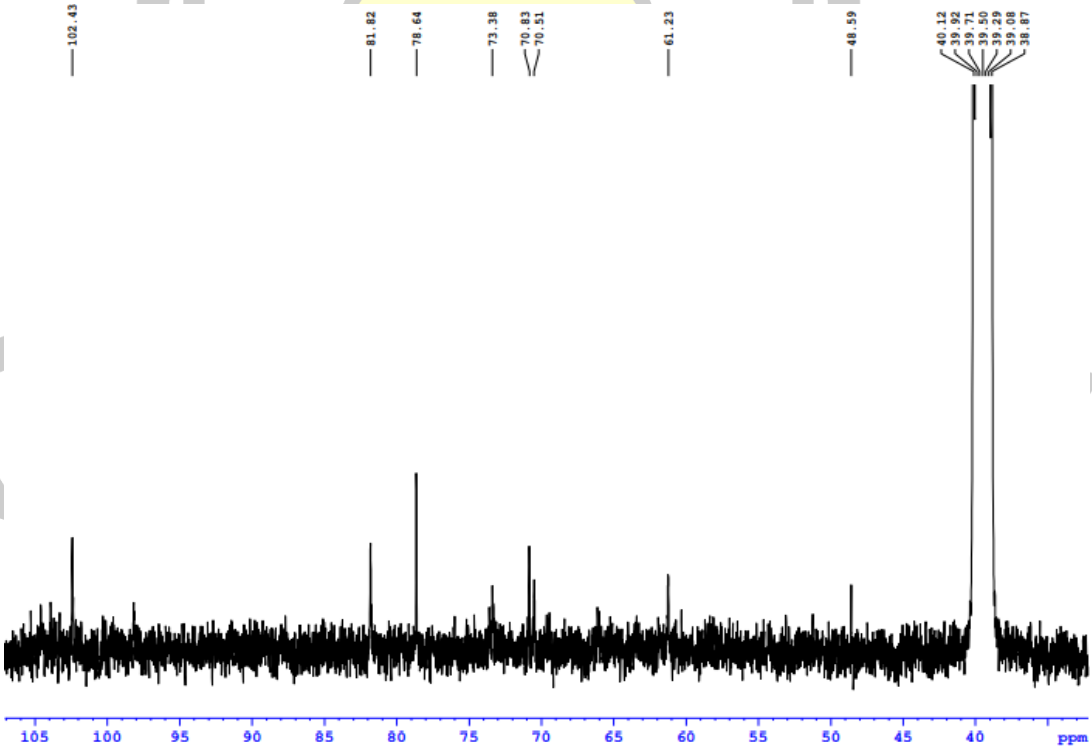

Figure A50. ^{13}C NMR (expansion 2) spectrum of **13** (DMSO-d_6, 100 MHz).

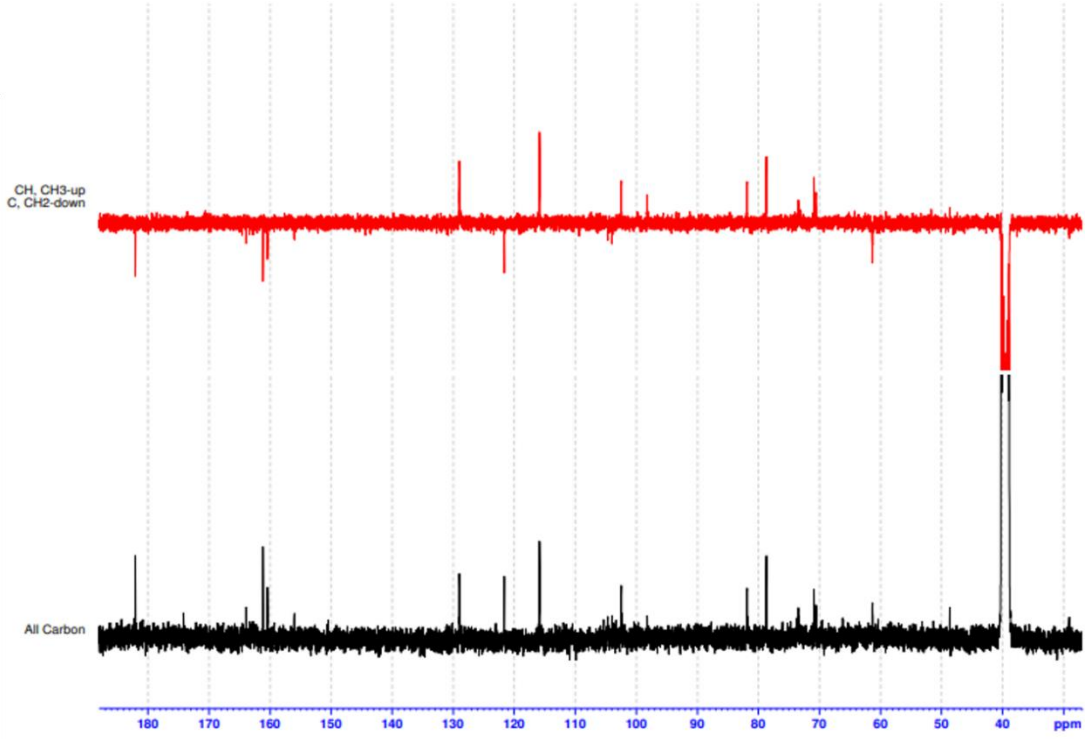

Figure A51. DEPT-135 spectrum of **13** (DMSO-d_6, 100 MHz).

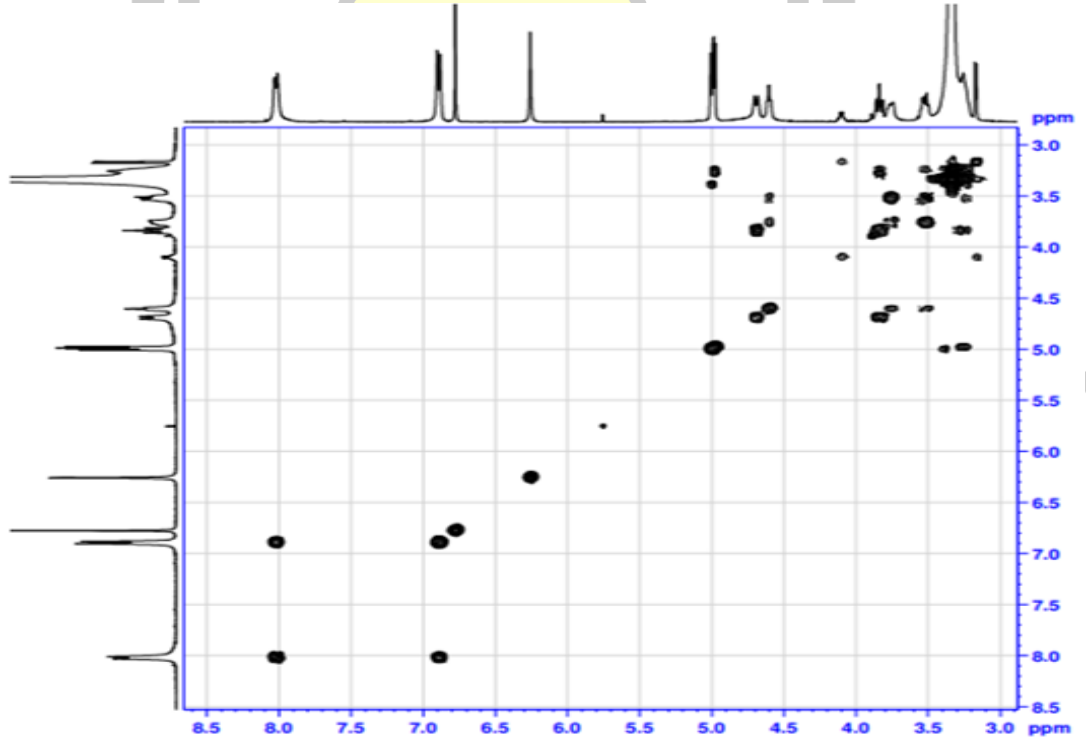

Figure A52. COSY spectrum of **13** (DMSO-d_6, 100 MHz).

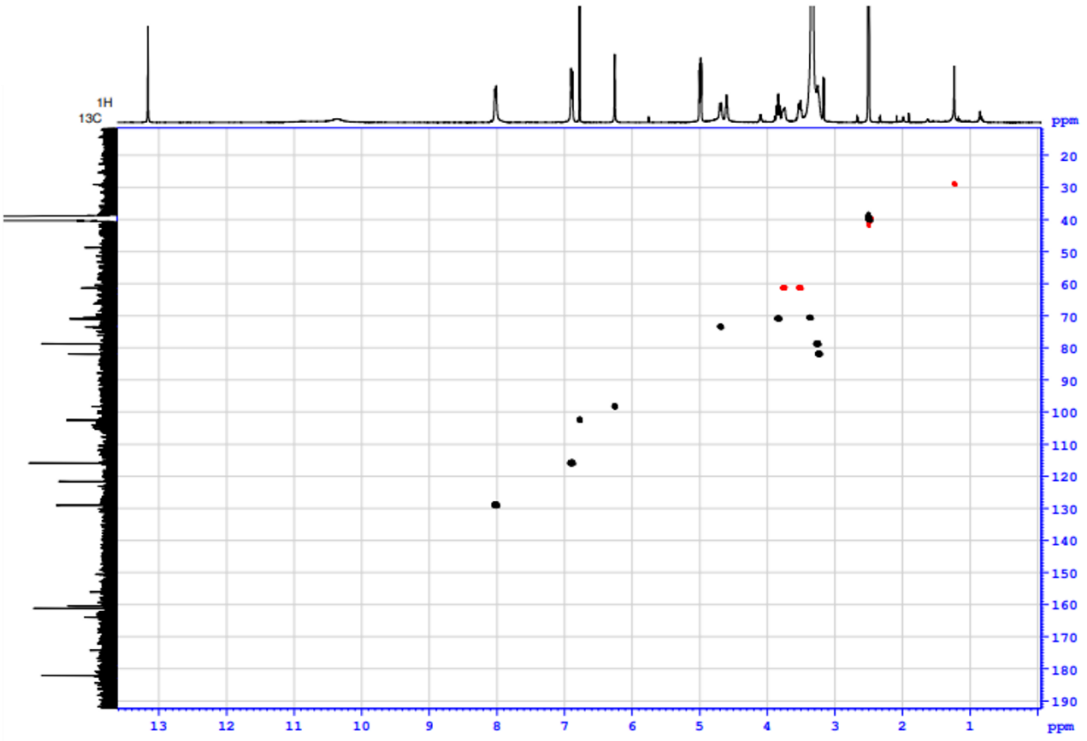

Figure A53. HSQC spectrum of **13** (DMSO-d_6, 100 MHz).

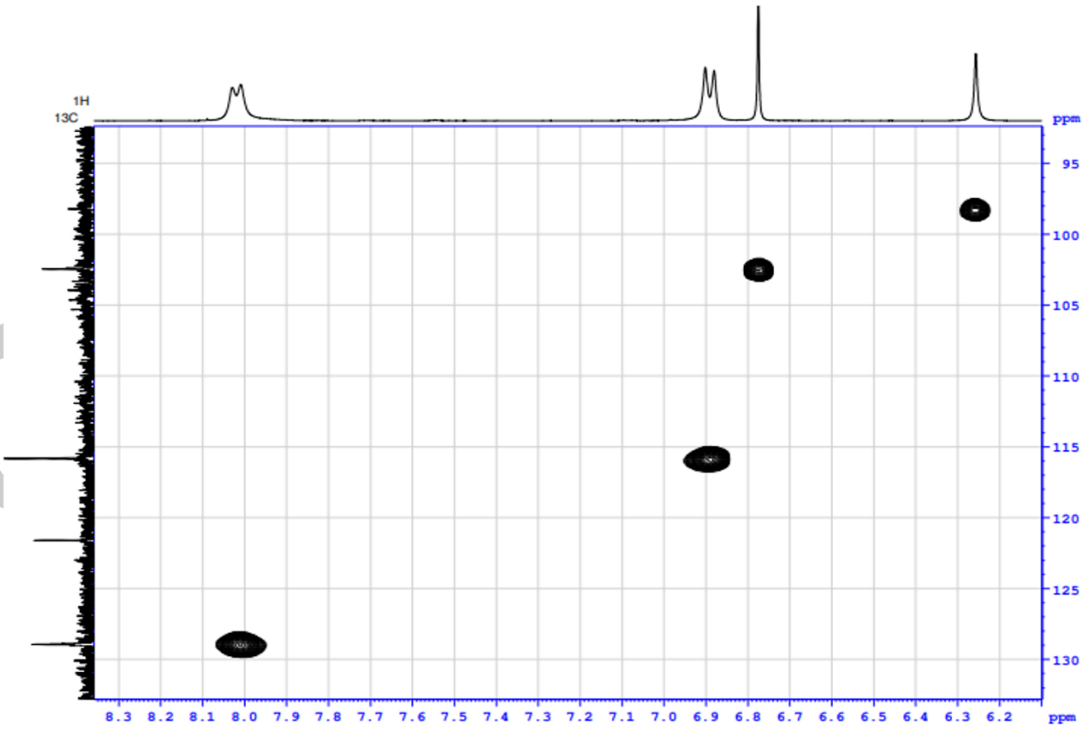

Figure A54. HSQC (expansion 1) spectrum of **13** (DMSO-d_6, 100 MHz).

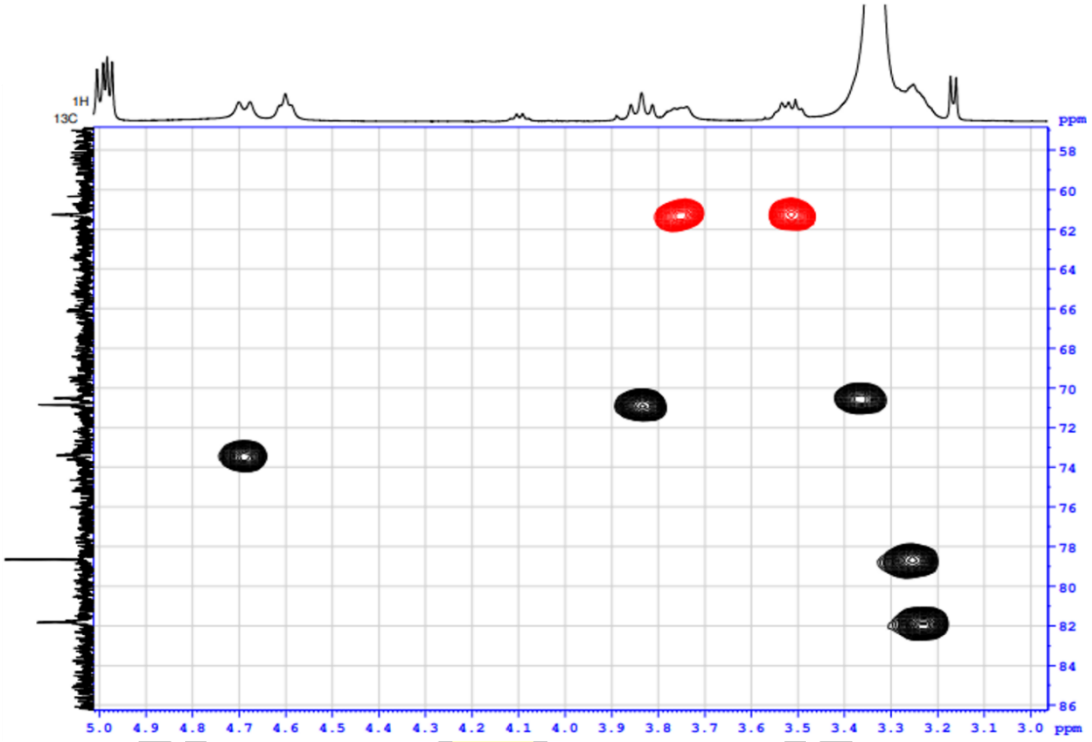

Figure A55. HSQC (expansion 2) spectrum of **13** (DMSO-d_6, 100 MHz).

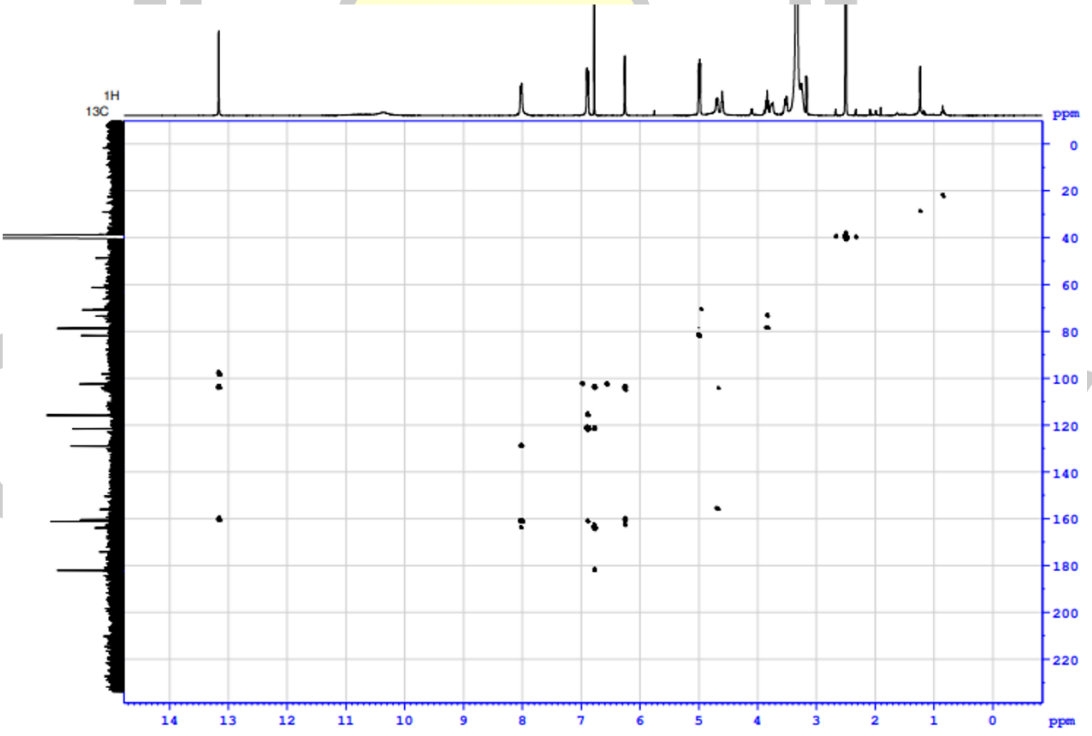

Figure A56. HMBC spectrum of **13** (DMSO-d_6, 100 MHz).

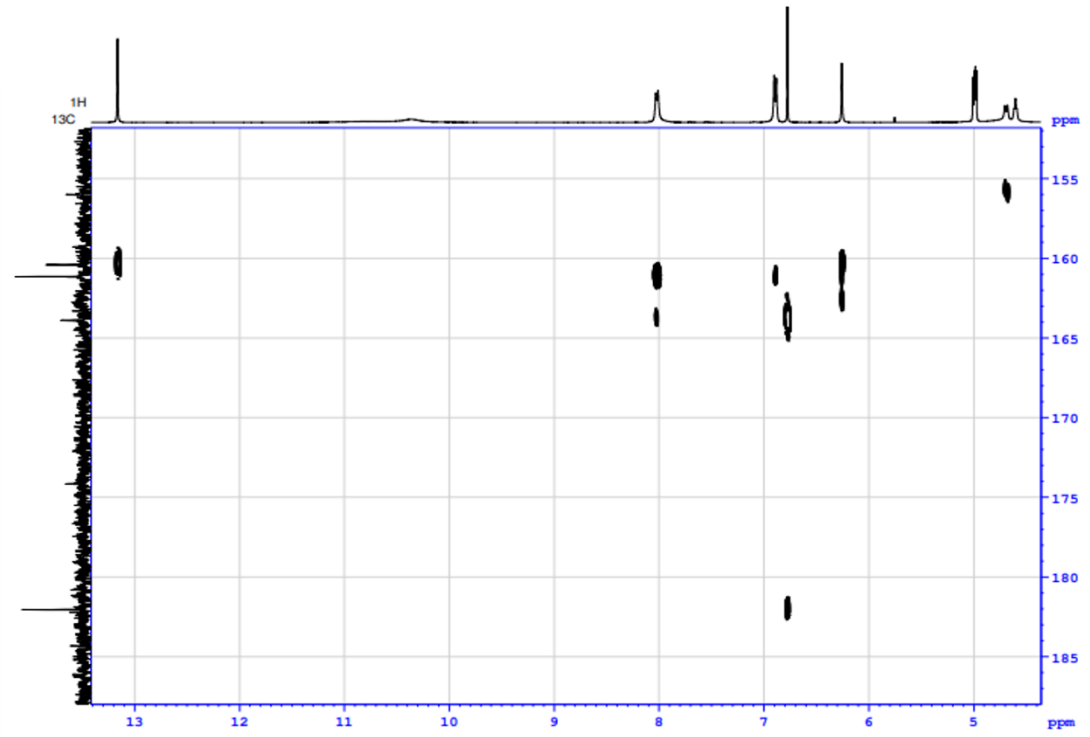

Figure A57. HMBC (expansion 1) spectrum of **13** (DMSO-d_6, 100 MHz).

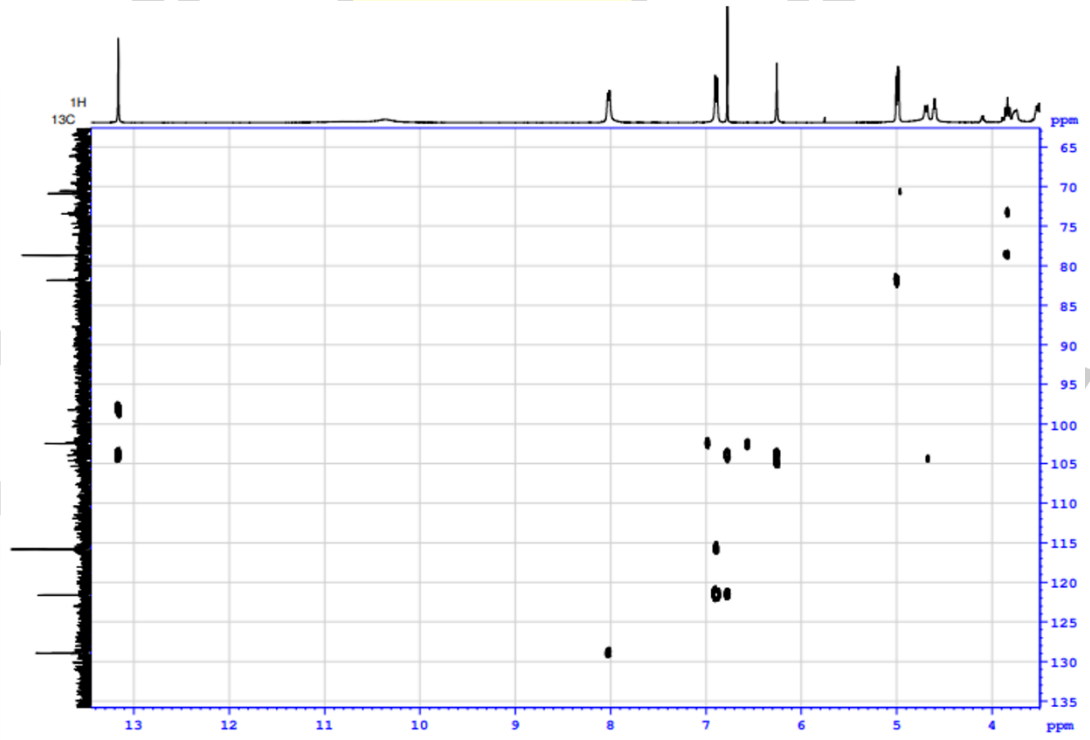

Figure A58. HMBC (expansion 2) spectrum of **13** (DMSO-d_6, 100 MHz).

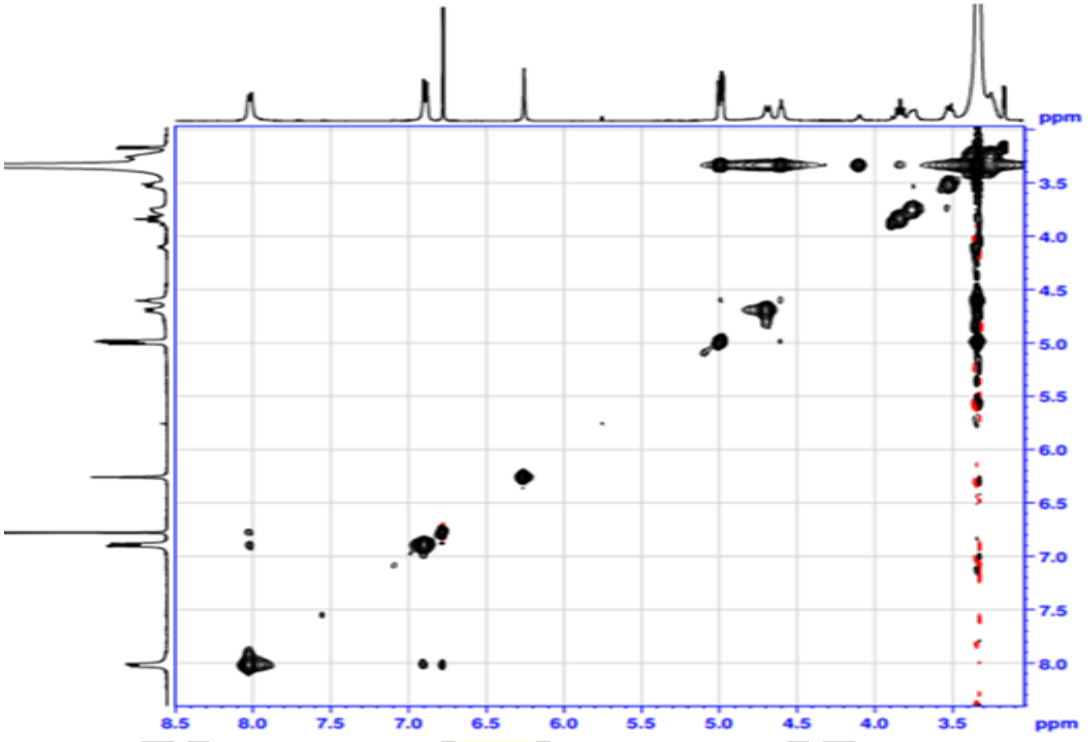

Figure A59. NOESY spectrum of **13** (DMSO-d_6, 100 MHz).

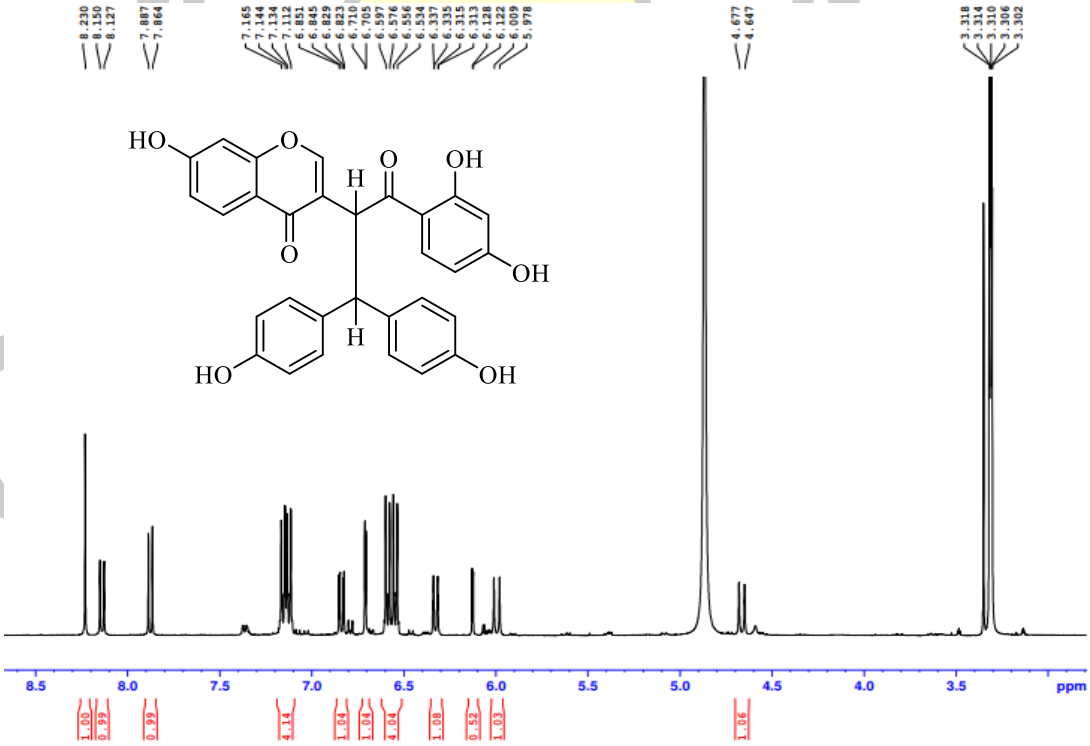

Figure A60. ^{1}H NMR spectrum of **20** (CD_3OD, 400 MHz).

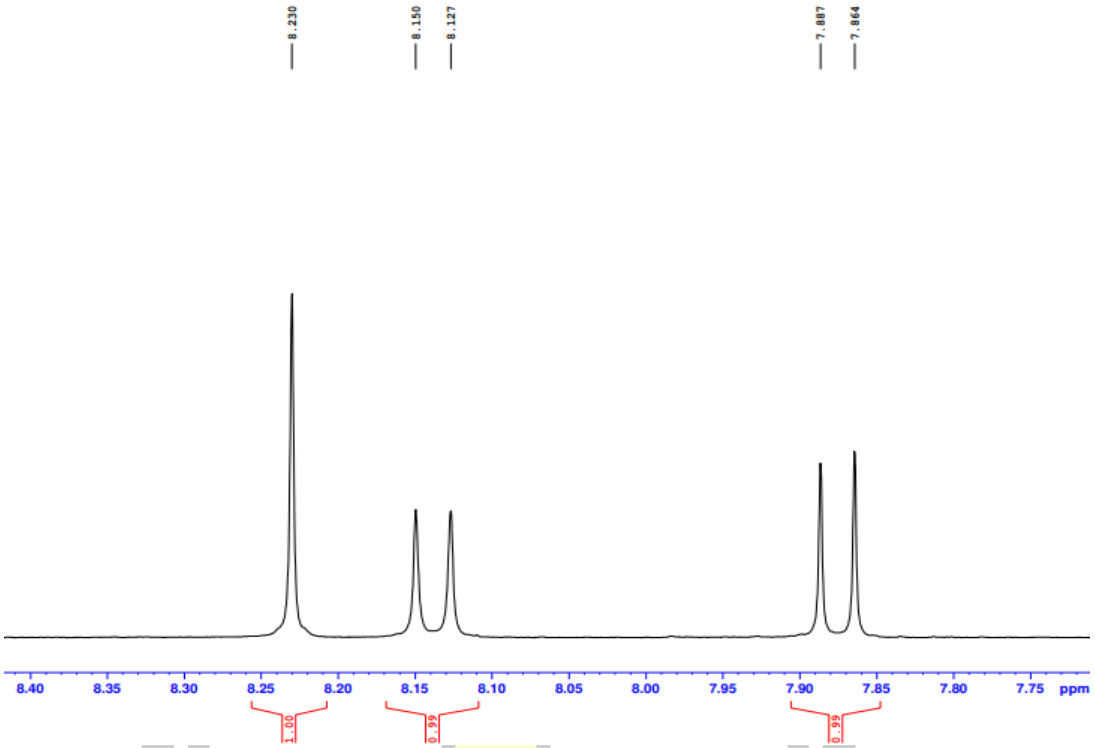

Figure A61. ^{1}H NMR (expansion 1) spectrum of **20** (CD_3OD, 400 MHz).

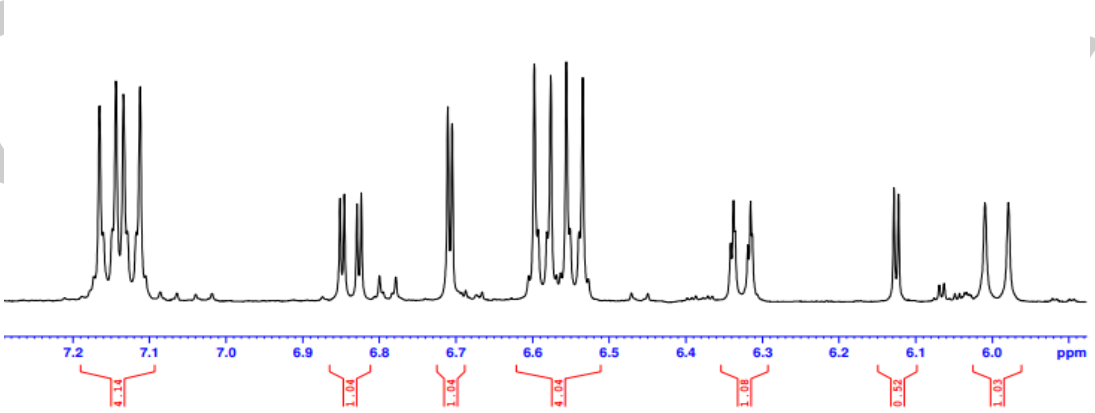

Figure A62. ^{1}H NMR (expansion 2) spectrum of **20** (CD_3OD, 400 MHz).

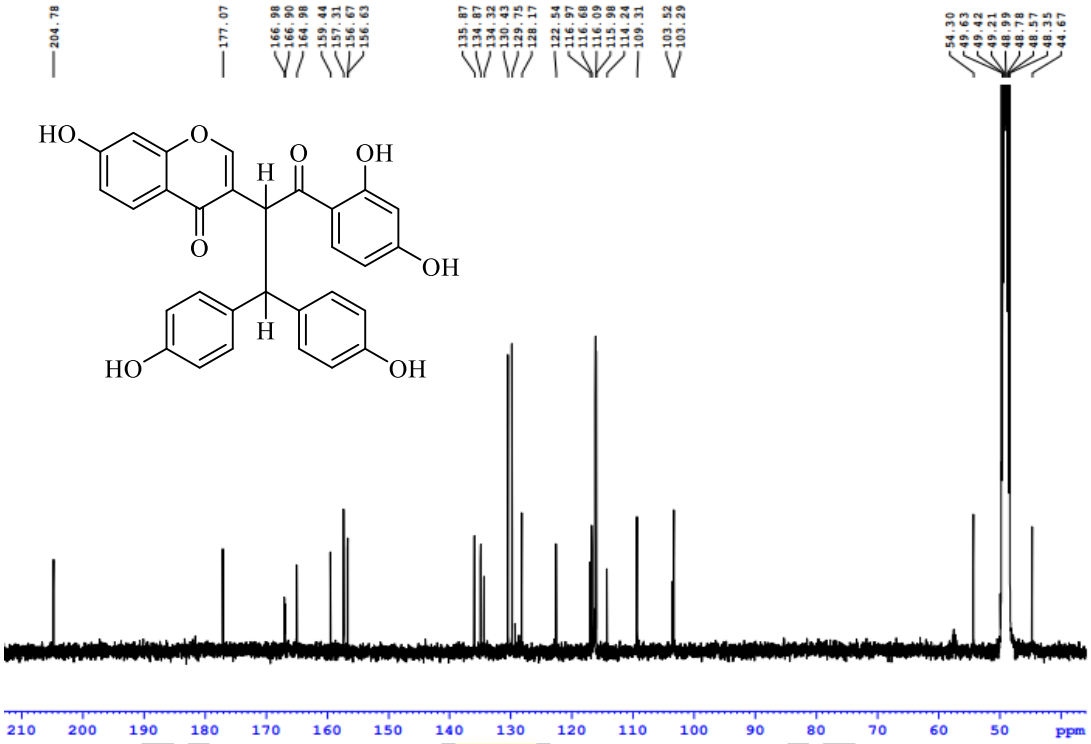

Figure A63. ^{13}C NMR spectrum of **20** (CD_3OD, 100 MHz).

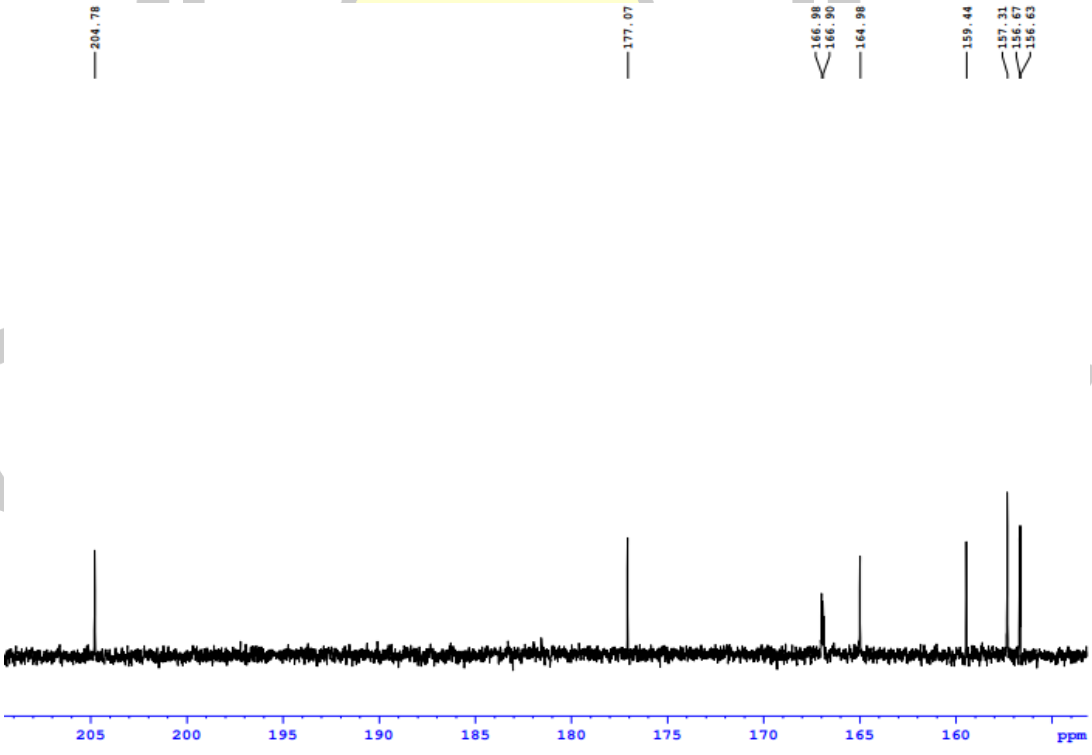

Figure A64. ^{13}C NMR (expansion 1) spectrum of **20** (CD_3OD, 100 MHz).

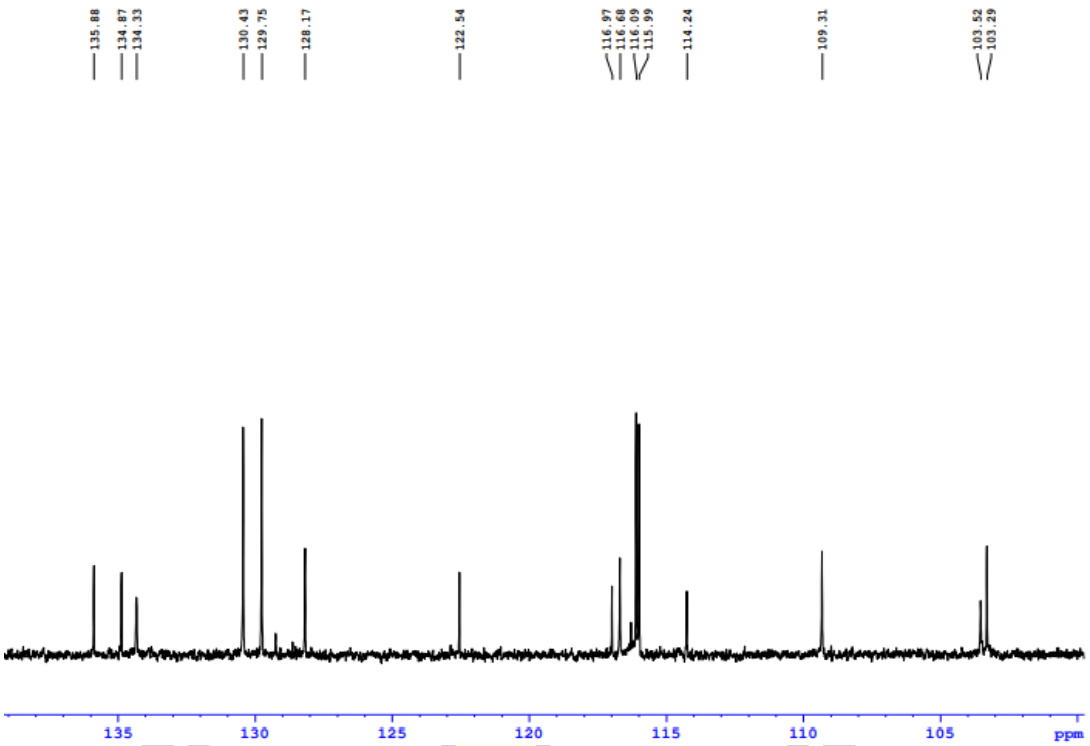

Figure A65. ^{13}C NMR (expansion 2) spectrum of **20** (CD_3OD, 100 MHz).

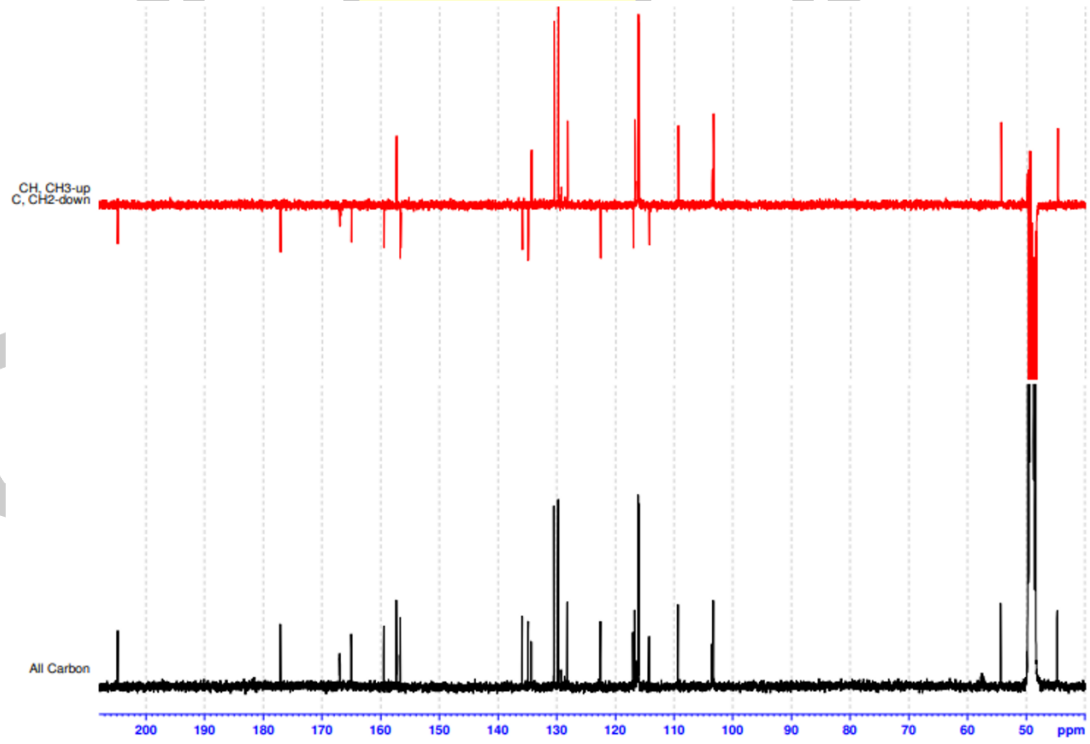

Figure A66. DEPT-135 spectrum of **20** (CD_3OD, 100 MHz).

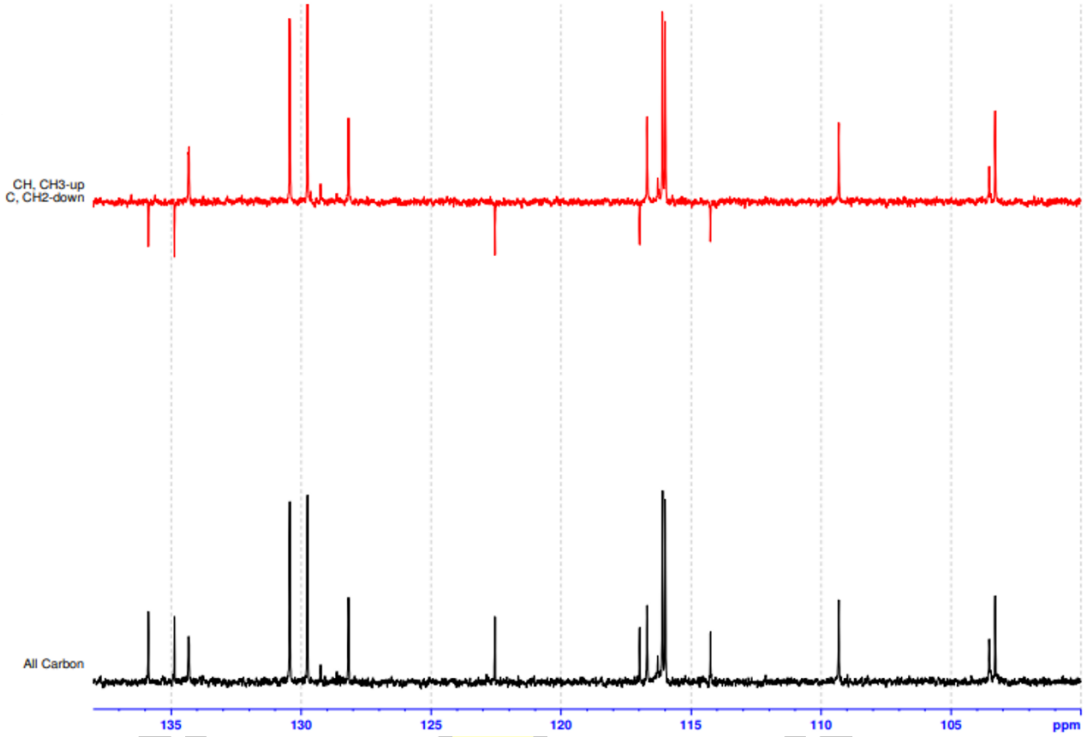

Figure A67. DEPT-135 (expansion 1) spectrum of **20** (CD_3OD, 100 MHz).

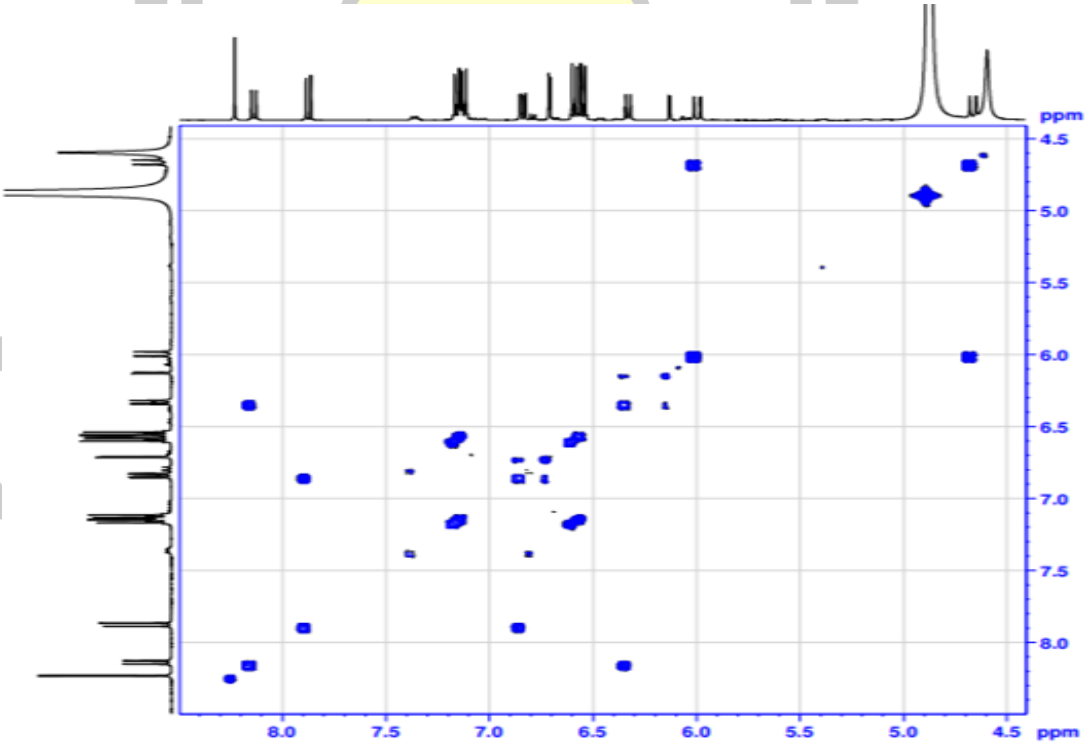

Figure A68. COSY spectrum of **20** (CD_3OD, 100 MHz).

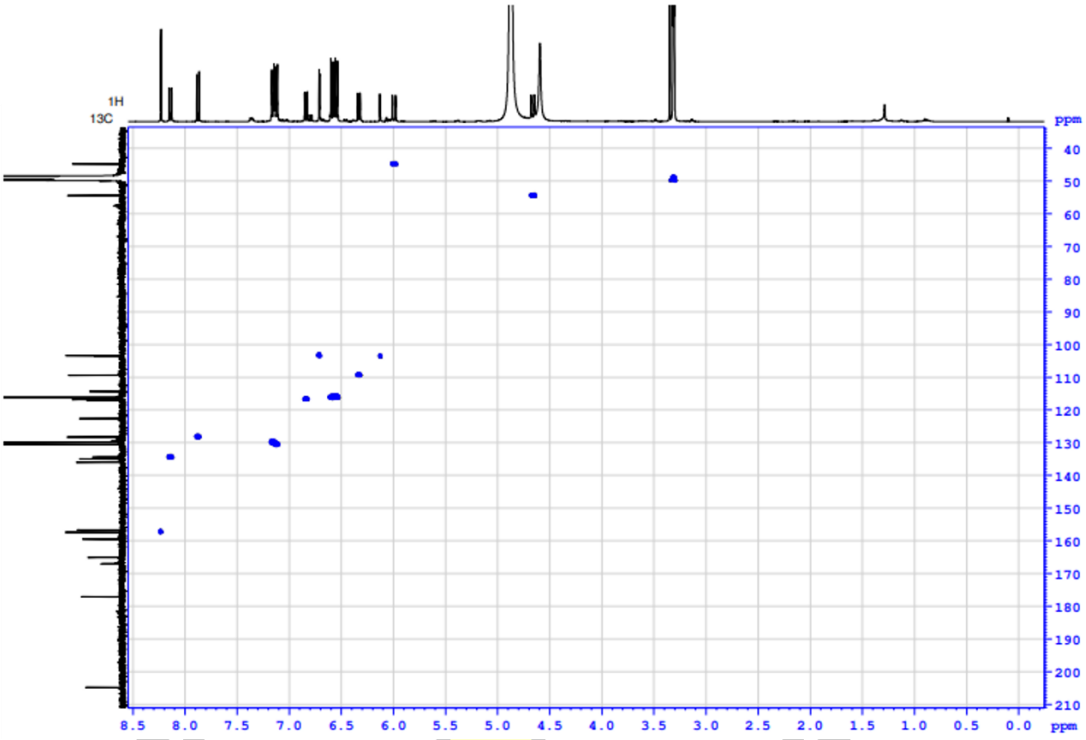

Figure A69. HSQC spectrum of **20** (CD_3OD, 100 MHz).

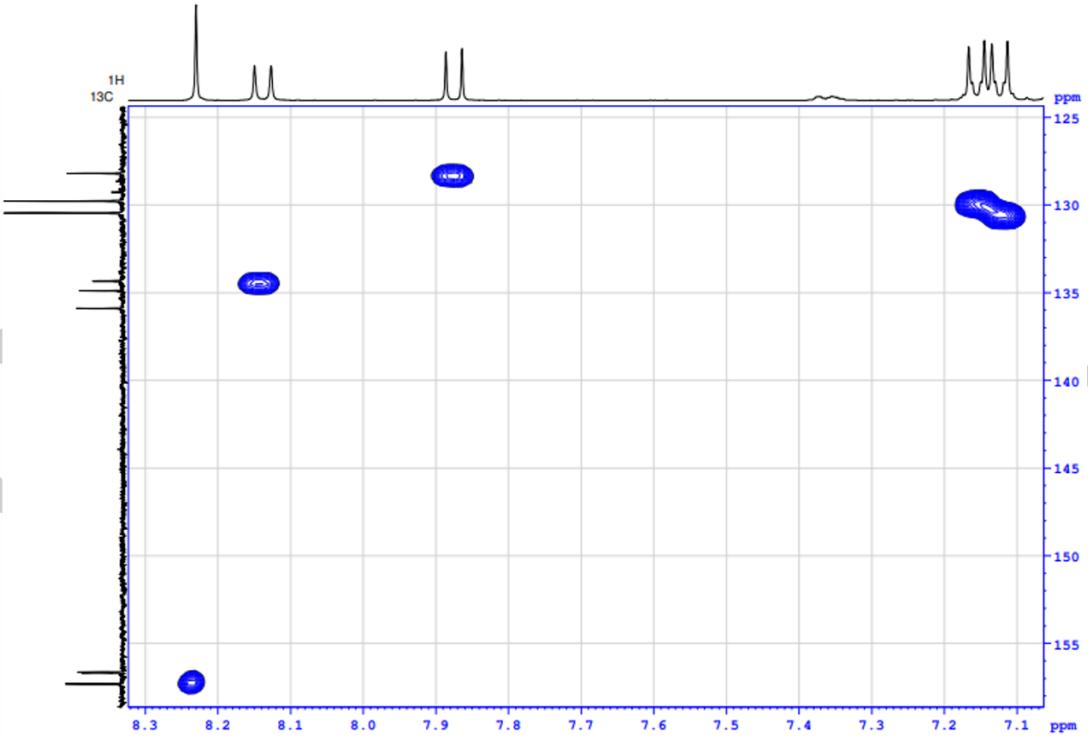

Figure A70. HSQC (expansion 1) spectrum of **20** (CD_3OD, 100 MHz).

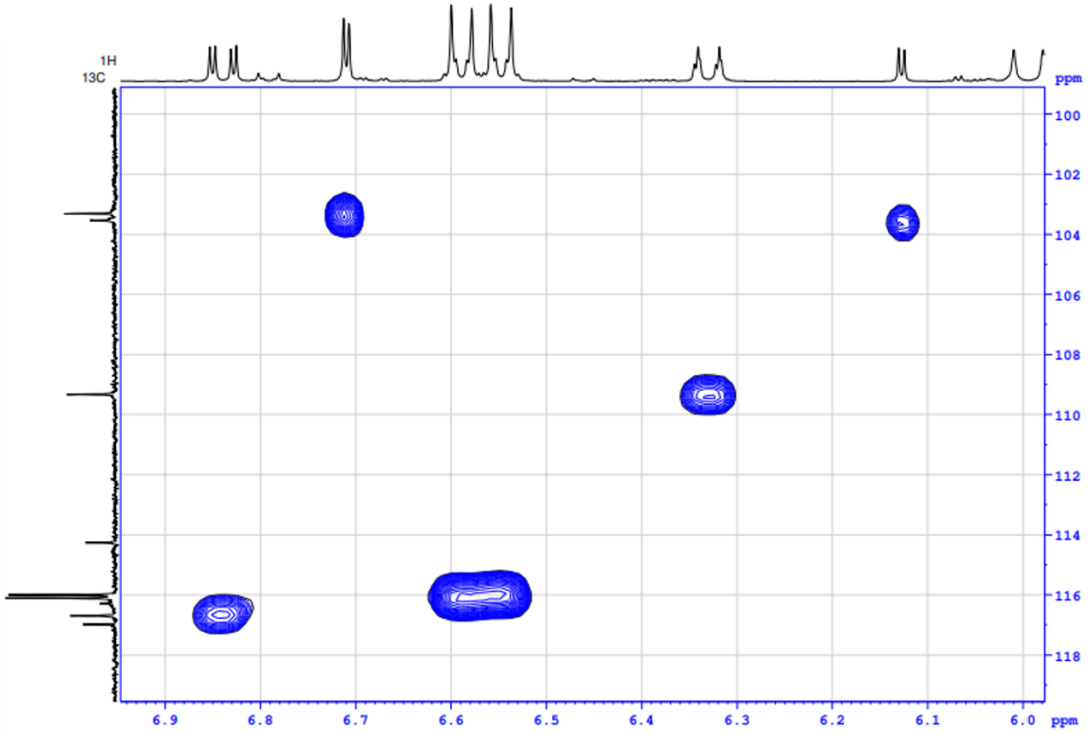

Figure A71. HSQC (expansion 2) spectrum of **20** (CD_3OD, 100 MHz).

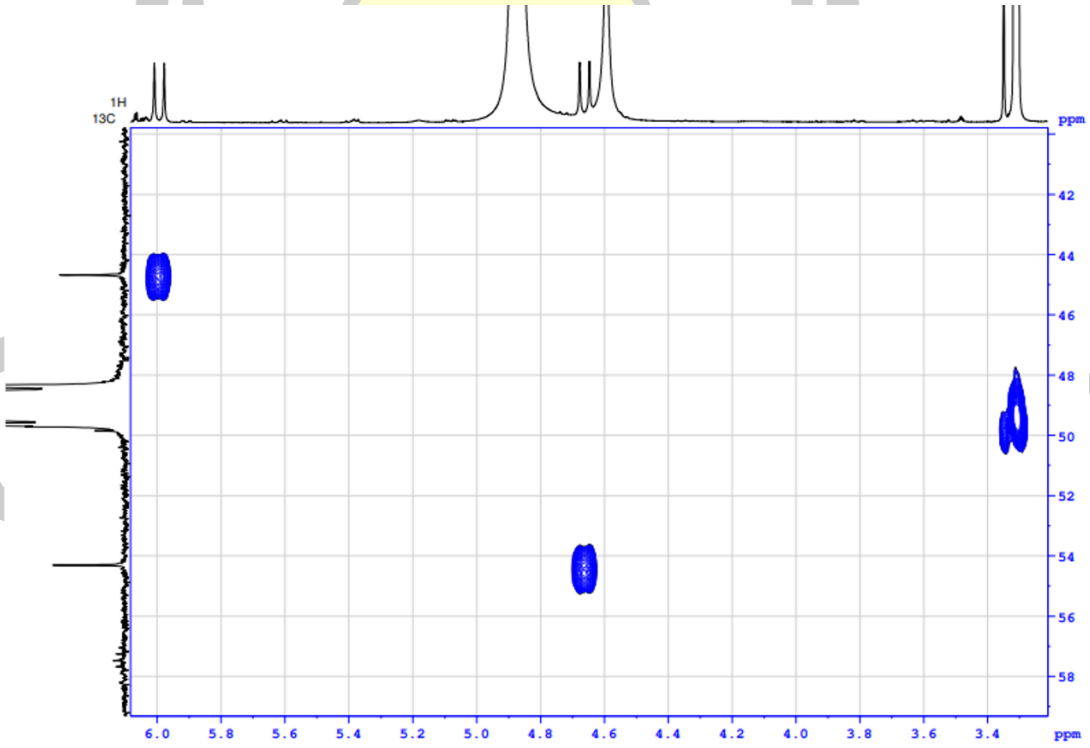

Figure A72. HSQC (expansion 3) spectrum of **20** (CD_3OD, 100 MHz).

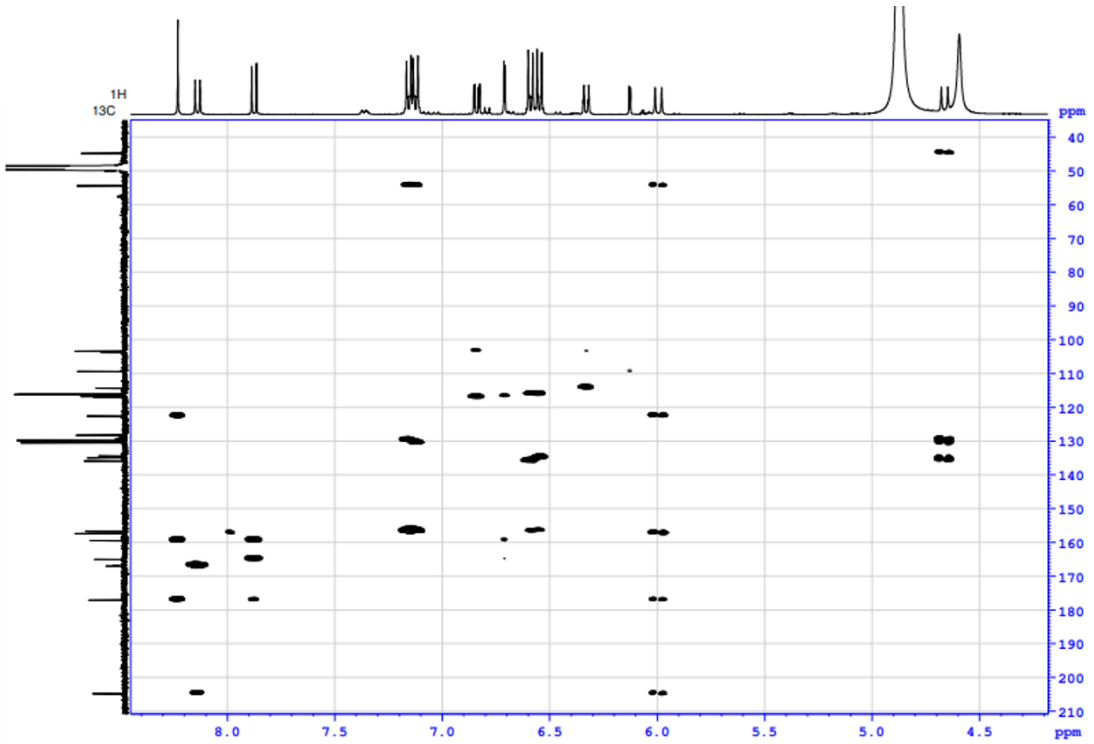

Figure A73. HMBC spectrum of **20** (CD_3OD, 100 MHz).

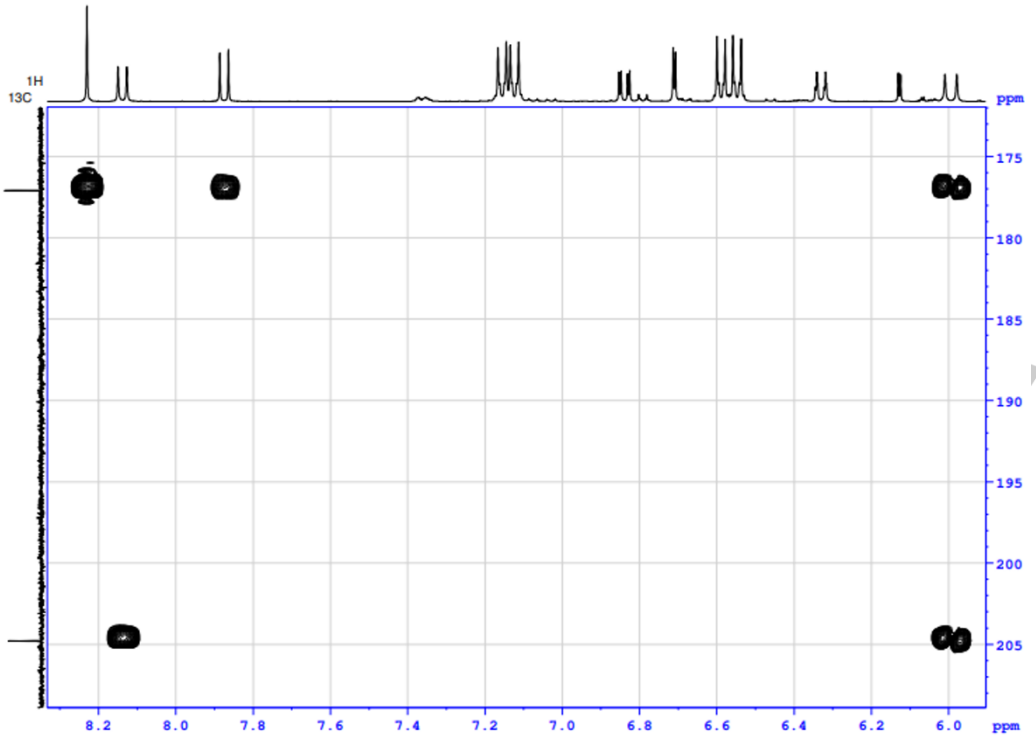

Figure A74. HMBC (expansion 1) spectrum of **20** (CD_3OD, 100 MHz).

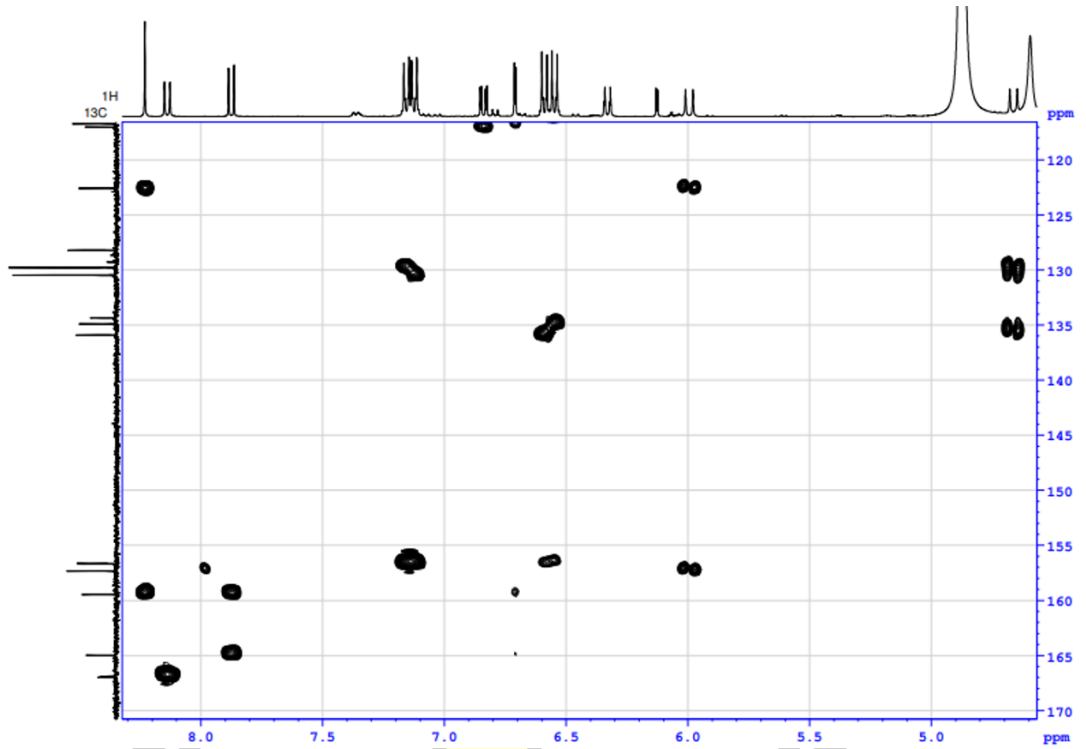

Figure A75. HMBC (expansion 2) spectrum of **20** (CD_3OD, 100 MHz).

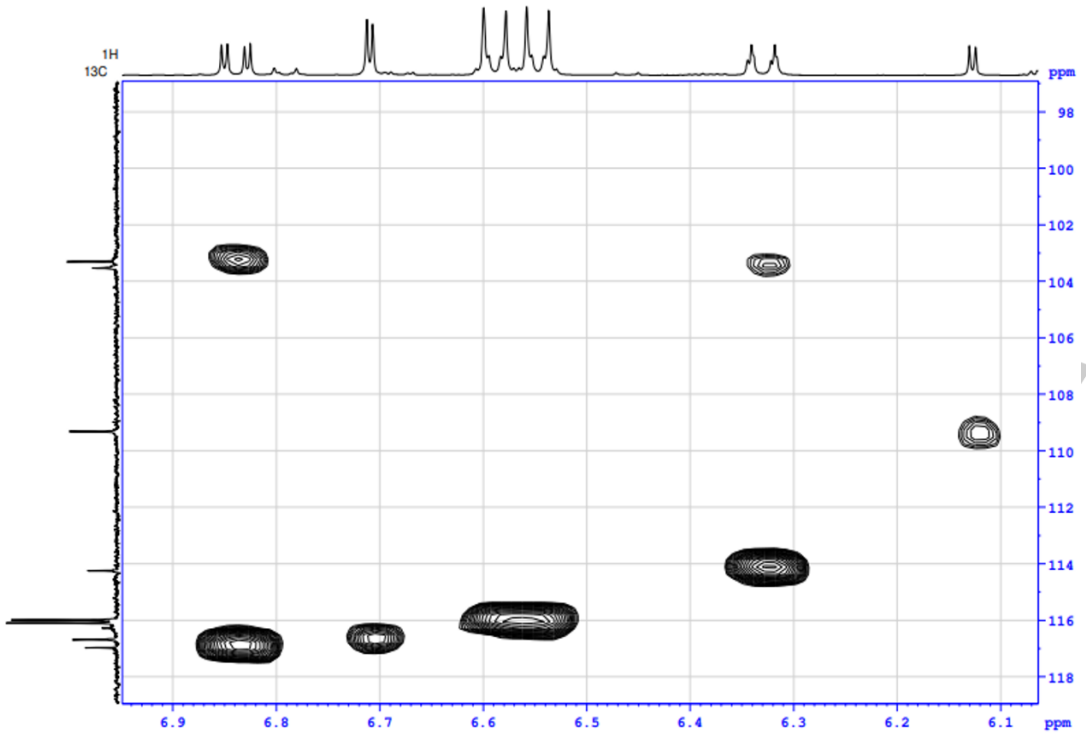

Figure A76. HMBC (expansion 3) spectrum of **20** (CD_3OD, 100 MHz).

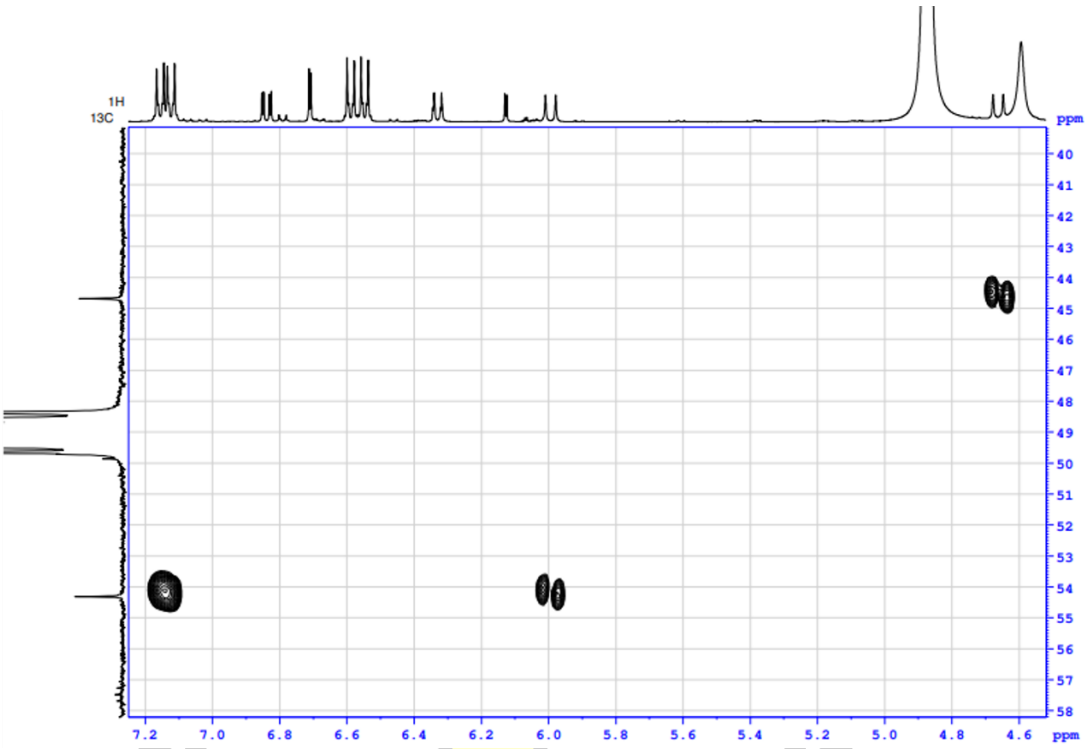

Figure A77. HMBC (expansion 4) spectrum of **20** (CD_3OD, 100 MHz).

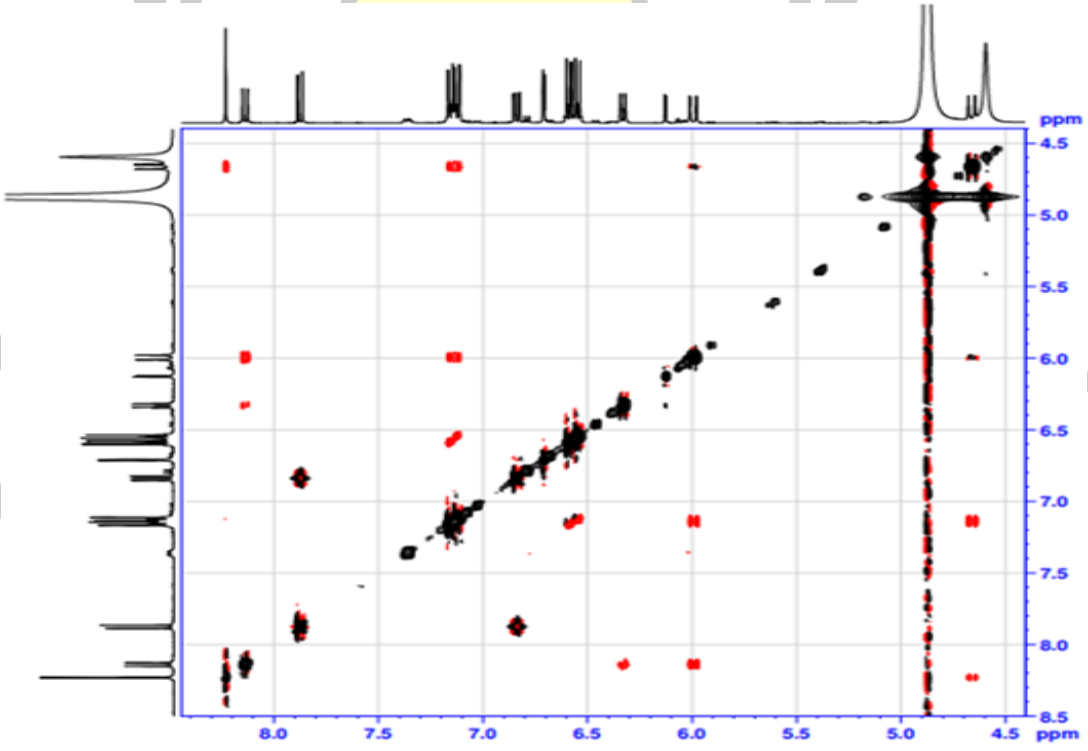

Figure A78. NOESY spectrum of **20** (CD_3OD, 100 MHz).

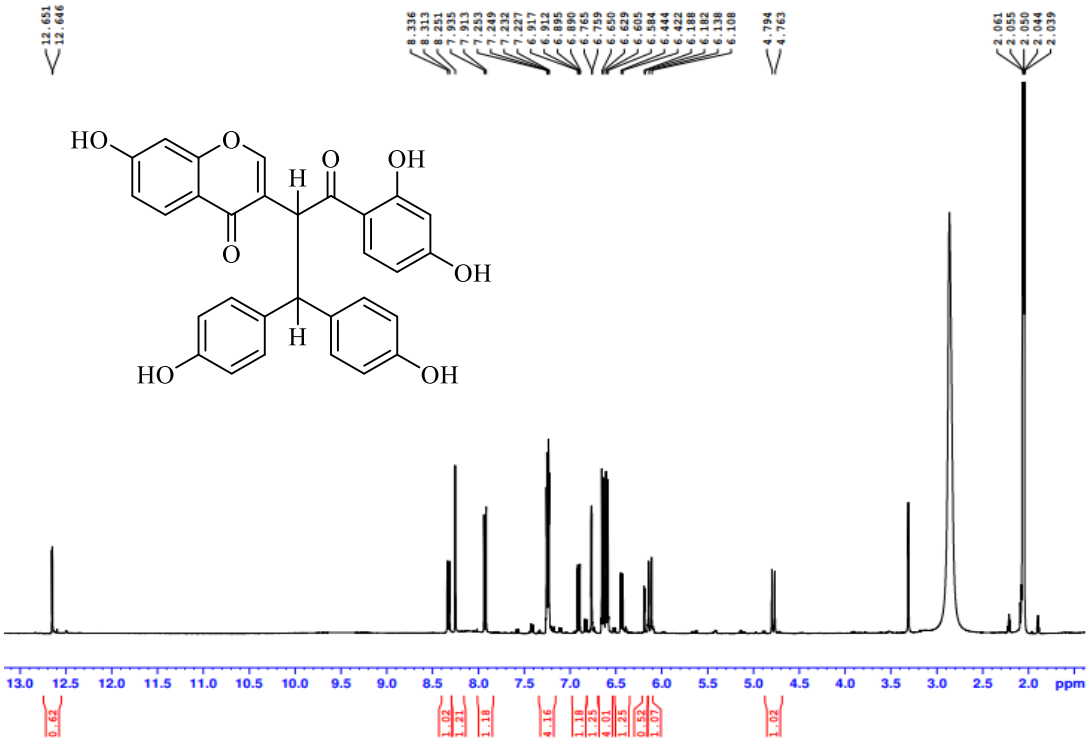

Figure A79. ^{1}H NMR spectrum of **20** (acetone-d_6, 400 MHz).

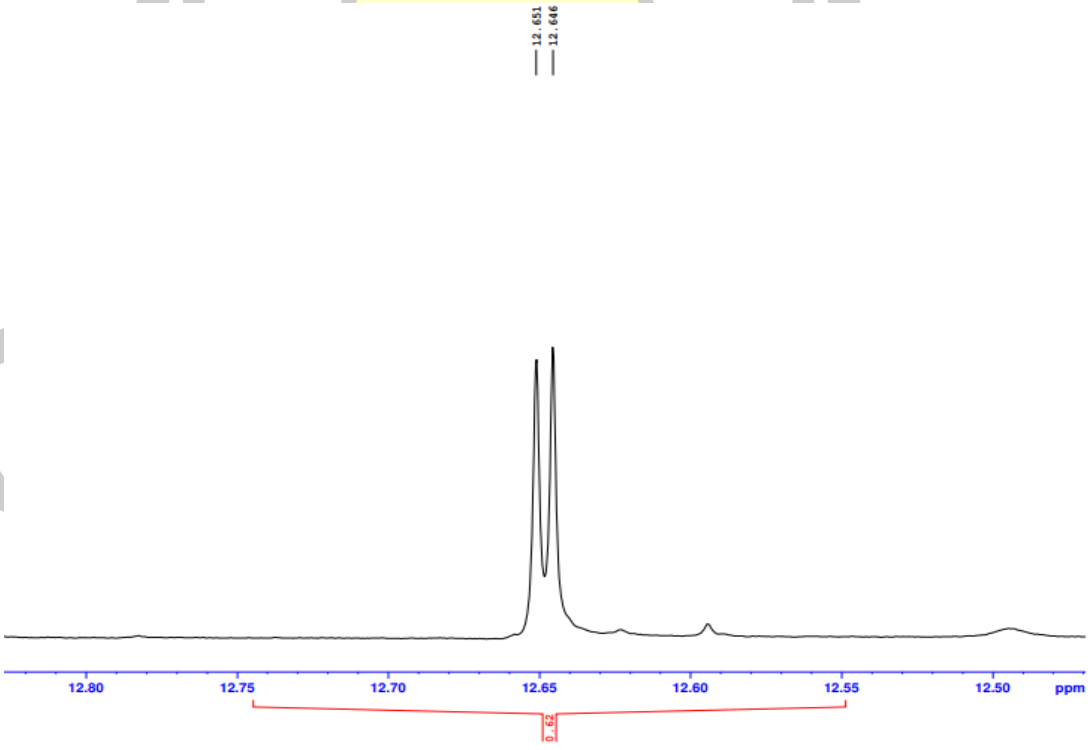

Figure A80. ^{1}H NMR (expansion 1) spectrum of **20** (acetone-d_6, 400 MHz).

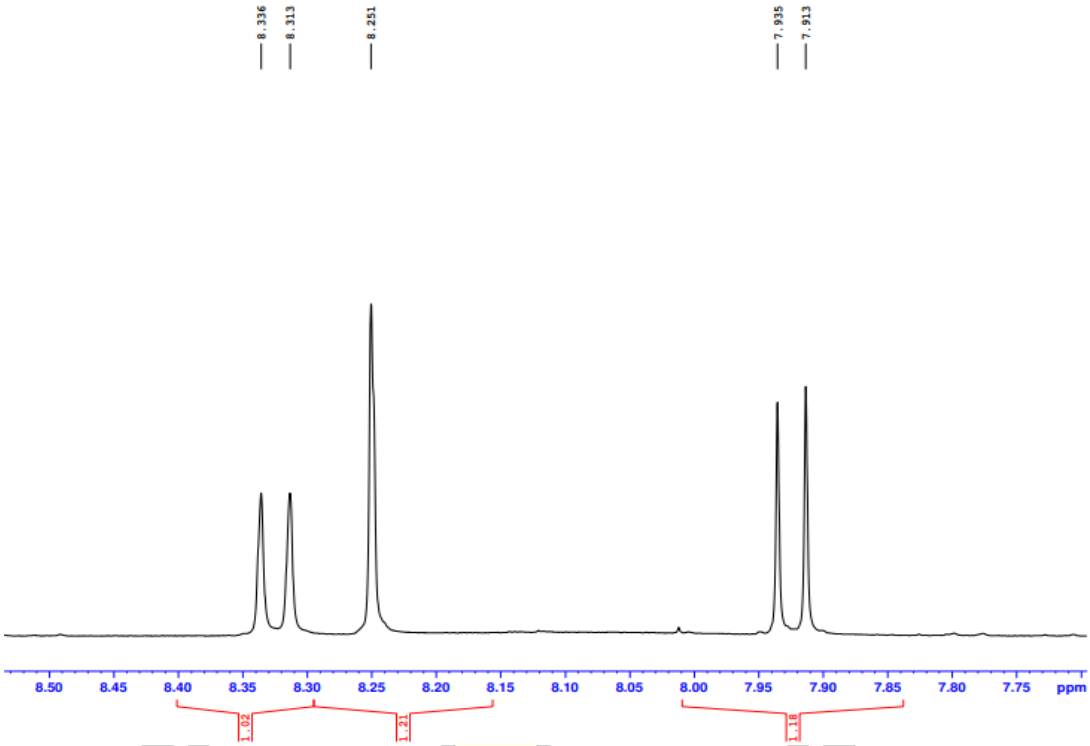

Figure A81. ^{1}H NMR (expansion 2) spectrum of **20** (acetone-d_6, 400 MHz).

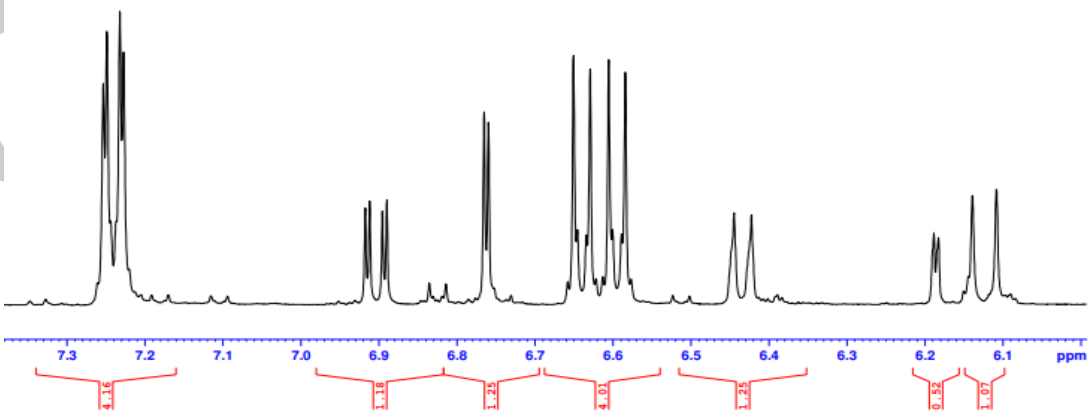

Figure A82. ^{1}H NMR (expansion 3) spectrum of **20** (acetone-d_6, 400 MHz).

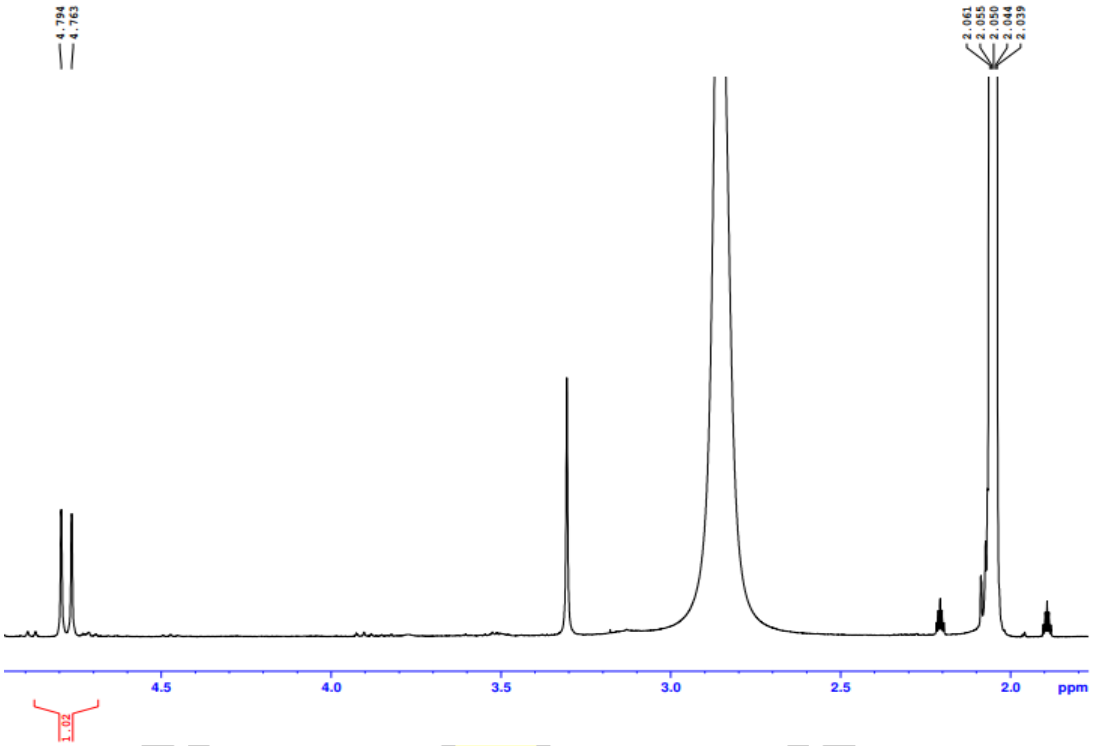

Figure A83. ^{1}H NMR (expansion 4) spectrum of **20** (acetone-d_6, 400 MHz).

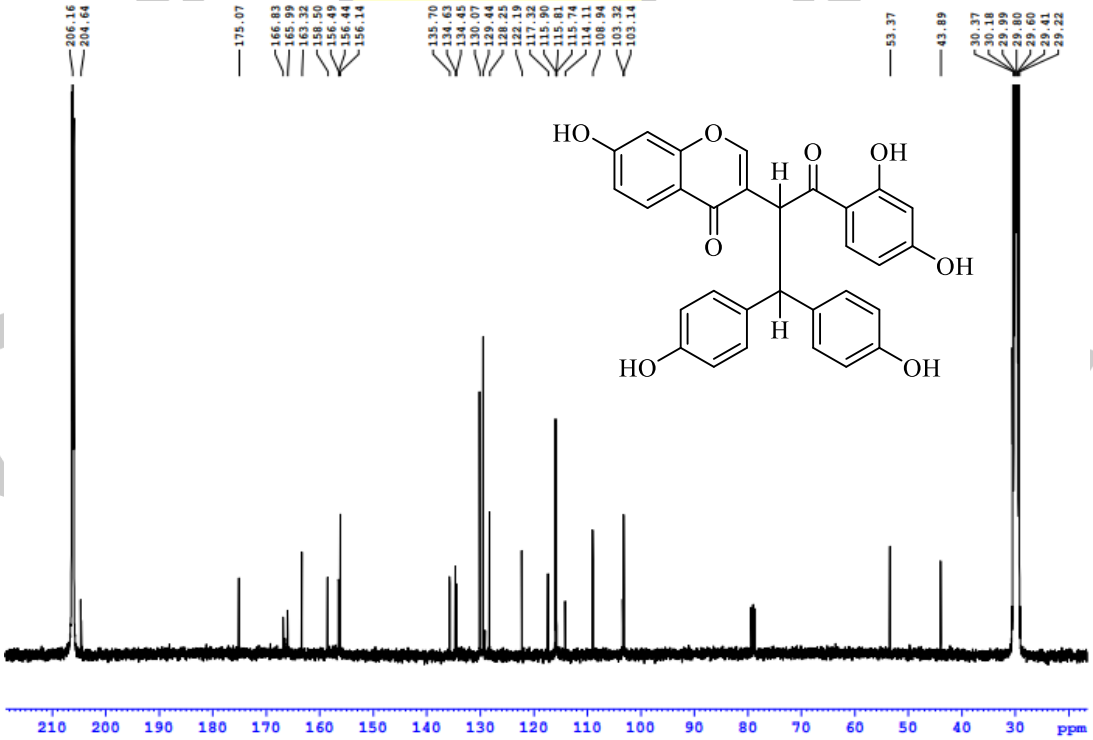

Figure A84. ^{13}C NMR spectrum of **20** (acetone-d_6, 100 MHz).

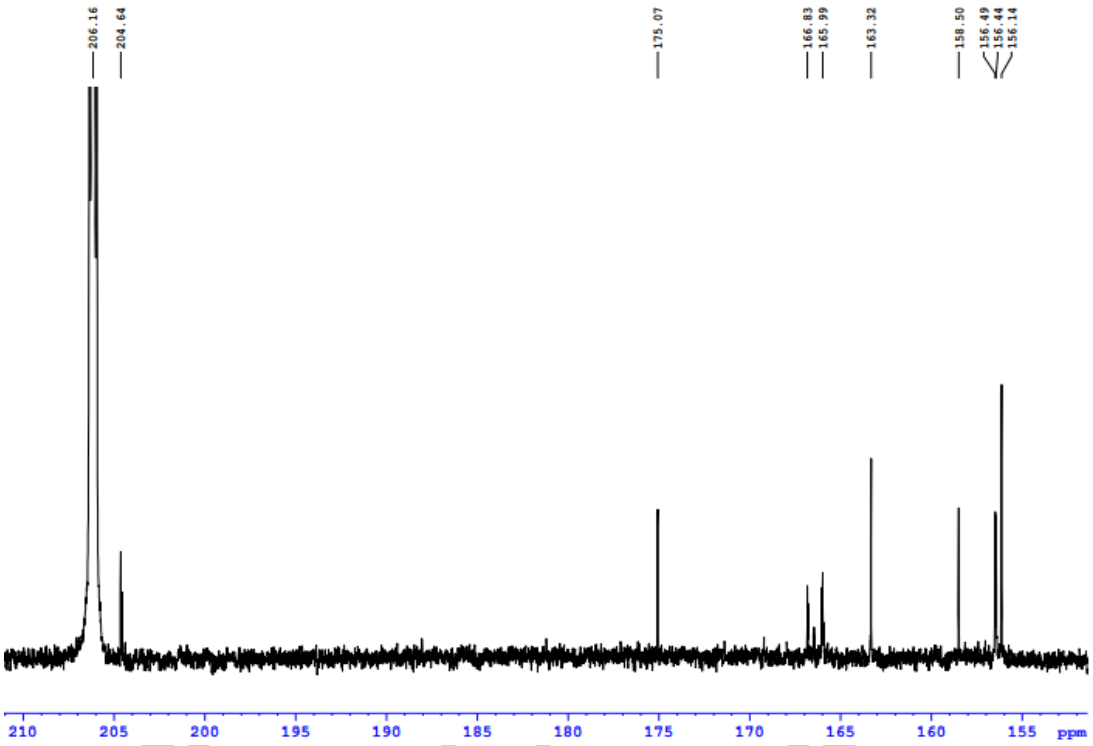

Figure A85. ^{13}C NMR (expansion 1) spectrum of **20** (acetone-d_6, 100 MHz).

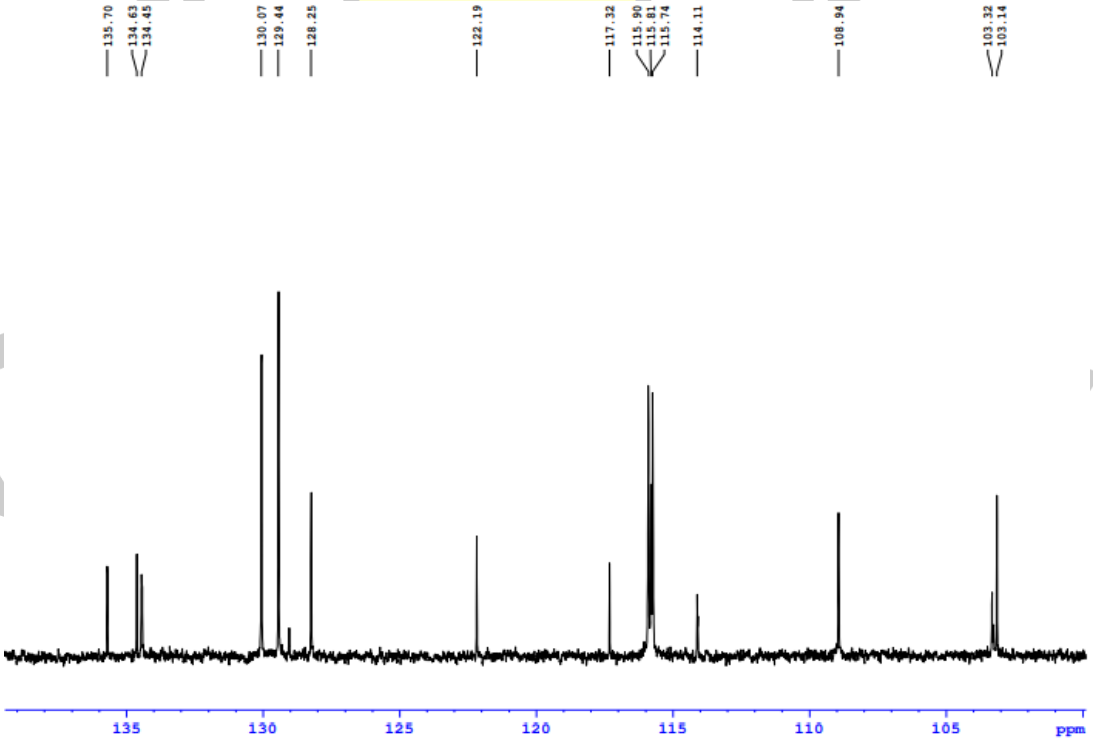

Figure A86. ^{13}C NMR (expansion 2) spectrum of **20** (acetone-d_6, 100 MHz).

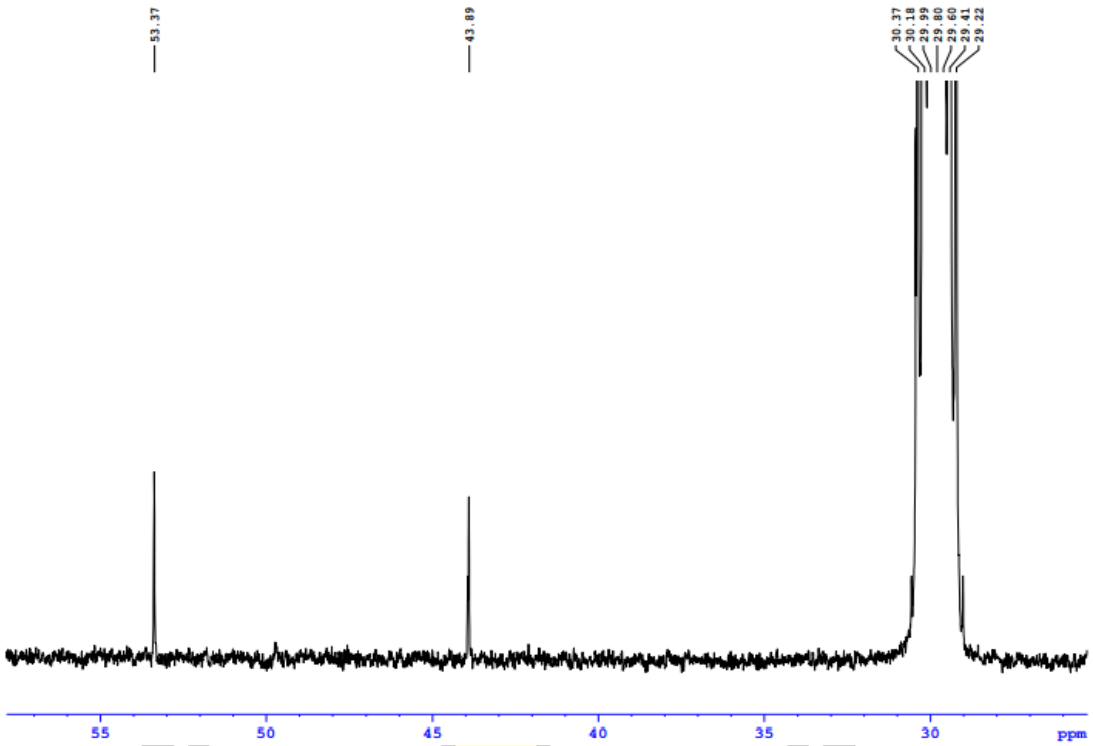

Figure A87. ^{13}C NMR (expansion 3) spectrum of **20** (acetone-d_6, 100 MHz).

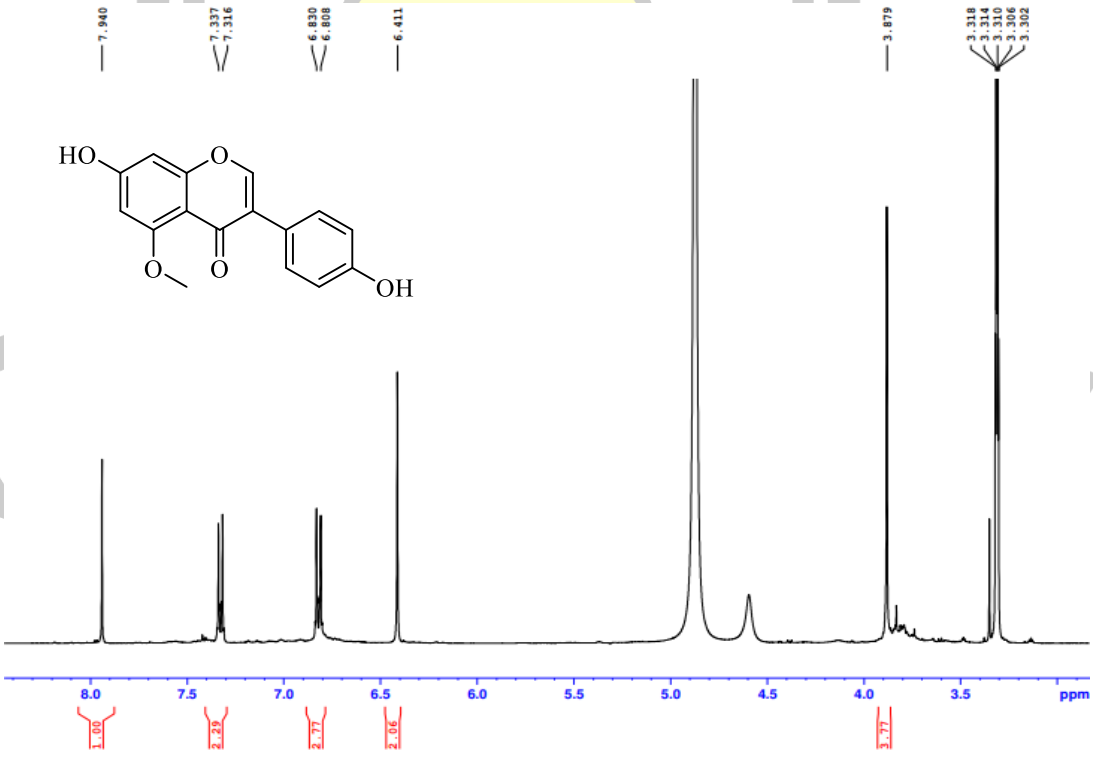

Figure A88. ^{1}H NMR spectrum of **26** (CD_3OD, 400 MHz).

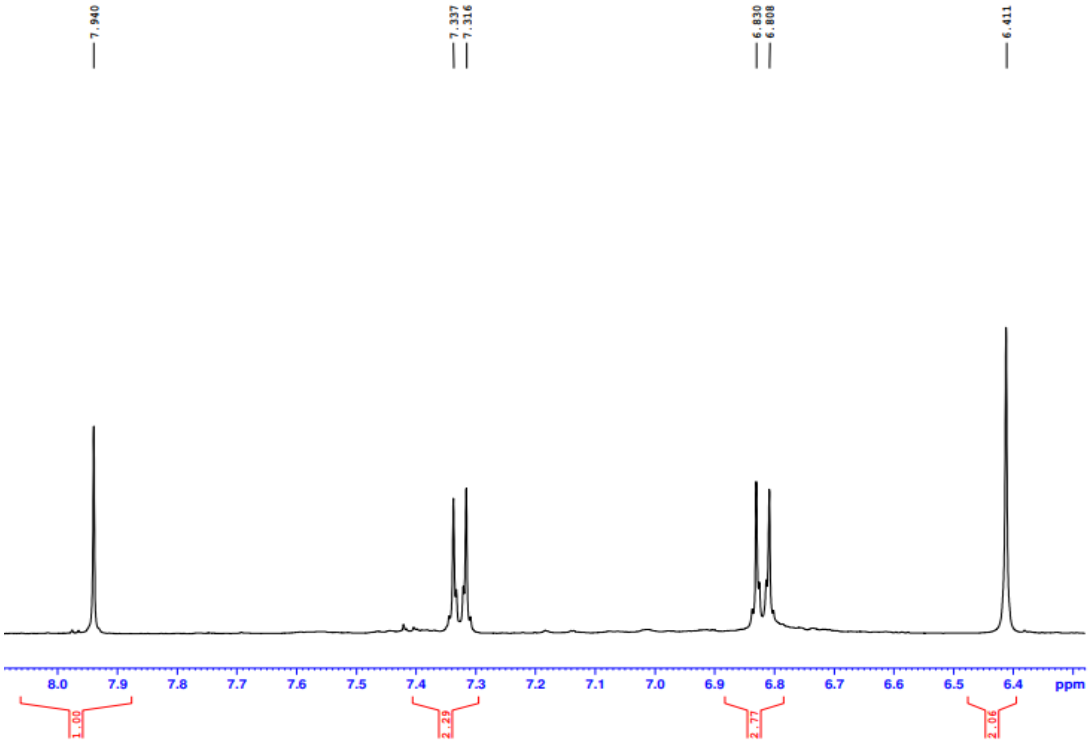

Figure A89. ^{1}H NMR (expansion 1) spectrum of **26** (CD_3OD, 400 MHz).

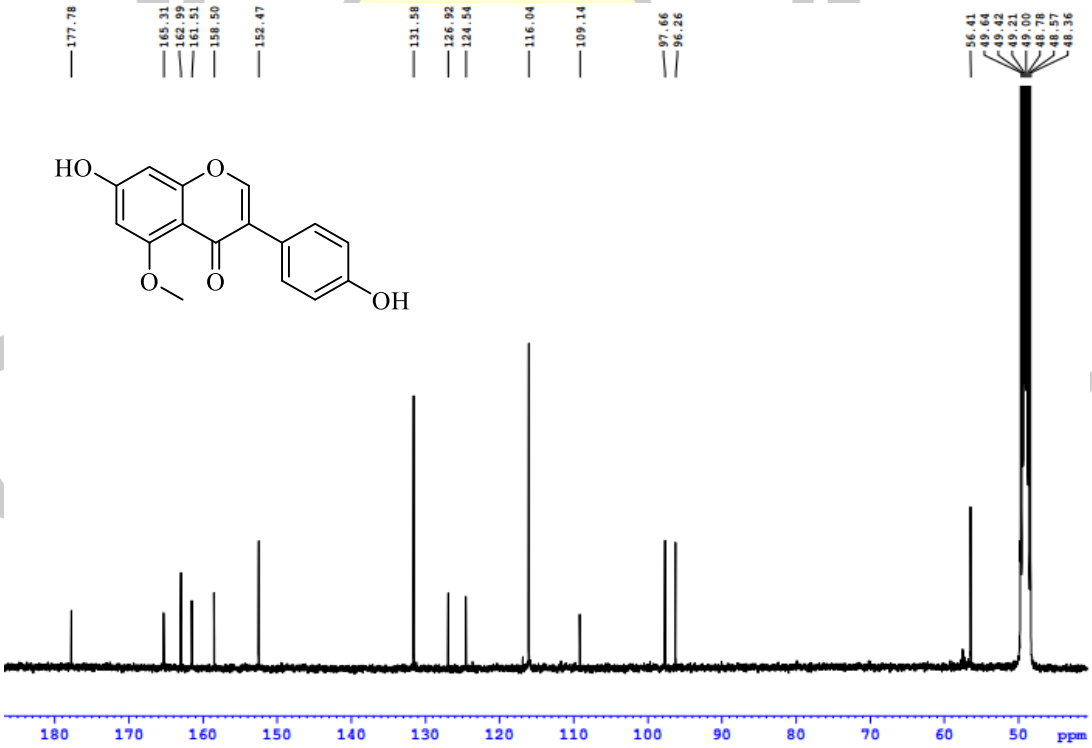

Figure A90. ^{13}C NMR spectrum of **26** (CD_3OD, 100 MHz).

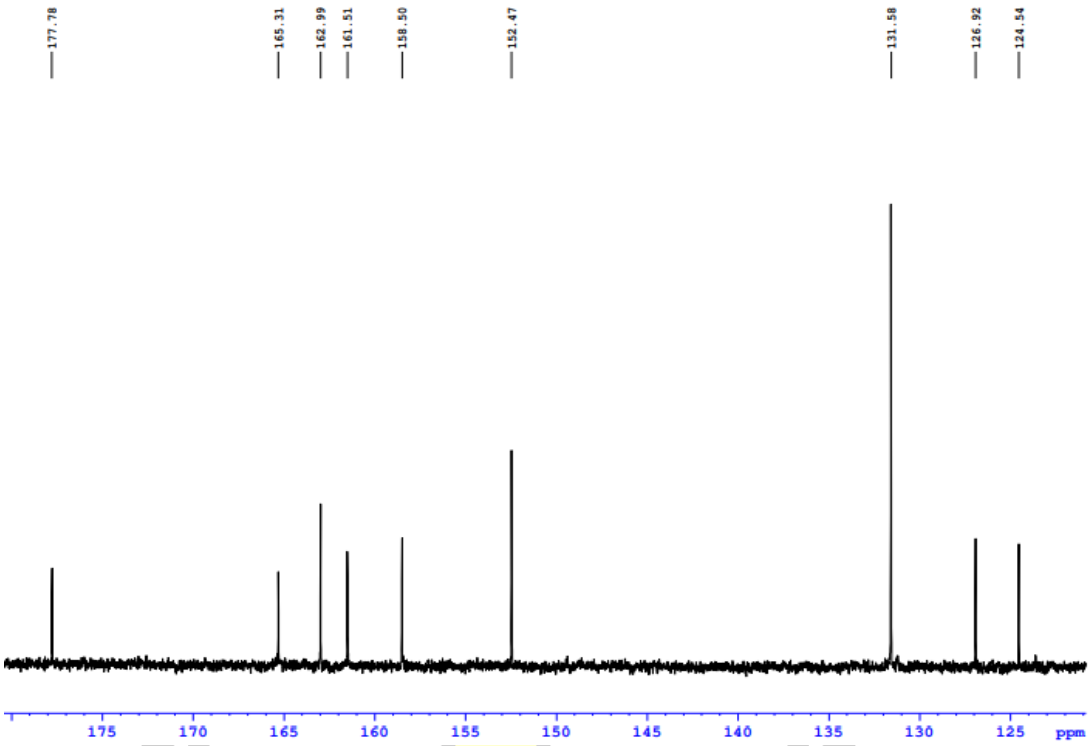

Figure A91. ^{13}C NMR (expansion 1) spectrum of **26** (CD_3OD, 100 MHz).

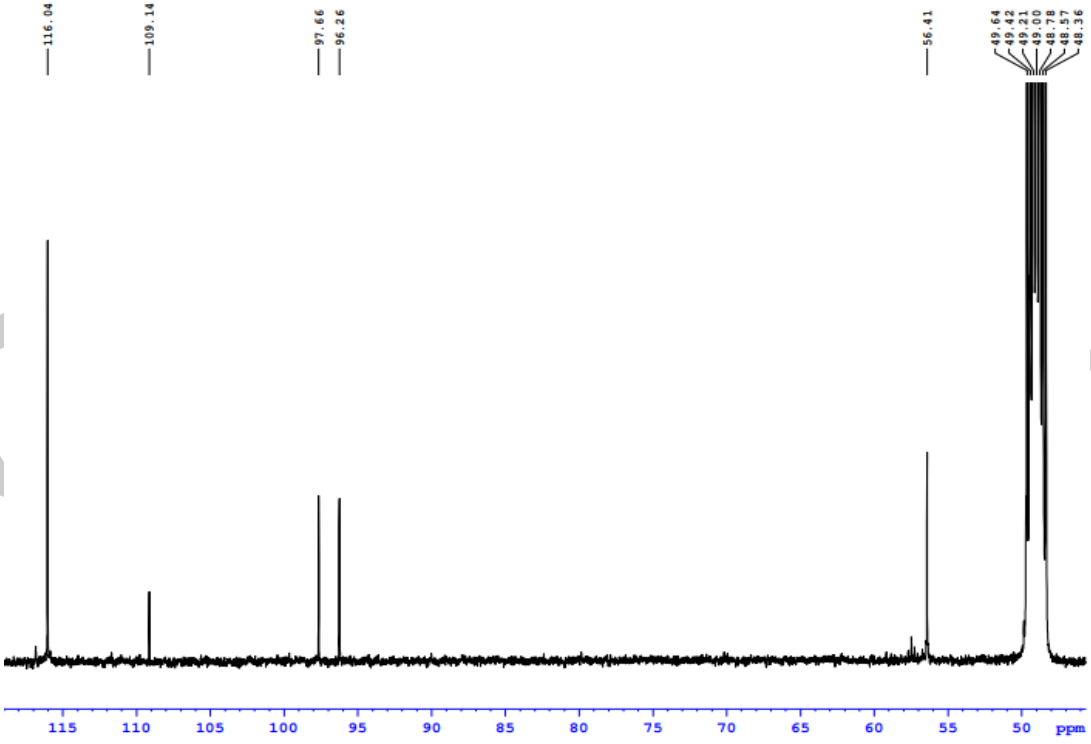

Figure A92. ^{13}C NMR (expansion 2) spectrum of **26** (CD_3OD, 100 MHz).

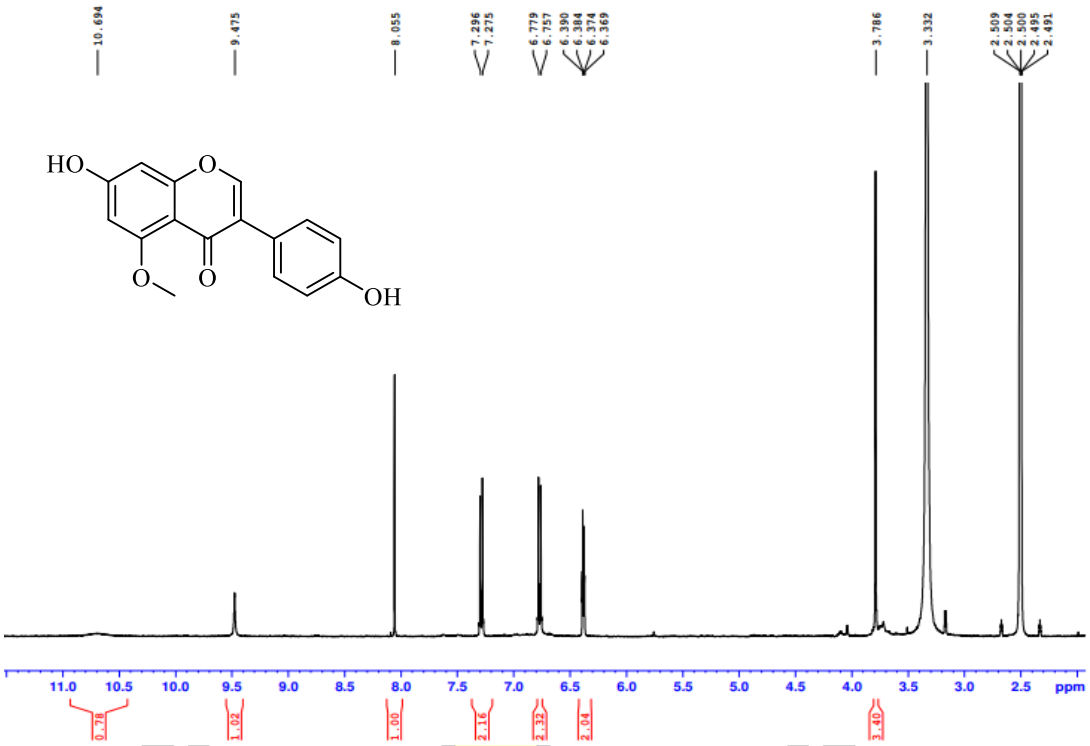

Figure A93. ^{1}H NMR spectrum of **26** (DMSO-d_6, 400 MHz).

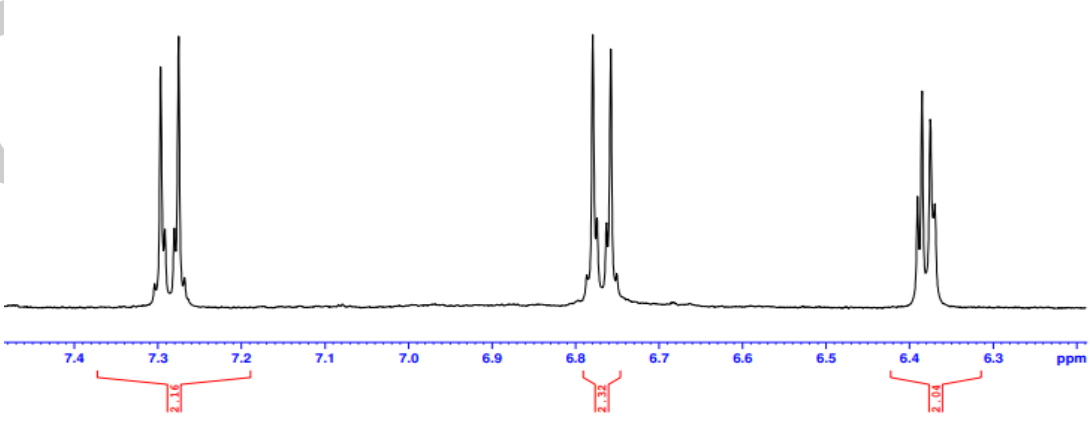

Figure A94. ^{1}H NMR (expansion 1) spectrum of **26** (DMSO-d_6, 400 MHz).

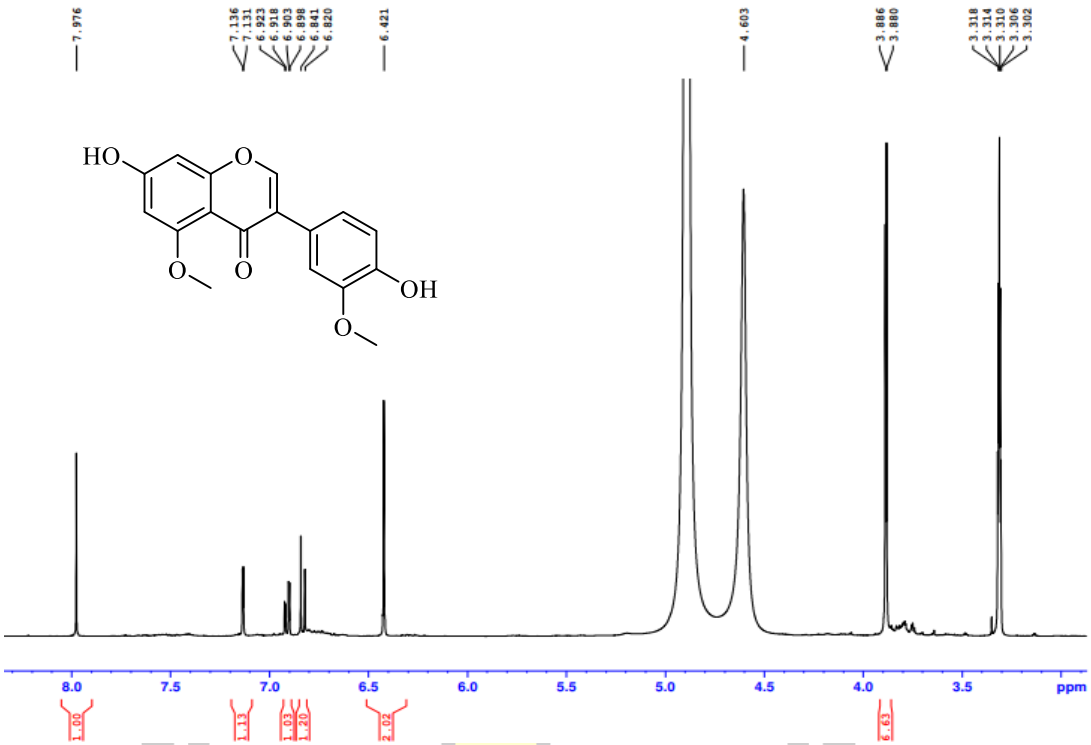

Figure A95. ^{1}H NMR spectrum of **27** (CD_3OD, 400 MHz).

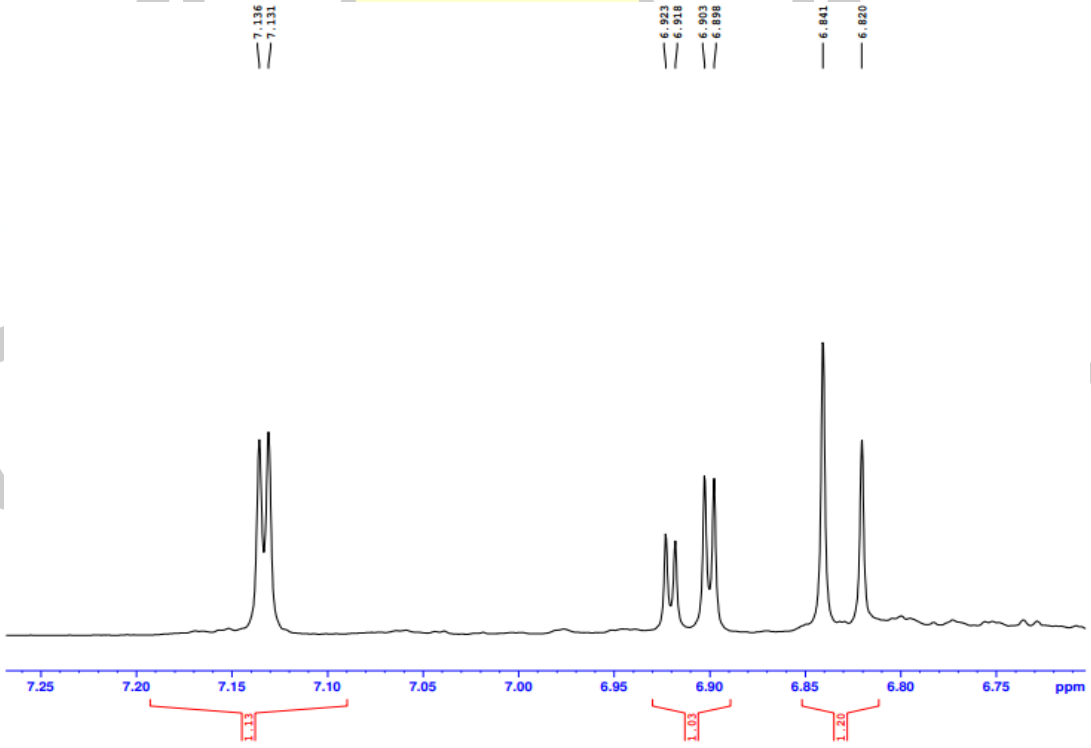

Figure A96. ^{1}H NMR (expansion 1) spectrum of **27** (CD_3OD, 400 MHz).

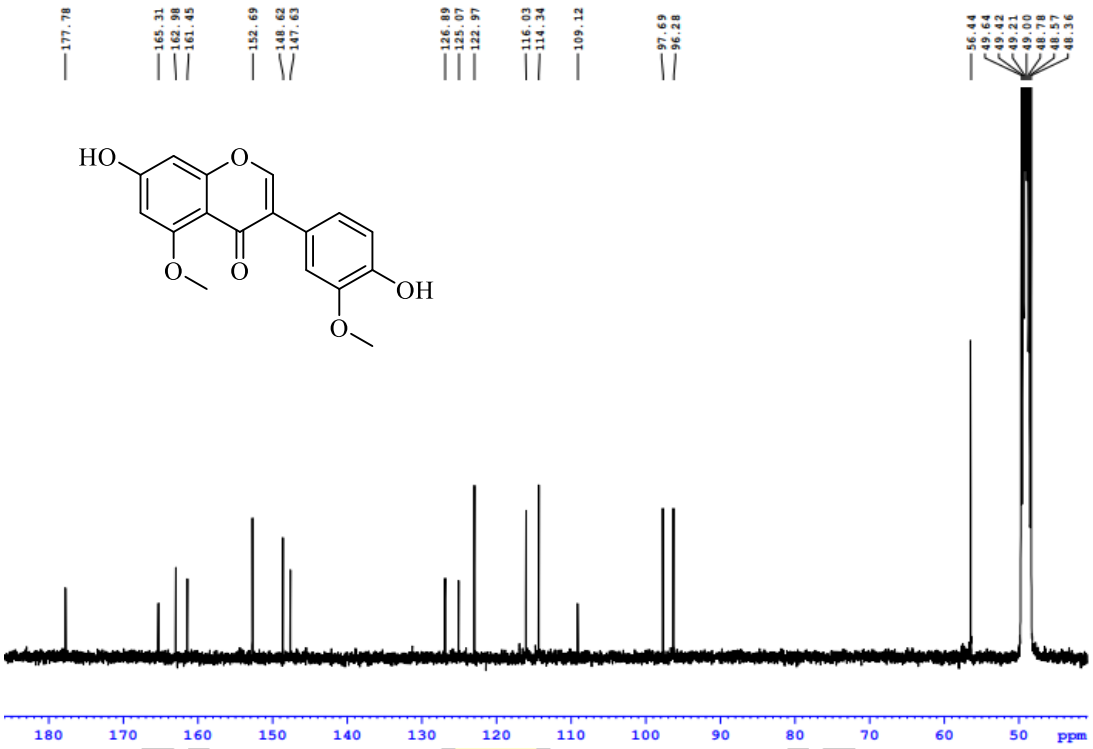

Figure A97. ^{13}C NMR spectrum of **27** (CD_3OD, 100 MHz).

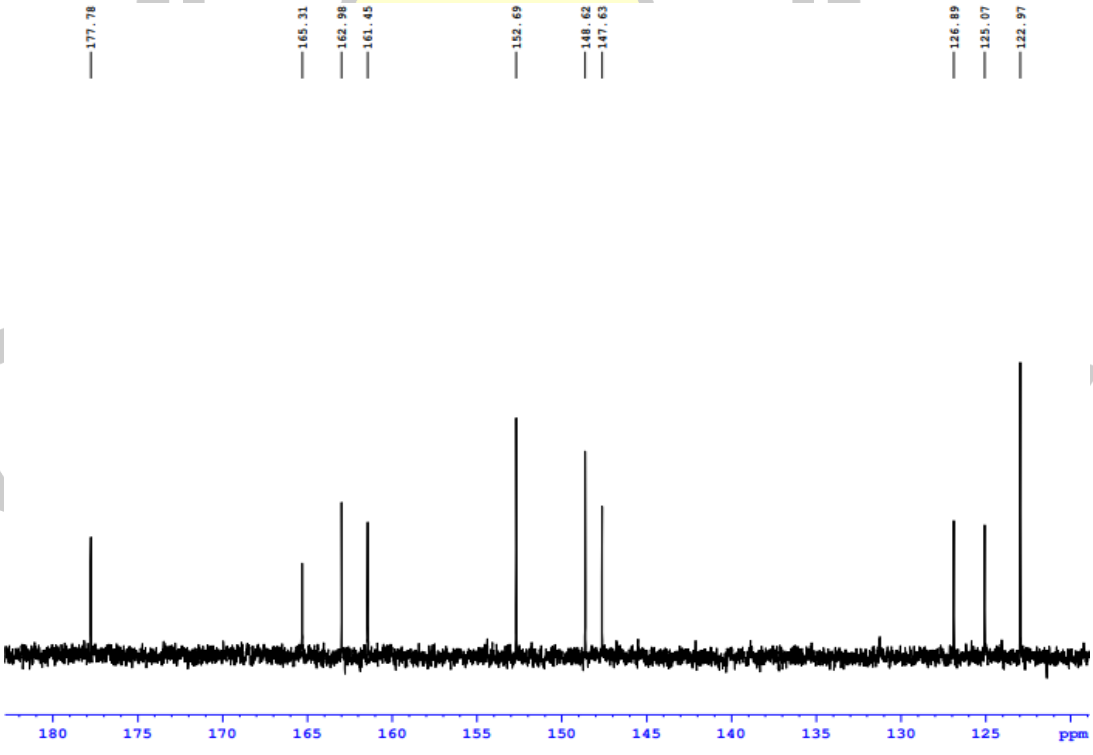

Figure A98. ^{13}C NMR (expansion 1) spectrum of **27** (CD_3OD, 100 MHz).

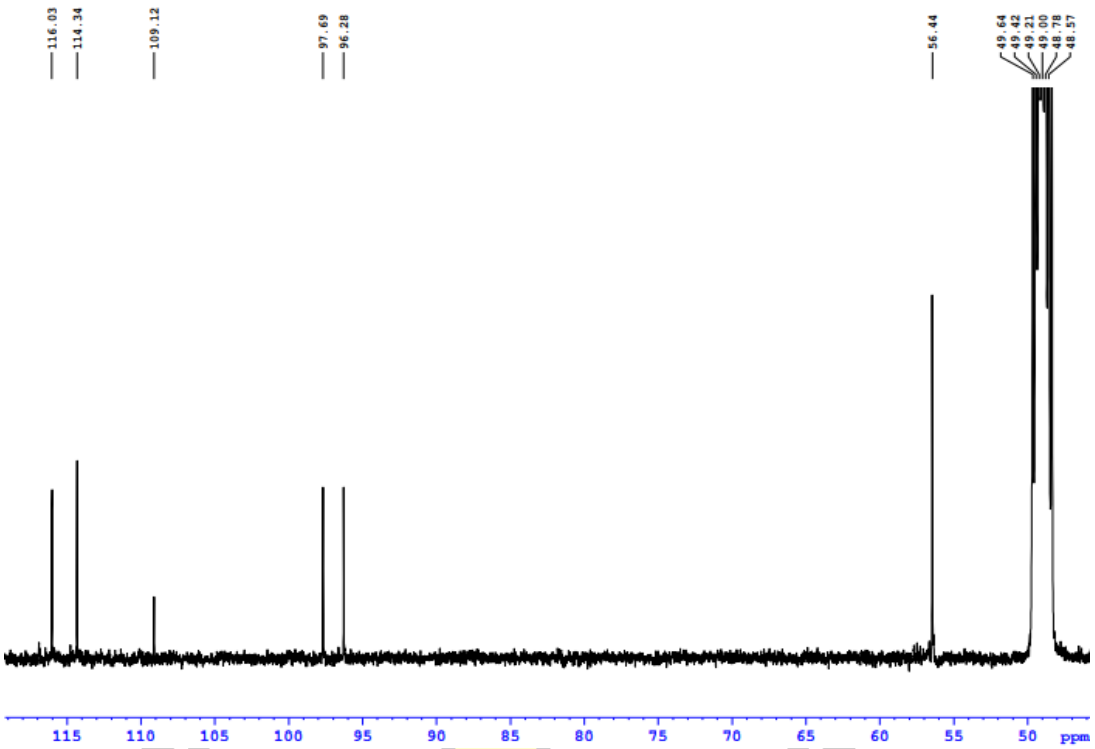

Figure A99. ^{13}C NMR (expansion 2) spectrum of **27** (CD_3OD, 100 MHz).

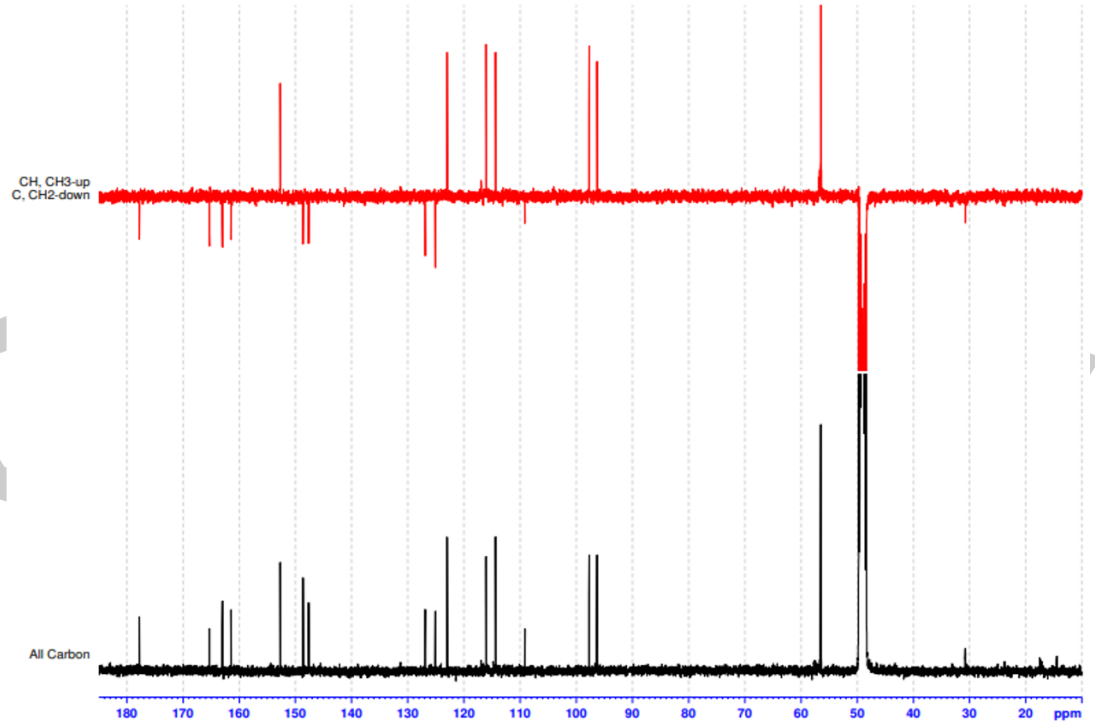

Figure A100. DEPT-135 spectrum of **27** (CD_3OD, 100 MHz).

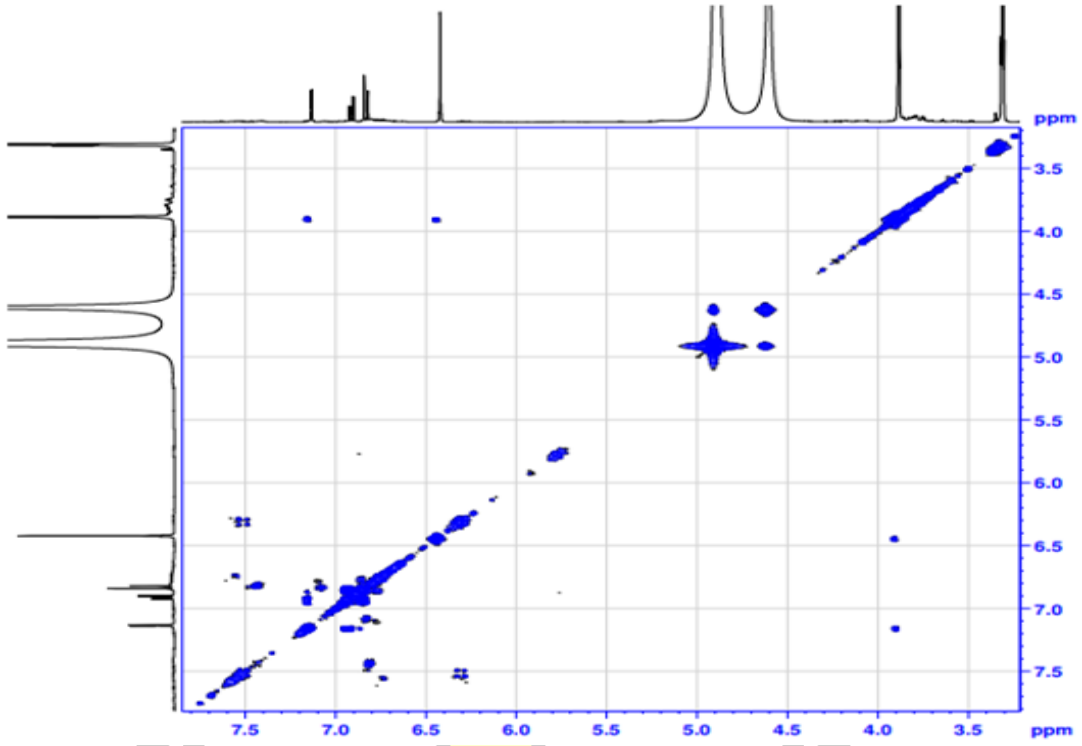

Figure A101. COSY spectrum of **27** (CD_3OD, 100 MHz).

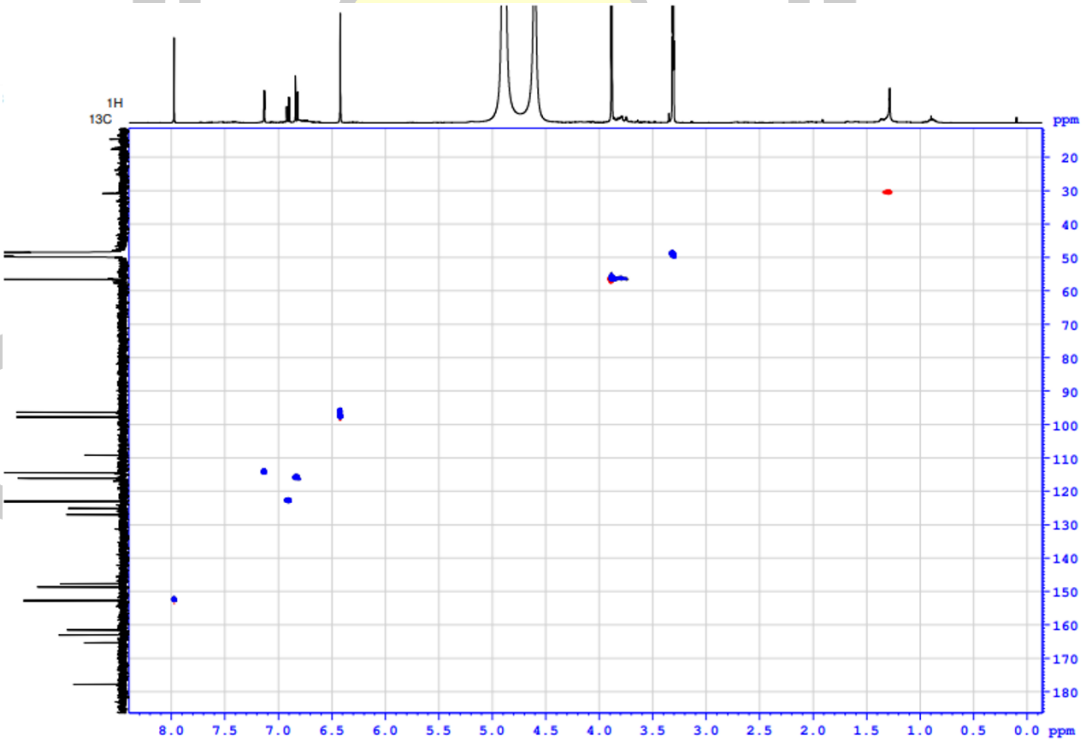

Figure A102. HSQC spectrum of **27** (CD_3OD, 100 MHz).

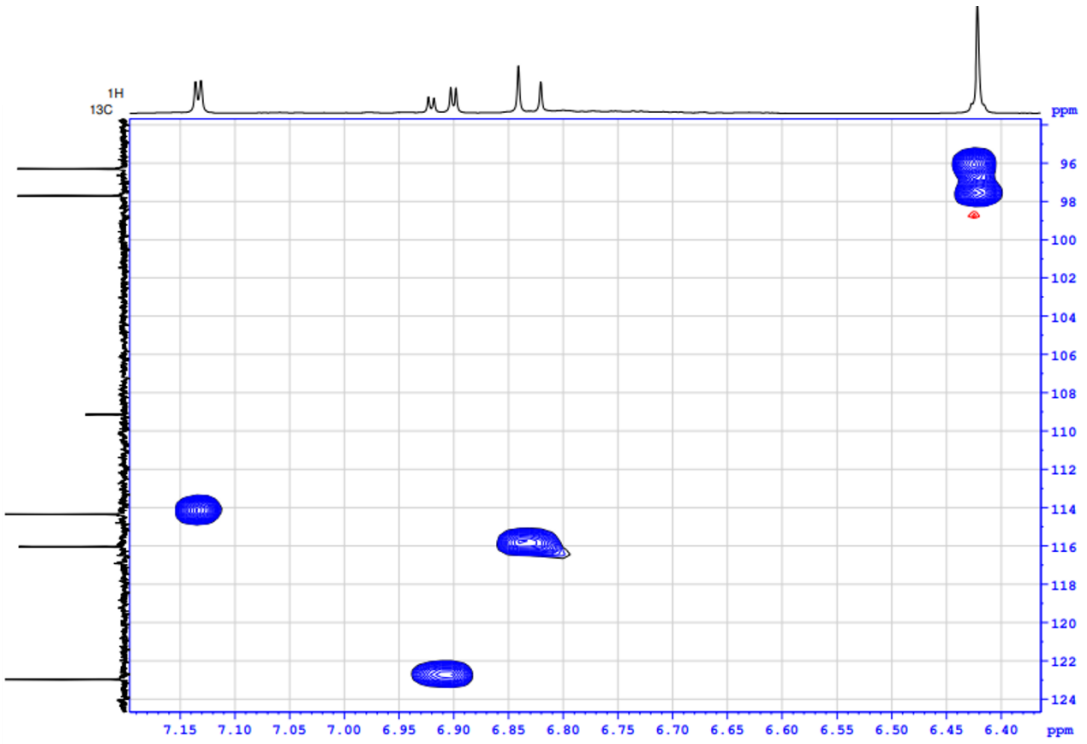

Figure A103. HSQC (expansion 1) spectrum of **27** (CD_3OD, 100 MHz).

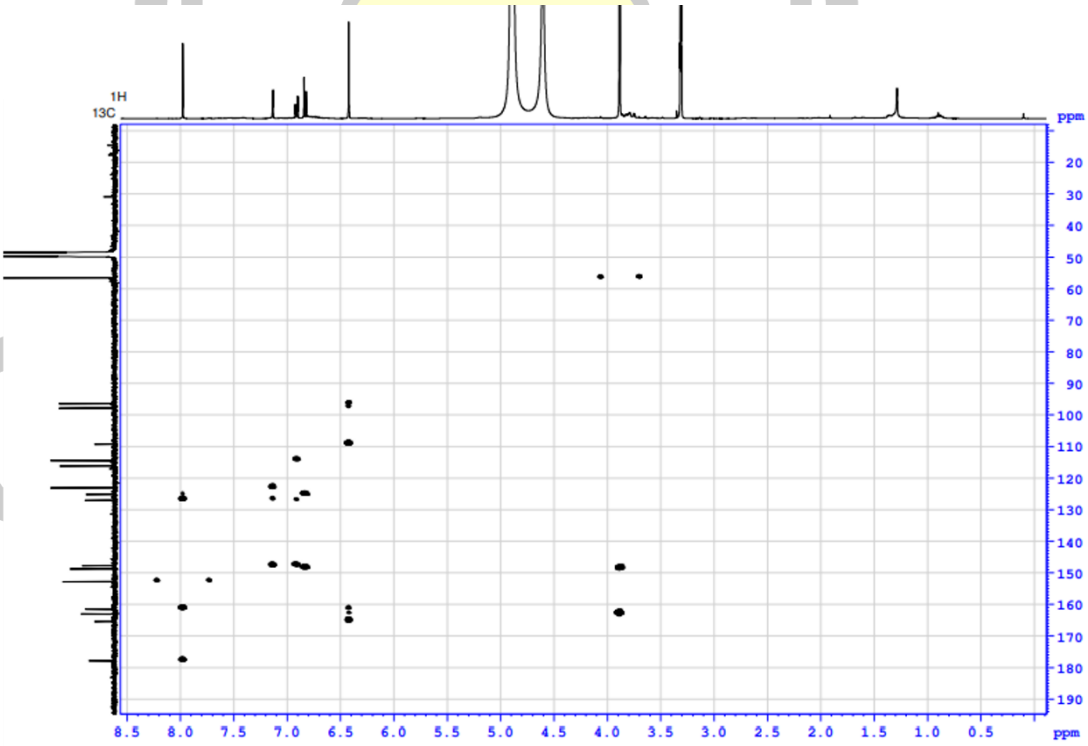

Figure A104. HMBC spectrum of **27** (CD_3OD, 100 MHz).

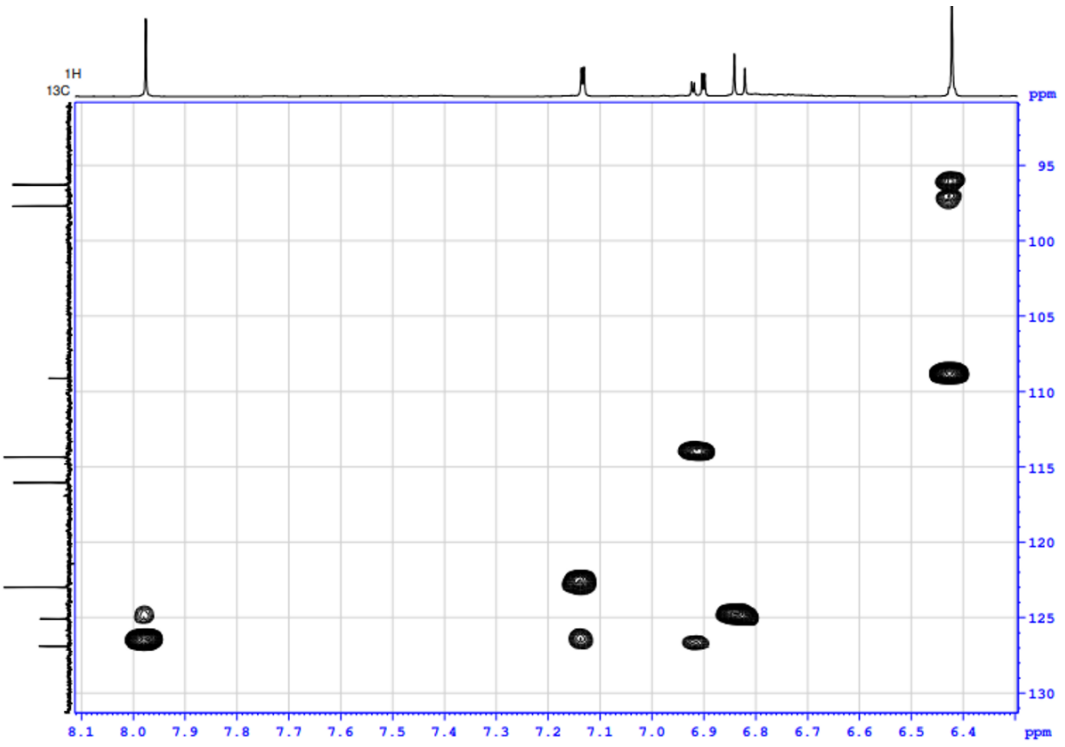

Figure A105. HMBC (expansion 1) spectrum of **27** (CD_3OD, 100 MHz).

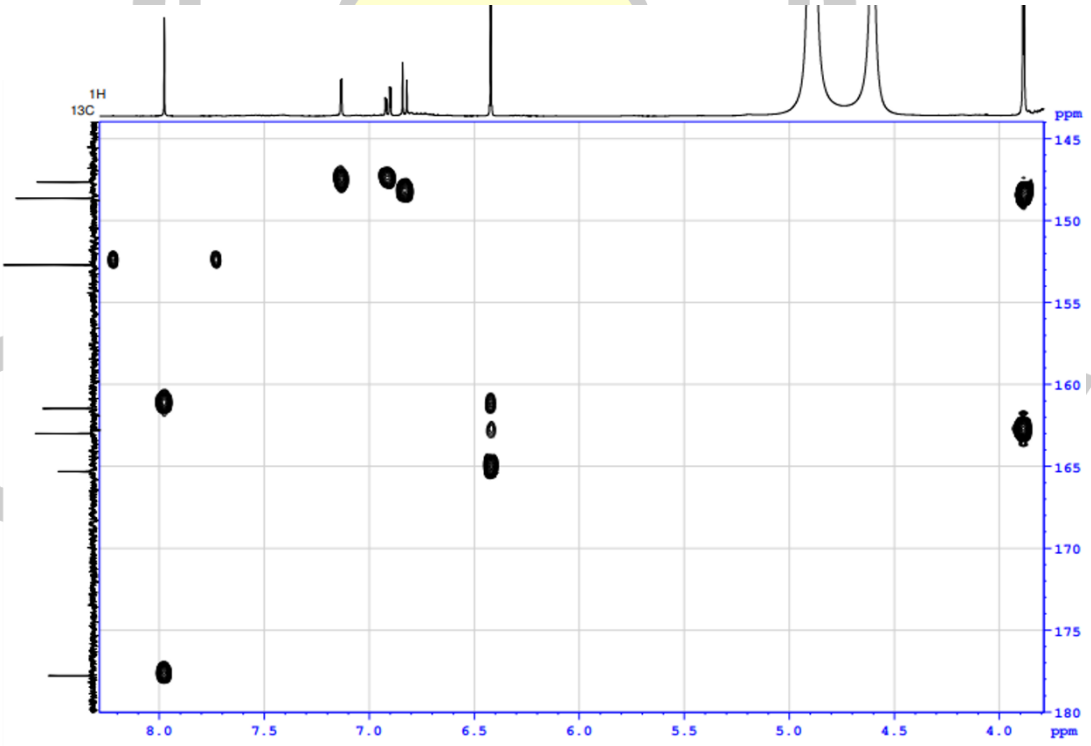

Figure A106. HMBC (expansion 2) spectrum of **27** (CD_3OD, 100 MHz).

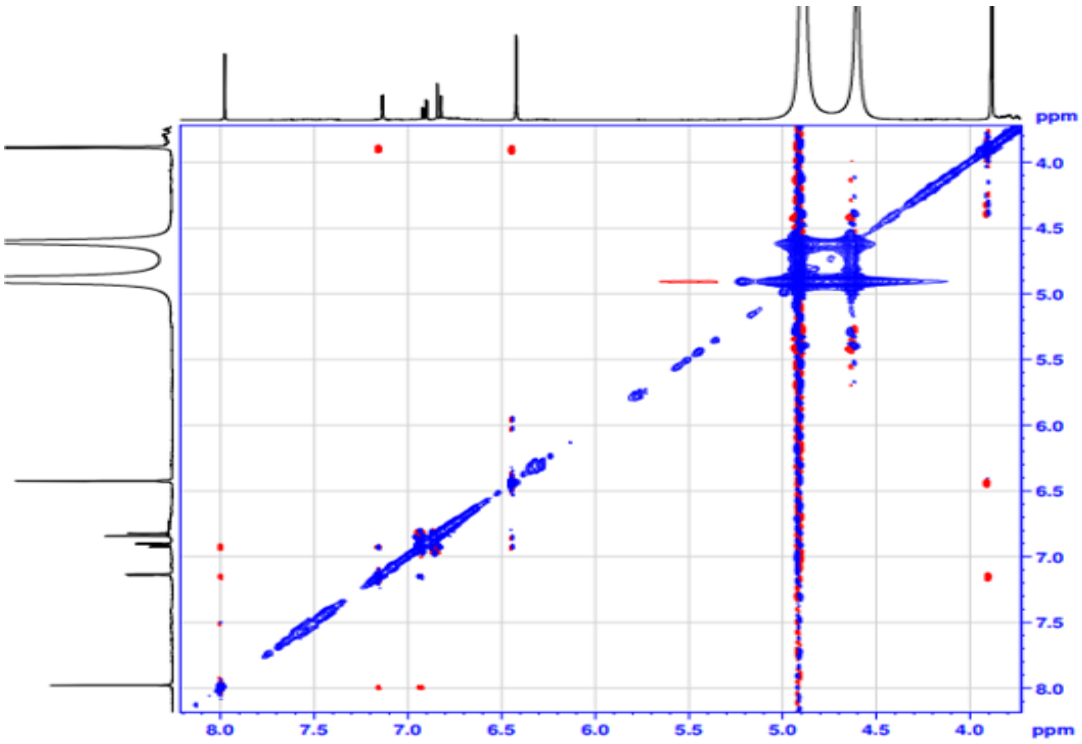

Figure A107. NOESY spectrum of **27** (CD_3OD, 100 MHz).

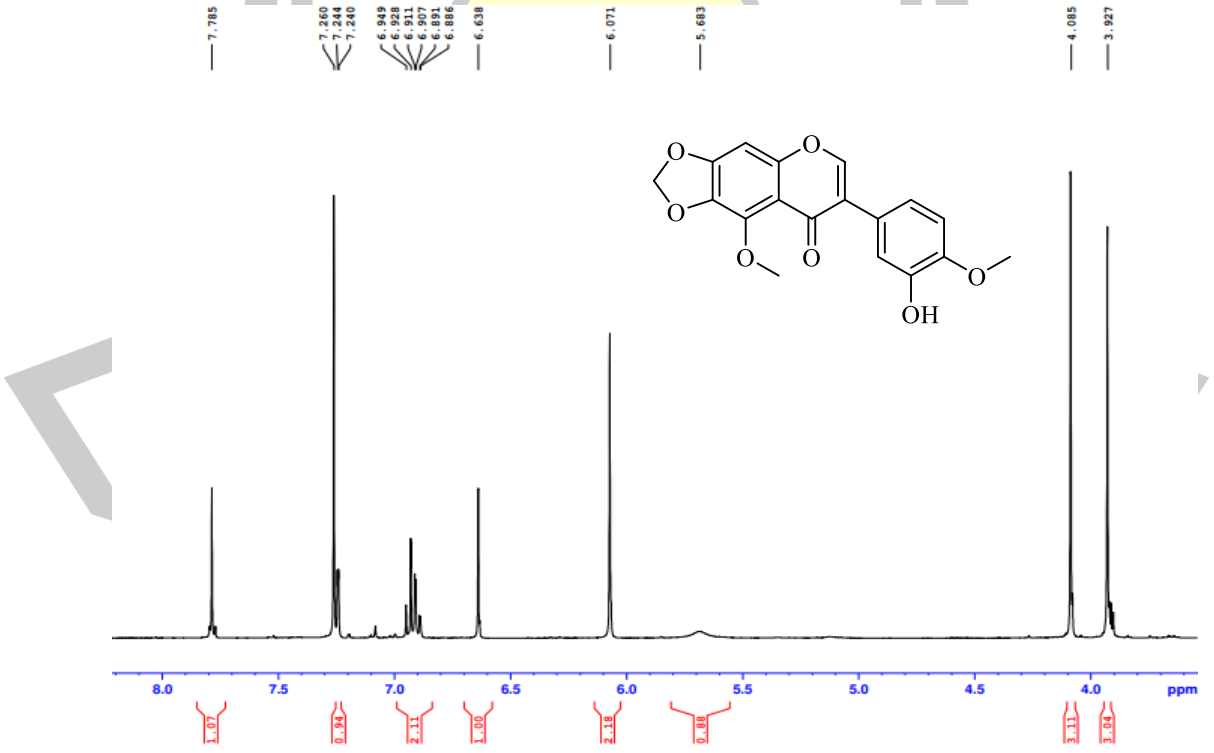

Figure A108. ^1H NMR spectrum of **36** ($CDCl_3$, 400 MHz).

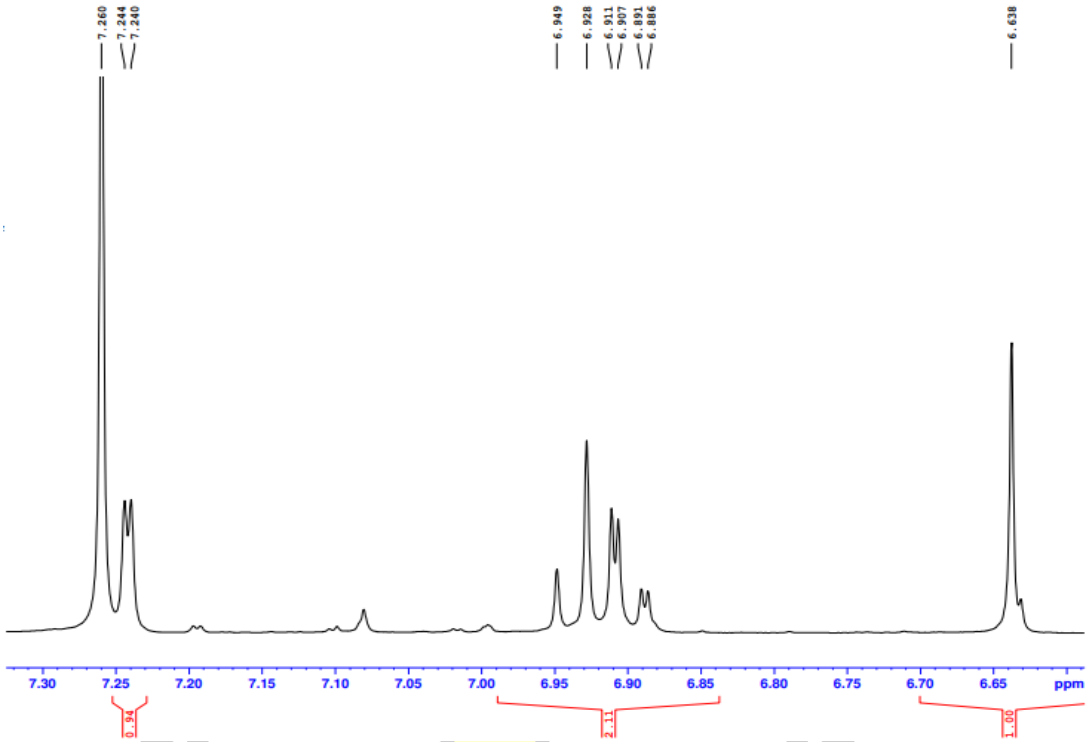

Figure A109. ^{1}H NMR (expansion 1) spectrum of **36** ($CDCl_3$, 400 MHz).

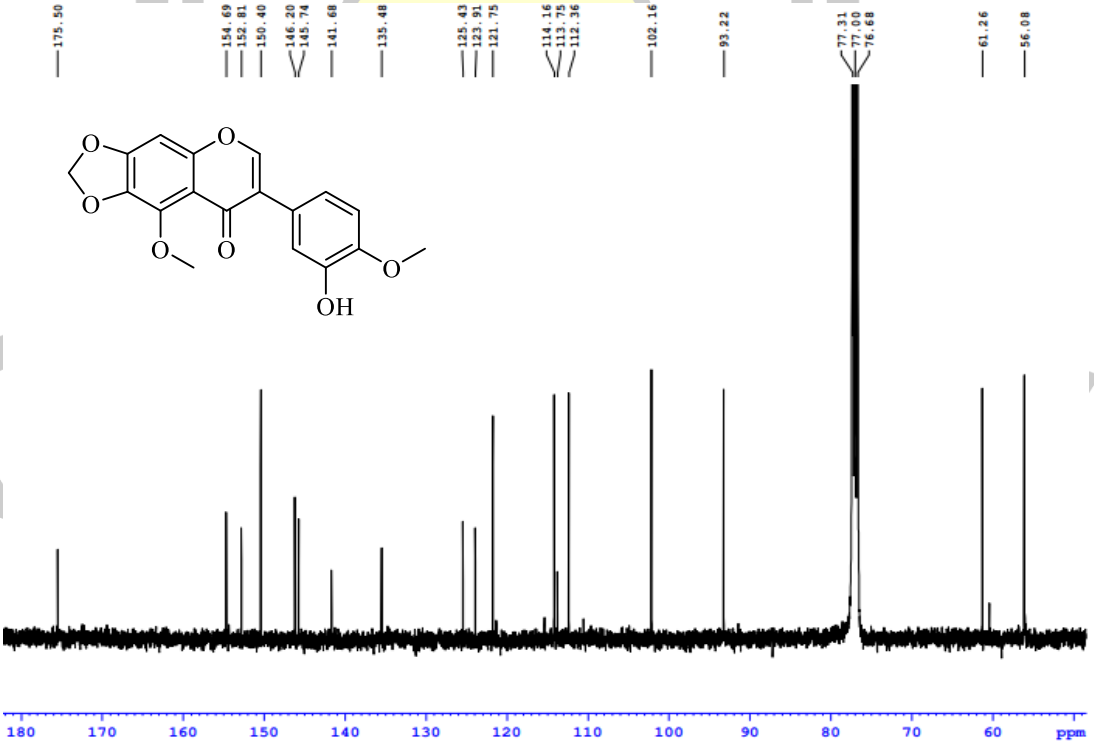

Figure A110. ^{13}C NMR spectrum of **36** ($CDCl_3$, 100 MHz).

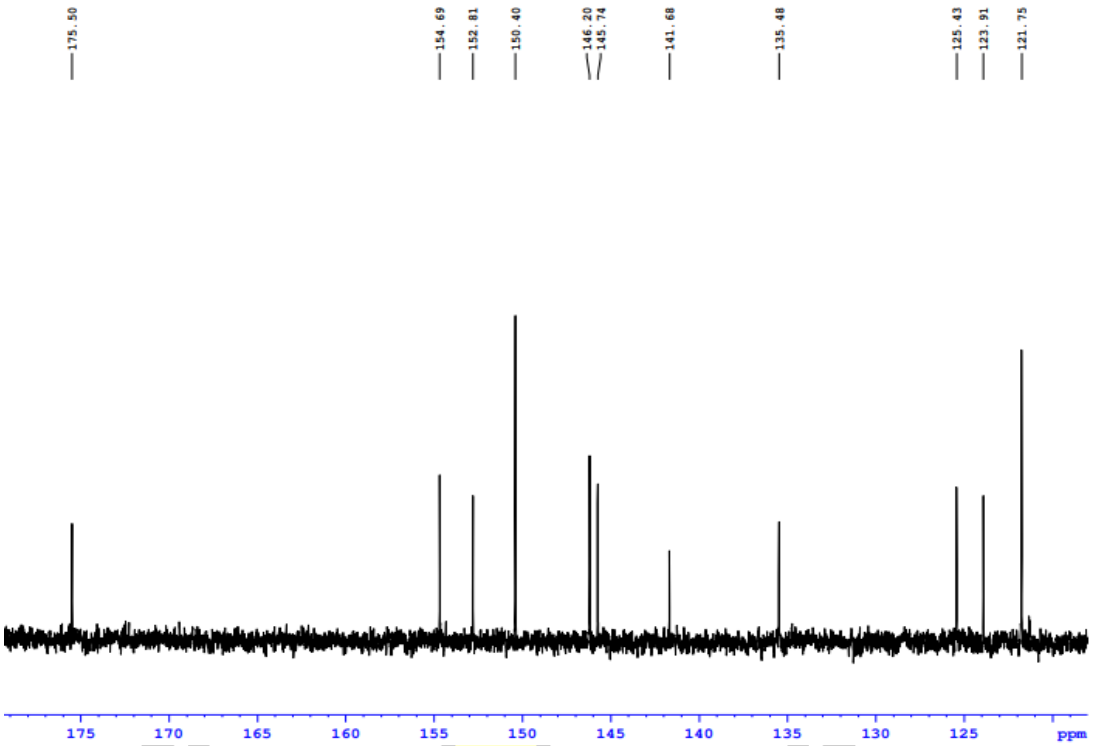

Figure A111. ^{13}C NMR (expansion 1) spectrum of **36** ($CDCl_3$, 100 MHz).

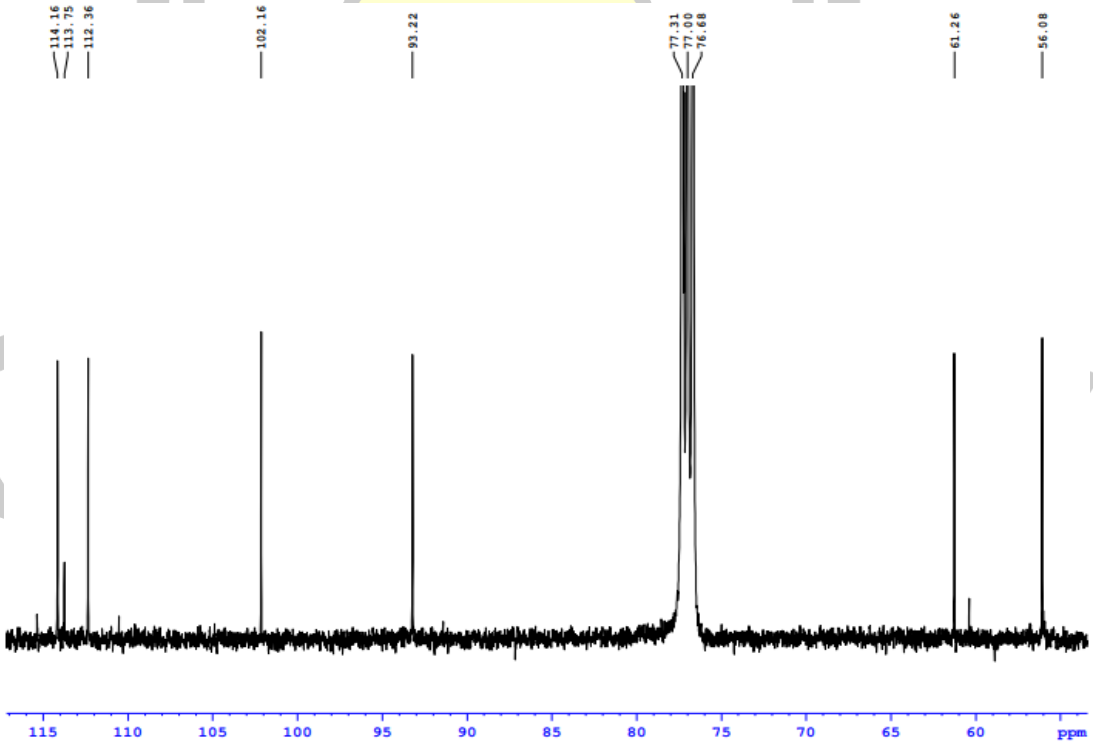

Figure A112. ^{13}C NMR (expansion 2) spectrum of **36** ($CDCl_3$, 100 MHz).

BIOGRAPHY

NAME	Sirilug Wongpakham
DATE OF BIRTH	24/07/1999
PLACE OF BIRTH	Sakon Nakhon, Thailand
ADDRESS	23 Village No. 5 Kho Khiao sub-district, Waritchaphum District, Sakon Nakhon, 47150
PLACE OF WORK	Mahasarakham University
EDUCATION	2015-2017 High School Certificate equivalent, Thambowonwittaya, Sakon Nakhon, Thailand 2018-2021 Bachelor of Science, Mahasarakham University, Maha Sarakham, Thailand 2022-Present Masters of Science, Mahasarakham University, Maha Sarakham, Thailand
Research grants & awards	Center of Excellence for Innovation in Chemistry (PERCH-CIC) Mahasarakham University (Postgraduate Research Scholarship)
Research output	Wongpakham, S.; Samsee, T.; Wongpakam, K.; Promden, W.; Thima, K.; Khulmanee, T.; Patrapuvich, R.; Sangdee, A.; Kijjoa, A.; Seephonkai, P. A New Isoflavone Xylopyranoside and Isoflavone Derivatives from the Roots of Ochna integerrima and Their DPPH Radical Scavenging Activity. Chemistry and Biodiversity. 2025; 22(2): e202401979.